

DIELECTRIC AND KERR EFFECT STUDIES
OF ELECTRO-ACTIVE POLYMER COMPLEXES

JOSEPH THLAMA DAWHA, B.Sc, M.Sc.

A thesis presented for the degree of
Doctor of Philosophy

to

THE UNIVERSITY OF ASTON IN BIRMINGHAM

January 1985

Dielectric and Kerr Effect Studies
of Electro-Active Polymer Complexes

A thesis presented for the degree of
Doctor of Philosophy
to
The University of Aston in Birmingham
by
Joseph Thlama Dawha, B.Sc, M.Sc
1985

Samples of polyphenylenes have been prepared from benzene, biphenyl and 1,4-dibromobenzene using a variety of synthetic procedures. The nature and composition of the polymers has been studied indirectly by solvent extraction of low-molecular weight material. Chromatographic techniques have shown that a major proportion of this material is comprised of para-substituted oligophenylenes. The reduction coupling of benzene has been found to yield a great variety of polyaryl compounds in addition to para-substituted polyphenylenes. The polymerization of biphenyl in solution in cyclohexane using $AlCl_3/CuCl_2$ catalysts gave predominantly para-substituted polyphenylenes and relatively large amounts of the odd membered oligomers. A reaction scheme has been prepared to account for these observations.

The dielectric and electro-optical properties of tetracyanoquinodimethane and iodine complexes of benzene, toluene, o-, m-, p-xylene, biphenyl, terphenyl and m-biphenylbenzene and those of the pure compounds was undertaken through the measurement of static dielectric permittivities and Kerr constants. Experimental molar Kerr constants have been derived for the complexes and compared to theoretical values calculated using bond and group polarizabilities taken from the literature. The experimental molar Kerr constants were in general considerably larger than the corresponding theoretical values and these differences were attributed to either increases in polarizability and/or increases in the anisotropy of polarizability of the complexes.

The effects of exhalation on the magnitudes of the molar Kerr constants has also been considered.

Kerr effect and dielectric studies have also been carried out on complexes formed between tetracyanoquinodimethane and different stereoregular forms of poly(N-vinylcarbazole) in solution in 1,4-dioxane. The magnitude of the Kerr effect was found to vary with changes in tacticity for the range of molecular weights and molecular weight distributions considered in this study.

Keywords:

Poly(p-phenylene), Oligophenylenes, Poly(N-vinylcarbazole), Tetracyanoquinodimethane, Iodine, Complexes, Tacticity, Synthetic routes, Kerr effect, Static dielectric permittivity.

ACKNOWLEDGEMENTS

I am grateful to my supervisor Dr.M.S.Beevers for his encouragement, dedication and intellectual involvement throughout the preparation of this work.

I am indebted to the Borno State College of Basic Studies and the Borno State Scholarship Board for their financial support during the period 1981-1984.

I would like to thank the staff of the chemistry workshop for the construction of numerous pieces of apparatus used for this study. My thanks are also extended to the technical staff of the Chemistry Department. I would like to express my appreciation to colleagues in the polymer research group for the interest they have shown in this work.

My thanks are also extended to Mrs.A.Howell for her patient typing of this manuscript.

Finally, I would like to thank members of my family and friends who have encouraged me throughout the course of this work.

CONTENTS

	Page
<u>CHAPTER 1</u> <u>Introduction</u>	1
<u>CHAPTER 2</u> <u>Poly(p-phenylenes) (PPP)</u>	12
2.01 Mechanism of the Polymerization	14
2.02 The Oxygen Effect (Radical Trapping)	18
2.03 Decomposition of Benzoyl Peroxide in Benzene-Cupric Chloride	20
2.04 Determination of Molecular Weight	24
2.05 Alkylation of Poly(p-phenylene)	26
2.06 Catalytic Hydrogenation of Poly(p- phenylene)	28
2.07 Control of Molecular Weight (Solvent effect)	30
2.08 The Lewis Acid-Catalyst-Oxidant System	31
2.09 Solid State Polymerization	34
2.10 PPP-Charge Transfer Complex and Electrical Conductivity	35
<u>CHAPTER 3</u> <u>Experimental Methods</u>	
3.01 Introduction	38
3.02 The Kerr Effect Apparatus	39
3.03 Optical Alignment	44
3.04 High-Voltage Pulse Former	45
3.05 Small Capacity Kerr Cell (K1)	48
3.06 Large Capacity Kerr Cell (K2)	50
3.07 Measurement of Experimental Kerr Constant B	53
3.08 Measurement of Relative Kerr Constant	54

	Page
3.09 Measurement of Kerr Constant by Double Cell Technique	57
3.10 The Dielectric Apparatus	59
3.11 Measurement of Static Dielectric Permittivity	62
3.12 The Automatic Sublimator	62
3.13 Power Controller for Automatic Sublimator	64
<u>CHAPTER 4</u> <u>Synthesis and Characterisation of</u> <u>Poly(p-phenylenes)</u>	67
4.01 Introduction	67
4.02 Bulk Polymerization of Benzene with $AlCl_3-CuCl_2$ Catalyst-Oxidant	68
4.03 Synthesis of Poly(p-phenylene) from Solutions of Benzene and Biphenyl in Cyclohexane	69
4.04 Polymerization of Biphenyl	70
4.05 Polymerization of Benzene-Ether Mixtures	71
4.06 Preparation of Poly(p-phenylene) by Transition Metal-Catalysed 'C-C' Coupling	73
4.07 Sulphonation of Poly(p-phenylene) (P1)	75
4.08 Infrared Analysis of Polyphenylenes	76
4.09 Analysis of Poly(p-phenylenes) using X-ray Diffraction	79

	Page
<u>CHAPTER 5</u> <u>Preparation and Chromatographic</u>	
<u>Characterisation of Oligophenylenes</u>	83
5.02 Extraction of Oligomers from Polymers	84
5.03 Gel Permeation Chromatography	85
5.04 Gel Permeation Chromatograph	88
5.05 Column Systems	91
5.06 Packing Material (Sephadex LH20 and LH60)	92
5.07 GPC Chromatograms	94
5.08 Gas Liquid Chromatography	109
5.09 Vapour Pressure Osmometry	113
 <u>CHAPTER 6</u> <u>Dielectric and Kerr Studies of Aryl-</u>	
<u>Iodine and Aryl-TCNQ Complexes</u>	114
6.01 Introduction	114
6.02 Solution Kerr Constants of Aryl-Iodine Complexes	120
6.03 Solution Kerr Constants of TCNQ-Xylene Complexes	131
6.04 Discussion of Results	134
6.05 TCNQ Complexes of Phenylene Oligomers in 1,4-dioxane	138
6.06 Preparation of TCNQ-Oligophenylene Complexes	139
6.07 Solution Molar Kerr Constants of Oligophenylene and Oligophenylene- TCNQ Complexes	140

	Page
6.08 Molar Kerr Constants of TCNQ- Oligophenylene Complexes in Solution in 1,4-dioxane at 298 K	141
6.09 Discussion of Results	144
<u>CHAPTER 7</u> <u>Calculation of Molar Kerr Constants of</u> <u>Bimolecular Complexes using Bond</u> <u>Polarizabilities</u>	150
7.01 Introduction	150
7.02 Theoretical Molar Kerr Constant of Iodine Complexes	156
7.03 Theoretical Kerr Constant of Tetracyanoquinodimethane	159
<u>CHAPTER 8</u> <u>Dielectric and Electro-Optical Properties</u> <u>of Poly(N-vinyl Carbazole) in Solution with</u> <u>with Tetracyanoquinodimethane</u>	167
8.01 Introduction	167
8.02 Synthesis and Characterisation of Stereoregular Poly(N-vinyl Carbazole)	169
8.03 Preparation of PVK:TCNQ Complexes in Solution in 1,4-dioxane	175
8.04 Kerr Effect of the PVK Samples S1-S4 and their TCNQ Complexes	176
8.05 Investigation of Molecular Weight Dependence on Kerr Constant for PVK Samples	187
8.06 Dielectric Permittivities of PVK and PVK:TCNQ Complexes in Solution in 1,4-dioxane	187

	Page
<u>CHAPTER 9</u> <u>General Conclusions and Suggestions</u> <u>for Future Work</u>	190
<u>APPENDIX 1</u> <u>Optical Theory of the Kerr Effect</u>	198
A1-I The Use of Quarter Wave Retarder	198
A1-II Measurements of Phase Difference, δ , using Static Electric Fields	201
A1-III Measurements of Phase Difference, δ , using Pulsed Electric Fields	203
<u>APPENDIX 2</u> <u>Computer Programs</u>	205
Program 1 Calculation of Theoretical Molar Kerr Constants	205
Program 2 Calculation of Solution Molar Refraction and Refractive Indices	218
Program 3 Calculation of Infinite Dilution Molar Kerr Constants	223
Program 4 Calculation of Dipole Moments	226
Program 5 Calculation of Solute Molar Kerr Constants using Alligation Formulae	228
<u>APPENDIX 3</u> <u>I.R.Spectra of Poly(p-phenylene) Samples</u>	234
<u>REFERENCES</u>	243

TABLES

<u>Table No.</u>		<u>Page</u>
1	Observed conductivities for unoriented $A_{S}F_{5}$ -doped polymers and copolymers	5
3.1	Kerr data for various concentrations of biphenyl in cyclohexane	56
4.1	I.R.Spectra data for various samples of poly(p-phenylene) and standard compounds	78
4.2	X-ray diffraction data for various poly(p-phenylene) samples and oligomers	81
6.01	Kerr effect data for solutions of I_{2} (0.2% w/v) in various solvents at 298 K	125
6.02	Dielectric data for solutions of I_{2} (0.2% w/v) in various solvents at 298 K	130
6.03	Kerr effect data for solutions of TCNQ (0.1% w/v) in various solvents at 298 K	132
6.04	Dielectric data for solutions of TCNQ (0.1% w/v) in various solvents at 298 K	132
6.05	Kerr effect and dielectric data for solutions of oligophenylenes in 1,4- dioxane at 298 K	145
6.06	Kerr effect and dielectric data for solutions of TCNQ and oligophenylenes in 1,4-dioxane	145

<u>Table No.</u>		<u>Page</u>
6.07	Dielectric data for solutions of TCNQ- oligophenylene in 1,4-dioxane at 298 K	146
7.01	Principal polarizabilities of the aryl compounds	160
7.02	Experimental molecular Kerr Constant and corresponding calculated dipole moment for the iodine-aryl compounds	163
7.03	Experimental molecular Kerr Constant for TCNQ-aryl complexes	164
8.01	Rotation of plane polarised light as a function of the square of the applied voltage, V, for pure PVK samples and their TCNQ complexes	181
8.02	Kerr effect data for PVK samples and their TCNQ complexes in 1,4-dioxane at 298 K	182
8.03	Dielectric data for various samples of PVK and their TCNQ complexes in solution in 1,4-dioxane	183
8.04	Kerr effect data for solutions of various molecular weights of PVK samples in 1,4-dioxane at 298 K	184

ILLUSTRATIONS

<u>Figure No.</u>		<u>Page</u>
3.1	Apparatus used to measure the electrically induced phase difference, δ	41
3.2	Electrical configuration of the electrode of the photomultiplier tube	43
3.3	Circuit diagram for the high voltage pulse former	46
3.4	Rectangular-shaped pulse as displayed on the oscilloscope	47
3.5	Diagram of the small capacity Kerr Cell (K1)	49
3.6	Cross-section diagram of the large capacity Kerr Cell (K2)	52
3.7	Rotation of plane polarised light as a function of the square of applied voltage for various concentrations (1-5% w/v) of biphenyl in cyclohexane at 298 K	55
3.8	Double Cell arrangement for the determination of Kerr effect	58
3.9	Configuration of the dielectric apparatus	60
3.10	The Dielectric Cell	61

<u>Figure No.</u>		<u>Page</u>
3.11	Diagram of the automatic sublimator with heating chamber	63
3.12	Circuit diagram of the power controller for automatic sublimator	65
4.1	X-ray diffraction pattern of polymer P1(A) and sulphonated P1(B)	82
5.1	Mode of separation in GPC	87
5.2	Model 7125 flow diagram	90
5.3	Block diagram of the gel permeation chromatograph	95
5.4	GPC chromatogram of oligomer extract from P1 (C1, sephadex LH-20) at 298 K	97
5.5	Plots of logarithm of molecular weight versus peak elution volume for oligomer extract from P1	98
5.6	GPC chromatogram of oligomer extract from P3 (C1, sephadex LH-20) at 298 K	100
5.7	GPC chromatogram of oligomer extract from P3 at 298 K (C2 system, sephadex LH-20)	101
5.8	GPC chromatogram of oligomer extract from P3 at 298 K (C2, sephadex LH-60)	103
5.9	GPC chromatogram of oligomer extract from P4 (C1, sephadex LH-20) at 298 K	104

<u>Figure No.</u>		<u>Page</u>
5.10	Plots of logarithm of molecular weight versus peak elution volume for oligomer extract from P4	106
5.11	GPC chromatogram of oligomer extract from P4 at 298 K (C2 system, sephadex LH-20)	107
5.12	GPC chromatogram of oligomer extract from P7 (C2, sephadex LH-20) at 298 K	108
5.13 (A)	U.V.Spectra of model compounds (Biphenyl, terphenyl and quarterphenyl)	110
(B)	U.V.Spectra of peaks 1, 2 and 3 from figure 5.12	
5.14	GLC chromatograph of oligomer extract from P3	112
6.1	Rotation of plane-polarised light as a function of the square of applied voltage for CCl_4 , benzene and their iodine solutions	124
6.2	Diagram of Benzene-Iodine complex	126
6.3	Overlap diagrams for TCNQ complexes with various aryl compounds	127
6.4	Molar Kerr constants, $m^m K$ as a function of the number of aromatic units for oligophenylene compounds	128

<u>Figure No.</u>		<u>Page</u>
7.1	Structure of TCNQ molecule	159
7.2	Structure of predicted 1,4-dioxane-TCNQ complex	165
8.1	Rotation of plane-polarised light as a function of square of applied voltage for PVK sample S1 and the TCNQ complex	177
8.2	Rotation of plane-polarised light as a function of the square of applied voltage for PVK sample S2 and the TCNQ complex	178
8.3	Rotation of plane-polarised light as a function of the square of applied voltage for PVK sample S3 and the TCNQ complex	179
8.4	Rotation of plane-polarised light as a function of the square of applied voltage for PVK sample S4 and the TCNQ complex	180

Dedicated to

Azumi Nkwa-Tarfa

Ka

Thlama Ali Dawha

INTRODUCTION

Conductivity of Polymer and Polymer/dopant Systems⁽⁵⁾

The performance, cost and processing advantages of organic polymers are responsible for the continuing displacement of conventional metals in a variety of areas. These range from structural applications to applications in photoconductor, pyroelectric and piezoelectric devices. Until recently, these applications have been limited to cases where high electrical conductivity was desired and in which composite structures with conventional metals were used. The situation changed with the discovery that polymers such as polyacetylene^(1,2), polyphenylenes^(3,4), could be transformed into semi-conducting and metallic conductors if suitably doped with either electron donors or electron acceptors.

Electrical conductivity can be varied as much as 18 orders of magnitude by varying dopant concentrations. This makes electronic property control feasible over a whole range from insulator to semi-conductor and then metal. But, to put things in perspective, it must be remembered that this research area is embryonic. Extending the technology of conducting polymers to provide materials having a total properties profile that is optimal is a challenging task. This process involves the development of a deeper understanding of the physics and chemistry of polymer complexes. Progress in understanding molecular charge-transfer

complexes has critically depended upon the availability of large dimension single crystals. Such crystals made possible the evaluation of inherent anisotropic electronic properties and sometimes subtle structural changes that determine these properties. The situation is completely different for conducting organic polymers that are formed by the addition of electron donors or acceptors to insulating polymers. The polycrystalline or amorphous nature of parent polymers and the disorder introduced during complex formation provided a barrier for determining critical aspects of their structure and properties. For these reasons, Baughman et al⁽⁵⁾ described conducting polymers as essentially a multicomponent 'black box' which can be experimentally examined in aggregate by electrical and spectroscopic methods, or theoretically examined by use of highly idealized and simplified concepts of the components of the box.

Baughman et al⁽⁵⁾ examined a variety of organic polymers to define the variation in molecular, crystallographic and defect structures that are compatible with high conductivities. They classified these materials into three categories depending upon backbone type: Polyacetylenes, polyphenylenes and polyphenylene chalcogenides.

They observed that dopant species and polymer dopant interactions are important for these analyses which were enormously complicated by irreversible chemical modification of polymer backbone that sometimes accompanies formation of conducting polymer complexes. The important factors which form the basis for conducting behaviour of polymer systems

was outlined by Baughman and co-workers. These include polymer structure, structure of 'simple complexes', covalent band formation with dopants and formation of molecular aggregates.

Polymer structures: The polymer chain structures present in undoped polymers and as modified by the doping process are thought to be the key determinant for the electronic properties of the polymer/dopant systems. Polymer and dopant components can occupy comparable volumes in heavily doped materials. However, there is no evidence from any investigated system that electronic conductivity along dopant molecular arrays provides the major contribution to observed conductivities. More specifically the signs of Hall Coefficients, thermo-power coefficients and polarity of junction devices suggest hole conductivity for acceptor-doped polymers and electron conductivity of donor-doped polymers.

Polymers that form highly conducting complexes need not have a planar backbone or a continuous system of overlapping Carbon π -orbitals. Structural investigations by Baughman et al⁽⁶⁾ and theoretical calculations by Bredas et al⁽⁷⁾ for cis- and trans-polyacetylene show consistency with planar backbone structures for these polymers. In contrast, poly(p-phenylene), poly(p-phenylene sulphide) and poly(m-phenylene) which form conducting complexes are noted for non-planar backbone structures. Structural data for phenylene oligomers predicts an angle of 23° between neighbouring phenyls in poly(p-phenylene). Nevertheless, poly(p-phenylene)

forms AsF_5 -complexes having a comparable conductivity to that for polyacetylene (about 500 and 1200 scm^{-1}) respectively for unoriented polymers^(1,4). A more interesting example is provided by poly(p-phenylene sulphide) which forms AsF_5 complexes with conductivities of about 1 Scm^{-1} ⁽⁸⁾. The neighbouring phenyl rings are inclined by alternating $+45^\circ$ and -45° with respect to the planar zig zag chain of the sulphurs⁽⁹⁾. The interaction of phenyl π -orbitals with sulphur P-orbitals has been suggested to provide the delocalized electronic system necessary for high conductivities in the doped polymers. The oligomer calculations by Duke and Patron⁽¹⁰⁾ and polymer calculations of Bredas et al⁽¹¹⁾ support this view. The introduction of methylene linkages (as an unbridged link in the polymer backbone) is known to dramatically decrease observed conductivities for the doped polymers. For example the replacement of chain chalcogens with methylene in poly(p-phenylene sulphide) or poly(p-phenylene oxide) reduces the electrical conductivity for the AsF_5 doped polymer from 1 and 10^{-3} Scm^{-1} respectively, to less than 10^{-7} Scm^{-1} . This change in backbone structure (supported by Bredas theoretical calculations⁽¹¹⁾) increases the ionisation potential of the polymer and also interrupts electronic delocalization thus explaining the observed conductivity results.

A	B	(A) _x	(B) _x	(AB) _x	(AB ₂) _x
HC=CH	C ₆ H ₄	1200	500	3	
C ₆ H ₄	C ₆ H ₄ S	500	1	0.3	0.02
C ₆ H ₄ S	C ₆ H ₄ O	1	10 ⁻³	10 ⁻⁴	5x10 ⁻⁶

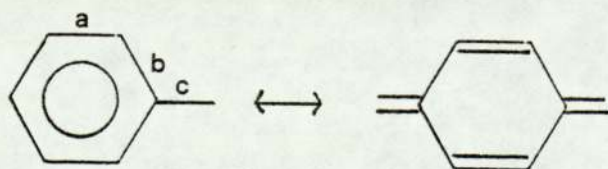
Table 1 Observed conductivities (Scm⁻¹) for unoriented AsF₅ - doped polymers and copolymers⁽⁵⁾

As shown in Table 1, homogeneous chain structures appear to give complexes with higher conductivities. Regular copolymers are observed to dope to lower conductivities than do homopolymers containing any one of the constituent chain elements. An exception to this correlation might occur where copolymerization removes steric hindrances to planarity which are present in one of the homopolymers. Also if one of the chain elements interrupts electronic connectivity in the polymer backbone, the copolymer complex might have a higher conductivity than the homopolymer having these linkages. Although this relationship cannot be generalized, the correlation suggested by the data in Table 1 provides a useful guidance for synthetic efforts aimed at optimizing electrical conductivity. The importance of the homogeneity of the backbone cannot be over emphasized since chemical heterogeneity can yield carrier localization on the chain unit which provides the lowest potential for holes (or electrons in the case of donor doping). This has been confirmed by Bredas et al⁽¹¹⁾ quantum chemical calculations which demonstrate the link between the homogeneous character of the polymer backbone and the width of the highest occupied

π -band. The width of the π -bands can be related to the degree of delocalization of the π -system along the polymer backbone and to some extent to the mobility of the carriers in these bands. The Bredas calculations showed that the band width of the highest occupied band for poly(p-phenylenevinylene) is about 2.8 eV (ionisation potential 5.1 eV), while for the constitutive homogeneous polymers, polyacetylene and poly(p-phenylene), the values are 6.5 eV (I.P. 4.7 eV) and 3.5 eV (I.P. 5.6 eV) respectively.

Structure of 'Simple' Complexes: Dopants generally function as either simple electron acceptors or donors for polymer chains. For example the alkali metal doping of polyacetylene and poly(p-phenylene). It was also another Bredas calculation on undoped and lithium doped trans-polyacetylene that provided insight into the effect of polymer-dopant interaction on backbone geometry. Their calculations suggested that even modest charge transfer drastically alters chain geometry and as a result electronic structure, and therefore cast doubt on the detailed use of rigid band structure models in the study of polymer-doped interactions.

Crystallographic data on biphenyl⁽¹²⁾ and biphenyl radical anions^(13,14) has been used to estimate structure changes during doping of poly(p-phenylene) with alkali metals. These changes are in the direction depicted for an increased admixture of the quinoidal resonance form:



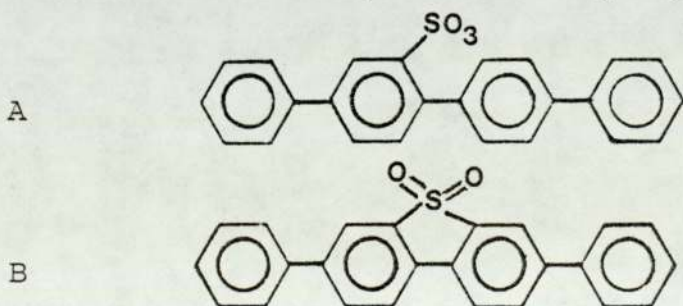
The bonds parallel to the chain direction (bonds 'a' and 'c') shorten and bonds inclined to this direction elongate in forming the biphenyl anion. While bonds 'a' and 'b' are nearly equal in the neutral species ('b'-'a' = 0.008 Å), the bonds differ by about 0.05 Å in the anion. Bonds 'b' and 'c' in the neutral species, which differ by about the same amount as do adjacent bonds in polyacetylene ('c'-'b' = 0.10 Å) become nearly equal in the anion ('c'-'b' = 0.008 Å). The biphenyl anion is non-planar in sodium triglyme complex and in a rubidium tetraglyme complex with rotation angles between phenyls are 7.2° and 9.4° as compared with 10.2° for the neutral species⁽¹²⁾. The anion is planar (or disordered) in potassium tetraglyme. Concentration of alkali metal in these biphenyl complexes (two phenyls per metal atom) nearly equals the highest observed sodium concentration in poly(p-phenylene), $(C_6H_4Na_{0.5})_x$ ⁽³⁾. By extrapolating the biphenyl results to poly(p-phenylene), it would be expected that the maximum bond-length difference in this polymer be approximately halved upon doping.

Halogen-doped polyacetylene also provides conducting systems that can be viewed as 'simple' charge-transfer complex. Raman, U.V., photoelectron and mass spectroscopy have all demonstrated the existence of I_3^- and I_5^- species for iodine-doped polyacetylene, Br_3^- for bromine-doped polyacetylene, and Cl_3^- for chlorine doped polyacetylene.

AsF_5 -doped poly(p-phenylene) is also another example of a 'simple' acceptor-doped charge-transfer complex. Hall coefficient measurements at high dopant level are consistent

with about one hole carrier per dopant molecule⁽⁴⁾. The only irreversible chemical modification that is observed on doping is an increase of molecular weight via para coupling of polymer chain ends and corresponding loss of hydrogen.

Covalent Bond Formation During Doping: Another important class of conducting polymers is comprised of those that undergo irreversible chemical modification during doping. In some cases this chemical modification provides a more extended conjugated structure, with corresponding reduction in ionisation potential and increase in π -band widths. In other cases this reaction interrupts conjugation and correspondingly limits conductivity of the complexes. The doping of polyphenylene with SO_3 from oleum provides an example where side reactions can occur to decrease the obtainable conductivity. I.R spectra of the polymer after doping suggested that there are three competing reactions. In the first case a conductive charge transfer complex is formed ($\sigma \approx 1 \text{ S cm}^{-1}$). This complex involves charge-transfer between a polymeric cationic species and a dopant anion. In the second case the SO_3 reacts directly with the polymer backbone to form a sulphonic acid group (A).



(Chemical modification of PPP induced by high temperature doping with SO_3)

The attachment of sulphonic acid groups leads to a soluble, non-conductive material. The third type of chemical modification (B) results after addition of a second SO_3 to an attached sulphonic acid group, followed by reaction with the neighbouring phenyl and liberation of H_2SO_4 .

Formation of Molecular Aggregates: There is hardly any experimental data available in the literature to show the relationship between electrical properties and supramolecular organisation. The enormous complexity of polymer structures poses the key problem. For example, the presence of folded, coiled or extended chains, segregated or non-segregated chain ends, intercrystallite tie molecules, and amorphous regions can affect microscopic electronic connectivity and the whole host of electronic properties.

Macroscopic d.c. conductivity measurements can be affected by such features, as well as by features which can occur from micro-to millimeter scales, such as spherulitic or fibre-like morphologies. All currently investigated polymers that can be doped to high conductivity levels are unfortunately, grossly inhomogeneous. Crystalline and amorphous regions of the undoped polymers can have different ionisation potentials, different electron affinities, different trap and scattering centre characteristics and concentration and different dopant diffusion coefficients. Likewise the equilibrium dopant concentration and the dopant concentration at which the semi-conductor-metal transition occurs can reasonably be expected to depend upon differing states of order in different regions of the polymer. The inhomogeneity

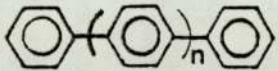
of the parent polymer could be replicated to a greater or lesser extent in the doped polymers. Measured properties would then be influenced by the composite structure. For example the often observed non-metallic temperature dependence of bulk d.c. conductivity for highly conducting doped polymers might commonly reflect the dominance of inter-phase and interparticle resistivities. There is generally an increase in conductivity for doped polymers with increasing perfection of the precursor polymer. However it is not true that three-dimensional crystallinity is a necessary prerequisite for obtaining highly conducting complexes ($\sigma > 10^{-2} \text{ Scm}^{-1}$). High-angle x-ray diffraction measurements indicate no significant long range three-dimensional order for AsF_5 doped poly(p-phenylene sulphide)^(8,15) despite the high conductivity observed (1 Scm^{-1}). Conductivity differences have been observed upon AsF_5 -doping of poly(p-phenylene) prepared with different synthetic methods, but no obvious correlation was made between conductivity and crystallinity of the precursor, undoped polymer. Comparable conductivity values have been obtained for the doping of either amorphous or crystalline poly(p-phenylene sulphide).

Areas of Application for Conducting Polymers: Although there still remain enormous potential areas for the application of conducting polymers, they have been employed successfully in low current circuitry systems, electromagnetic and electrostatic shieldings, batteries, stabilized electrodes, semiconductor devices and in solar cells, etc.

Perhaps the most important application of conducting polymer

systems to date is the use of poly(N-vinyl carbazole), PVK in the electroreprographic industry. In xerography, for instance, the surface of a drum, coated with a photoconductive material, is first uniformly charged by a corona and then exposed to a bright image of the item to be copied. Where the light falls, the charge leaks away to the underlying earthed, metal drum. The remaining charged, originally dark, areas are able to attract the dry ink or toner for transfer to the copy paper. Amorphous selenium used to be the photoconductive material on the drum, but now PVK is also used extensively. It has an added advantage in toughness and is easy to fabricate. PVK complexes are discussed further in Chapter (VI).

POLY (P-PHENYLENES) (PPP)

The polyphenyls comprise a series of hydrocarbons of the general formula $C_n H_{n-2(N-1)}$, where n is the number of carbon atoms and N is the number of phenyl nuclei. However, it is the aromatic hydrocarbons in the p-polyphenyl () series which have attracted considerable attention because of their good thermal stability, high melting points, insolubility, electronic configuration and their use as moderators in nuclear reactors.

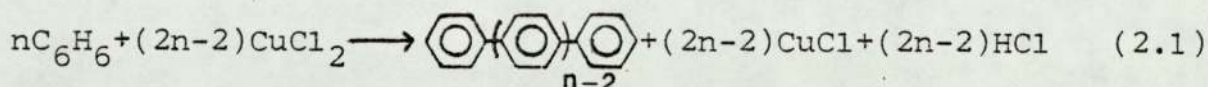
Previously, the individual, higher, isolable p-polyphenyls have usually been prepared by classical methods, such as Ullman coupling, the Fittig reaction, or Grignard synthesis. These routes however, suffer from one or more of the following limitations; very low yields, necessity for drastic conditions, tedious purifications, difficulties in reproducing results, multistep synthesis from the aromatic hydrocarbon precursor, and the formation of gross mixtures due to competing reactions. For example in the Ullman synthesis of p-sexiphenyl from 4-iodo-p-terphenyl and silver powder at 330°C, Pummerer and Bittner⁽¹⁶⁾ remarked on the difficulty of effecting condensation, and subsequently applied the method to a mixture of 4-iodobiphenyl, 4,4'-diiodobiphenyl and copper powder which provided a 25% yield based upon the iodo-aromatics⁽¹⁷⁾. In a modified version, Kuhn⁽¹⁸⁾ obtained p-sexiphenyl by zinc-acetic acid reduction of the product derived from 4,4'-diiodobiphenyl and copper.

Nozaki and co-workers⁽¹⁹⁾ also investigated the Ullman procedure with 4-iodo-p-terphenyl and reported a 10% yield based upon the p-terphenyl precursor in this multistep synthesis. In connection with their studies of p-polyphenyls and the corresponding methylated derivatives, Kern and Wirth⁽²⁰⁾ utilized the Ullman and Grignard reactions for preparative purposes. In addition the catalytic reduction of p-dibromobenzene in the presence of methanol afforded a gross mixture from which p-sexiphenyl was isolated in only 0.7% yield⁽²¹⁾. P-quarterphenyl was also conveniently prepared from 4-bromo or 4-iodo-biphenyl, magnesium, and cupric chloride by a method described by Krizewsky and Turner⁽²²⁾ for the production of biphenyl from magnesium phenyl halide. It has also been obtained by the pyrolysis of biphenyl; the yield however was very low, with a considerable formation of carbon, and the product contaminated with isomeric quaterphenyl and octaphenyl.

Poly(p-phenylenes) are however now available commercially due to an easy preparative route pioneered by Kovacic and co-workers⁽²³⁾. Marvel and Hartzell⁽²⁴⁾ were the first to obtain the impure polymer by the chloranil oxidation of poly-1,3-cyclohexadiene prepared by Ziegler polymerisation. It was however, the works of Kovacic et al⁽²³⁾ that constituted the first case wherein an aromatic monomer functioned in a well defined polymerization leading to homopolymer. They converted benzene to p-polyphenyl in Lewis acid-catalyst oxidant systems such as ferric chloride, molybdenum pentachloride and aluminium chloride-cupric chloride⁽²³⁾.

The C₆H₆-AlCl₃-CuCl₂ System According to Kovacic.

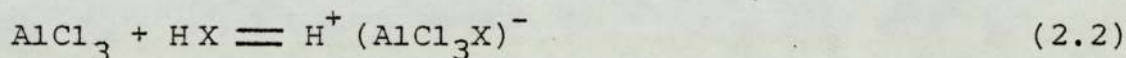
Poly(p-phenylenes) may be readily prepared by the treatment of benzene with aluminium chloride-cupric chloride under mild conditions according to Kovacic as shown by equation (2.1)



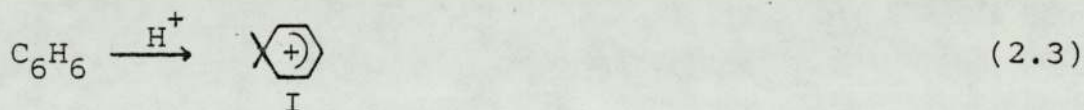
2.01 Mechanism of the Polymerization.

Initiation

Three modes of initiation have been proposed, namely cationic, radical cationic, and radical. The possible involvement of a sigma complex⁽²⁵⁾ is depicted in equations 2.2 and 2.3.



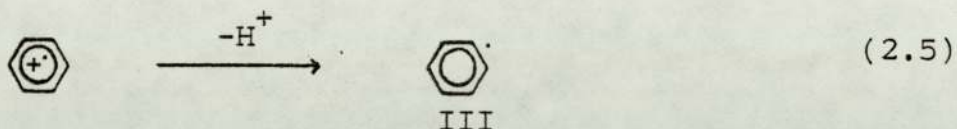
where X is a halogen.



This approach is analogous to that generally accepted for the cationic polymerisation of olefines catalysed by metal halides⁽²⁶⁾. The importance of the Lewis acid catalyst was demonstrated in the aluminium chloride-cupric chloride system by a control experiment⁽²⁷⁾. The possible intermediacy of radical cations was first advanced by Kovacic and Koch⁽²³⁾, and subsequently favoured by Mano and Alves⁽²⁸⁾. This pathway involves loss of an electron from the π -cloud of benzene (equation 2.4).



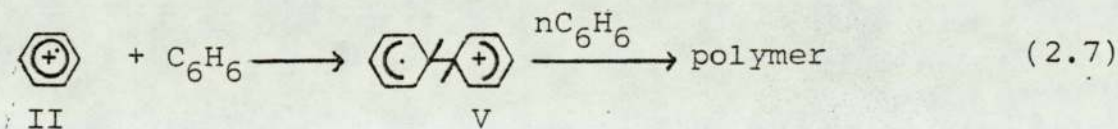
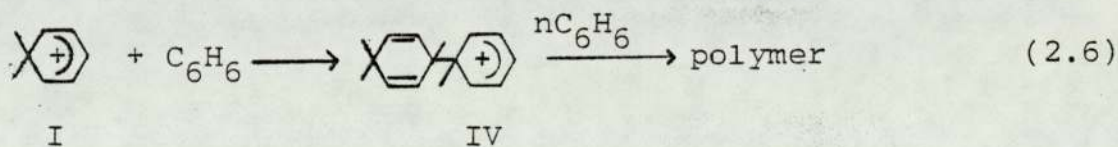
With $\text{AlCl}_3\text{-CuCl}_2$, the electron acceptor would be CuCl_2 or a $\text{CuCl}_2\text{-AlCl}_3$ complex. Of interest is the observation by Kuwana and co-workers⁽²⁹⁾ that electro-oxidation of benzene yields mixed polyphenylenes via a radical cation. Initiation by phenyl radicals obtained by deprotonation of initially formed radical cations was suggested by Mano and Alves⁽²⁸⁾ (equation 2.5).



Elimination of a ring proton from a radical cation in sufficiently basic media has been noted in the prior literature⁽²⁹⁾.

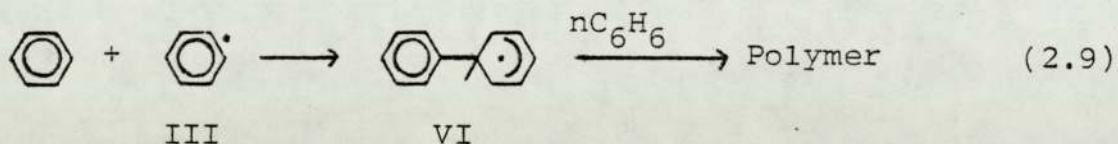
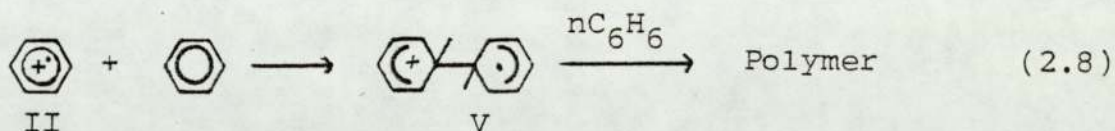
Propagation

Several modes of propagation for the benzene polymerisation by $\text{AlCl}_3\text{-CuCl}_2$ have been advanced by several investigators. Kovacic and co-workers proposed a cationic pathway which could involve either the Sigma Complex, I, or the radical cation, II⁽²⁷⁾, from the initiation step. Propagation by these moieties are shown in equations 2.6 and 2.7.



Further chain extension with 'V' is then believed to proceed via the positive end of the species.

In marked disagreement, Mano and Alves⁽²⁸⁾ proposed a different method of propagation entailing radical entities. Their concepts are depicted in equations 2.8 and 2.9.



Species II and III are obtained from the initiation step. Their mechanism entails the radical end of structure V as the propagating species.

Regardless of the polymerization mechanism, radical or cationic, one point of agreement^(25,28) is that propagation leads to structures, such as VII, which are subsequently oxidized to poly(p-phenylene).



VII

Kovacic and Kyriakis⁽²⁷⁾ noted that the exact stage at which rearomatization occurs is unknown. Presumably restoration of an aromatic nucleus at some point in VII, prevents reversal of the propagation step. Mano and Alves⁽²⁸⁾ concluded from their studies that rapid chain extension to VII occurs before appreciable oxidation.

Kovacic and Engstrom⁽³⁰⁾ carried out further work with the aim of determining whether a cationic or radical pathway was

involved in the propagation step in the polymerization of benzene. The work was based on the differences in reactivity of the propagating species with aromatic substrates containing substituents. Their key reference point comprised the known relative rates of reaction for radicals and electrophiles toward substituted aromatic nuclei. For example, the relative rates, 'K' haloarene / 'K' benzene in radical phenylation⁽³¹⁾ and cyclohexylation⁽³²⁾ increases from chlorobenzene, o - and p-dichlorobenzene, and 1,3,5 trichlorobenzene with the increase in degree of substitution. In contrast electrophilic substitution^(33,34) shows a decrease in relative rates as the number of chlorine substituents increases. It is for this reason that Kovacic and Engstrom carried out polymerisation of equimolar mixtures of benzene and haloarene under standard conditions. It was expected that a growing end which is radical in character would yield a polymer containing appreciable amounts of chlorinated monomer and the degree of incorporation in the copolymer would be predicted to increase in the order $C_6H_5Cl < o - \text{ and } p - C_6H_4Cl_2 < 1,3,5 - C_6H_3Cl_3$. If the propagating species is cationic, the resulting copolymer would be composed almost exclusively of benzene monomer, with relatively small quantities of haloarene, and the degree of participation would be expected to follow the trend, $1,3,5 - C_6H_3Cl_3 < o - \text{ and } p - C_6H_4Cl_2 < C_6H_5Cl$.

Poly(p-phenylene) prepared in neat benzene contains small amounts of chlorine (2.7 - 3.3%) as has been shown⁽³⁵⁾ by elemental analysis: C, 88.7-92.6%; H, 4.9-5.3%; and Cl, 1.6-4.8%. The polymer also contains about 14-16 phenyl units per

Cl atom and a C/(H+Cl) ratio of 1.46-1.51. It also shows characteristic infra-red band $\sim 804 \text{ cm}^{-1}$ indicative of para substitution. These data fit into a consistent pattern strongly supporting propagation by an electrophilic entity. Kovacic and Engstrom⁽³⁰⁾ found that analytical figures for the polymers obtained in their mixed system were very close to those for the product formed with benzene alone, indicating a strong preference by the growing end for the benzene monomer. Microanalysis and C/(H+Cl) ratios for the product formed in presence of o- and p- dichlorobenzene and 1,3,5-trichlorobenzene were virtually identical to those obtained from the poly(p-phenylene) produced in the standard polymerization (no haloarene) demonstrating that these highly deactivated aromatics are being incorporated in negligible quantities. These workers further observed that I.R. spectrum of poly(p-phenylene) (prepared from neat benzene) which exhibits the following absorptions: 695 and 765 cm^{-1} (monosubstitution from end groups), 804-807 cm^{-1} (strongest band, parasubstitution from the repeating units), 1000, 1400 and 1480 cm^{-1} were indistinguishable from spectra of polymer prepared in presence of haloarenes, and therefore verified the conclusions drawn from the microanalysis as to the identity and composition of the polymers.

2.02 The Oxygen Effect (Radical Trapping)

The use of scavengers, such as oxygen, to inhibit free-radical reactions in solution is well documented⁽³⁶⁻³⁸⁾. Most carbon radicals react rapidly with oxygen to yield peroxy radicals⁽³⁹⁾ which are relatively unreactive in

relation to the chain sequence. The combination of alkyl radicals with oxygen has been shown to occur with a rate constant of approximately 10^8 - 10^{10} l/mol-sec, approaching diffusion control⁽³⁷⁾. In the polymerization of styrene, interception occurs 2.5×10^5 times faster than chain propagation⁽³⁹⁾. If a species known to react rapidly with radicals affect the rate of reaction, it is a good indication that radicals are involved. Depending on the particular system and the fate of the peroxy radicals produced, such trapping of free radicals may result in rate retardation or complete inhibition. It is for this reason that Kovacic and Engstrom⁽³⁰⁾ studied the effect of O_2 on the polymerization system to strengthen their claim regarding the nature of the propagating species.

The effect of oxygen on the polymerization of benzene in the lewis acid - oxidant system has been determined principally by two sets of workers, but with conflicting results. Kovacic and Wu⁽⁴⁰⁾, using ferric chloride as a combined catalyst and oxidant, found no noticeable difference between polymerizations carried out under nitrogen and those performed with oxygen continuously bubbled through the reaction mixture. In sharp contrast, Mano and Alves⁽²⁸⁾ investigating the aluminium chloride-cupric chloride system, noted a retardation of the polymerization as a result of the presence of oxygen. The insensitivity of the ferric chloride system suggested therefore a characteristic of a non-radical propagating species, such as IV (equation 2.6) and the inhibition reported for the $AlCl_3$ - $CuCl_2$ was used to support the claim of an involvement of a cyclohexadienyl type

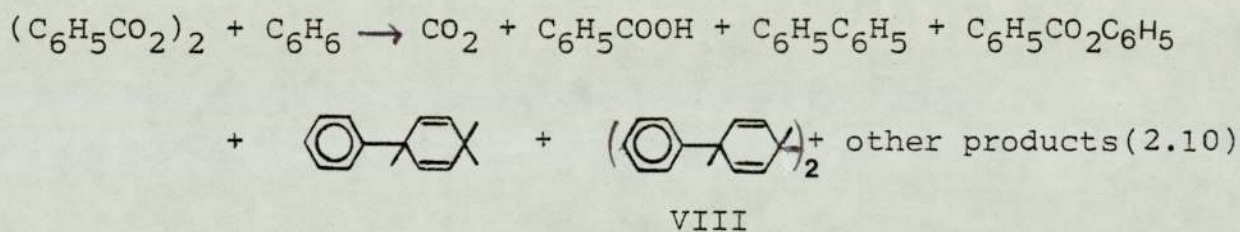
radical VI (equation 2.9) as the growing entity.

In order to gain further insight into the nature of the propagating moiety and to resolve the discrepancy, Kovacic and Engstrom⁽³⁰⁾ carried out a check on the findings of Mano and Alves by polymerizing benzene in a standard system under nitrogen and oxygen atmospheres. They monitored the progress of the reaction by titrating the evolved hydrogen chloride gas with standard caustic soda. The method was based on the stoichiometry of equation 2.1. They found a plot of hydrogen chloride gas evolved against time for the nitrogen run identical to the plot for the oxygen run. They also found a further evidence for the lack of participation by oxygen in the early stages of the reaction, where no retardation or inhibition was evident. Some types of chain terminators produce prolonged induction periods after which reaction proceeds at the uninhibited rate⁽³⁶⁾. In addition, they did not observe any significant decrease in product yield as compared with the 23% decrease from the presence of oxygen observed by Mano and Alves. Based on the negligible effect of oxygen on product yield and hydrogen chloride evolution in their work, Kovacic and Engstrom further suggested that it is unlikely that radicals are involved in the propagation as set forth by Mano and Alves. This data also supports their earlier conclusions from the ferric chloride reaction.

2.03 Decomposition of Benzoyl Peroxide in Benzene- Cupric Chloride

Kovacic and Engstrom went further and argued that if the

Mano-Alves mechanism was valid, then generation of phenyl radicals by alternate, unequivocal means in the presence of benzene and cupric chloride should give rise to poly(p-phenylene). Thermal decomposition of benzoyl peroxide in benzene has long been an important source of phenyl radicals which have been intensively studied in homolytic aromatic substitution^(31,39). The overall process in dilute benzene has been summarised according to equation (2.10) by De Tar and co-workers⁽⁴¹⁾.



The major products in the reaction being benzoic acid and biphenyl, together with a great deal of higher molecular weight material from which quarterphenyl and tetrahydro-quarterphenyls have been isolated in low yields. The biphenyl is obtained from the intermediate phenylcyclohexadienyl radical VI, identical to the proposed propagating species in the polymerization of benzene. The higher molecular weight material is the result of side reactions involving dimerization of VI.

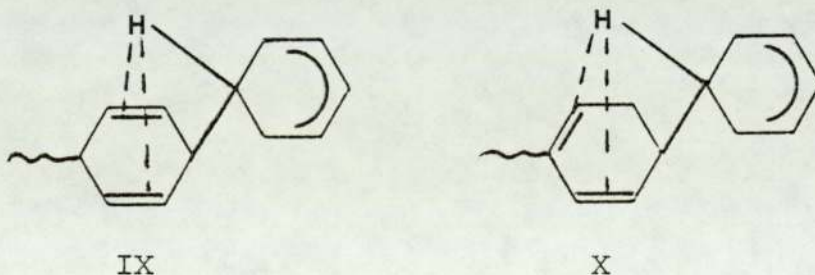
Decomposition of benzoyl peroxide in benzene with cupric-chloride was then performed by Kovacic and Engstrom. Their results indicated an increase in benzoic acid and biphenyl at the expense of the higher molecular weight dimerization products. In addition, no polyphenylene was detected in the small amount of residue obtained after work up. They there-

fore suggested that the absence of poly(p-phenylene) in the decomposition products was unexpected if VI was involved in propagation. The increase in biphenyl and the resultant disappearance of higher molecular weight products observed by Kovacic and Engstrom was attributed to oxidation of the intermediate phenylcyclohexadienyl radicals 'VI' by cupric chloride. They explained the effect of cupric chloride on their reaction by the well known behaviour of Cu(II) salts towards free radicals. Cupric ions have been shown to function as an efficient trap through oxidation of the intermediate radicals^(37,42,43). With certain carbon radicals cupric halides accomplish this primarily through ligand transfer resulting in excellent yields of halogenated substrates^(44,45) and this type of reaction has been determined⁽³⁶⁾ to occur extremely rapidly in the case of sec.-butyl radicals $k \sim 10^8$ l/mol sec. These workers concluded that the absence of poly(p-phenylenes) among the products in the presence of CuCl_2 sheds serious doubt on the ability of phenyl radicals to initiate the polymerization of benzene. Their result was further confirmed by the works of Hey and co-workers⁽⁴⁶⁾ on the thermal decomposition of benzoyl peroxide in benzene with cupric benzoate and copper bronze. The terminating effect of Cu(II) ion on intermediate 'VI' produced in dilute solution employed by Hey et al produced even more dramatic results. Biphenyl accounts nearly quantitatively for the phenyl radicals produced. It was also significant, they noted, that other oxidants employed in the Lewis acid-oxidant system display similar behaviour toward free-radicals. Ferric chloride, chloranil, benzoquinone and nitrogen-dioxide all function as oxidants leading to the

production of material resembling poly(p-phenylene).

It is now generally accepted from these findings that a radical species, as proposed by Mano and Alves, would be incapable of propagation in a system containing such efficient radical traps as cupric chloride, ferric chloride, p-benzoquinone, chloranil or nitrogen dioxide, since rapid termination would be expected. The designation of the polymerization as oxidative cationic is now most favoured.

A puzzling aspect though, of the proposed polymerization pathway (oxidative cationic) is that propagation occurs rather than rearomatization by proton loss. The rearomatization reaction is energetically favoured in almost 100% of the cases for simple aromatic substrates. Kovacic et al⁽⁴⁹⁾ suggested that a modifying feature may be the presence of electron density in the unsaturated ring adjacent to the complex. They examined a model of the propagating end (IX and X) which indicates stereochemical feasibility of interaction between the somewhat acidic Sp^3 hydrogen of the complex and the π -orbitals of the neighbouring diene.



Co-ordination in this manner could thus render loss of a proton more difficult.

2.04 Determination of Molecular Weight

The extreme insolubility of poly(p-phenylene) has made the determination of its accurate molecular weight almost impossible. Approximate determination of its molecular weight has however, been obtained from elemental analysis, I.R. spectroscopy, soluble derivatives and catalytically hydrogenated products.

Elemental analysis: Theoretically, the data from elemental analysis could provide information pertinent to the molecular weight problem. For example the C/H atomic ratio varies from 1.285 for p-terphenyl to a limiting value of 1.5 for an infinitely long poly(p-phenylene) chain. Practically, this approach has serious limitations, considering that a polyphenylene of quite low molecular weight ($n = 20$) possesses a C/H value = 1.46 which is experimentally indistinguishable from the limiting value. This approach is further complicated by the fact that all polyphenylenes contain chlorine usually in small amounts and therefore, the C/H ratio for the parent hydrocarbon is better obtained from the expression $C/(H + Cl)$, assuming that chlorine is introduced by replacement of hydrogen.

I.R. Spectroscopic analysis: Approximate indications of relative molecular weights in the polyphenylene series have been obtained from the ratio of intensity (para band) to intensity (mono band) in their I.R. spectra. The oligo - and polyphenylenes exhibit characteristic I.R. absorptions corresponding to parasubstitution ($800-840\text{ cm}^{-1}$, arising from

internal phenylene rings) and monosubstitution ($730-770\text{ cm}^{-1}$ and $690-710\text{ cm}^{-1}$, arising from the end phenyl units). Quantitative analysis (base line technique)^(47,48) of the absorption values for the para and mono bands of quaterphenyl, quinquephenyl and sexiphenyl yielded a linear relationship between the ratio of para/ $(\Sigma\text{ mono})$ and the number of rings. As the molecular weight increases, this ratio becomes larger. A regression analysis of the data for the first three compounds (quarterphenyl, quinquephenyl and sexiphenyl) produced a value of '9' rings for poly(p-phenylene), which is in good agreement with the average value ($n=8$) observed from GPC of hydrogenated PPP and slightly more than one-half the 'n' value determined for alkylated PPP⁽⁴⁹⁾. Caution must however, be exercised in interpreting the I.R. data. From elemental analysis⁽³⁵⁾, chlorine (1-2%) and oxygen (1-2%) are known to be present in PPP prepared by standard methods. Substitution along the polymer backbone would alter the infrared spectrum, decreasing the intensity of the para band relative to the mono bands. There is also the possibility of the presence of non-aromatic rings in the polymer chain. Structural irregularities such as p-quinoid or cyclohexadiene units, arising from incomplete oxidation have been used to rationalize the brown colour⁽⁴⁸⁾. The interruption of conjugation would have an effect on the spectral results and therefore the values of 'n' obtained from I.R. data should probably be considered at least a lower limit for the degree of polymerisation. Also, the position of the para band in oligo(p-phenylenes) is known to shift to a lower wave number as the number of units increases in the p-poly(p-phenylene) series⁽²⁷⁾ and the shift is also known to decrease with

increasing molecular weight. The shift in the para band position provide a reasonable comparison of the lower molecular weight polymers and PPP which differ widely in molecular weight.

Soluble derivatives: Sulphonated derivative of PPP for molecular weight determination was first attempted by Kovacic and co-workers⁽⁴⁹⁾ but the undesirable features of drastic reaction conditions (concentrated H_2SO_4 at $264^\circ C$ for 24 hours) and the presence of both highly polar and non-polar moieties in the end product induced them to pursue an alternate course, namely Friedel-Crafts alkylation.

The solubility of the alkylated polymer is enhanced for two reasons: a decrease in the regularity (non-planarity of the nuclei and presence of side chains) and introduction of solubilizing alkyl moieties.

2.05 Alkylation of Poly(p-Phenylene)

Kovacic and co-workers carried out a successful alkylation of the polymer with n-propyl bromide, n-propyl chloride and isopropyl bromide. They also unsuccessfully attempted to alkylate the polymer with ethyl bromide, n-butyl bromide, 4-methyl-1-pentene and 4-methyl-2-bromopentene.

n-propyl bromide or n-propyl chloride alkylation⁽⁴⁹⁾: In this method, crude PPP (3-5 g) was placed in a 100 ml, three-necked, round-bottomed flask equipped with thermometer and condenser with $CaCl_2$ drying tube. Excess n-propyl halide

(50 ml) was added with stirring, and the suspension was heated to reflux (46°C for chloride, 66°C for bromide) for 24 hours. After addition of 18% HCl (50 ml), the mixture was filtered to yield a black, tarry mass. Repeated extraction with acetone provides a light golden-tan powder which was then treated with boiling 18% HCl and boiling water. The solid was then dried overnight at 110°C . A typically recovered weight is 300%. The material does not melt at elevated temperatures. Infrared spectrum of the sample (KBr pellet) indicates absorptions at 2950, 1450, 1360 (gem-dimethyl), 1060 and 890 cm^{-1} . The diffuse reflectance visible spectrum had a λ_{max} 360 nm.

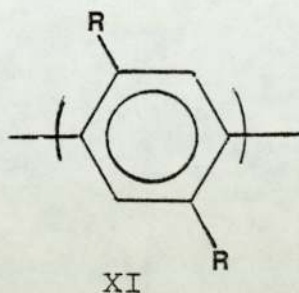
Calculated elemental analysis for $(\text{C}_{18}\text{H}_{28})_n$: C, 88.52%; H, 11.48%.

Found: C, 88.68%; H, 9.79%.

Isopropyl bromide alkylation:⁽⁴⁹⁾ In this method, purified PPP (0.08 g) and anhydrous AlCl_3 (1.5 g) were placed in a three-necked round-bottomed flask equipped with thermometer and condenser with CaCl_2 drying tube. Excess isopropyl bromide (20 ml) was added with stirring, and the suspension was heated at reflux (59°C) for 24 hours. Work up as in the preceding sections, yielded 0.14 g (172% recovered weight) of light brown powder. The I.R. spectrum (KBr pellet) of the product exhibited bands at 1950, 1460, 1360, 1060, 875 and 805 cm^{-1} .

Calculated elemental analysis for $(\text{C}_{21}\text{H}_{26})_n$: C, 90.65%; H, 9.35%. Found : C, 90.15%; H, 9.23%.

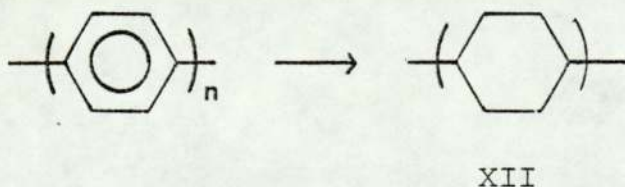
These I.R. spectral studies of the alkylated polymers suggest the structure 'XI' with the occurrence of



disubstitution on opposite sides of the ring. Substitution beyond the stage shown in XI was considered unlikely. Steric hindrance to nuclear attack on XI by another alkyl moiety would be great. Also by analogy, according to prior investigations, alkylation of p-xylene with alkenes under a variety of conditions yielded mono and dialkylated material, but no tri or tetra alkylated derivatives⁽⁵⁰⁾. Kovacic et al then determined the number average molecular weight ' \bar{M}_n ' of their alkylated polymer (XI) by vapour phase osmometry and found a value of 3755. This corresponded to an average of 15 aromatic units.

2.06 Catalytic Hydrogenation of Poly(P-Phenylene)

Kovacic and Durham⁽⁵¹⁾ carried out the catalytic hydrogenation of PPP, thereby forming a completely reduced, soluble product containing 1,4-cyclohexylene (1,4-cyclohexadienyl) (XII) units.



The following method was adapted by these workers for the catalytic hydrogenation.

A 500 ml rocker-type high-pressure 'parn' bomb was charged with the polymer (1 g), catalyst (or polymer with deposited catalyst), cyclohexane (150 ml), and glass beads to aid in mixing. After hydrogen was introduced to the desired pressure the bomb was rocked at 193-200^o to ensure thorough mixing. After the reaction, the mixture was filtered, and the solid was washed well with the solvent used in the reduction. Further extraction of the insoluble material with hot benzene gave negligible amounts of soluble product. The combined dried cyclohexane filtrate was freed of solvent under reduced pressure. The residue was dissolved in the minimum amount of benzene at room temperature and then precipitated by addition of methanol. After the suspension was centrifuged and the liquid decanted, the procedure was repeated five times. The resultant white powder was dried under vacuum overnight. The product softened slightly at 135^oC and melted at 180-210^oC.

Calculated elemental analysis for $(C_6H_{10})_n$: C, 87.7%; H, 12.29%. Found: C, 85.04%; H, 12.22%.

Molecular weight determination of the hydrogenated polymer 'XII' using Waters gel-permeation chromatograph (model 200) equipped with three Styrogel Columns (900, 400, 45 \AA) and employing perhydro-p-sexiphenyl (0.1% in THF) as standard demonstrated that the average number of cyclohexane units per chain was 7.5, with a maximum of 16 and a minimum of 4.

These workers also ran a gas chromatography of crude 'XII' (6 ft x $\frac{1}{4}$ in column, 30% SE-30 on 45-60 mesh chromosorb W(AW), 190°C, 48 ml/min) and observed the presence of a small amount of dicyclohexyl (retention time, 9.0 min) and a higher molecular weight component (retention time 11.5 min). These results compare favourably with the data obtained from the vapour phase osmometry.

Although the molecular weight of poly(p-phenylene) remains unknown, the study of the alkylated and hydrogenated polymers by Kovacic and co-workers has shown that the polymer contains chains at least 16 phenyl units in length.

2.07 Control of Molecular Weight (Solvent effect)

The molecular weight of PPP prepared by reaction of benzene with $\text{AlCl}_3\text{-CuCl}_2$ in different kinds of solvent was found to vary with the nature of solvent, concentration of solution and to some extent the reaction temperature. Kovacic and Li-Chen HSU⁽⁴⁸⁾ carried out a detailed study of such effects. They found a good agreement among solubility, infrared and reflectance analysis in relation to the relative changes in molecular weight. They noted the following extremes: Solubility in chloroform (2.2-20%), infrared para-band position ($801\text{-}804\text{ cm}^{-1}$) and reflectance λ_{max} ($395\text{-}385\text{ cm}^{-1}$). They also found the following order of effectiveness of the solvents in reducing molecular weight: $o\text{-C}_6\text{H}_4\text{Cl}_2 > 1,2,4\text{-C}_6\text{H}_3\text{Cl}_3 > p\text{-C}_6\text{H}_4\text{Cl}_2 > \text{TiCl}_4 > \text{SnCl}_4 > \text{C}_6\text{H}_6$.

A good correlation has also been found to exist between

increasing dielectric constant and increasing effectiveness of solvent in decreasing molecular weight. The following order of effectiveness in reducing molecular weight was observed: $o\text{-C}_6\text{H}_4\text{Cl}_2 > 1,2,4\text{-C}_6\text{H}_3\text{Cl}_3 > \text{SnCl}_4 > \text{CS}_2 > \text{C}_6\text{H}_6$ which have dielectric constants of 7.5, 3.98, 2.87, 2.64 and 2.28 respectively. A further rationalisation of the effect of aromatic solvents on polymerisation was also attempted using the observation that ' π ' and ' n ' complexes⁽⁵³⁾ might so deactivate the growing end that the rate of propagation decreases and termination by proton loss assumes a more favoured status.

2.08 The Lewis Acid - Catalyst-Oxidant Systems:

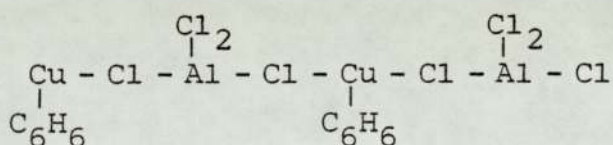
Having established the process, Kovacic and Hsu⁽⁴⁸⁾ proceeded with a series of investigations to define the scope of benzene polymerization in the system benzene-Lewis acid catalyst oxidant. In particular, they carried out an exhaustive study of the reactions, benzene- AlCl_3 - CuCl_2 to determine the effect of water, cuprous chloride and the variation in catalyst-oxidant ratio on polymer yield. In a previous investigation by Kovacic and Wu⁽⁴⁰⁾ evidence was found in benzene-ferric chloride reactions for co-catalysis by Bronsted acids such as water, acetic acid and nitro ethane. Bearing this observation in mind, Kovacic and Hsu undertook an investigation of water as a potential co-catalyst in the AlCl_3 - CuCl_2 system. They observed that polymer yield varied inversely with the amount of water added to the system and suggested a rather plausible interpretation for their observation. This involves the destruction of aluminium

chloride by hydrolysis on the assumption that large quantities of catalysts were required for high yields. Another suggestion was that some water was consumed in a chain termination reaction which was in keeping with the small amounts of oxygen in the polymers. However, there was no simple correlation which was apparent entailing oxygen content and the amount of added water.

AlCl₃-CuCl₂ molar ratio: These workers also investigated the effect of variation in AlCl₃-CuCl₂ molar ratio at 30-32°C for 2 hours and found that polymer yield rose rapidly with increasing molar ratio, reached a maximum at 2:1 and then remained constant. This observation prompted them to ask the question; why the necessity for large quantities of catalyst? To find an answer to this question, they examined the influence of initially added cuprous chloride to the system and found very strikingly, no essential polymerization occurred even at reflux temperature when cuprous chloride and aluminium chloride were used in equimolar ratio. They also found that at a CuCl₂-AlCl₃ molar ratio of 1:2 the yield was 39% and closely corresponded with a 35% yield obtained with half this amount of aluminium chloride in the absence of added cuprous chloride. These findings led them to suggest that cuprous chloride generated during the course of the C₆H₆-AlCl₃-CuCl₂ reaction acts as a powerful inhibitor by associating with aluminium chloride. The union apparently results in a 1:1 complex which contains the aluminium chloride in a catalytically inactive form. An examination of benzene filtrate of the reaction mixture by the addition of water to the dark green solution produced an exothermic

reaction resulting in evolution of acid fumes and precipitation of copious quantities of cuprous chloride. They suggested that since the salt itself is very insoluble in benzene, their observation compellingly argues for the presence of cuprous chloride in complex form. They obtained confirmation from solubility measurements on cuprous chloride and aluminium chloride individually (which were found to be only slightly soluble < 3% in benzene) while a mixture containing equimolar quantities of the two salts dissolved almost completely at room temperature with the formation of a yellow solution.

A further evidence for this complex formation was provided by Amma and Turner⁽⁵²⁾ in a detailed x-ray analysis which revealed that the compound was formed in the ratio $C_6H_6-CuCl-AlCl_3$ 1:1:1 and possessed the structure 'XIII'.



XIII

Kovacic and co-workers also observed that the polymerization reaction was characterised by induction periods varying from 15 to 25 minutes when carried out in the absence of added water. However, cuprous chloride virtually eliminated the induction period when introduced in the ratio $CuCl-AlCl_3$ 1:2. Thus cuprous chloride may function both as an inhibitor and a promotor, and although the precise nature of the promoting action is unknown, several conjectures were considered; among which include:-

- i) the cuprous chloride might be an efficient catalyst at some stage in the reaction sequence; and
- ii) that a cuprous-cupric complex comprises the actual dehydrogenating agent.

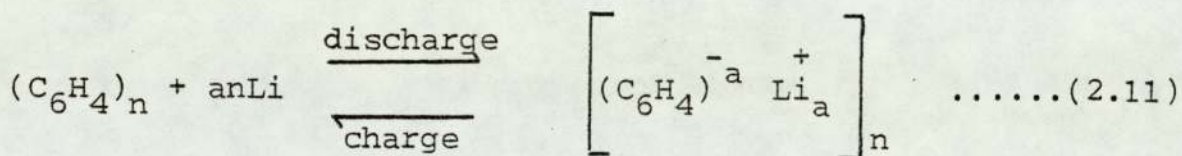
2.09 Solid State Polymerisation

Recently, Baughman et al⁽⁵⁷⁾ discovered a novel method for the preparation of highly conducting poly(p-phenylene). The method involved the simultaneous solid state polymerisation and doping of p-phenylene oligomers (p-terphenyl, p-quarterphenyl, p-quinquephenyl and p-hexaphenyl) by a prolonged exposure of their AsF_5 -complexes to 400 torr AsF_5 . This lead to a highly conducting charge transfer complex. The polymer material prepared in this way, when compensated with $(\text{CH}_3)_2\text{OH}$ and annealed to remove residual oligomer resulted in a highly crystalline polymer. The x-ray diffraction studies of the annealed material unambiguously indicate poly(p-phenylene). The discovery of the solid state polymerisation in presence of AsF_5 is particularly significant because it allows the use of the highly processible p-phenylene oligomer as precursors to the insoluble, infusible poly(p-phenylene). In this way, thin conducting films of metallic poly(p-phenylene) can be prepared directly from films of the oligomers, which have in turn been deposited from the vapour phase or from solution. Alternatively chain-oriented poly(p-phenylene) can be produced by reacting single crystals or epitaxially grown films of the oligomer with AsF_5 . Single crystal plates of terphenyl have been reacted with AsF_5 to form oriented poly(p-phenylene)

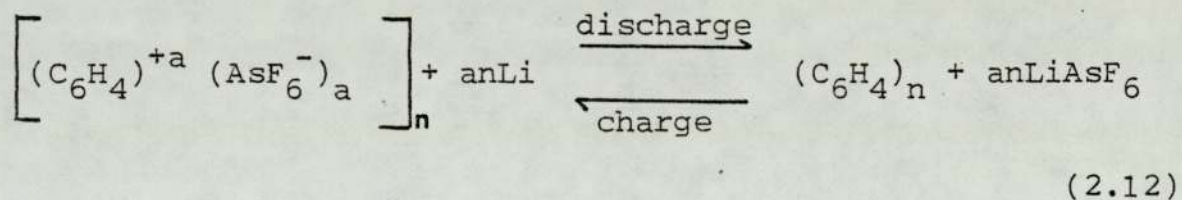
complexed with AsF_5 . The oriented complex has been shown to be optically polarizing and exhibits a strong conductivity anisotropy.

2.10 PPP-Charge Transfer Complex and Electrical Conductivity

Poly(p-phenylene) prepared by the Kovacic method is a good insulator ($\sigma \ll 10^{-2} \text{ S cm}^{-1}$). However, doping of the polymer with AsF_5 , NOBF_4 and lithium naphthalide increases its conductivity markedly, and conductivities over 10^4 S m^{-1} for doped polymer has been measured⁽³⁾. The increase in conductivity is due to the ability of PPP to form complexes with both 'n' and p-type dopants. It has been shown that the conductivity of the 'pre-doped' polymer can further be increased by electrochemical doping⁽⁵⁴⁾. For acceptor doping, the polymer electrode was maintained at a positive potential with respect to a platinum counter electrode in an electrochemical cell. For example doping with PF_6^- was accomplished from a 0.5 m solution of tetraethylammonium hexafluorophosphate in rigorously dried propylene carbonate. Conductivities of 50 S cm^{-1} has been obtained in this manner with dopant PF_6^- . Donor doping with lithium has also been done by employing a counter electrode of lithium in a 0.5 m solution of lithium perchlorate in THF. The configuration itself being an electrochemical cell and doping proceeds spontaneously when electrons are allowed to flow from the lithium to the polymer through an external circuit. The doping process corresponds to the discharge of the cell as shown in equation (2.11).



Baughman et al⁽⁵⁷⁾ observed that the stoichiometry 'a' in equation (2.11) given for discharge varied from 0 to 0.5, and that the cell has a rather low open circuit voltage with a discharge characteristic extending from ca 0.9 to ca 0.4 V. The major portion of the discharge plateau was between 0.6 and 0.4 V. These workers further obtained a much higher voltage cell by combining an acceptor-doped polyphenylene cathode with a lithium anode in an electrolyte composed of 1 m LiAsF₆ in a propylene carbonate. The cell reaction proceeds according to equation (2.12) where they observed electrochemical doping levels up to a = 0.10.



During charge, the PPP was oxidised and the AsF₆⁻ anions from the electrolyte enter the polymer to provide counter ions for the positively charged polymeric cation. During discharge these ions diffuse back into the electrolyte. Cells using the salts LiBF₄, LiPF₆ and LiAsF₆ have been constructed by Baughman and co-workers⁽⁵⁷⁾ and each displayed approximately the same open circuit voltage (OCV) vs lithium, 4.4 V, for a charge level corresponding to a=0.10. These workers also constructed cells with alkali-metal doped PPP as an anode and acceptor-doped PPP as a cathode and observed an open circuit voltage of ca. 3.3 V.

Although solvent compatibility is still a problem area and obviously requires further investigations, batteries employing poly(p-phenylene) electrodes have been shown to have a great potential since doped PPP exhibits many of the attributes of the ideal electrode: high electronic conductivity, high ionic mobility, insolubility, structural integrity and high voltage.

EXPERIMENTAL METHODS

3.01 Introduction

The measurement of dielectric permittivity and electrically induced optical birefringence (Kerr effect) forms the main basis of this work. The apparatus and techniques employed to facilitate these measurements are described in this chapter.

The phenomenon of electrical double-refraction discovered by John Kerr whilst studying glasses is known as the electro-optical Kerr effect. If a transparent isotropic substance is placed in a uniform static electric field it becomes optically anisotropic and doubly refracting. In liquids this is due to the orientation and polarisation of the molecules brought about by coupling of the electric field with their induced and permanent dipole moments. Although the tendency to orientate in the applied electric field is opposed by thermal motions, a steady state will exist for a given temperature and electric field strength. If the molecules are not perfectly symmetrical, a difference in the velocity of light and hence refractive index in the directions parallel and perpendicular to the electric field will be observed. Thus, if a molecule is electrically anisotropic at low frequencies, then it usually follows that the molecule will exhibit optical anisotropy. A more detailed description of the theory is given in Appendix 1.

The measurement and interpretation of the anisotropy of polarizability which is sensitively dependent on bond type, molecular structure, conformation and morphology (for solids) forms the analytical basis of the electro-optical Kerr effect.

Gans⁽⁵⁸⁾ was the first to realise the relationship between Kerr constant and the magnitude of the optical anisotropy of a molecule. His discovery then led to the first use of the Kerr effect as a powerful investigative technique for molecular behaviour. Since then, equations relating macroscopic phenomena of refractivity, light scattering, dielectric polarization to molecular properties have been developed^(59,60). The Kerr effect is now used widely in the study of macromolecules.

Static dielectric permittivity measurements on the other hand are less complicated than the Kerr effect and are used extensively for calculating dipole moments of molecules in the investigation of molecular structures. It is a useful technique for the study of polymeric materials, but is often difficult to interpret because of the large number of conformations which can be adopted by polymer molecules.

3.02 The Kerr Effect Apparatus

The molar Kerr constant of a substance may be visualised as the difference in molecular refraction for directions, E , in the parallel and perpendicular to a unit electric field in the substance. The quantity that is of interest is the experimen-

tal Kerr constant B, defined simply by the equation:

$$B = \frac{n_p - n_s}{E^2 \lambda} = \frac{\delta}{2\pi l E^2} \quad (3.1)$$

where n_p and n_s are the refractive indices for the component of the light in the medium parallel and perpendicular to the electric field E, λ is the wavelength of light, l is the optical pathlength and δ is the phase difference between components of light parallel and perpendicular to E.

The Kerr effect apparatus was designed to measure the Kerr constant B of non-conducting liquid system by application of rectangular-shaped high voltage pulses of short duration across liquid samples. The diagram of the apparatus used to measure the electrically-induced phase difference, δ , is shown in Figure 3.1. A parallel plane-polarized beam of monochromatic light is passed through the Kerr cell such that the plane of polarization of the light is at an angle of 45° relative to the direction of the applied electric field. In the presence of this electric field the light leaving the cell is generally elliptically polarized. After passing through a quarter-wave retarder (de Senarmont compensator) orientated with its principal optical axis at 45° to the direction of the applied electric field, the light is transformed into plane polarized light which can be extinguished by rotating the analyser. The angular difference, α , between the principal planes of the polarizer and the analyser is then equal to $\delta/4$ provided that the electric field is applied as a rectangular pulse (cf $\delta/2$ if a d.c. electric field is used).

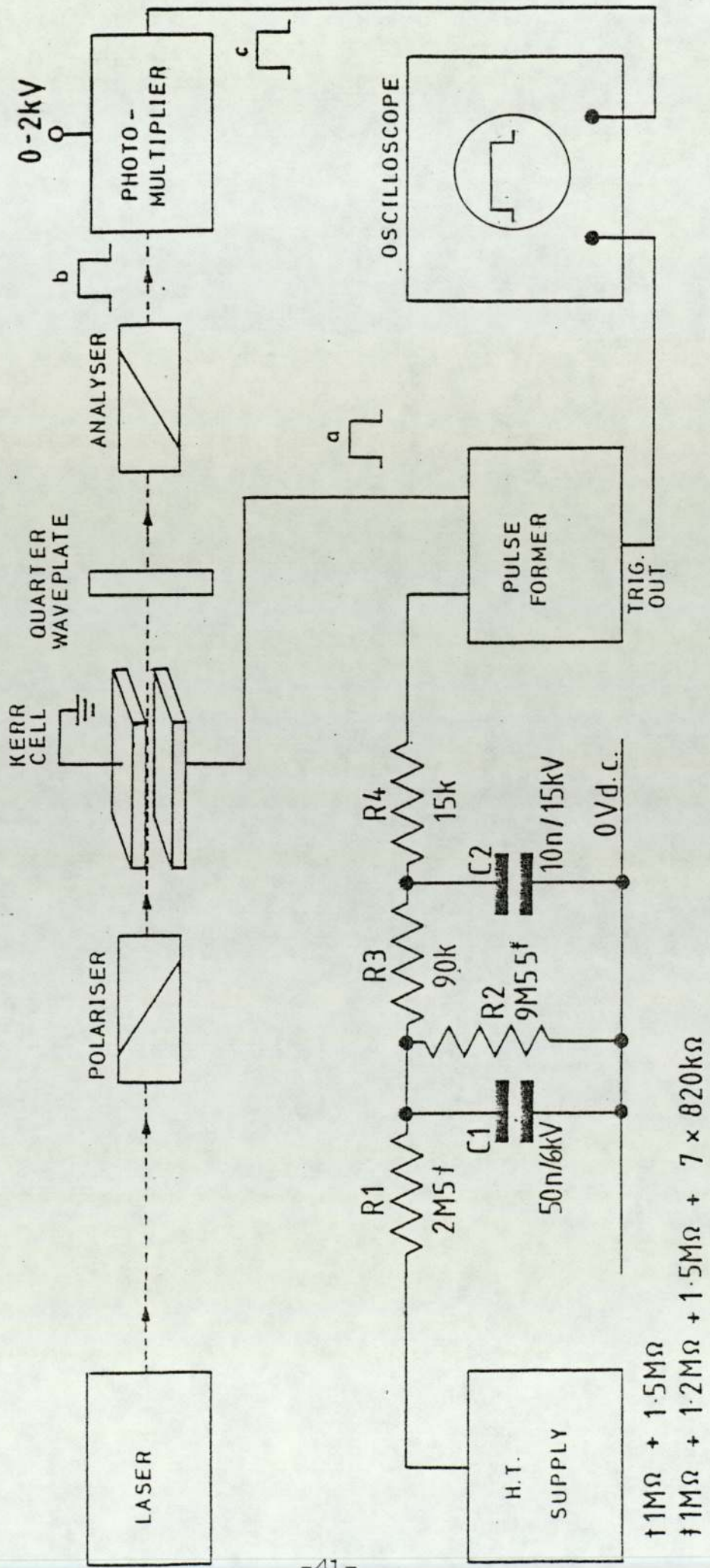
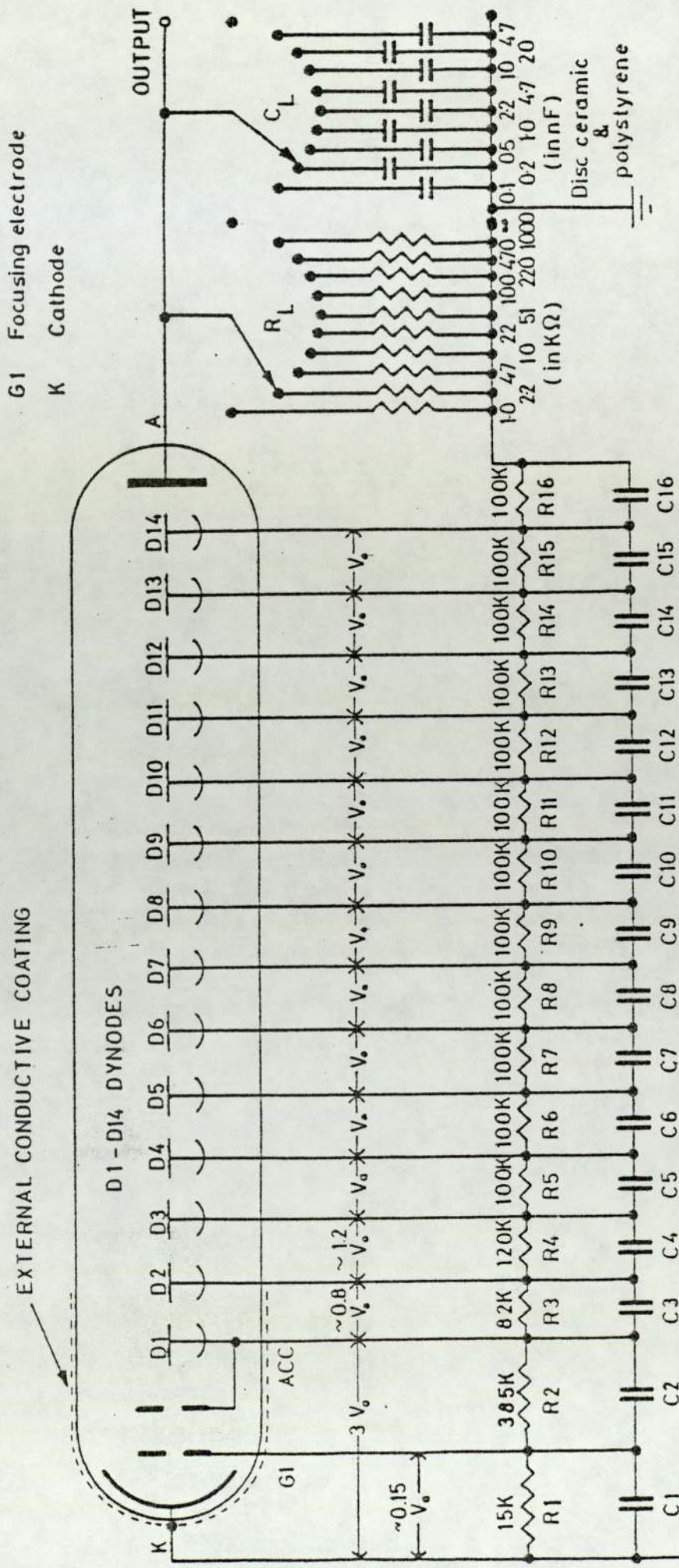


Figure 3.1 Apparatus used to measure the electrically induced phase difference, δ .

Two light sources were used. One was a 2.6 mW helium-neon laser (Scientifica and Cook, model SLH/2) emitting at a wavelength of 632.8 nm. A second He/Ne laser from the same manufacturer was also used. It emitted light at the same wavelength as the former but it was more powerful (~ 10 mW) and gave a brighter beam of light. It was therefore, mostly used in this work. The plane of polarization of the light emitted from these laser sources was horizontal. The degree of polarization of the light entering the Kerr cell was improved by passing the beam through a high quality polarizer. Both the polarizer and analyser were Glan-type prisms (Ealing Beck Ltd.) mounted in brass tubes. The analyser could be rotated by means of a series of gears connected to a graduated disc which allowed rotations as small as 0.005 degrees to be read with an accuracy of ± 0.002 degrees. The quarter-wave retarder was cleaved from mica (F. Wiggins and Sons Ltd.), used at 632.8 nm and mounted between glass discs.

Changes in levels of light were detected by a photomultiplier. The output of the photomultiplier was connected to an oscilloscope (Tektronix Inc., type 465B) thus enabling the electrically-induced optical pulse to be effectively displayed. The electrical configuration of the electrodes of the photomultiplier tube (E.M.I. 9816B) is shown in Figure 3.2 and is recommended by the manufacturer for high gain use. A quanta of light impinging upon the semi-transparent caesium-antimony photo cathode, K, causes the emission of an electron. After being focused and accelerated this electron gives rise to an avalanche of electrons along the dynode chain, d_1-d_{14} . The resulting electrical photo-

- A Anode
- ACC Accelerating electrode
- G1 Focusing electrode
- K Cathode



C1-C16 DISC CERAMIC 10F/750Vdc.

010 - 2kVdc.

Figure 3:2 Electrical configuration of the electrodes of the photomultiplier tube.

induced current is collected at the anode, A., and converted into a voltage drop across the anode load resistor, R_L . The extent of the gain and/or smoothing of the output from the photomultiplier tube may be adjusted by changing the values of R_L and C_L , respectively. A Brandenberg model 472R power pack was used to supply the high-tension voltage which was continuously variable in the range 0-2 kV.

3.03 Optical Alignment

In optical systems, light is lost due to reflection and refractions from the optical components. Such loss of light increases with any misalignment of the optical components and would consequently reduce the signal/noise ratio. It is therefore important to properly align the optical components of the Kerr apparatus to minimise scattering and to prevent the hindrance of light beam passing through the Kerr cell and other components to the photomultiplier tube. Deformations of the photocurrent pulses from a rectangular shape are usually observed when there is an improper position of light beam between the electrodes in the Kerr cell. The lateral position of the Kerr cell containing the electrodes and liquid sample was achieved by fine adjustment of a transverse mechanism while observing the image of the light beam on a paper screen was judged to be satisfactory (a single circular spot of uniform intensity). The screen was also placed between the analyser and the photomultiplier in order to observe the quality of the extinction of the image when the polarizers are crossed. A non-extinction of the image would usually indicate the presence of a mechanically-induced

optical strain due to overtightening of securing screws in the windows of the cell. The light beam could also be moved vertically as desired by means of adjusting screws on the laser mounting.

3.04 High-Voltage Pulse Former

A rectangular-shaped pulse of high voltage is applied to the electrodes of the Kerr cell using the pulse former circuit shown in Figure 3.3. Only the essential aspects are given here. For a more detailed description of the circuit and its operation the reader is referred to reference (61).

The pulseformer can be operated in one of two modes. In the first mode (S_1 closed) a relaxation oscillator based on a unijunction transistor, resistor R_1 and capacitor C_1 provides an accurately timed sequence of narrow pulse which triggers a monostable (Timer 1). The output of Timer 1 is a rectangular pulse of duration $T_2 - T_1$ determined by R_2 and C_2 . The leading edge of this pulse triggers a second monostable (Timer 2) which energises a solenoid to close a high-voltage reed switch S_3 at time T_1 . This action applies a high voltage to the Kerr cell. The trailing edge of the pulse output from Timer 1 triggers a third monostable (Timer 3), the output of which closes a second reed switch, S_4 , at time T_2 . This action shorts the high voltage of the Kerr cell to ground. The on-time of Timer 2 is not very important provided that R_3 and C_3 are chosen so that the duration of the output exceeds the longest time ($T_2 - T_1$) set by the variable resistor R_2 and C_2 . The output of Timer 3 after

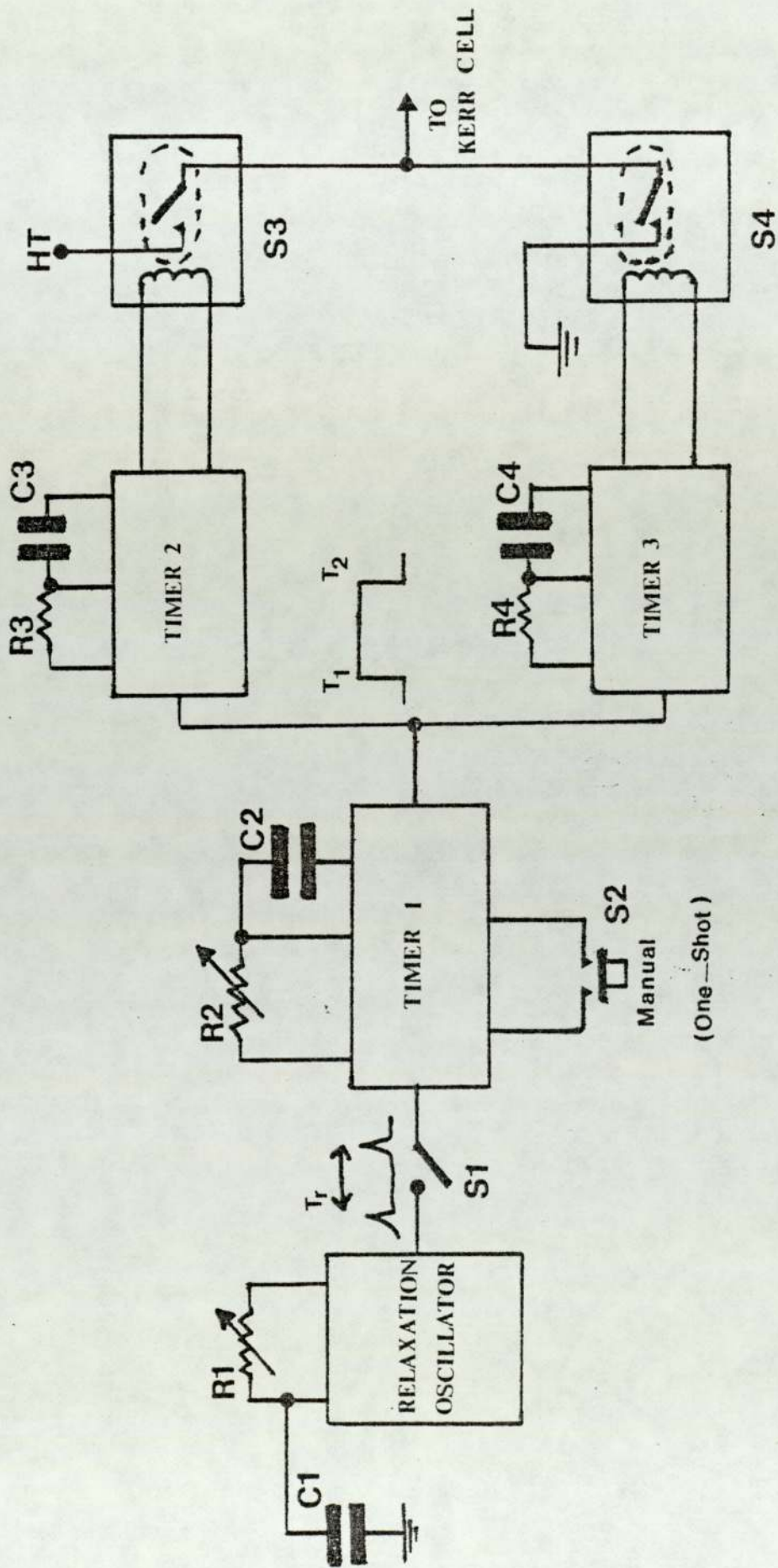


Figure 3.3 Circuit diagram for the high voltage pulse former

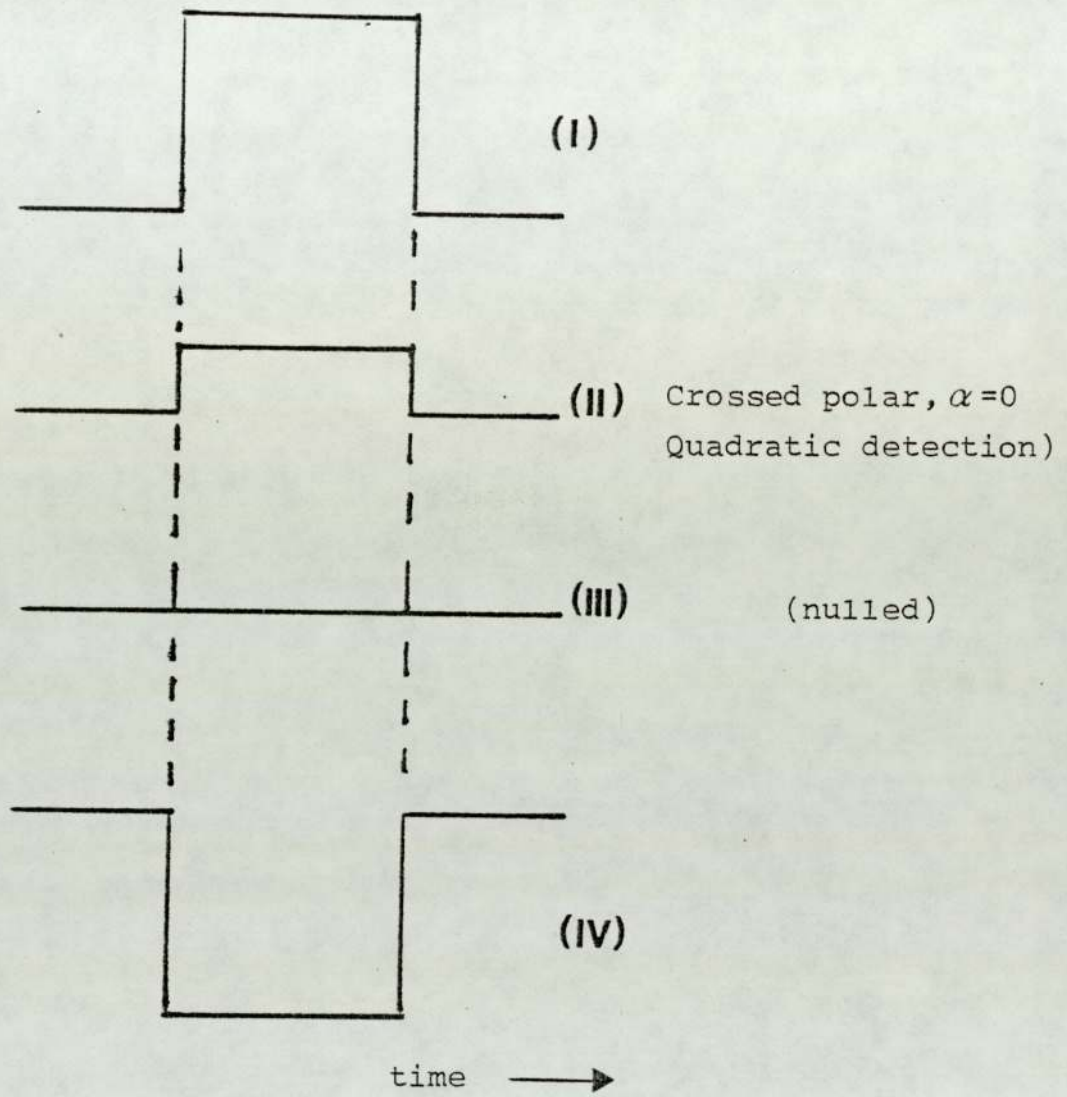


Figure 3.4 Rectangular-shaped pulse as displayed on the oscilloscope

triggering must be held for a time sufficient to ensure that the high voltage electrodes are completely grounded. Finally, Timer 2 releases S_3 to the open position and Timer 3 acts similarly with respect to reed switch S_4 . In the second mode of operation (S_1 open) the pulse-former may be operated manually on a one-shot basis, by closing switch S_2 .

3.05 Small Capacity Kerr Cell (K1)

A diagram of the small capacity Kerr cell is shown in Figure 3.5. The body of the cell was fabricated by milling a rectangular channel through one face of a solid stainless steel cuboid. The two electrodes, also of stainless steel, are positioned in this channel. The high voltage electrode is isolated from the body of the cell by two pieces of glass or teflon which cover the bottom and one side wall of the channel. The earthed electrode makes electrical contact with the cell body by means of two stainless steel ball bearings housed in the electrodes which may be pressed firmly into contact with the inner wall of the cell by screwing down two Allen-Key grub screws. This locking mechanism also serves to keep the electrode assembly rigid. The electrode gap is set by four glass spacers, which fit into opposite holes drilled in the two electrodes. The depth of the holes in the high voltage electrode may be varied by adjusting four Allen-Key grub screws and in this way the electrode gap may be varied. In the present study the electrode gap was set at 1.35 mm. The earth electrode was dressed back 2 mm along its upper edge to prevent arcing between the electrode gap above the liquid level. The high-voltage electrode was made shorter

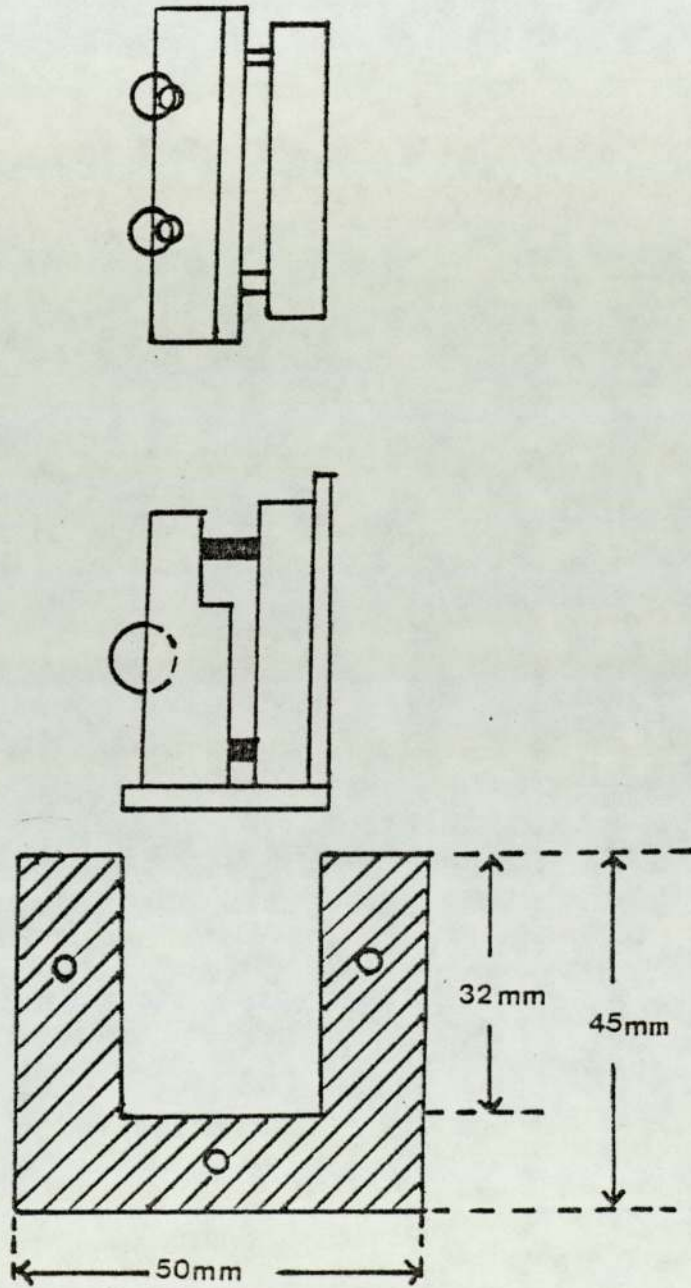


Figure 3.5 Diagram of the small capacity Kerr Cell (K1)

than the earth one to prevent arcing between the ends of the high-voltage electrode and the window assembly. The length of the high-voltage electrode (42 mm) was taken as the effective optical pathlength between the electrodes. The stainless steel window seating rings were fastened to the cell body using three screws and sealed with epoxy resin. The windows of the cell consisted of two optical quality quartz discs which were carefully selected for their freedom from strain bire-fringence. Each window was secured to the cell by a stainless steel retaining ring and three screws. A leak-proof seal was achieved between each window and its mounting using paper washers. A rubber O-ring cushioned the seal of the retaining ring upon the window. The electrical connections to the electrodes passed through holes in the stainless steel lid of the cell and each hole was fitted with an electrically insulating PTFE sleeve. The temperature of the cell could be controlled to within ± 0.05 K by means of a close fitting water-jacket connected to a Churchill water pump/thermostat. A Wallis (Worthington) model S103/3 power pack was used to supply the high-tension voltage, which was continuously variable in the range 0-10 kV. The voltage applied across the Kerr cell was measured on a digital Keithley model 616 electrometer.

3.06 Large Capacity Kerr Cell (K2)

The large capacity Kerr cell (K2) was used in this work only in conjunction with the Kerr cell (K1) to demonstrate the use of a double cell technique for the measurement of the Kerr effect of solutes in solution.

A cross-sectional diagram of the cell is shown in Figure 3.6. The design used in the construction of the cell resembles that used by other workers⁽⁶¹⁾. The cylindrical body of the cell and window mountings were made from brass, whilst the two electrodes were made from stainless steel. The brass body was electro-plated with nickel. The lower electrode was semi-circular in cross-section and made electrical contact with the cell wall, which was earthed. The upper electrode, also semi-circular in cross-section, had a smaller radius than the lower electrode and was electrically insulated from the cell by means of a PTFE sleeve through which passed the high-voltage electrical connection. The central stainless steel screw also served to keep the electrode assembly rigid. The inter-electrode separation was 1.08 mm and was set by means of two uniformly ground glass spacers. The length of the electrodes was 99 mm and this was taken to be the effective optical path length between the electrodes. The windows of the cell consisted of two optical quality quartz discs which were carefully selected for their freedom from strain birefringence. Each window was secured between a window seating and a window retaining ring by three spring-loaded nuts. A leak proof seal was achieved using washers cut from good quality paper. A rubber O-ring was used to effect a liquid tight seal between the window mounting assembly and the end faces of the Kerr cell.

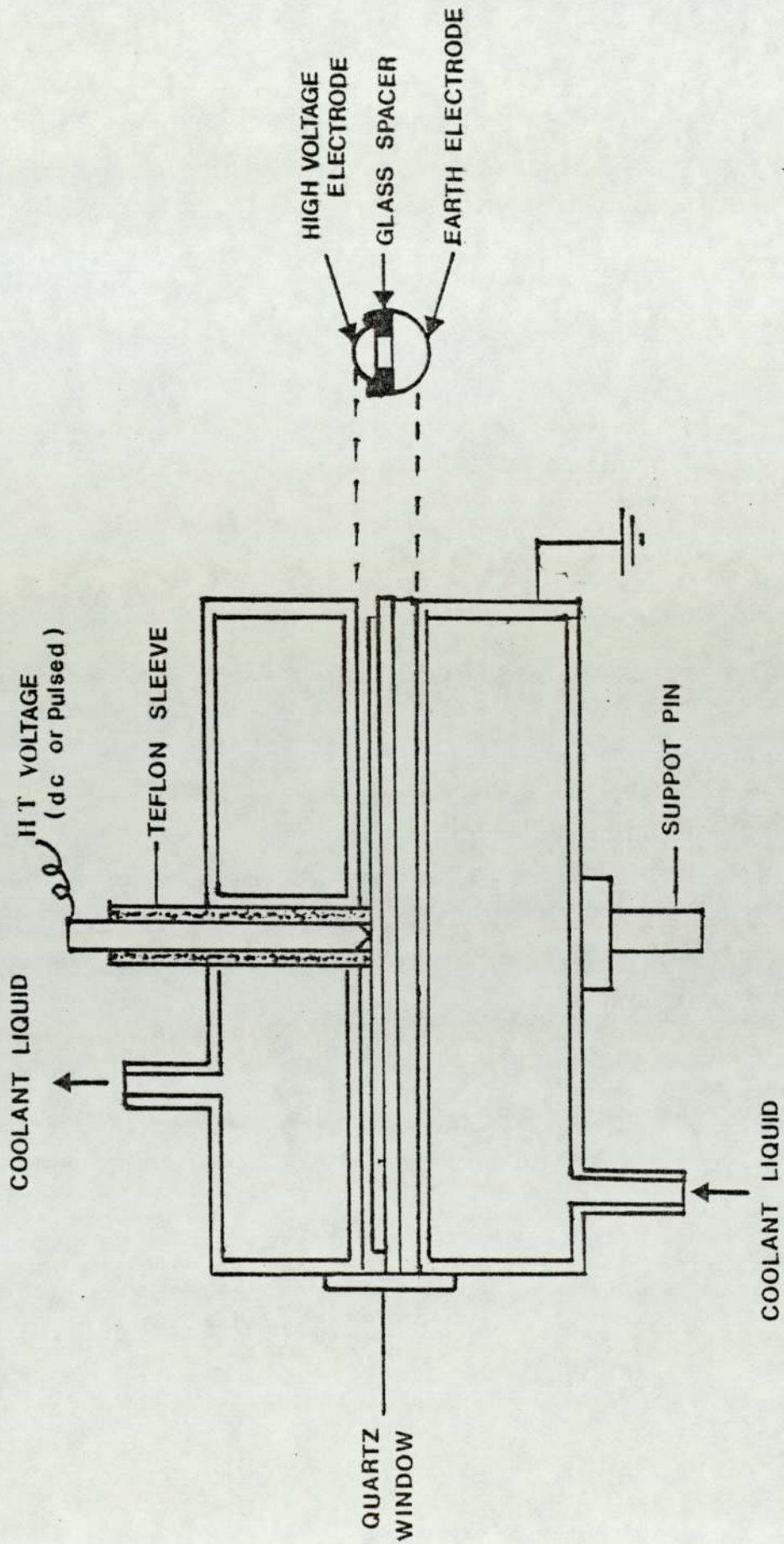


Figure 3.6 Cross section diagram of the large capacity Kerr Cell (K2)

3.07 Measurement of Experimental Kerr Constant B

The experimentally determined Kerr constant B, is defined by the equation:

$$B = \frac{\delta}{2\pi l (v/d)^2} \dots\dots\dots(3.2)$$

where δ is the electrically-induced phase difference between the components of light parallel and perpendicular to the applied electric field E, l is the optical path length between the electrodes, v is the applied voltage and d is the electrode separation.

If the Kerr effect is measured using a pulsed electric field, the rotation of the plane of polarization, α from the crossed position in the absence of an electric field, is related to the phase difference, δ , by

$$\alpha = \frac{\delta}{4} \dots\dots\dots(3.3)$$

Eliminating δ from equation 3.2 and rearranging gives:

$$\alpha = \frac{\pi l (v/d)^2}{2} B \dots\dots\dots(3.4)$$

If the Kerr law is obeyed then a plot of α versus v^2 should give a straight line graph passing through the origin with a gradient of $(\pi l B)/2d^2$, from which the experimental Kerr constant B may be determined. In practice the true rotation, α' , proportional to α was obtained from an arbitrarily calibrated dial. The rotation α is related to α' by a constant factor (0.9) governed by the overall ratio of the gear train used to rotate the analyser. Thus, the true

angular rotation, α , of the plane of polarization of the light is given by

$$= 0.9 \alpha \quad \dots\dots(3.5)$$

Note that equation (3.5) requires α to be expressed in radians. ($1^\circ = 0.0174532$ radian).

3.08 Measurement of Relative Kerr Constant

The Kerr constant of liquid sample was determined by comparing its electrically induced phase difference, δ with that of a standard. The Kerr cell was first calibrated with a liquid of known Kerr constant, B_s . Using M_x and M_s to denote the gradients of plots of α' versus v^2 for the unknown and standard liquids respectively, the experimental Kerr constant of the unknown material B_x can be readily calculated from the Kerr constant of the standard liquid using the simple relationship:

$$B_x = \frac{M_x}{M_s} B_s \quad \dots\dots(3.6)$$

Plots of α' versus v^2 for solutions of biphenyl in cyclohexane are shown in Figure 3.7. The slopes of the graphs and the correspondingly calculated Kerr constant using equation (3.6) are shown in Table (3.1).

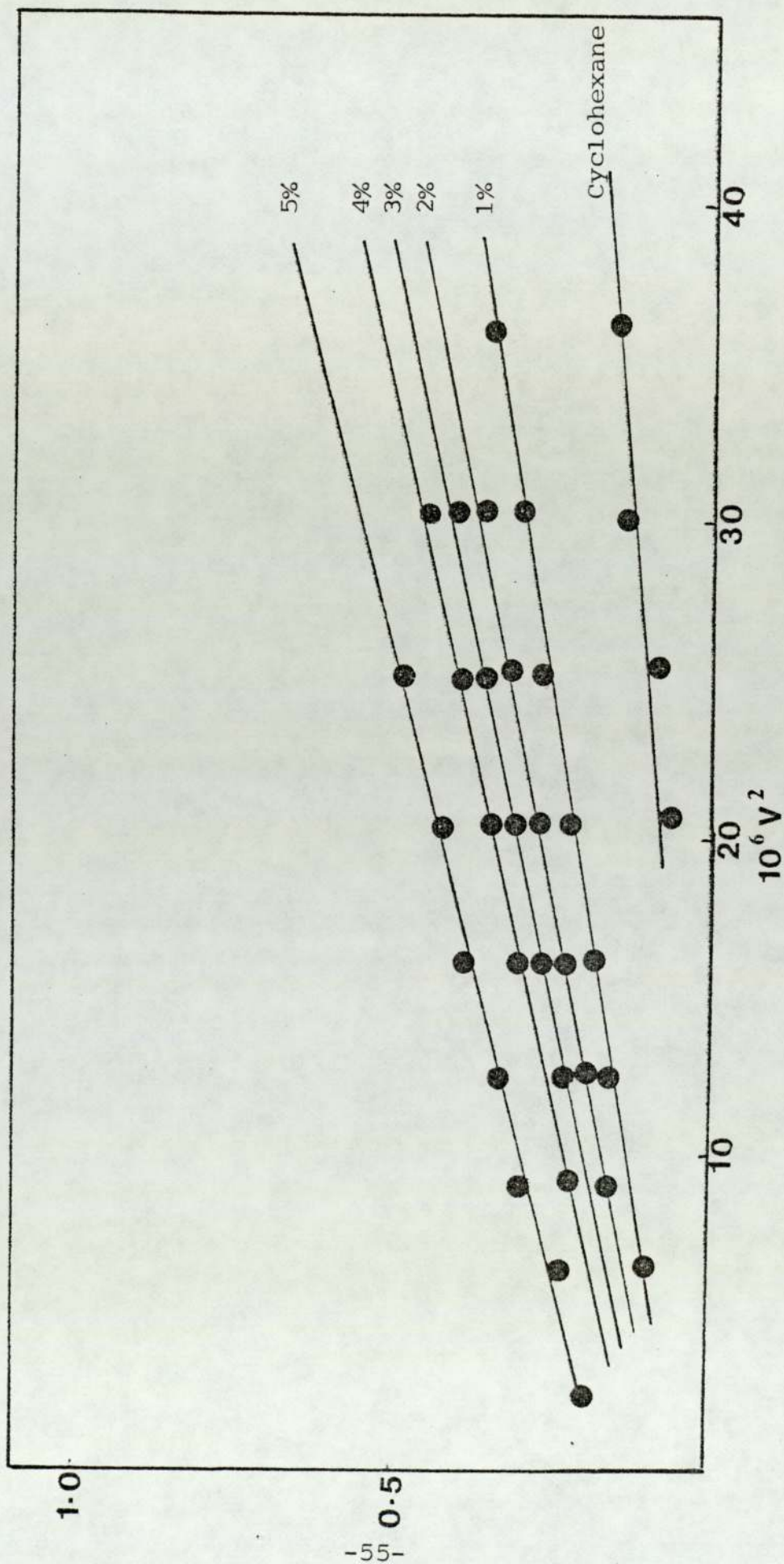


Figure 3.7 Plots of the rotation of plane polarised light against the square of voltage for various concentrations (1-5% w/v) of biphenyl in cyclohexane at 298 K

Cyclohexane	α'	0.06	0.1	0.15	0.17				Gradient	B ($v^{-2}m$)
	$10^6 v^2$	20.34	25.0	30.25	36.0				0.0058 ± 0.0002	
1% Biphenyl	α'	0.5	0.56	0.59	0.63	0.67	0.70	0.70	0.0082	0.086
	$10^6 v^2$	6.4	12.32	16.08	20.34	25.0	30.25	30.25	± 0.00026	
2% Biphenyl	α'	0.56	0.59	0.63	0.67	0.71	0.75	0.75	0.0091	0.094
	$10^6 v^2$	9.0	12.46	16.16	20.25	25.0	30.25	30.25	± 0.00026	
3% Biphenyl	α'	0.52	0.58	0.62	0.66	0.70	0.75	0.75	0.0104	0.108
	$10^6 v^2$	4.49	9.12	12.25	16.18	20.25	25.0	25.0	± 0.00039	
4% Biphenyl	α'	0.06	0.08	0.11	0.15	0.19	0.23	0.23	0.0109	0.112
	$10^6 v^2$	4.66	6.30	9.12	12.32	16.08	20.34	20.34	± 0.00024	
5% Biphenyl	α'	1.00	1.04	1.10	1.14	1.19	1.22	1.22	0.0377	0.132
	$10^6 v^2$	2.26	6.25	9.0	12.25	16.08	20.25	20.25	± 0.015	

Table 3.1 Kerr data for various concentrations of biphenyl in cyclohexane

3.09 Measurement of Kerr Constant by Double Cell Technique

The measurement of Kerr effect by a double cell method was demonstrated using Kerr cells K1 and K2. This arrangement, first suggested by des Coudres⁽⁶²⁾ employs the use of a second cell which compensates the birefringence developed in the first cell. This occurs when the configuration of the electrodes in the second cell are perpendicular to those in the first or when one cell contains a liquid with positive birefringence while the second contains a liquid with negative birefringence.

The method was applied when the Kerr effect due to solvent tends to mask the effects due to the solute being investigated. The Kerr cell, K2 was filled with solution of material under investigation. The two cells were then arranged in series between the polarizer and the quarter-wave plate. In this way the birefringence due to solvent in K1 is partially cancelled out by the phase retardation induced in K2. The resultant measured effect was therefore attributable in greater proportion to solute under investigation. The technique was successfully demonstrated for a solution of p-terphenyl in chloroform. The double cell arrangement is shown in Figure 3.8.

For perfect cancellation of solvent effect the Kerr effect will be entirely attributable to the solute. However, in practice, because of slight mismatch between the cells, it is impossible to achieve a perfect compensation. Under these

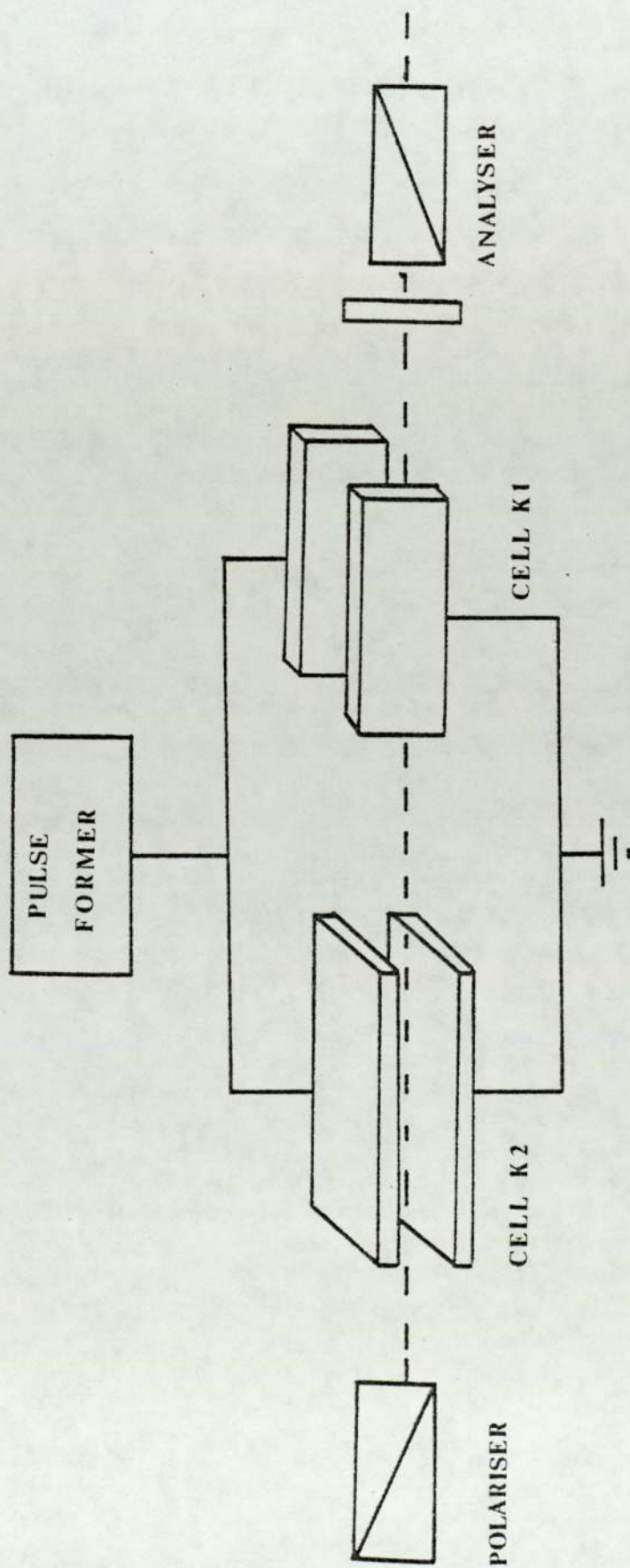


Figure 3.8 Double cell arrangement for the determination of Kerr effect

circumstances the resultant Kerr effect may be regarded as that due to a solute dissolved in a solvent possessing a very small Kerr constant.

3.10 The Dielectric Apparatus

The arrangement of the dielectric apparatus used for this study is shown in Figure 3.9. The apparatus consists of a variable frequency oscillator (V.F.O), a variable air capacitor, (C_S pF) (Sullivan and Griffiths precision variable air capacitor), a dielectric cell (C_{CELL} pF) and a precision frequency counter (Venner Electronics Ltd., type T5A 6636/2m). The dielectric cell (manufacturer unknown) was comprised of two cylindrical blocks of brass (Figure 3.10). The external surfaces were nickel plated and the internal surfaces in contact with the sample were gold plated. The outer cylinder, C, was hollow to allow passage of coolant liquid. The cell was fitted with an external screw-top lid, B, through which the cell could be filled and an internal perforated lid. The latter ensured that the effective volume of the dielectric cell was reproducibly constant and independent of the actual volume ($\sim 20 \text{ cm}^3$) of liquid sample in the cell, provided that the liquid level was above the internal lid. The height and diameter of the inner cylindrical electrode, D, were 35 mm and 33 mm respectively. The electrode gap was approximately 1.5 mm and the vacuum capacitance of the empty cell was determined to be 47 pF.

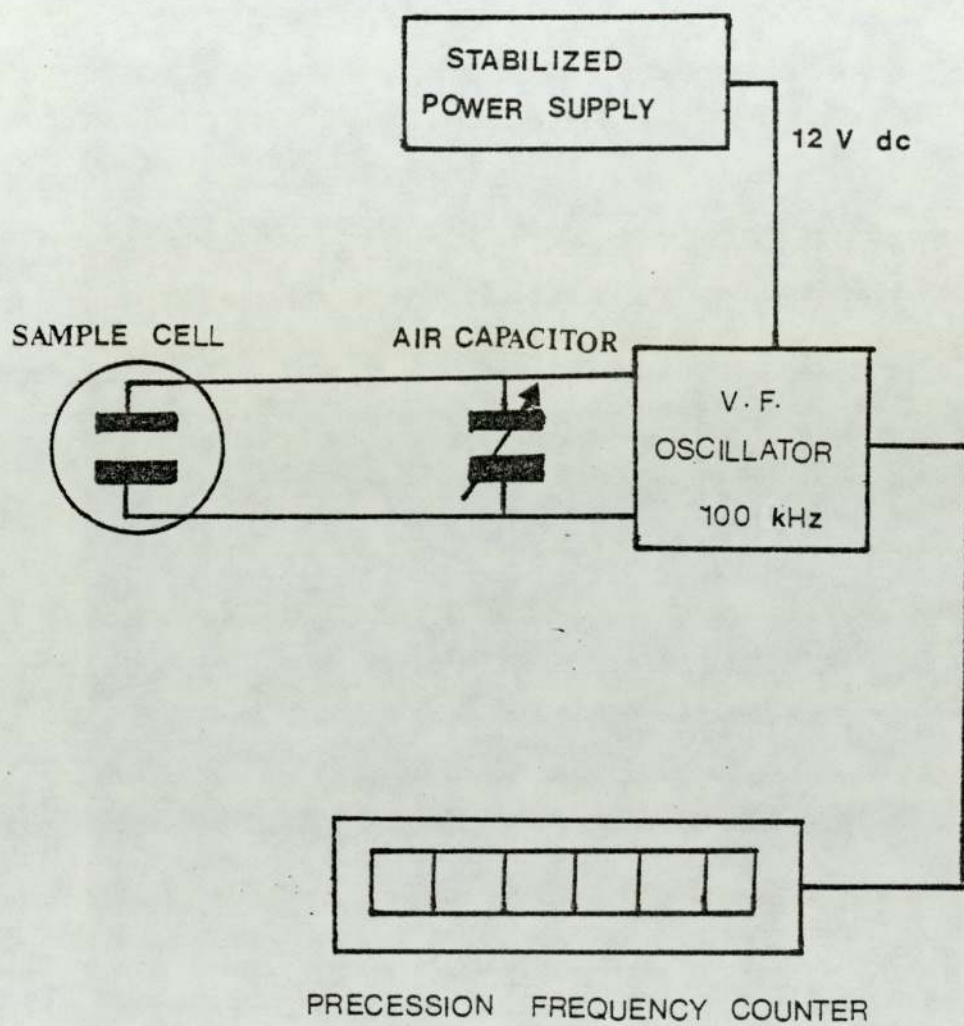


Figure 3.9 Configuration of the dielectric apparatus

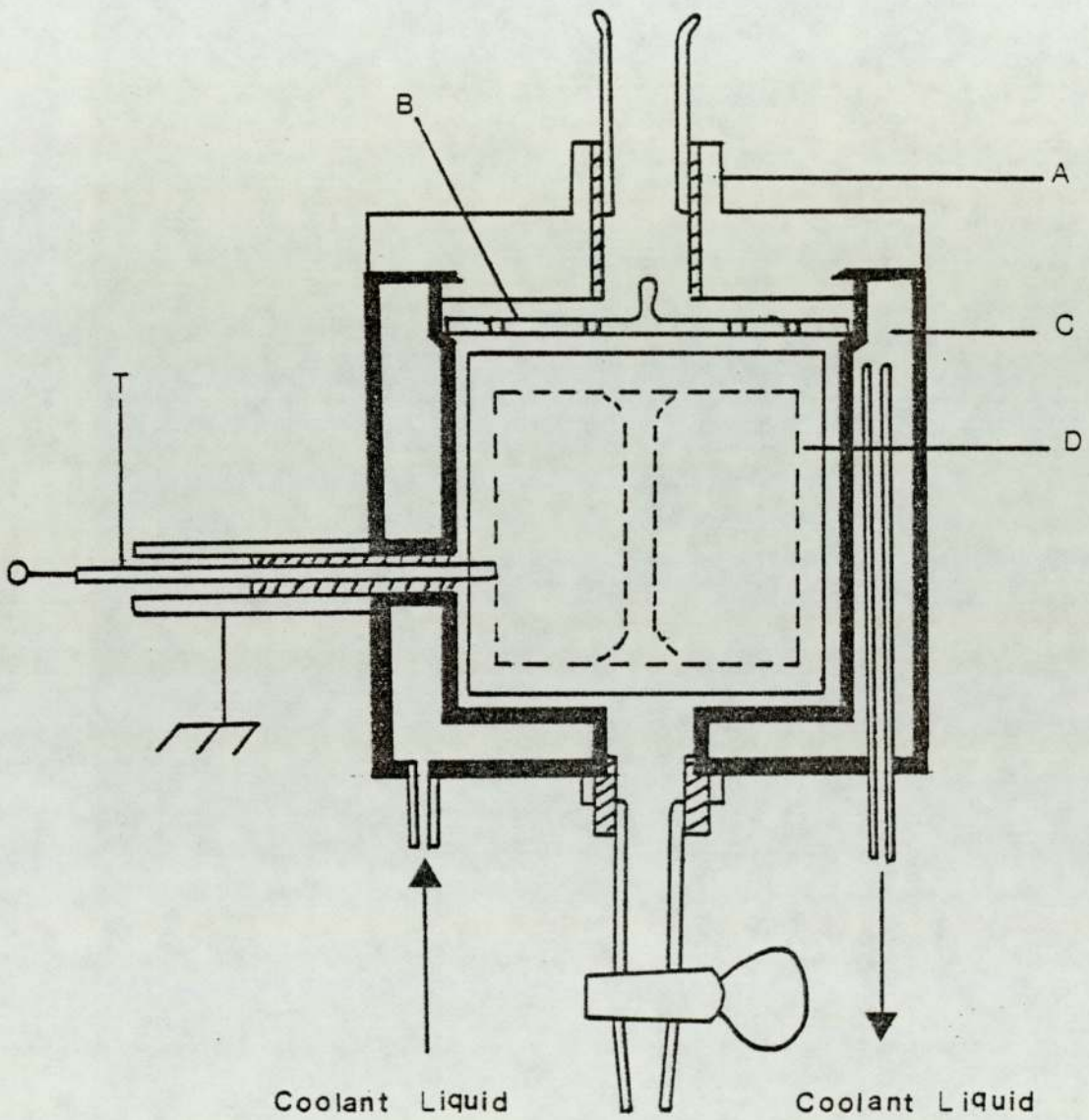


Figure 3.10 The Dielectric Cell

 Teflon

3.11 Measurement of Static Dielectric Permittivity

The dielectric apparatus shown in Figure 3.9 permits the determination of capacitances indirectly by the measurement of the frequency of the V.F.O. The cell acted as one of the principal capacititive elements of the variable frequency oscillator. The frequency of operation of the V.F.O. was measured using the precision frequency counter to an accuracy of 1 part in 10^5 .

The frequency of the V.F.O. was measured for the empty cell (f_{air}), the cell filled with solvent (f_1) and for the cell filled with a series of solutions (f_{12}) covering a range of concentrations. All measurements were conducted at 298 K.

The static dielectric permittivity, ϵ_{12} , of the solution was calculated using the expression

$$\epsilon_{12} = 1 + \left[\frac{1/f_{12}^2 - 1/f_{\text{air}}^2}{1/f_1^2 - 1/f_{\text{air}}^2} \right] (\epsilon_1 - 1) \quad \dots\dots(3.7)$$

where ϵ_1 is the dielectric permittivity of solvent at 298 K.

3.12 The Automatic Sublimator

The automatic sublimator used in this work was designed and built in the Department of Chemistry work shops. It consists of a molecular still, a heating chamber, an electrically driven motor and a power controller unit. The molecular still enclosed in the heating chamber is shown in Figure (3.11). The still, made of pyrex glass (~ 300 mm long),

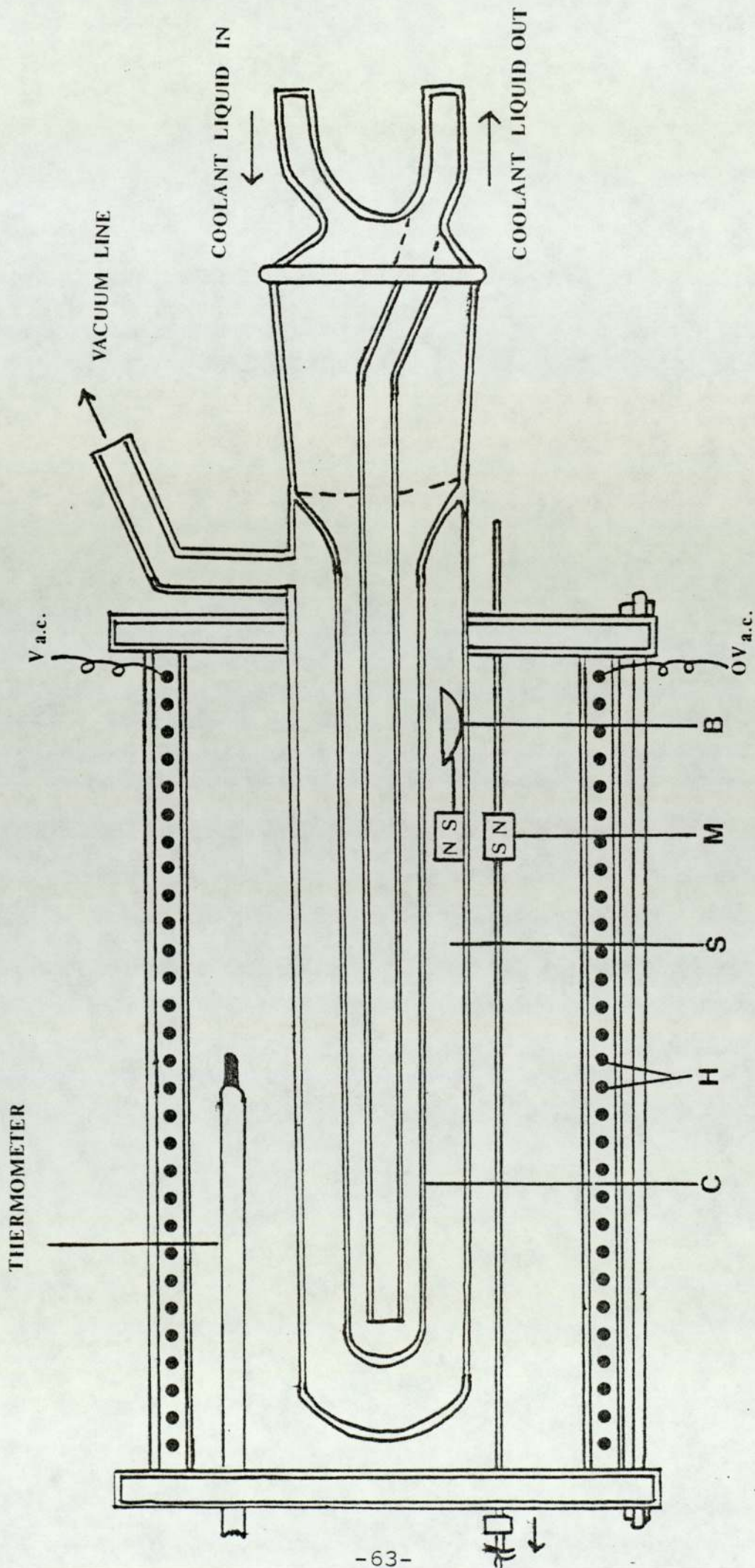


Figure 3.11 Diagram of automatic sublimator with heating chamber

consists of a sublimation chamber, S, containing a cold finger, C (~ 8 mm from the inner walls of the chamber) through which coolant liquid is circulated. A pyrex sample boat, B (~ 40 mm long) fitted with a magnet is placed about 6 mm from the cold finger (glass pimples at the bottom of the boat reduces the gap between the cold finger and the inner wall of the chamber to 6 mm). The heating chamber consists of two concentric glass cylinders. The heating coil, H, is wound round the inner cylinder and connected to the output of the power controller unit, while the outer cylinder serves as a protective shielding. A second magnet attached to a brass rod is driven along the length of the sublimator by an electric motor and gear box and in so doing moves the magnet and the attached sample boat in the sublimation chamber.

3.13 Power Controller for Automatic Sublimator

The temperature of the sublimator is controlled by the magnitude of the electric current passing through the heater coils. Accurate control of the electric current was achieved using a triac-based power controller, the circuit of which is shown in Figure 3.12. The controller consists of one triac, a diac, a coil (L1) of capacitor (C1) to suppress radio interference and an RC network. The charging and discharging times of capacitor C2 can be set by one of four potentiometers P1 through P4. The latter are selected sequentially at preset intervals of time by three micro-switches S3-S5 operated by a sliding rod driven by an electric motor and a 4 speed gear box. The times taken for the sample tray to transverse the sublimator could be set by

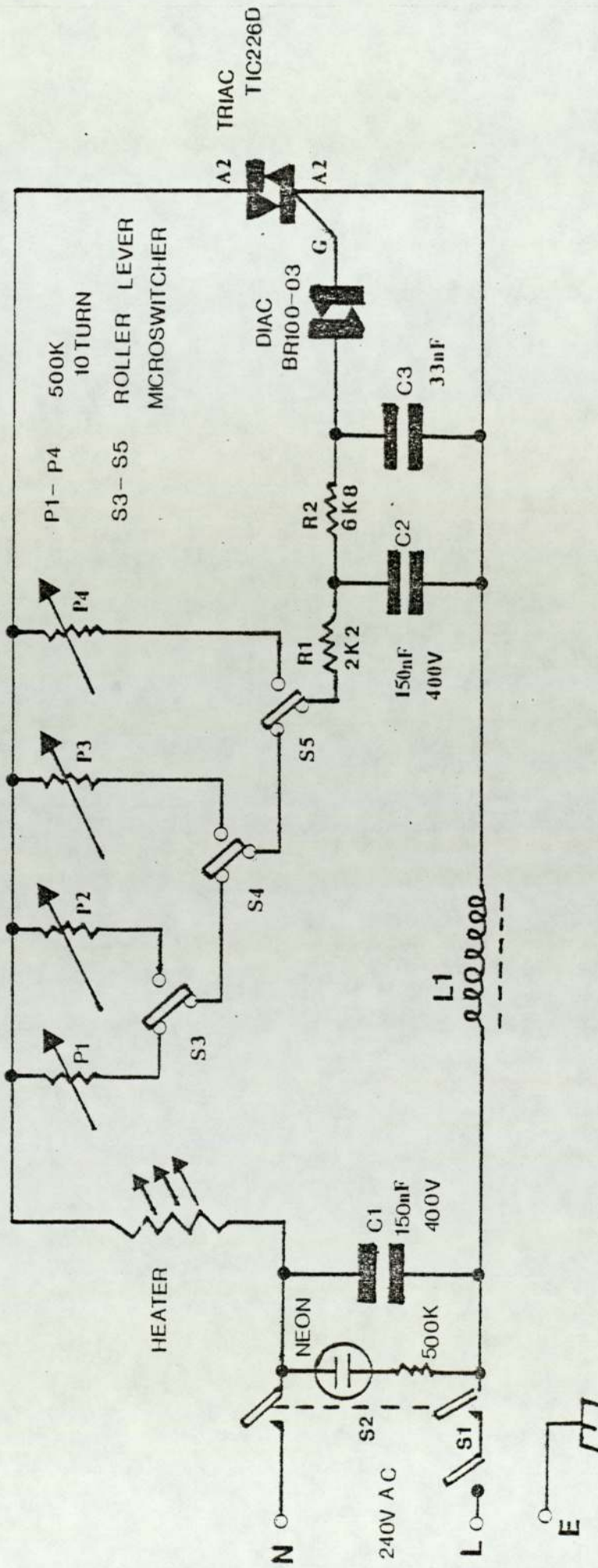


Figure 3.12 Circuit diagram of the power controller for the automatic sublimator

the gear box to 3, 14, 51 and 215 minutes.

Using this apparatus the sample could be subjected to a programmed sequence of temperature versus time. The sublimator was fitted with a cut-out (stop) switch for automatic running. The temperature was recorded by means of a thermometer.

SYNTHESIS AND CHARACTERISATION OF POLY(P-PHENYLENES)

4.01 Introduction

Poly(p-phenylenes) employed in this work were mainly prepared by the oxidative cationic polymerization method developed by Kovacic and co-workers, according to the procedure outlined in reference (23).

These polymerizations were performed in a three-necked flask equipped with a thermometer, paddle stirrer and a nitrogen inlet, and according to the Kovacic procedures. Since poly-phenylenes are highly insoluble in almost any known solvent, measurements in solution to study their properties are virtually impossible. The oligomers (e.g biphenyl, p-terphenyl, p-quarterphenyl, p-quinquephenyl, etc.) are however, reasonably soluble particularly in chloroform. For this reason, some modifications of the basic polymerization process were attempted in order to produce polymers with increased molecular weight distributions and to provide materials with variable compositions containing soluble extractable oligomers for subsequent studies. This involved the polymerization of benzene in bulk and its polymerization in various 'inert' solvents. The Kovacic method was also used to polymerize biphenyl to polyphenylene. The polymer was also prepared by a novel type of polycondensation utilizing transition metal-catalysed 'C-C' coupling.



It was our view that electrical properties of this highly insoluble polymer could be studied indirectly by looking at properties of oligomers from the polymer. Measurement of their dielectric and electro-optical properties in solution would be useful in explaining the electronic properties of the polymer. Thus, a study of solutions of pure oligomer and solutions of oligomer/dopant systems could provide useful information on the nature of the reported highly conducting charge-transfer complexes that the polymer forms with both donor and acceptor dopants⁽³⁾.

4.02 Bulk Polymerization of Benzene with $AlCl_3$ - $CuCl_2$ Catalyst-Oxidant

In this method of preparation, benzene was polymerized by the Kovacic method in bulk (no solvent) under mild conditions (30-35°C, 30-40 minutes). The proportions of monomer, catalyst and oxidant were 1:0.5:0.5 respectively. The polymer produced was a light brown, insoluble, infusible powder. The total quantity obtained was 8.4 g which corresponded to a 10.8 percent yield based on benzene. Elemental analysis of the polymer gave: C = 76.1, H = 4.0, Cl = 6.5 and copper and oxygen amounted to 13.4%.

The I.R. spectra (KBr disc) of the polymer exhibited a strong absorption band at 810 cm^{-1} indicative of para band, and rather weak mono band absorptions at 695 and 770 cm^{-1} . These observations suggests that the polymer was formed by the linkages of phenyl rings para to one another to give poly(p-phenylenes). For convenience, the polymer sample produced by this method will be subsequently referred to as sample P1.

4.03 Synthesis of Poly(P-Phenylene) from Solutions of Benzene and Biphenyl in Cyclohexane

Medium dilution: In this method, the polymerization of benzene was effected in a solvent (cyclohexane). The proportion of benzene/cyclohexane was 1:1 by volume and the catalyst-oxidant ($\text{AlCl}_3\text{-CuCl}_2$) ratio and preparation conditions remain the same as in the bulk process. The product was a black powder and proved to be insoluble in common solvents and infusible. The total yield is 2.9 g, which corresponded to 7.4 percent based on benzene. Elemental analysis of the polymer gave C = 87.3, H = 4.6, Cl = 6.6 and copper and oxygen amounted to only 1.6 percent.

The I.R spectrum (KBr disc) of the polymer exhibited strong absorption at 810, 755 and 700 cm^{-1} . The absorption at 810 is due to the para band and the absorptions at 755 and 700 cm^{-1} leads to a small para/ mono band ratio and therefore suggests that the polymer is of low molecular weight. The product of this preparation will be subsequently referred to as P2.

High dilution: In this method, the polymerization was carried out in high dilution with a total monomer/solvent volume ratio of 1:6 (benzene/cyclohexane). Cyclohexane (250 cm^3) with the catalyst-oxidant ($\text{AlCl}_3\text{-CuCl}_2$) was placed in a three-necked reaction flask and 100 cm^3 of the mixture of benzene and cyclohexane (1:1 v/v) was introduced dropwise into the polymerization system from a dropping funnel at a rate of about 1 cm^3 per minute while stirring continuously.

The polymeric product was dark brown in colour and similar in appearance to material obtained by the medium dilution method. It was also insoluble and infusible. The yield based on benzene, was calculated to be 7.8 percent.

Elemental analysis of the polymer gave: C = 84.2, H = 4.6, Cl = 6.8. Copper and oxygen accounted for the remaining 4.4 percent.

The I.R spectrum (KBr disc) exhibited a para band absorption at 820 cm^{-1} and mono bands at 770 and 700 cm^{-1} . The para band intensity is weaker than either of the two mono band intensities. The $\text{para}/\Sigma\text{mono}$ ratio is even smaller than that for P2. This therefore suggests that the polymer has a lower molecular weight than P2. The polymer produced by this method will subsequently be referred to as P3.

4.04 Polymerization of Biphenyl

This preparation closely followed the Kovacic method but employed biphenyl as the monomer and cyclohexane as the solvent. Biphenyl(0.5moles) was dissolved in 50 cm^3 of cyclohexane and placed into a three-necked flask together with $\text{AlCl}_3\text{-CuCl}_2$ catalyst-oxidant system. The proportions of biphenyl, aluminium chloride and cupric chloridewere 1:1:1. The reaction apparatus was assembled as previously (section 4.01) and polymerization was allowed to proceed for 40 minutes at $30\text{-}35^\circ\text{C}$. This was followed by the work up procedure as described in reference (23). The polymer produced was yellow in colour and the total yield amounted to 34 percent based

on biphenyl.

Elemental analysis of the polymer gave: C = 89, H = 5.7, Cl = 3.2.

The I.R spectra gave strong para absorption peak at 820 and mono peaks at 765 and 700 cm^{-1} . This suggests that the polymer is essentially formed by linkages of phenyl rings at the para positions to one another. The para/ Σ mono ratio also suggests that the polymer has a low molecular weight. The polymer produced by this method will be subsequently referred to as P4.

4.05 Polymerization of Benzene-Ether Mixtures

The polymerization of benzene in the presence of ethers (diethyl ether and dioxane) was attempted to study the possibility of incorporation of the ethers into the final product. An incorporation of the ethers into the polymer would provide additional peak in the I.R spectrum and could influence the para and mono bands of the polymer. The effect of the presence of ether on product yield, molecular weight and oligomers could also be studied. The system could also provide additional information about the mechanism of polymerization proposed previously^(25,28).

Benzene and 1,4 - Dioxane:

The experimental method was basically the same as that employed in the bulk synthesis of poly(p-phenylene) but was carried out in the presence of small amounts of 1,4 dioxane.

With a benzene/1,4-dioxane ratio of 50:1 (v/v), the total yield based on benzene was 1.4 percent. When the proportion of 1,4 dioxane was increased to give a benzene/1,4 dioxane ratio of 10:1 (v/v), complete inhibition occurred and no polymer was formed. However, when an excess of catalyst ($\text{AlCl}_3\text{-CuCl}_2 = 4:1$) was employed while still maintaining a benzene/1,4 dioxane ratio of 10:1 (v/v), a yield of ca 0.5 percent was obtained.

Elemental analysis of the polymer produced by this method gave: C = 87.1, H = 4.8, Cl = 6.5 and copper and oxygen amounted to 1.6 percent.

The I.R.spectrum (KBr disc) exhibited a strong para absorption at 810 and weak mono absorptions at 770 and 700 cm^{-1} . This gives a high para/ Σ mono ratio and therefore suggests the polymer may have a high molecular weight. For convenience, the polymer produced by this method will be subsequently referred to as P5.

Benzene and Diethyl Ether

In this method of preparing poly(p-phenylene), benzene was polymerized according to the Kovacic method in the presence of varying proportions of diethyl ether. For a benzene/diethyl ether volume ratio of 5:1 the yield of polymer was ca 7.3 percent. When the quantity of diethyl ether was increased to give a benzene/diethyl ether volume ratio of 1:1, no visible polymerization occurred. However for benzene/diethyl ether ratios of 1:1 together with a modified catalyst-oxidant mix ($\text{AlCl}_3\text{-CuCl}_2 = 4:1$), some polymer was

formed (yield ca 5.7 percent). The polymeric product obtained was light brown in colour and similar in appearance to P1.

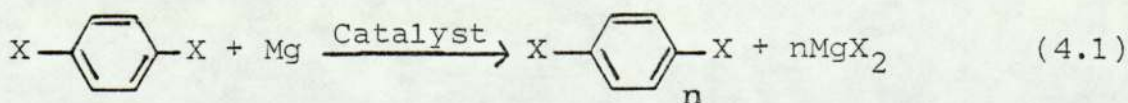
Elemental analysis showed: C = 88.5, H = 4, Cl = 6.5, and copper and oxygen amounted to only 1 percent.

The I.R spectrum (KBr disc) gave strong para band at 810 and weak mono bands at 770 and 700 cm^{-1} . The polymer obtained by this method will be subsequently referred to as P6.

4.06 Preparation of Poly(P-Phenylene) by Transition Metal-Catalysed 'C-C' Coupling

Transition metals or their compounds are known to catalyze the coupling of Grignard reagents with aryl halides⁽⁶³⁾ and since this transition metal catalyzed coupling reaction proceeds selectively and quantitatively under mild conditions, it has been applied to the preparation of various organic aromatic compounds⁽⁶³⁾.

The principle of the transition metal catalyzed coupling was extended by Yamamoto et al⁽⁶⁴⁾ who applied it for the preparation of polyphenylene type polymers having regular recurring units by starting from dihalogenated aromatics. P-dihalobenzene, for example, can be dehalogenated by reacting with magnesium in the presence of a suitable transition metal catalyst. In this reaction, linear polyphenylenes are formed according to the equation (4.1)



Polymerization of 1,4 Dibromobenzene:

The Yamamoto method⁽⁶⁴⁾ was employed in the present study to prepare poly(p-phenylene) from p-dibromobenzene using magnesium metal and a catalyst of nickel bipyridyl in dry tetrahydrofuran.

The nickel bipyridyl complex used in this method was prepared from anhydrous nickel chloride and 2,2'-bipyridyl. This was achieved by dissolving a 1:1 by weight mixture of anhydrous nickel chloride and 2,2' bipyridyl in absolute ethyl alcohol which formed an intense red solution of the bipyridyl complex. On standing the solution turned to intense blue. This change in colour is due to the transformation of the unstable red complex (square planar) to the more stable blue complex (tetrahedral). The blue complex was isolated from solution by gradual evaporation of the solvent at room temperature.

The tetrahydrofuran (THF) used as solvent for the polymerization was dried over sodium naphthalide according to the following procedures: To 250-350 cm³ of THF in a three-necked flask fitted with a reflux condenser, 1-2 g of sodium metal and the molar equivalent of naphthalene was added. A deep blue solution was obtained due to the formation of sodium naphthalide. The solution was refluxed for 30 minutes and then distilled to give anhydrous THF. The THF was either used immediately or left to stand for brief periods in a tightly stoppered flask.

P-dibromobenzene (11.8 g) and magnesium metal turnings (1.2 g)

were thoroughly mixed in the dried THF (50 cm^3) in a round-bottomed flask. The nickel chloride - bipyridyl complex (51 mg) was added to the mixture which was then refluxed for 5 hours. The reaction mixture was poured into 500 cm^3 of ethyl alcohol. The precipitated polymer was collected using a sintered glass filter funnel, washed with dilute hydrochloric acid followed by ethyl alcohol and then dried in a vacuum oven at 80°C . The polymer was light yellow in colour and the yield was 3.1 g (26.3%) based on dibromobenzene.

Elemental analysis of the polymer gave: C = 62, H = 4.5, Br = 30.5.

The I.R spectrum shows a strong para band absorption at 810 and mono absorptions at 770 and 700 cm^{-1} . This observation suggests that the polymer was formed by the linkages of phenyl rings in positions para to one another. The spectra also shows a prominent absorption at $1075\text{-}1080 \text{ cm}^{-1}$ due to 'C-Br'. Bromine has already been shown to be present in significant amounts in the polymer from the elemental analysis. Samples of polymer obtained using this method will be subsequently referred to as P7.

4.07 Sulphonation of Poly(P-Phenylene) (P1)

The sulphonation of the polymer was carried out as follows: Into a three-necked, round-bottomed flask equipped with a thermometer, mechanical stirrer, gas inlet and gas outlet were placed 50 cm^3 of sulphuric acid and 1 g of P1. The mixture was heated to $\text{ca.}150^\circ\text{C}$ under a nitrogen atmosphere

for about six hours. The black reaction product was cooled to room temperature and poured over ice. A black solid was isolated by suction filtration, washed thoroughly with deionized water and then dried in an oven at 120°C.

4.08 Infrared Analysis of Polyphenylenes

I.R. spectra of the polyphenylenes and oligomers were obtained using Pye Unicam Sp 1000. KBr discs were prepared with the composition of polymer amounting to about 10 percent of the disc. Pure samples of p-terphenyl and p-quarterphenyl were obtained from Aldrich Chemicals. P-quinquephenyl was obtained from K and K Chemicals Ltd. Polymer samples P1-P6 were synthesized in this laboratory according to methods described in previous sections of this chapter.

All these materials exhibit I.R absorption bands characteristic of para substitution and mono substitutions discussed in Section 2.04. The position and relative intensities of para and mono bands for these samples are listed in Table 4.1. The para band position in the spectrum is seen to shift to a lower wave number ($845-810\text{ cm}^{-1}$) with increase in phenyl units in the polyphenylene series p-terphenyl to polyphenylene (P1-P6). This observation complements comments made by Kovacic et al⁽⁴⁸⁾ and Jozefowicz⁽⁶⁵⁾.

The para absorption band for polymer P3 and P4 was found to be at 820 cm^{-1} , significantly higher than that (810 cm^{-1}) observed for samples P1, P2, P5, P6 and P7. The observations correlate with the amount of oligomers extractable from

these polymers. P3 and P4 had the highest proportion of extractable oligomers. This is only possible if P3 and P4 have a broad molecular weight distribution. The ratio of intensities (Para/ Σ mono bands) has also been used to give an approximate indication of relative molecular weights in the polyphenylene series⁽⁴⁸⁾. These ratios listed in Table 4.1, Column 8) increase, as expected from p-terphenyl to p-quinquiphenyl. However for the polymers there are important exceptions to this trend. For example P2 and P3 have the ratio of intensities (para/ Σ mono) lower than p-terphenyl. This discrepancy could not be attributed to differences in molecular weights since the polymers P2 and P3 have higher molecular weights than the p-terphenyl and therefore would be expected to have the higher para/ Σ mono band ratios. A probable explanation for this reversed trend could be the presence of substituents e.g. chlorine and oxygen along polymer backbones in P2 and P3 which is known⁽⁴⁸⁾ to decrease the intensities of the para bands relative to the mono bands. This argument is supported by elemental analysis of the polymers which indicates the presence of chlorine and oxygen. The differences in the para band position (P2 = 810 cm^{-1} and P3 = 820 cm^{-1}) and the ratios of para/ Σ mono bands (P2 = 0.31 and P3 = 0.2) appear to depend on the method of preparation. The polymer P3 has been prepared in greater solvent presence (50 cm^3 benzene in 300 cm^3 cyclohexane) than P2 (50 cm^3 benzene in 50 cm^3 of cyclohexane). The greater solvent presence would not significantly alter the rate of initiation but would quite significantly decrease the rate of propagation and hence the kinetic chain length. Polymers with low molecular weight would consequently be formed. This is seen to be

Polyphenylene Samples and Oligomers	Absorption maxima (cm^{-1})								Ratio of Para/ Σ mono band intensities
	Para band		Mono band 1		Mono band 2		Position	Int. (cm)	
	Position	Int. (cm)	Position	Int. (cm)	Position	Int. (cm)			
P-terphenyl	845	6.6	750	6.8	695	6.5		0.49	
P-quarterphenyl	830	5.7	755	5.6	690	4.9		0.54	
P-quinquephenyl	820	5.8	760	6.0	690	3.1		0.64	
P1	810	7.9	770	2.5	695	0.9		2.3	
P2	810	1.1	755	2.1	700	1.4		0.31	
P3	820	1.0	755	2.5	700	2.5		0.2	
P4	820	5.2	765	7.1	700	5.2		0.42	
P5	810	4.3	770	1.9	700	0.5		1.79	
P6	810	4.0	770	1.9	700	0.5		1.66	
P7	810	7.0	770	3.8	700	2.1		1.18	

Table 4.1 I.R. Spectral data for various samples of poly(p-phenylene) and standard compounds

the case for P3.

4.09 Analysis of Poly(phenylenes) using X-ray Diffraction

X-ray diffraction study of poly(p-phenylene) was shown previously by Marvel and Hartzell⁽²⁴⁾ and Kovacic et al⁽⁶⁶⁾ that the polymer is significantly crystalline. Kovacic et al⁽⁶⁶⁾ also demonstrated from their x-ray diffraction study, that crystallinity in the polymer increases as a result of pressing of the powder, increase in moulding temperature and subsequent heat annealing at 400-500°C. They observed a decrease in the half-width of the strongest crystalline reflection as crystallinity increases, indicating an increase in crystallite size. The d-spacing of this reflection was also observed to systematically decrease as the crystallinity increases. These workers attributed the increase in crystallinity, crystallite size and the decrease in d-spacing of the most intense reflection to the annealing effects and loss of chlorine at the high temperature (400-500°C). They also suggested that such thermal treatment would enhance mobility of chains in the amorphous portion of the polymer and hence induce additional crystallinity. Marvel and Hartzell⁽²⁴⁾ previously suggested that the most intense reflection at 4.53 Å could be due to repeat distance along the chain of the polymer. This was refuted by Kovacic et al⁽⁶⁶⁾ who argued that a repeat of one p-phenylene unit should be 4.20-4.30 Å (and not 4.53 Å), and suggested that the reflection at 4.53 Å is most probably related to the lateral packing of the poly(p-phenylene) chains.

X-ray diffraction work has proved to be a useful and quick method for looking at crystallinity in polymers, and was employed for this work.

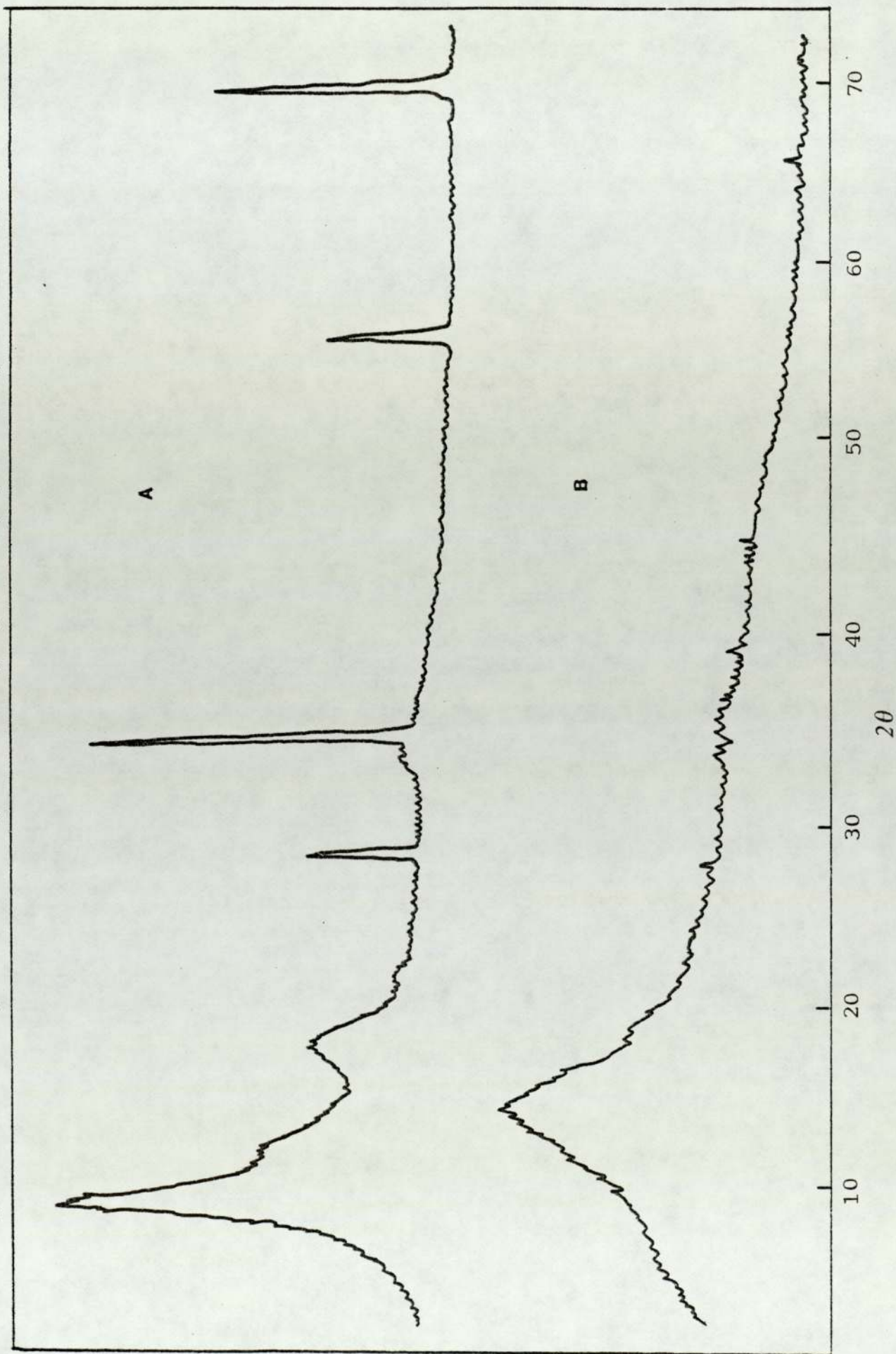
All the polyphenylenes synthesized in this study were crystalline, exhibiting similar d-spacing characteristics to each other, and to the d-spacing characteristics of p-quarterphenyl, p-quinquiphenyl and p-sexiphenyl reported by Toussaint and Vos⁽⁶⁷⁾. The d-spacings for these polymers and oligomers are shown in Table 4.2. As shown in the table, the pattern is in good agreement with the data published by Kovacic et al⁽⁶⁶⁾ and Marvel and Hartzell⁽²⁴⁾ for polyphenylenes prepared by the oxidative cationic polymerization of benzene and by the 1,4 polymerization of 1,3-cyclohexadiene followed by dehydrogenation methods respectively. The similarities would therefore suggest that the various methods of synthesis studied do not produce any change in crystallinity of the polymer.

Figure 4.1 shows a comparison of the x-ray diffraction patterns of P1 before and after sulphonation with concentrated sulphuric acid. The disappearance of the sharp diffraction pattern characteristic of crystallinity after sulphonation is as expected. This is because treatment of the polymer with sulphuric acid (see section 4.07) leads to the introduction of sulphonic acid groups into the polymer backbones and hinders easy packing of the polymer chains on a regular lattice. As a result an amorphous polymer is produced with an appropriate x-ray diffraction pattern (Fig.4.1B).

Table 4.2 X-ray diffraction data for various poly(p-phenylene) samples and oligomers

Sample	d Spacings (Å)								
P1	4.54	3.93	3.20	2.38	2.05	1.445	1.443	1.23	1.226
P2	4.52		3.28		2.01	1.45		1.228	1.226
P4	4.24	3.50	3.14	2.36	2.03	1.457			
P7	4.43	3.70	3.07						
p-quarterphenyl	4.53	3.87	3.18	2.37	2.08				
p-quinquiphenyl	4.60	3.83	3.16	2.35	2.04				
p-sexiphenyl	4.60	3.86	3.18	2.34	2.05				

Figure 4.1 X-ray diffraction pattern of polymer PI (A) and Sulphonated PI (B)



5.01 Preparation and Chromatographic Characterisation
of Oligophenylenes

This chapter details experimental investigations largely concerned with the extraction and characterisation of phenylene oligomers from the polymers. The extractions were accomplished by Soxhlet extraction technique and by a continuous solvent reflux action on the polymers. The polymer P4, prepared by the polymerisation of biphenyl gave the highest percentage (48.2%) of chloroform soluble oligomers per dry weight of polymer. This could be rather misleading because of a substantial presence of unpolymerised biphenyl in the extract. The polymerisation of benzene in solvent (cyclohexane) produced polymers with a substantial increase in the proportion of chloroform extractable oligomers compared with polymers prepared in the bulk (percentage extraction from P1 = 0.08, while percentage extraction from P3 = 22.3). This observation was anticipated because the polymerisation in 'inert' solvent (cyclohexane) would have little or no effect on the rate of initiation but would significantly reduce the rate of propagation and consequently the kinetic chain length. Polymers with broad molecular weight distribution and high proportion of extractable oligomers would then be produced.

The polymerisation of dibromobenzene to produce polymer P7, also gave materials with significant proportions of chloroform extractable oligomers (7.8%) per dry weight.

Gel permeation chromatographic and gas liquid chromatographic methods were used for the characterisation. Outlines of these techniques are given together with some description of instrumentation.

5.02 Extraction of Oligomers from Polymers

Two methods of extraction were employed using chloroform as solvent and gave similar extraction efficiencies. In the continuous solvent reflux action method, a weighed amount of finely powdered polymer and a known volume of chloroform were placed in a round-bottomed flask fitted with a condenser and refluxed for 24 hours. The refluxed material was then filtered and its chloroform soluble portions were collected into a clean beaker. The chloroform was then evaporated in a vacuum oven leaving a mixture of solid oligophenylenes. The second method of extraction was by a soxhlet extraction technique. A weighed amount of polymer material was taken in a porous thimble (made from tough filter paper) and placed in the soxhlet apparatus which consists of a solvent round-bottomed flask fitted with a reflux condenser. The arrangement provides a continuous condensation of solvent vapour into the thimble, and extracts the oligomers which sieve through the porous thimble back into the bulk solvent flask. This process is automatically repeated until complete extraction was effected, after which the solvent (chloroform) was evaporated to give solid oligomers.

5.03 Gel Permeation Chromatography

Gel permeation chromatography, GPC, is a rapid technique for separating mixtures of soluble organic species into their different sizes. The separation is made regardless of chemical nature of the species in most cases, and separation of materials of the same chemical structure and different molecular weights are made to good effect. The size parameter involved is the size of the solubilized molecule. Often two materials of different molecular weight and different chemical structure possess the same size in a particular solvent and no separation would be detected unless detectors specific to one component were used. Similarly, molecules of the same molecular weight but different chemical structure may have different effective sizes.

Mechanism of GPC

The separating medium in GPC is usually a porous cross linked polystyrene gel having a mean particle size of 35-75 μ . The gel contains pores which may range from around 30 \AA to 10⁷ \AA in diameter. The gel is packed into tubes and is retained with fine sinters at either end and are commonly called columns. These columns when in use are maintained saturated with solvent which flows through continuously. When a polymer solution is passed through the column, the dissolved molecules "permeate" into and out of the gel pores. The molecules are only able to enter the gel pores that are large enough to accept them. Hence a separation will be effected through the difference in pore volume available to each species. The larger molecules will pass through the

column fairly quickly with the time of elution becoming progressively slower for the smaller molecules. This is illustrated in Figure 5.1. The residence time of each species in the column is measured from the quantity of solvent emerging from the columns from the point of injection, i.e. the "retention volume" or "elution volume".

The use of particular dextran gels for separations according to size was first introduced by Porath and Flodin⁽⁶⁸⁾ in a process termed gel filtration chromatography and has found many applications in Biochemistry. It is however the technique of gel permeation chromatography (GPC) introduced by Moore⁽⁶⁹⁾ in 1964 that has proved to be a versatile tool for fractionation of a homologous series of macromolecules according to size. The technique is now applied not only in the determination of molecular weight distribution of polymers, but also in the separation of organic compounds and oligomers. For example, low-molecular weight homologs of poly(ethylene glycol) have been separated using cross-linked dextran gels (Sephadex)⁽⁷⁰⁾; and higher oligomers in several polyamides have been isolated on a preparative scale using Sephadex G 25 and Bio-Gel P-10⁽⁷¹⁾. Determann et al⁽⁷²⁾ also prepared a copolymer of methyl methacrylate and ethyl glycol dimethacrylate which they successfully used for fractionation of low-molecular weight polystyrenes. Heitz et al⁽⁷³⁾ also fractionated oligophenylenes and oligourethanes using several cross linked gels.

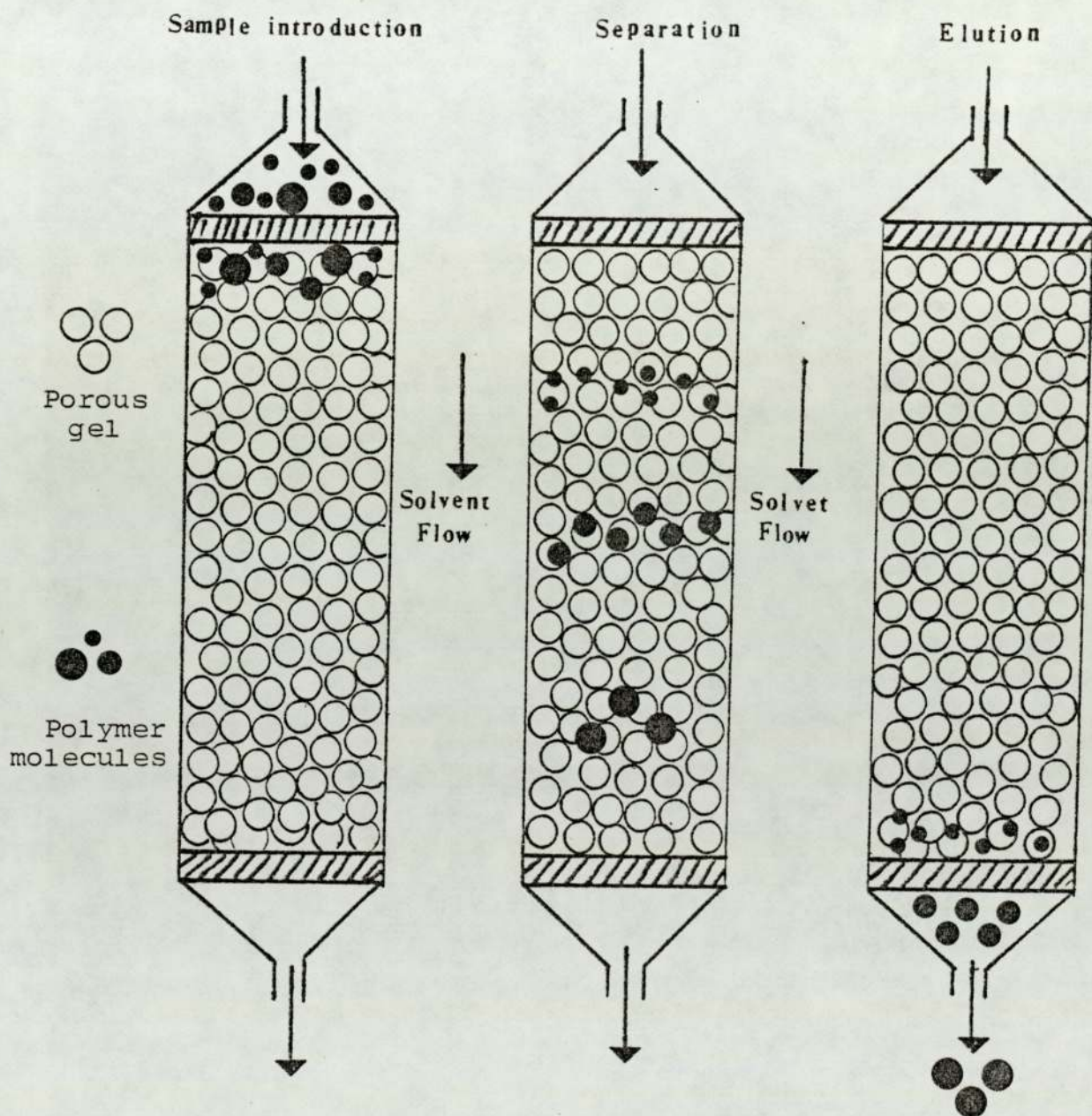


Figure 5.1 Mode of separation in GPC

5.04 Gel Permeation Chromatograph

The basic essential components of the gel permeation chromatograph used for this work are: a solvent delivery system, a column unit with a syringe loading sample injector, a detector system for monitoring flow and concentration, a chart recorder to continuously monitor solute concentration and an automatic fraction collector.

The solvent delivery system consists of a large solvent reservoir (to minimise fluctuations in solvent quality), a solvent filter, a system of teflon and steel connection tubes and a pump.

ACS-HDLC Model 300 Pump: The pump is a single-head reciprocating type, with a unique feature of controlling and eliminating all pulses without increasing the dead volume. Changes in flow rate are achieved by changing piston stroke length, but is so arranged that the maximum extension of its piston is constant thus ensuring the emptying of liquid in its cylinder at each stroke. Because its piston stroke is very rapid (23 per second), much greater than the systems response, no pulsations are observed. Its flow control system incorporates automatic feedback which measures the actual flow at each stroke and automatically adjusts the piston stroke length thereby compensating for any variations in solvent compressability or back pressure.

Syringe.Loading Sample Injector: The sample injector employed was the Rheodyne model 7125. It consists of a six-

port sample injection valve in which loading of sample loop is accomplished with a syringe through a needle port built into the valve shaft. Figure 5.2 shows the flow diagram of the valve. The view is of the stator-rotor interface, where flow switching takes place, as seen from the front of the injector. The six small circles represent the ports in the valve stator (rear of injector). The two heavy arcs represent the connecting passages in the rotor. The large circle represents the needle port (front of injector). The needle port is used to fill the sample loop in the load position. In the inject position the loop is switched into the solvent stream and the needle port is vented through valve port 5. Rotation of the knob through 60° switches the valve from load to inject position. Two methods of loading samples can be used with the injector: the complete loop filling method and partial loop filling method. The complete loop filling method is most widely adapted and it employs the use of excess sample to insure that the sample loop is completely filled. The volume of sample is then determined precisely by the loop volume to give a high degree of precision. The partially filling method is used only when small quantities of sample are available. A microsyringe is used to determine the volume of sample delivered to the loop. It is possible with this method to inject samples ranging from less than one microlitre up to approximately 50% of the loop capacity and the injector is capable of accommodating sample loops ranging from 10 microlitre capacity up to 2 millilitres.

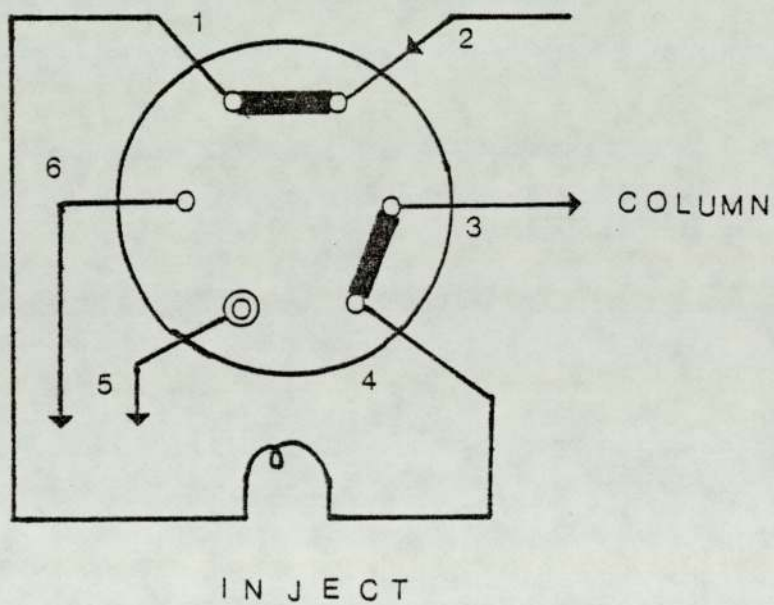
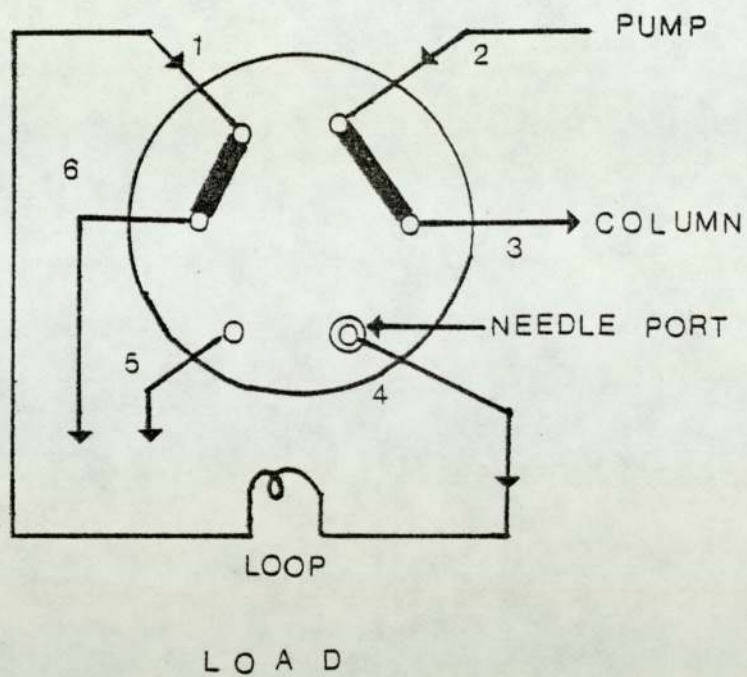


Figure 5.2 Model 7125 Flow diagram

5.05 Column Systems

Two types of columns were adapted for this work and were designated as systems C1 and C2. The column system C1, was designed and built in the Department of Chemistry. It consists of a cylindrical glass tube 1 cm in diameter and 180 cm long. Attached to the upper end of the tube is a 250 cm³ solvent reservoir and at the bottom end is fitted an adaptor for connecting the narrow bore steel tubing to a spectromonitor equipped with a flow cell. The material used for packing this column was sephadex LH-20 obtained from Pharmacia Fine Chemicals. Dry gels of sephadex LH-20 were first suspended in chloroform for 24 hours to form swollen gels. The column was mounted vertically and small pieces of glass wool were laid over the outlet capillaries. A slurry of the swollen gel was then packed into the column by introducing it gently at the top and gradually draining off the chloroform until a continuous gel was formed. Separation was effected by simple gravimetric flow through the column. The solvent reservoir provided a continuous stream of the liquid phase with an elution rate of ca. 30 cm³ per hour.

Column system C2 (SR 25/100) was obtained from Pharmacia Fine Chemicals. It is suitable for all kinds of liquid chromatography in aqueous or organic solvents. Each column is complete with two flow adaptors for perfect bed protection and easy sample application and allows the use of recycling chromatography, upward flow elution and columns in series. The column is capable of resisting pressures up to

1 Kg cm⁻² (14 psi) and can be used at temperatures up to 60°C.

5.06 Packing Material (Sephadex LH20 and LH60)

The packing materials used for the columns are Sephadex LH 20 and LH 60 obtained from Pharmacia Chemicals. These are highly cross linked dextran gels which swell in both aqueous and organic solvents. They have wide applicability in the fractionation of lipids, steroids, fatty acid, hormones, vitamins, oligomers and other small molecules. Apart from gel filtration in organic solvents, Sephadex LH 20 and LH 60 are useful for adsorption and partition chromatography. The Sephadex LH 60 has a higher fractionation range while the Sephadex LH 20 has a stronger adsorptive property for aromatic and polycyclic compounds.

Spectromonitor(HPLC MONITOR 750-11): The spectromonitor used for sample detection was HPLC Monitor 750-11 obtained from Applied Chromatography Systems. It is characterised by its selectable wavelength range, by the use of filter cassettes, in the range 200 nm to 300 nm. It has a wide spectral range deuterium lamp as a source of UV light, and the filters allow the transmission of the UV light beam at the wavelength selected through a sample cell to a detector. The sample cell has an inlet, for connection to the chromatographic column, at the bottom of the cell and an outlet to a fraction collector. Absorbance range selection is push button controlled on the front panel of the monitor giving 0.005, 0.01, 0.02, 0.05, 0.1, 0.2, 1.0 and 2.0 absorbance units (AU) full scale on a 10 mV recorder.

Fraction Collector (Frac-100): The fraction collector employed was the Pharmacia Fine Chemicals fraction collector model, Frac-100. It is a versatile instrument for automatic fraction collection and evaluation of chromatograms. In its standard form it can collect up to 95 fractions in tubes with diameters 10-18 mm. When connected to a suitable monitor, it can measure peak heights, areas and elution volumes or times for up to 11 peaks as well as indicating into which tubes the peaks have been collected.

Fractions can be collected in a variety of different ways, based either on time or volume and is controlled via simple specified programs. For example uniform fractions of fixed time can be collected until all tubes are used up and then the Frac-100 automatically switches off. In other collection sequences, an induction period could be specified before collection. The liquid corresponding to the induction period is then collected in a separate container from the collection tubes. Collections may be done by collecting peaks in smaller fixed fractions than the main part of the eluents, thus readily providing a means of distinguishing between tubes containing peaks and those without. Collection may also be done only for peaks, while the remaining part of the eluent is allowed to run into a separate container. The fraction collector may either be time or volume programmed to switch itself and a connected pump off automatically.

Chart recorder: The chart recorder used was the Knauer Single-channel recorder No.41.20.00. It has the special feature of automatically doubling its chart width from 25 to

50 cm via a polarity change, if the signal to be measured exceeds the maximum input voltage corresponding to full-scale deflection. A block diagram illustrating the principal components of the chromatograph is shown in Figure 5.3. The operation of the instrument is as follows: The eluent (chloroform) was drawn from the solvent reservoir, filtered and then pumped through the sample columns, into and out of the UV detector. The operating pressure and hence the flow rate is controlled by a press button system on the front panel of the pump. Where the use of more than one column was necessary, the columns were connected in series by a narrow bore teflon tubing. Measured quantities of samples were loaded into the column via the sample loading injector. Detection of the separated components was based upon their absorption of UV light at a fixed wavelength (254 nm). The absorptions are automatically traced into chromatograms by the chart recorder which is connected to the detector.

5.07 GPC Chromatograms

Chromatograms were obtained using the two column systems C1 and C2 on oligomers extracted from the polymers. These column systems gave similar chromatograms in terms of resolution when packed with Sephadex LH-20 in both cases. Packing with Sephadex LH-60 produces chromatograms different in terms of resolution to the Sephadex LH-20. We found rather unexpectedly, that using two columns in series in the C2 system does not improve the resolution. This is rather surprising because connecting two columns in series would effectively increase the number of theoretical plates and

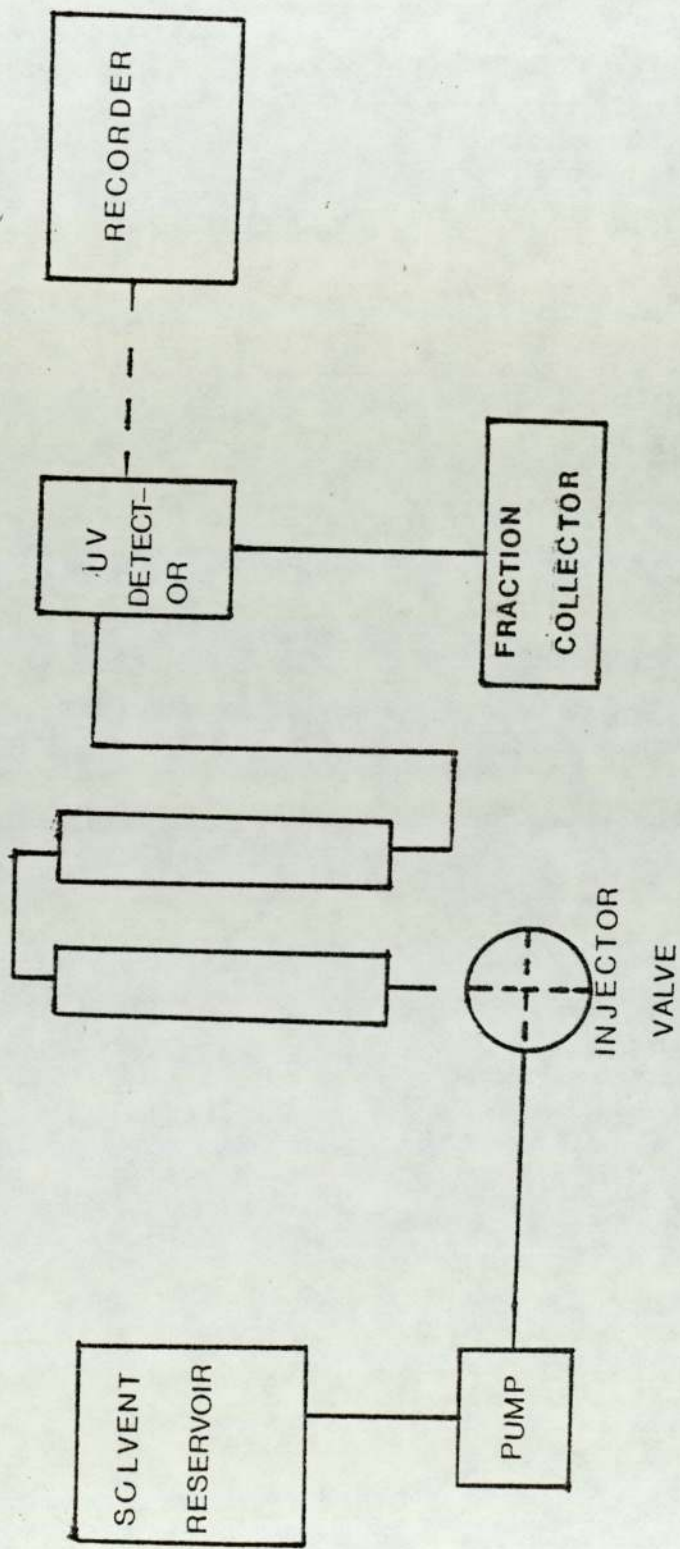


Figure 5.3 Block diagram of the gel permeation chromatograph

therefore be expected to improve on resolution of a single column.

Figure 5.4 shows the chromatogram of the phenylene oligomers extracted from P1 using the column system C1. The chromatogram was obtained at room temperature (299°K) using an elution rate of 30 cm^3 per hour. The spectromonitor was set at a fixed wavelength of 275 nm and a sensitivity of 0.5 AUFS. Chart recorder speed was 120 mm per hour and set at 10 mV fsd. The chromatogram indicates five distinct peaks with peak elution volumes: $\text{Ve}_1 = 95$; $\text{Ve}_2 = 102$; $\text{Ve}_3 = 107$; $\text{Ve}_4 = 114$ and $\text{Ve}_5 = 124\text{ cm}^3$. To identify the various peaks, the chromatogram was spiked with standard oligomer compounds. This was done by individually adding the pure model compounds of biphenyl, p-terphenyl, p-quarterphenyl and p-quinquiphenyl to the oligomer extract and a chromatogram for each spiked sample was obtained.

A reinforcement of peaks 5, 4, 3 and 2 by biphenyl, p-terphenyl, p-quarterphenyl and p-quinquiphenyl respectively suggested their presence in the extract. A plot of the logarithms of molecular weights of the model compounds against their peak elution volume produced a straight line (See Figure 5.5). This observation suggests a homologous series of compounds in the extract. The chromatograms were not sufficiently well resolved to enable isolation of the individual components. This problem was further complicated by the rather broad peak on top of which the narrower component peaks appear to be located. An attempt to obtain better resolution using the C2 type column system was not

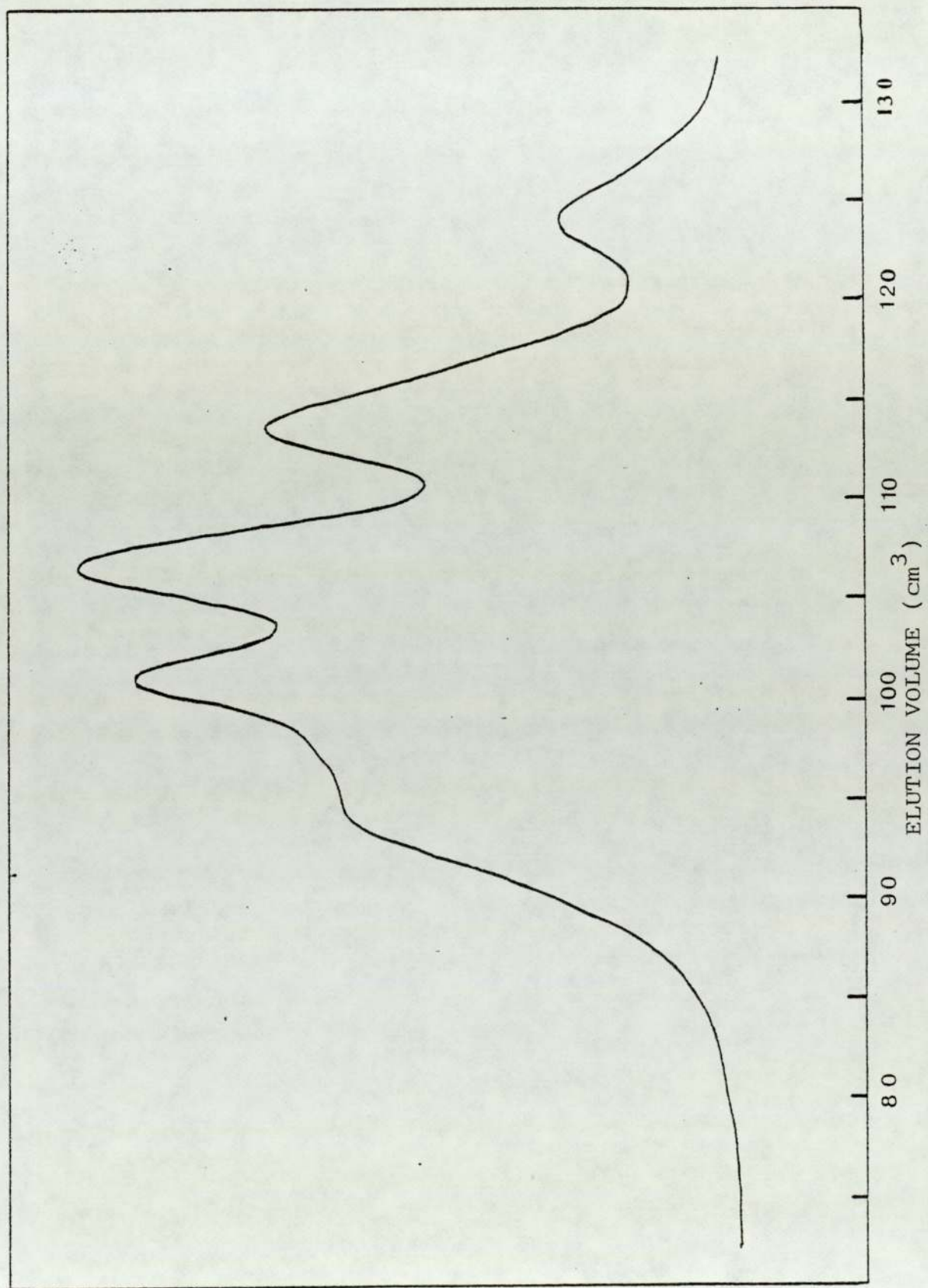


Figure 5.4 GPC chromatogram of oligomer extract from P1 (Cl, Sephadex LH-20) at 299 K

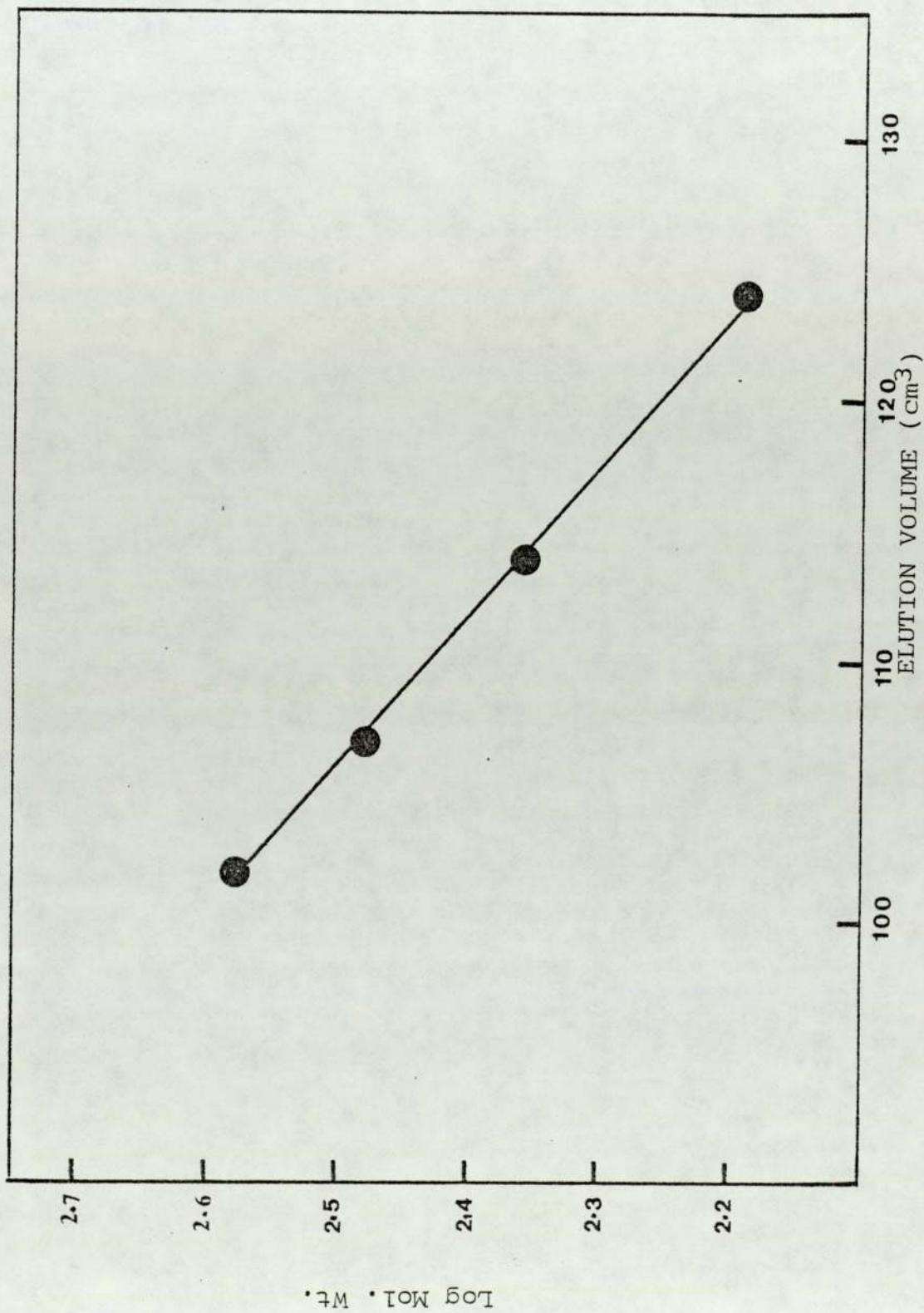


Figure 5.5. Plots of logarithm of molecular weight versus peak elution volume for oligomer extract from P1

successful. The poor resolution observed even with the lengthening of column (Two C2 columns connected in series) could be due to peak broadening by diffusion or caused by the presence of dead volumes often encountered in GPC systems.

Figure 5.6 shows the GPC chromatograms of oligophenylenes obtained using column system C1 on extract from P3. It indicates distinct peaks 5 and 4 and broad and less distinct peaks designated 1, 2 and 3. The distinct peaks 4 and 5 were identified as previously to be terphenyl and biphenyl respectively, but the broadening and overlap in the case of peaks 1-3 made identification impossible. An interesting observation is the peak elution volume V_{e1} (corresponding to peak 1), it was the same as the exclusion volume (V_o) of the column. This could be the reason for the non-resolution of peaks at the higher molecular weight end of the chromatogram. It also provided information that oligophenylenes large enough to be excluded from the column but sufficiently soluble in chloroform were extracted. A chromatogram of oligomers from the P3 extract was also obtained using the column system C2. This is shown in Figure 5.7 and is very similar in terms of resolution to that obtained using C1 (see Figure 5.6). The peaks 2, 3, 4 and 5 in the chromatogram were identified (by spiking with the model compounds) as p-quinquiphenyl, p-quarterphenyl, p-terphenyl and biphenyl respectively. Peak 1 represents oligomers that are excluded from the column. It is clear from Figures 5.6 and 5.7 that there is little difference in resolution between C1 and C2 systems. A trial run using the C2 system employing two columns in series did not produce any change in resolut-

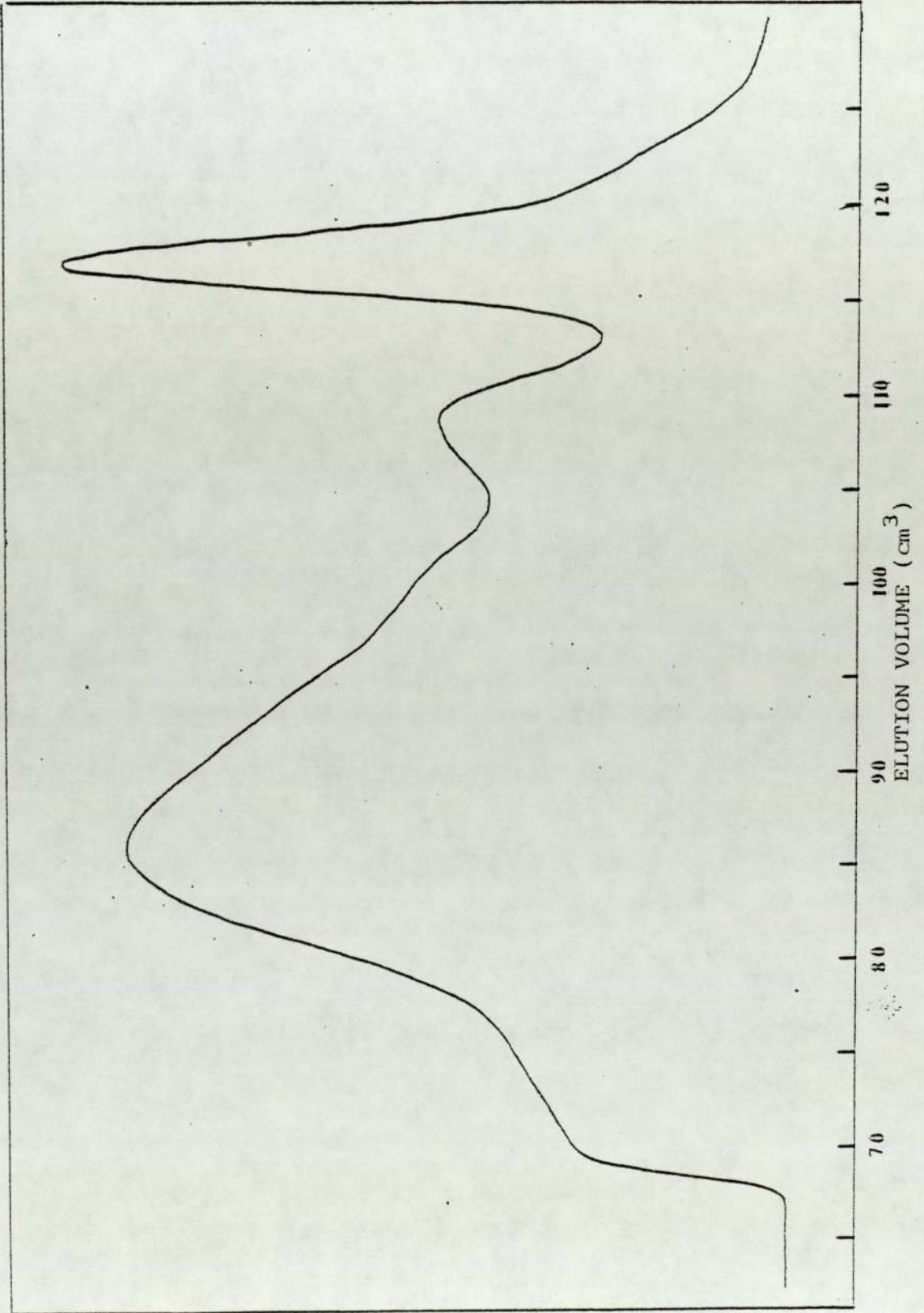


Figure 5.6 GPC chromatogram of oligomer extract from P3 (C1, Sephadex LH-20) at 298 K

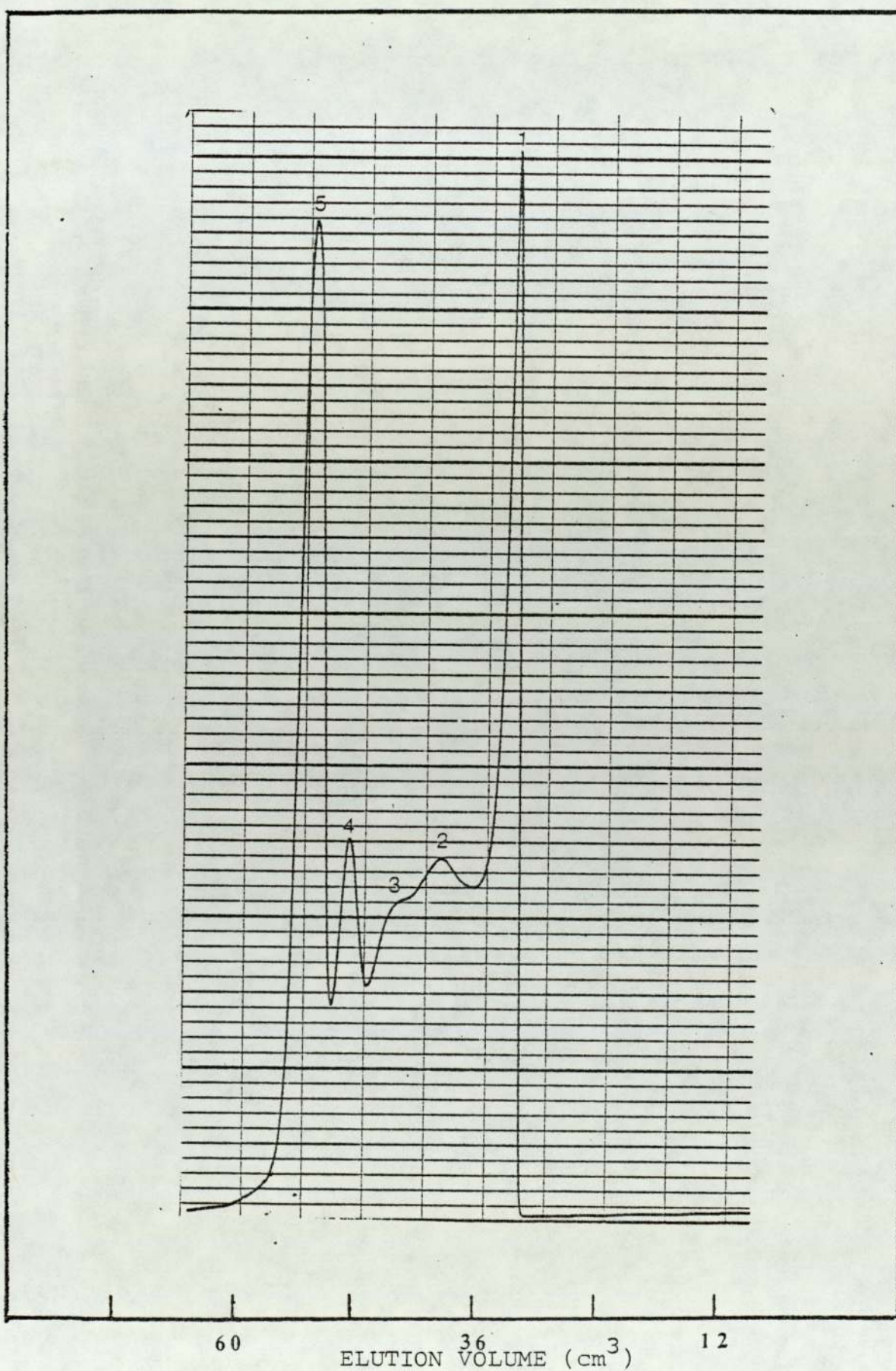


Figure 5.7 GPC chromatogram of oligomer extract from P3
at 298 K
(C2 System, Sephadex LH-20)

ion as explained previously.

The column system C2 was packed with Sephadex LH-60 and used to separate oligomers from the P3 extract. Figure 5.8 shows the GPC chromatogram obtained and it shows quite clearly that Sephadex LH-60 was not as capable of separating the oligomers as Sephadex LH-20. It was however, capable of isolating the higher molecular weight oligomers (peak 1, which are also excluded from the column) from the lower molecular weight portions (peak 2).

Figure 5.9 shows the chromatogram of oligophenylenes extracted from polymer P4 obtained using the column system C1 packed with Sephadex LH-20. The chromatogram indicates six distinct peaks labelled 1-6, with peak elution volumes; 75, 82, 87, 96, 107 and 118 cm³ respectively. Peaks 3, 4, 5 and 6 were identified by spiking with model compounds to be p-quinquiphenyl, p-quarterphenyl, p-terphenyl and biphenyl respectively. A plot of logarithms of molecular weights of these model compounds against the peak elution volumes was constructed and gave a straight line as shown in Figure 5.10, suggesting that the components eluting are members of a homologous series. An important feature of Figure 5.9 is that the peaks appear well resolved compared to the previous cases (i.e. Figures 5.4 and 5.6). This appears to suggest that the polymerization of biphenyl (to produce P4) is a cleaner process than the bulk and solvent polymerisation of benzene. It is rather surprising that p-terphenyl and p-quinquiphenyl peaks appear in the GPC chromatogram (Figure 5.9), because if the polymerization occurred only by an

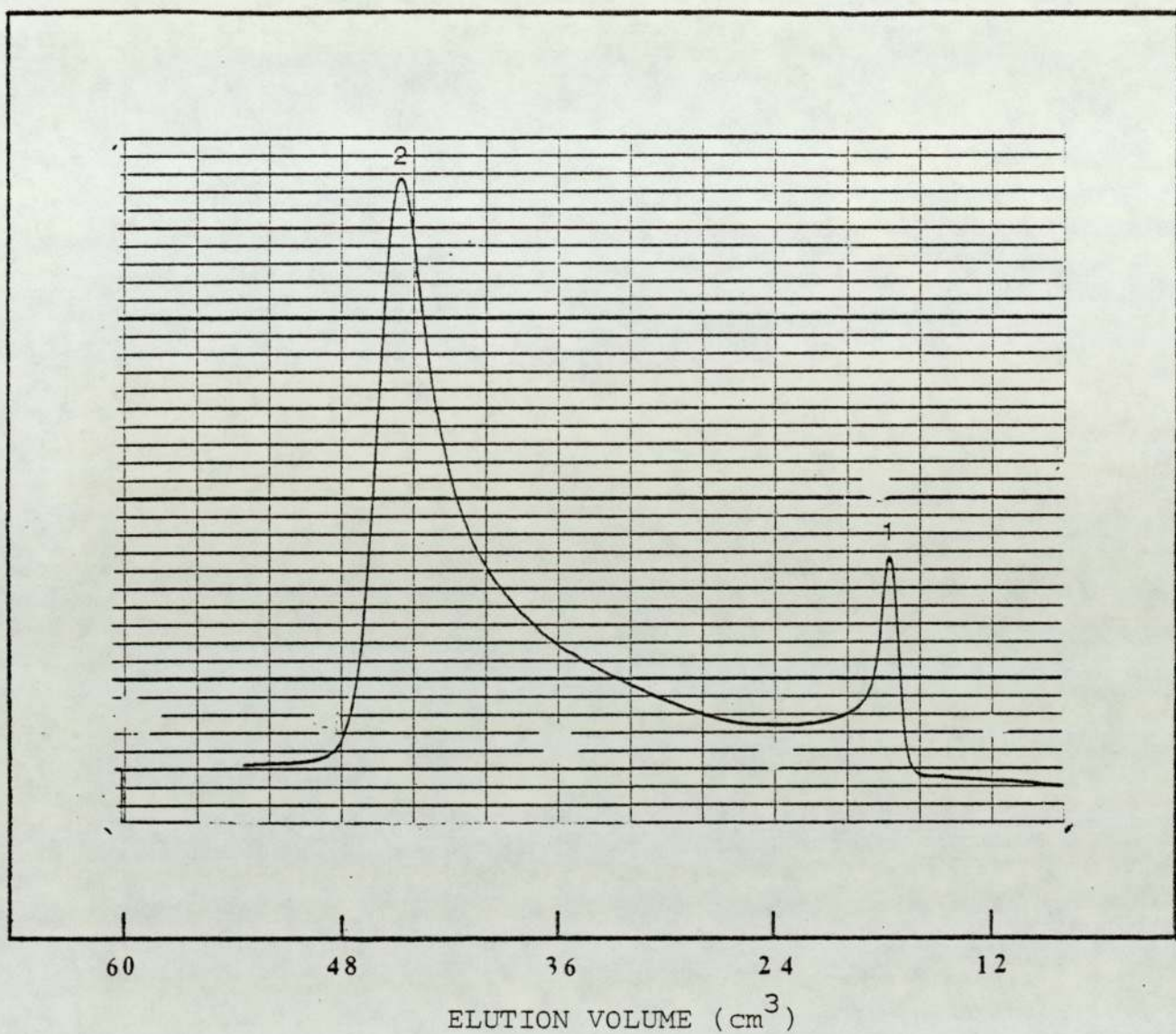
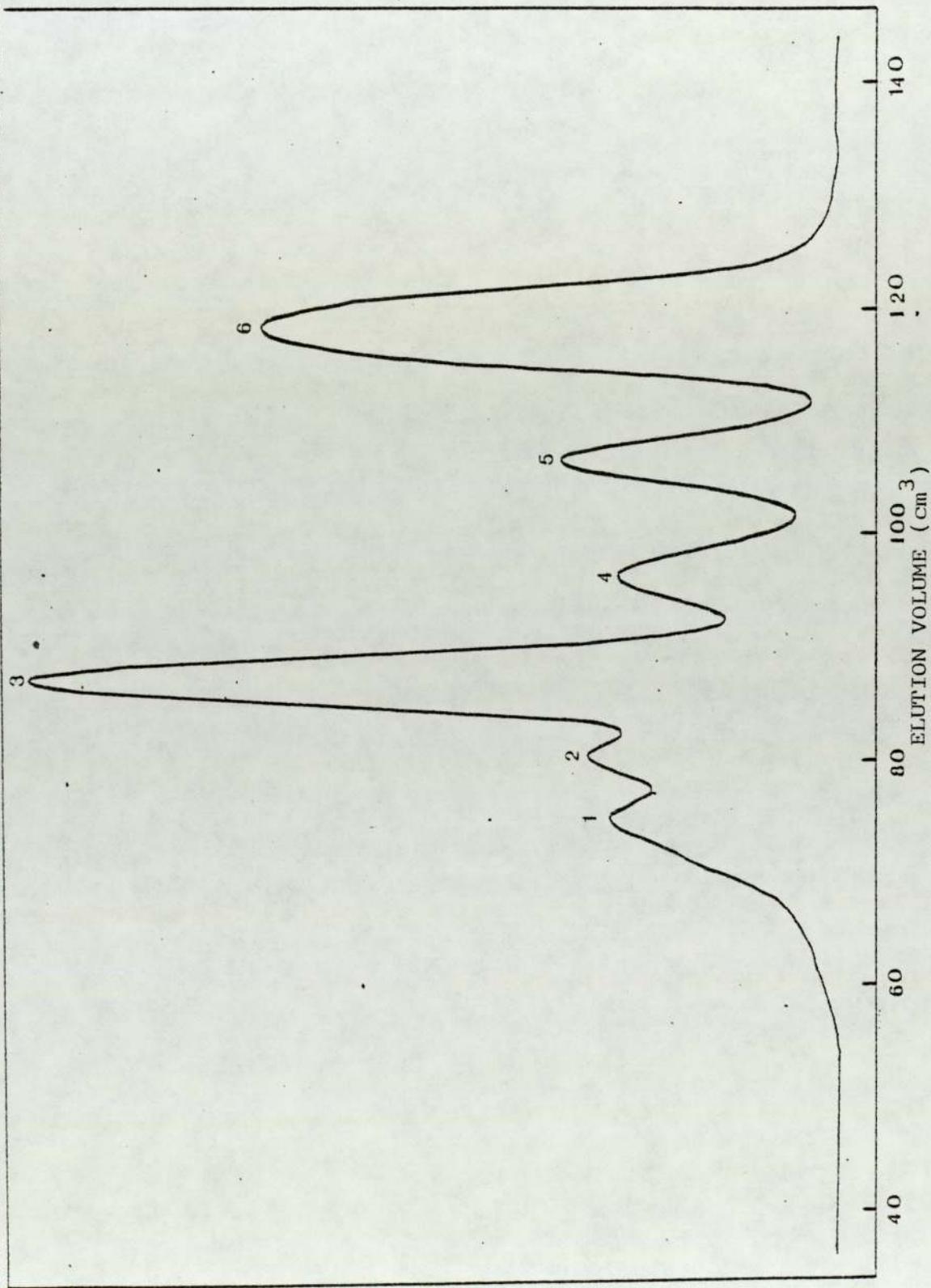


Figure 5.8 GPC chromatogram of oligomer extract from P3 at 298 K (C2, Sephadex LH-60)

Figure 5.9 GPC chromatogram of oligomer extract from P4 (Cl, Sephadex LH20) at 298 K



irreversible stepwise addition of biphenyl to the propagating species, it would not be expected to produce terphenyl and quinquiphenyl. This observation therefore suggests the existence of a reversible depolymerization process. Although the peaks appeared well-resolved in the chromatogram, collection based on the peaks (except biphenyl peak 6) did not produce single components as shown by their individual U.V spectrum. Although peaks 1 and 2 were not identified by the spiking experiment, they were assumed to be the next two higher members in the series and are seen to fit well in Figure 5.10.

A chromatogram for the oligomer extract from P4 was also obtained using the C2 column system packed with Sephadex LH-20. This is shown in Figure 5.11 and exhibited similar resolution to the one obtained using the C1 system (Figure 5.9).

In Figure 5.11 the peaks 1, 2, 3 and 4 were identified by spiking with the model compounds as p-quinquiphenyl, p-quarterphenyl, p-terphenyl and biphenyl respectively. The two additional peaks corresponding to hexaphenyl and heptaphenyl observed previously in Figure 5.9 appear to be absent or present only in very small concentration in Figure 5.11. The analysis of the chromatogram shown in Figure 5.11 was monitored at a fixed wavelength 254 nm, a region where the hexaphenyl and heptaphenyl have no appreciable absorptions.

Figure 5.12 shows the GPC chromatogram of oligomers obtained using column system C2 to analyse the extract from

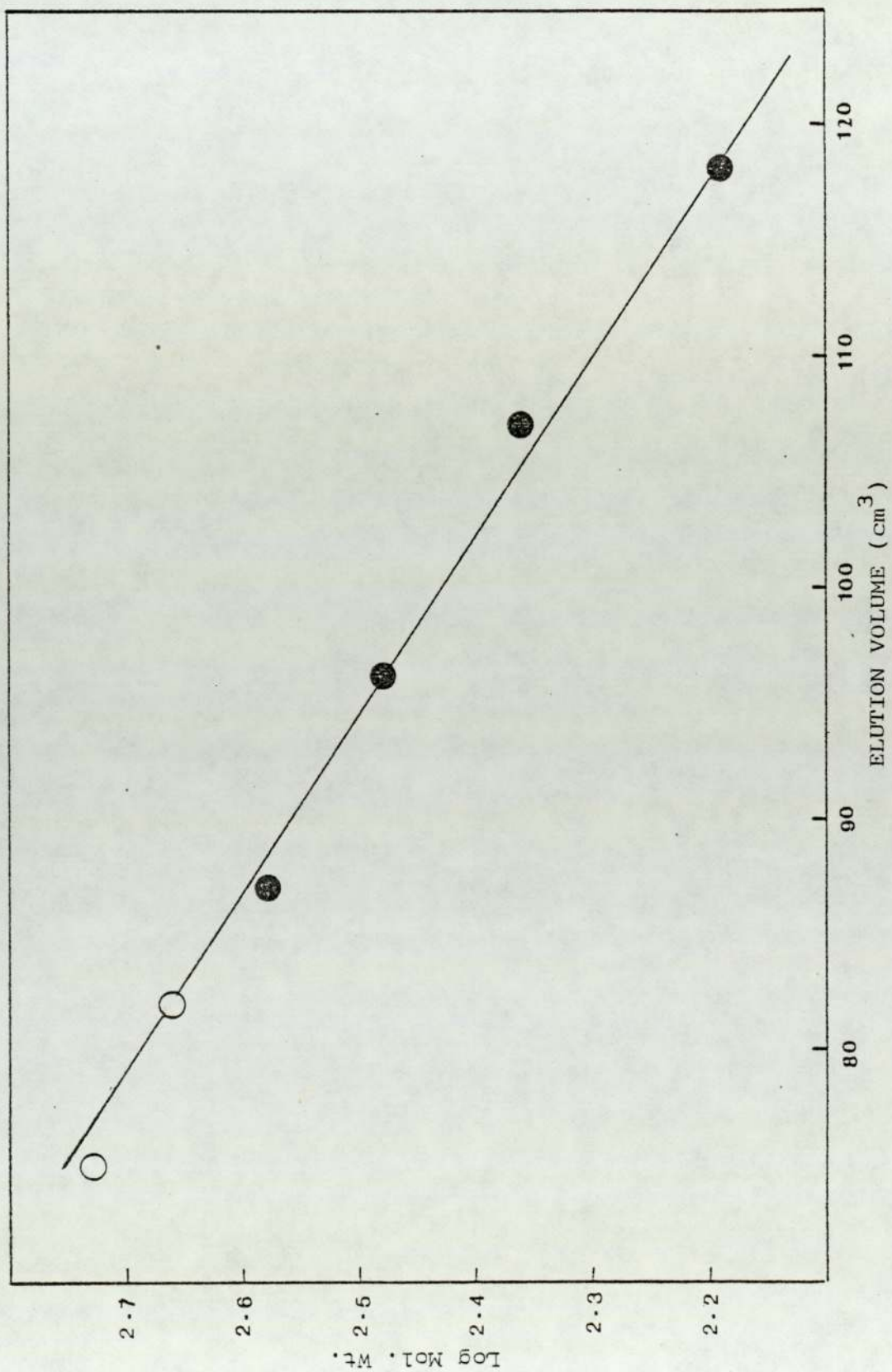


Figure 5.10 Plots of logarithm of molecular weight versus peak elution volume for oligomer extract from P4. ○ Correspond to Hexa- and Hepta phenyl

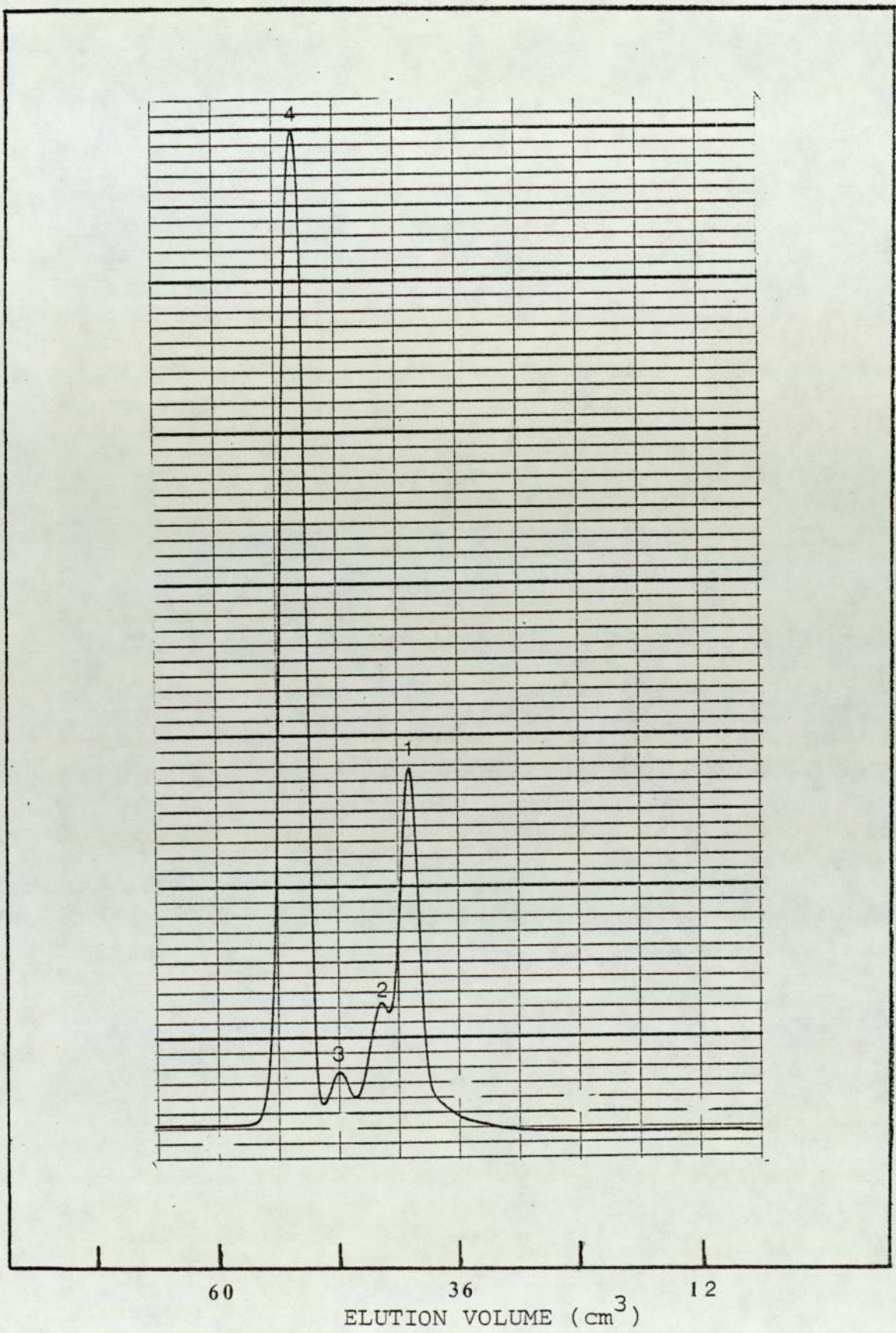


Figure 5.11 GPC chromatogram of oligomer extract from P4 at 298 K (C2 System with Sephadex LH-20)

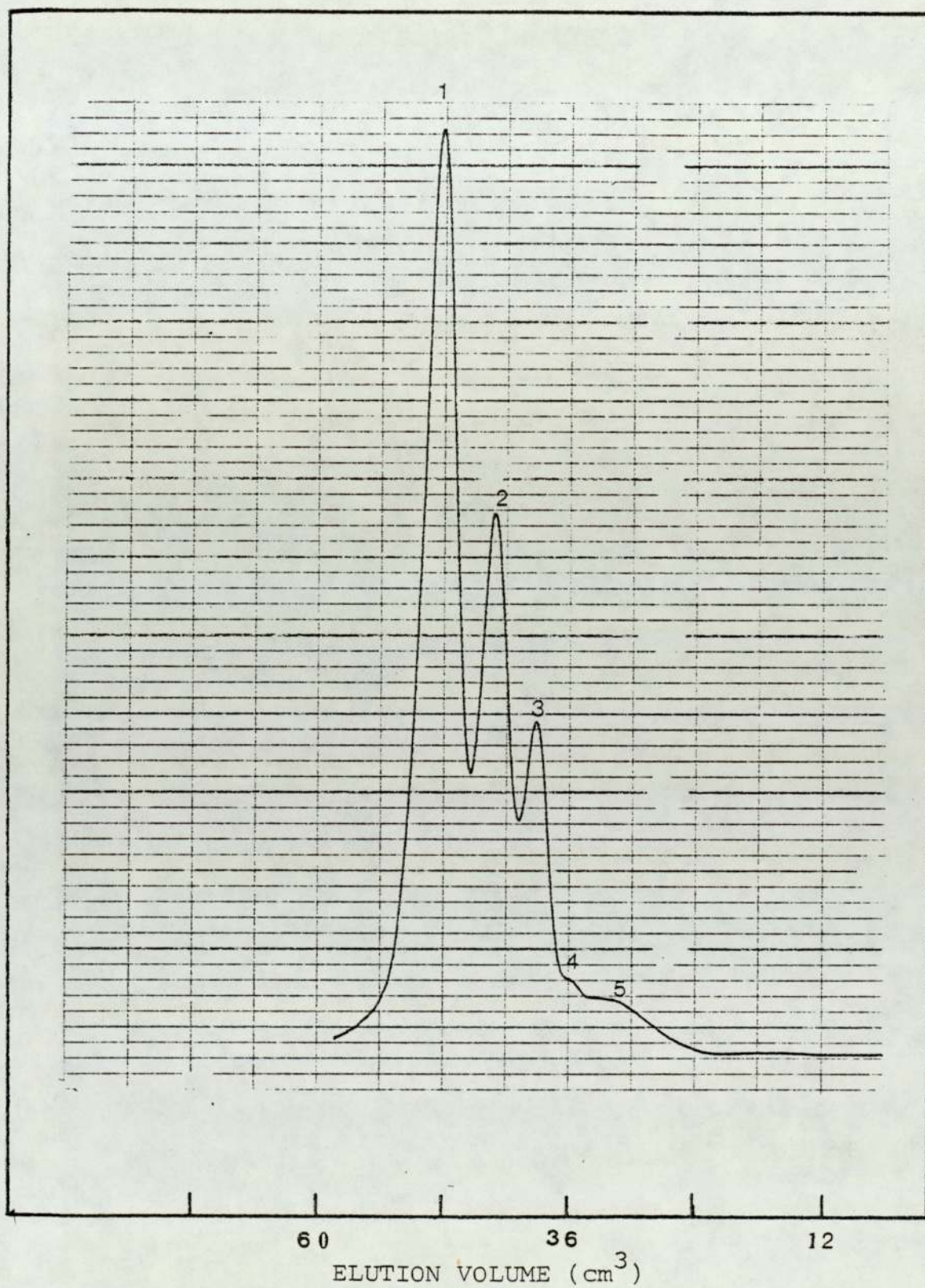


Figure 5.12 GPC chromatogram of oligomer extract from P7 (C2, Sephadex LH-20) at 298 K

P7. It shows three distinct peaks 1, 2 and 3 and two shoulders 4 and 5. Peaks 1, 2 and 3 were identified through spiking with model compounds as biphenyl, p-terphenyl and p-quarterphenyl respectively. Although the shoulders 4 and 5 were not identified by the spiking experiment, they appear to be the next two higher members of the series. Collection based on peaks was carried out on peaks 1, 2 and 3 and their individual U.V spectrum was determined using a **pye** Unicam Sp 800. The U.V spectrum of these peaks suggested single components with λ_{\max} positions at 260, 292 and 305nm for the peaks 1, 2 and 3 respectively. The absorption maxima of these peaks shows a shift to higher values compared with the corresponding pure model compounds (measured λ_{\max} for biphenyl, p-terphenyl and p-quarterphenyl are 250, 279 and ²⁹⁷279 nm respectively). A comparison of λ_{\max} positions for the model compounds and the corresponding individual peaks from Figure 5.12 is shown in Figure 5.13. The model compounds have a lower λ_{\max} value. This is expected because elemental analysis on P7 indicated substantial presence of bromine (30.5%) which could only be present as substituents in the polymer. Such bromine substitution would produce a bathochromic shift in λ_{\max} position from that of the corresponding unsubstituted polymer and hence the effect will also be reflected in the oligomers extracted from the polymers.

5.08 Gas Liquid Chromatography

Gas-liquid chromatography (GLC) first proposed by Martin and Synge⁽⁷⁴⁾ as a suitable method for separating volatile compounds has since developed into a highly automated tech-

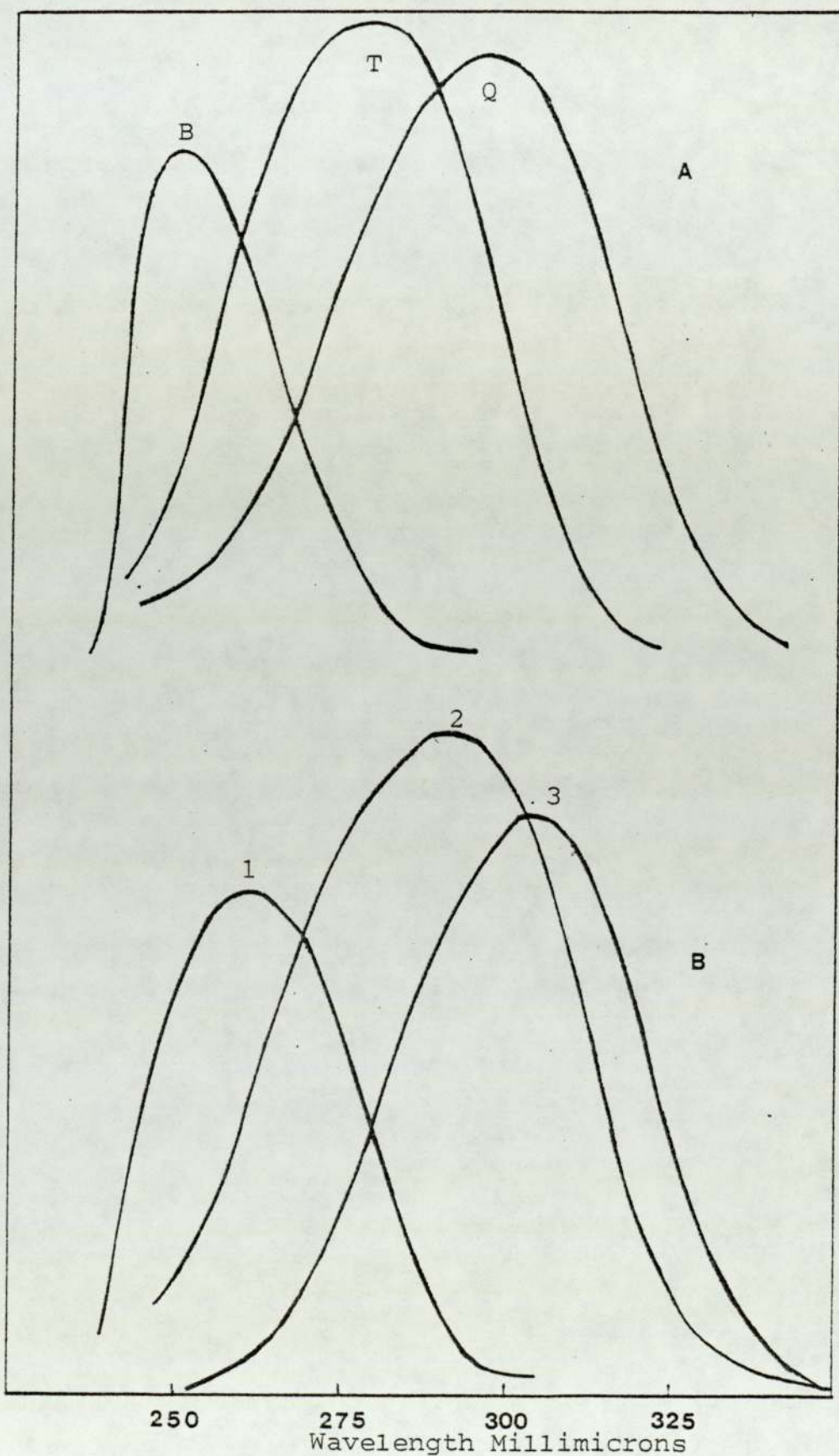


Figure 5.13 (A) U.V. spectra of model compounds
 (Biphenyl, terphenyl and quarterphenyl)
 (B) U.V. spectra of peaks 1,2 and 3 from Fig.5.12

nique with a variety of applications. The fundamental principles, however, have remained the same. Samples or mixtures, whose components are required to be separated, are volatilised in a carrier gas and then passed through a column which is packed with a finely-sieved, inert, granular material. The latter serves as a support for a thin, liquid layer, which acts as a solvent for the sample components. The degree of separation of these components depends upon differences in their distribution partition coefficients between the mobile gas phase and the stationary liquid phase. The separated components emerge from the column and pass through a suitable detector producing an electrical signal which is fed into an amplifier/recorder system.

The chromatograph used in this work was the Pye Unicam GCD chromatograph. This was fitted with a dual high vacuum silicon grease column (12 ft long on glass-phase prep A60-85 mesh). The chromatograph employed a flame ionization detector.

The GLC chromatography was employed in this work to investigate the presence of any species other than oligomers in the chloroform extract of the polymers. Figure 5.14 shows the GLC chromatogram of the oligomer extract from polymer P3. A systematic spiking of the extract with standard compounds led to the identification of some of the peaks as shown. Peaks arising due to impurities from the column were also identified by a blank run on the column and are marked 'X' in Figure 5.14. There are however some species as indicated on the chromatogram which were not identified. This tends to

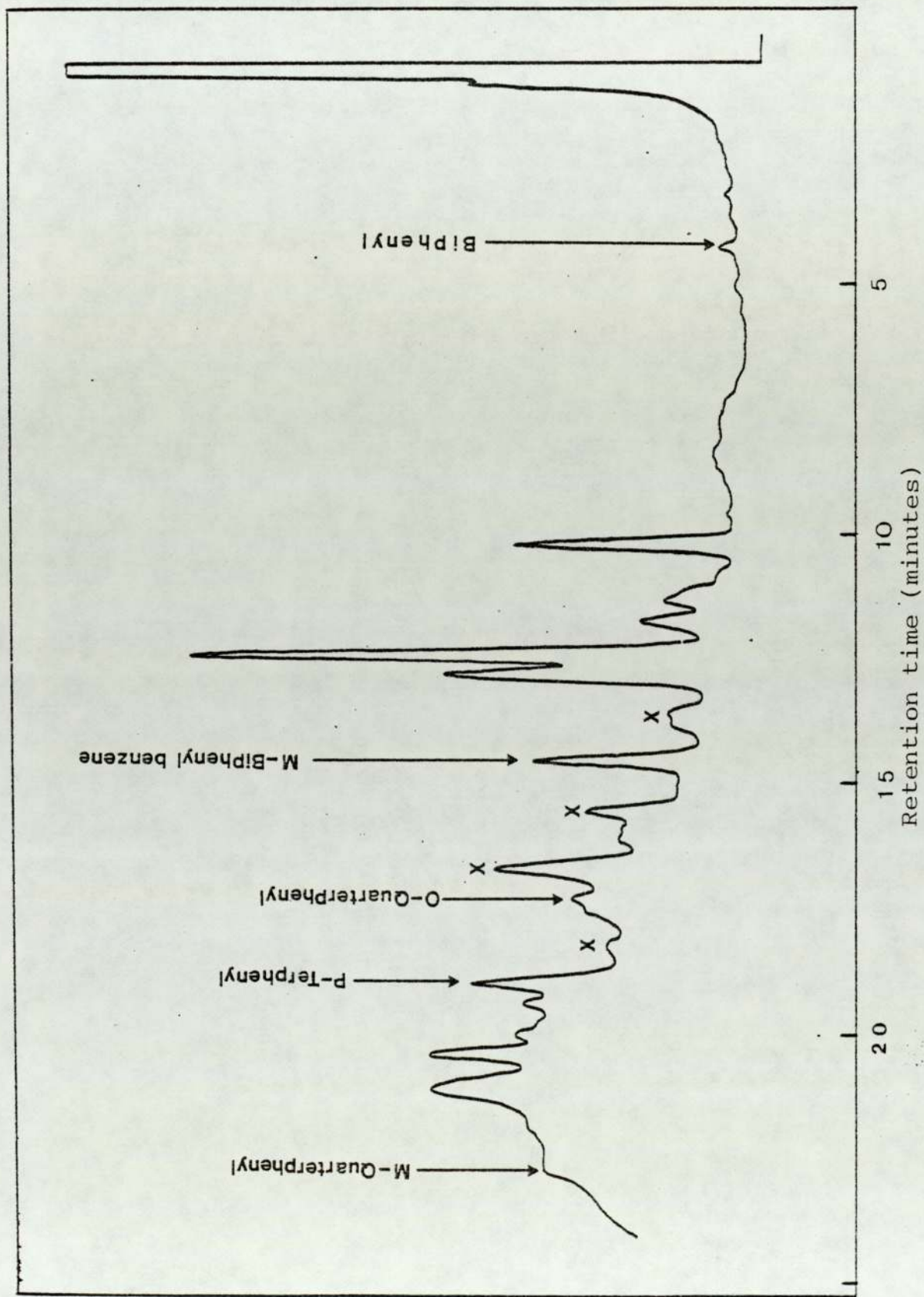


Figure 5.14 GLC chromatogram of oligomer extract from P3

suggest that the benzene polymerization according to the Kovacic method is not an entirely 'clean' process since some species in addition to the pure polymer and oligomers seem to be produced.

5.09 Vapour Pressure Osmometry

The average molecular weight of the chloroform soluble portions (oligophenylenes) from the polymers was determined with a Mechrolab 301 A vapour pressure osmometer using chloroform as solvent at 298^oK.

Molecular weight determination was first carried out on a molecule of known molecular weight (m-biphenyl benzene) to check the accuracy of the instrument. The molecular weight measured for m-biphenyl benzene was 227 and compares favourably with the actual molecular weight of 230.

Measurements under the same conditions were carried out to determine the average molecular weight of oligophenylenes from the polymers. The oligomers extracted from P3 gave an average molecular weight of 839 which corresponded to 11 phenylene units while oligomers extracted from P4 gave an average molecular weight of 341 and therefore correspond to an average of 3-4 phenylene units.

Dielectric and Kerr Effect Studies of Aryl-Iodine
and Aryl-Tetracyanoquinodimethane Complexes

6.01 Introduction

It is well known that iodine solutions may be either violet or brown depending on the nature of the solvent. The halogen is violet in media such as the aliphatic hydrocarbons and carbon tetrachloride, and brown in solvents such as alcohols, ethers, ketones, organic acids etc. The visible absorption maximum of the violet solutions is located in the 520-540 nm region and the overall spectrum is similar to that of iodine in the vapour state. The maximum for brown solutions occur at lower wavelengths (460-480 nm). The ultraviolet and visible spectra of iodine in different solvents have been of interest to chemists for over half a century. Numerous explanations were proposed to account for the 'abnormal' (i.e. non-violet) colouration. Early explanations based on the formation of iodine dimers or complex aggregates, were discounted when Beckmann⁽⁷⁵⁾ demonstrated by cryoscopic methods that dissolved iodine molecules are in the diatomic state regardless of the colour of the solution. He then suggested that the brown colour was characteristic of solvent-solute addition products. Lachmann⁽⁷⁶⁾ supported this explanation pointing out that solvents which give rise to violet colour are unsaturated. He

observed that small additions of alcohol to a solution of iodine in chloroform shift the colour stepwise from violet to brown. Hilderbrand and Glascock⁽⁷⁷⁾ also found that when iodine and an alcohol were both added to a 'violet' solvent (e.g. bromoform or ethylene bromide), the molal lowering of the freezing point was considerably less than additive, indicating combination of iodine with alcohol. Furthermore, they investigated colorimetrically the equilibria of iodine with ethyl alcohol, ethylacetate and nitrobenzene dissolved together in a 'violet' solvent such as carbon tetrachloride, chloroform or carbondisulphide and found in each case an equilibrium constant corresponding to a 1:1 complex. Many workers have since shown curiosity about the chemical basis for the solvation of iodine. Walker⁽⁷⁸⁾ first suggested dipole moment interaction as an explanation, but this was quickly and conclusively discounted by Hilderbrand and Benesi⁽⁷⁹⁾ when they showed that iodine solubility (which would be altered by solvation effects) bears little or no relation to the dipole moment of the solvent molecule. They observed that for molecules such as alcohols, which possess relatively large dipole moments, their effect was readily understandable but the interaction between iodine and benzene (which form a brown colour with iodine) was puzzling, since it was previously considered to be a normal non-polar liquid. These workers suggested the presence of a complex (brown colour) formed via an acid-base interaction and subsequently regarded a donor-acceptor pair, similar to the formation of I_3 from the base I^- and the acid I_2 . Evidence of

such basic character in benzene has long been observed in its interaction with aluminium chloride⁽⁸⁰⁾, sulphur dioxide⁽⁸¹⁾ and trinitrobenzene⁽⁸²⁾. Fairbrother⁽⁸³⁾ also supported this view by reporting that iodine had an abnormally high dielectric polarization in dioxane, isobutylene, p-xylene and benzene and concluded that the high polarization was due to the presence of a solvent - I^+I^- complex. Perhaps the most dramatic contribution relating to the formation of iodine solvent complexes was made by Benesi and Hilderbrand⁽⁷⁹⁾, who examined not only the visible but also the ultraviolet spectra of solutions of iodine in carbontetrachloride, benzene, toluene, xylene and mesitylene. More significant, however, was the discovery of an intense ultraviolet absorption peak for the aromatic hydrocarbon solutions which was absent for solutions of iodine in carbontetrachloride. The position of the ultraviolet absorption maximum in the hydrocarbon solutions ranged from 297 nm for benzene to 333 nm for mesitylene.

The ability of quinones to form stable solid complexes with aromatic amines has been known for many decades⁽⁸⁴⁾. Such complex formation is due to interaction of the electron deficient π -orbital system of the quinone (a π -acid or an acceptor) with the electron rich π -orbitals of the amine (a π -base or a donor). In certain cases, where solid complexes are formed between aromatic diamines and relatively strong π -acids such as polyhaloquinones, strong paramagnetic resonance absorptions⁽⁸⁵⁾ are exhibited

The unique characteristic of the TCNQ as a π -acid derives partly from the high electron affinity of the polyene system conferred by the powerful electron withdrawing effect of the four cyano groups and partly from the planarity and high symmetry of the TCNQ structure. The molecule forms three types of electrically conducting compounds. First, in keeping with its quinoid character, the TCNQ forms crystalline π -complexes (charge-transfer complexes) with aromatic hydrocarbons, amines and polyhydric phenols. These complexes are characterised by intermediate to high resistivity (10^3 to 10^{14} ohm cm). The TCNQ also forms two series of stable, salt-like derivatives, each involving complete transfer of an electron to TCNQ with the formation of the anion-radical. Simple salts, thus formed, could be represented by the formula $m^{+n}(\text{TCNQ}^{\cdot-})_n$, in which 'm' may be a metallic or organic cation, and are characterised by resistivities in the range 10^4 to 10^{12} ohm cm. In some cases, the salt formed is of the type $m^{+n}(\text{TCNQ}^{\cdot-})_n(\text{TCNQ})$ in which a molecule of formally neutral TCNQ is present in addition to the radical-anion $\text{TCNQ}^{\cdot-}$. This type of complex are characterised by low electrical resistivities (10^{-2} to 10^3 ohm cm)⁽⁸⁶⁾.

TCNQ: π -complexes: In most organic solvents, the complexes formed between TCNQ and suitable donor compounds are much less soluble than either of the individual components thereby permitting their isolation. With very few exceptions these are found to be 1:1 complexes and are usually obtained by adding solutions of the donor to

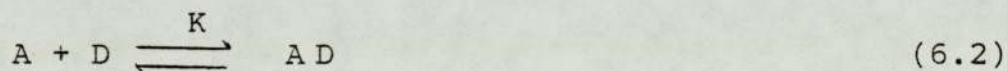
solutions of TCNQ in solvents such as tetrahydrofuran, chloroform and dichloromethane. These 1:1 complexes generally have interesting electrical properties. Although donors possessing high basicity (i.e. the diamines) have been shown to give highly conductive complexes, no consistent correlation has been made between structure or basicity of the donor and electrical conductivity of the corresponding TCNQ complex. For example, 1:1 p-phenylenediamine-TCNQ complex has a resistivity of about 10^3 ohm cm. On the other hand, N,N,N',N'-tetramethyl-p-phenylenediamine affords a complex with a resistivity of about 10^6 - 10^8 ohm cm even though one would expect the methylated amine to have a higher π -base strength by virtue of hyperconjugative effects⁽⁸⁷⁾. It has been suggested that these differences may be related to molecular packing within crystals and that smaller NH₂ groups of the unmethylated amine allow greater continuity of the donor/acceptor pair with consequently increased π -orbital overlap. This would be expected to present a lower energy barrier to the electron transport required for conductivity. In addition, impurity effects may be important in accounting for these differences.

Both iodine and tetracyanoquinodimethane have been used extensively as dopants to enhance the electrical conductivities of polymeric materials (e.g. iodine doping of polyacetylene and TCNQ doping of poly(N-vinylcarbazole)). These dopants also form complexes with simple aryl compounds. This chapter details an experimental study of

some 'simple' aryl complexes with iodine and TCNQ carried out as preliminary work with a view to understanding the nature of complexes they form with poly(p-phenylene) and poly(N-vinyl carbazole). The static dielectric permittivities and electro-optical Kerr effects of a series of aryl compounds (benzene, toluene, p-, o- and m-xylene) were first measured in the pure state and when complexed with iodine and TCNQ. The complexes were usually prepared by dissolving a fixed amount of the dopants in the various aryl solvents so as to form a binary system.

6.02 Solution Kerr Constants of Aryl-Iodine Complexes

The formation of a complex between the aryl compounds benzene, toluene, p-, o- and m-xylene and iodine can be represented by the following equation



where A, denotes the acceptor (iodine), D the donor (aryl compound), AD the iodine-aryl complex and K is the equilibrium constant.

Therefore
$$K = \frac{[AD]}{[A][D]} \quad (6.3)$$

The quantities [A], [D] and [AD] represent the concentration in moles per litre of uncomplexed iodine, uncomplexed aryl compound and iodine-aryl complex, respectively.

Thus, the total amount of iodine in the system will be

equal to the sum of iodine in the free-state and in the complex form.

$$\text{Hence } [A]_{\text{total}} = [A]_{\text{free}} + [AD] \quad (6.4)$$

$$[A]_{\text{free}} = [A]_{\text{total}} - [AD] \quad (6.5)$$

Substituting equation (6.5) into (6.3) and rearranging gives

$$K[D]_{\text{free}} = \frac{[AD]}{[A]_{\text{total}} - [AD]} \quad (6.6)$$

However the concentration of donor is usually chosen to be in excess of all other components, hence the concentration of the donor is approximately constant. Thus we may write

$$[D]_{\text{free}} \approx [D]_{\text{total}} \quad (6.7)$$

Substituting (6.7) into (6.6) gives

$$K[D]_{\text{total}} = \frac{[AD]}{[A]_{\text{total}} - [AD]} \quad (6.8)$$

Thus (6.8) may be used to calculate the concentration of complex, provided K , $[A]_{\text{total}}$ and $[D]_{\text{total}}$ are known.

For the benzene-iodine system the stoichiometric quantities of benzene $[D]_{\text{total}}$ and iodine $[A]_{\text{total}}$ for a 0.2% (w/v) solution of iodine in benzene are 11.19 mol.l^{-1} and $0.0078 \text{ mol.l}^{-1}$ respectively. Substituting these values into equation (6.8) permits the calculation of the concentration of the benzene-iodine complex $[AD]$, for

a known value of the equilibrium constant, $K(0.21 \text{ mol}^{-1})$,⁽⁸⁸⁾

$$\text{Thus } 0.2 \times 11.19(0.0078 - [\text{AD}]) = [\text{AD}]$$

$$[\text{AD}] = 0.00539 \text{ mol.l}^{-1}$$

$$\text{Hence } [\text{A}]_{\text{free}} = (0.0078 - 0.00539) = 0.0024 \text{ mol.l}^{-1}$$

The amount of free iodine in a 0.2% w/v solution of iodine in benzene is $0.0024 \text{ mol.l}^{-1}$ which implies that the concentration of 1:1 complex (I_2 - benzene) is $0.0078 - 0.0024 = 0.0054 \text{ mol.l}^{-1}$.

The equilibrium constant used in this calculation was determined for a dilute solution of iodine and benzene in n-heptane⁽⁸⁸⁾. This method of calculating the concentration of complex was used to determine the molecular composition of the other aryl-iodine systems.

Solution Molar Kerr Constants ${}_m K_{12}$

Solution molar Kerr constants may be calculated using the equation

$${}_m K_{12} = 6\lambda n_{12} B_{12} M_{12} / (n_{12}^2 + 2)^2 (\epsilon_{12} + 2)^2 d_{12} \quad (6.9)$$

where M_{12} is the molecular weight, n_{12} the refractive index, d_{12} , density of the medium. λ is the wavelength of light employed in the determination of the Kerr constant.

Typical data for benzene- I_2 and CCl_4 - I_2 systems are shown

in figure 6. 1. The solution Kerr constants, B_{12} were calculated as described in Chapter 4 and are presented in table 6.01. The dielectric data are also presented in table 6.02.

For a dilute solution of polar solutes the following approximations are normally acceptable;

$$n_1 \simeq n_{12}, \quad d_1 \simeq d_{12} \quad \text{and} \quad M_{12} \simeq M_1$$

where n_1 , d_1 , and M_1 are refractive index, density and molecular weight of solvent respectively. Equation (6.9) then becomes

$${}_m K_{12} = 6\lambda n_1 B_{12} M_1 / (n_1^2 + 2)^2 (\epsilon_{12} + 2)^2 d_1 \quad (6.10)$$

where the experimental Kerr constant, B_{12} for a 0.2% w/v solution of iodine in benzene was determined to be $0.66 \times 10^{-14} \text{ V}^{-2} \text{ m}$. The corresponding static dielectric permittivity, ϵ_{12} was found to be 2.277. The refractive index, n_1 , the density d_1 , and molecular weight, M_1 of benzene was taken as 1.4973, 873.8 Kg m^{-3} and 78 respectively. The wavelength of light, λ , for which measurements were performed was $632.8 \times 10^{-9} \text{ nm}$.

Substituting these values into equation 6.10, the solution molar Kerr constant was calculated to be $10.2 \times 10^{-26} \text{ V}^{-2} \text{ m}^5 \text{ mol}^{-1}$.

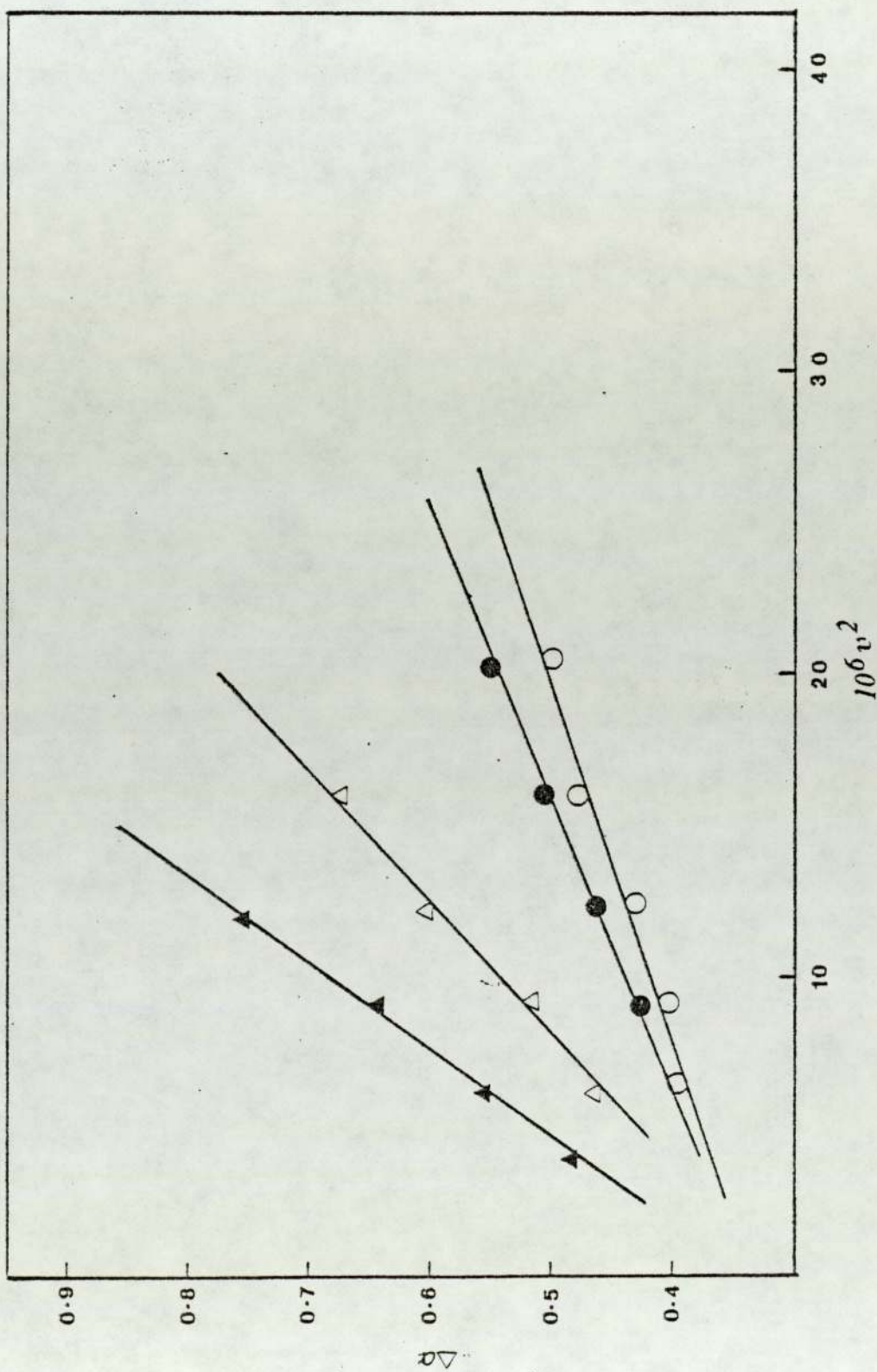


Figure 6.1 Rotation of plane-polarised light as a function of the square of applied voltage for CCl_4 (\circ), $0.2\% \text{ w/v I}_2$ in CCl_4 (\bullet), Benzene (\triangle) and $0.2\% \text{ I}_2$ in benzene (\blacktriangle) at 298 K

Solvent	$10^{14} B_1$ ($v^{-2} m$)	$10^{14} B_{12}$ (or B_{13}) ($v^{-2} m$)	$10^{27} K_1$ ($v^{-2.5} m^{0.1} l^{-1}$)	* $10^{27} K_{12}$ (or K_{13}) ($v^{-2.5} m^{0.1} l^{-1}$)	$10^{27} K_3$ ($v^{-2.5} m^{0.1} l^{-1}$)
CCl ₄	0.092	0.12	1.64	2.15	654 ± 130 ^a
Benzene	0.45	0.66	69.5	102	6760 ± 1200
Toluene	1.09	1.17	20.5	21.9	2290 ± 330
o-xylene	1.77	2.39	32.2	43.5	30600 ± 5000
p-xylene	1.53	2.07	32.7	44.2	15100 ± 500
m-xylene	1.34	1.39	27	28	30 ± 300

Table 6.01 Kerr effect data for solutions of I₂ (0.2% w/v) in various solvents at 298 K

^a Molar Kerr constant K_m^2 for iodine

* Solution molar Kerr constant for CCl₄-I₂ is denoted by K_{m12} . The other aryl-I₂ systems are denoted by K_{m13} and their experimental Kerr constants B, are denoted similarly

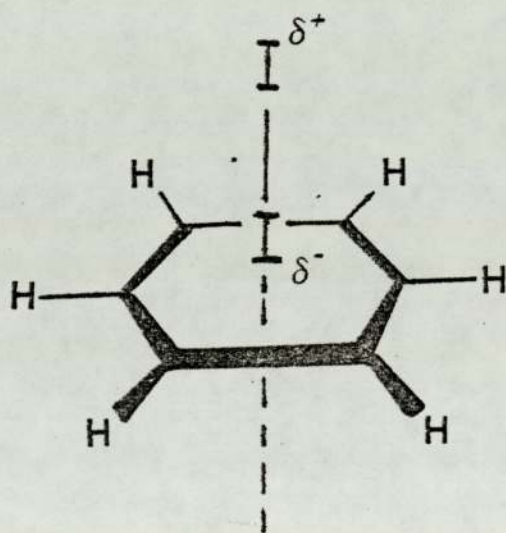
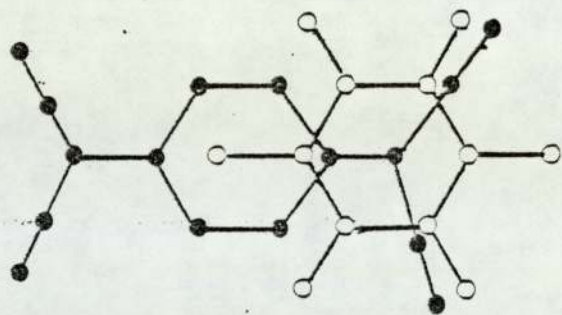
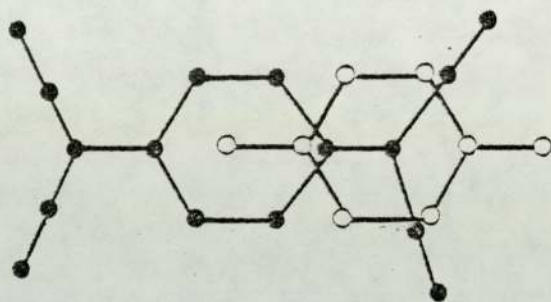


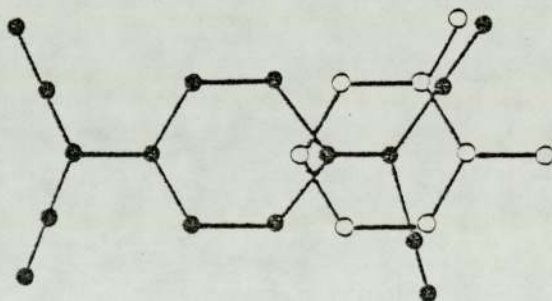
Figure 6.2 Diagram of Benzene-Iodine Complex



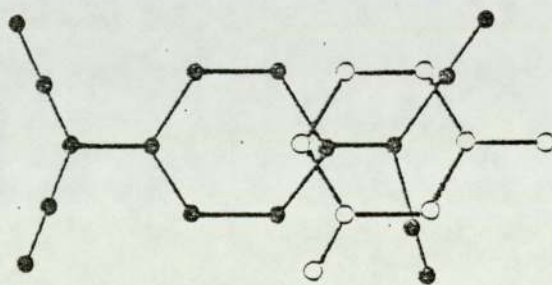
(a)



(b)



(c)



(d)

Figure 6.3 Overlap diagrams for TCNQ complexes with various aryl compounds: (a) hexamethylbenzene (b) p-xylene (c) o-xylene (d) m-xylene

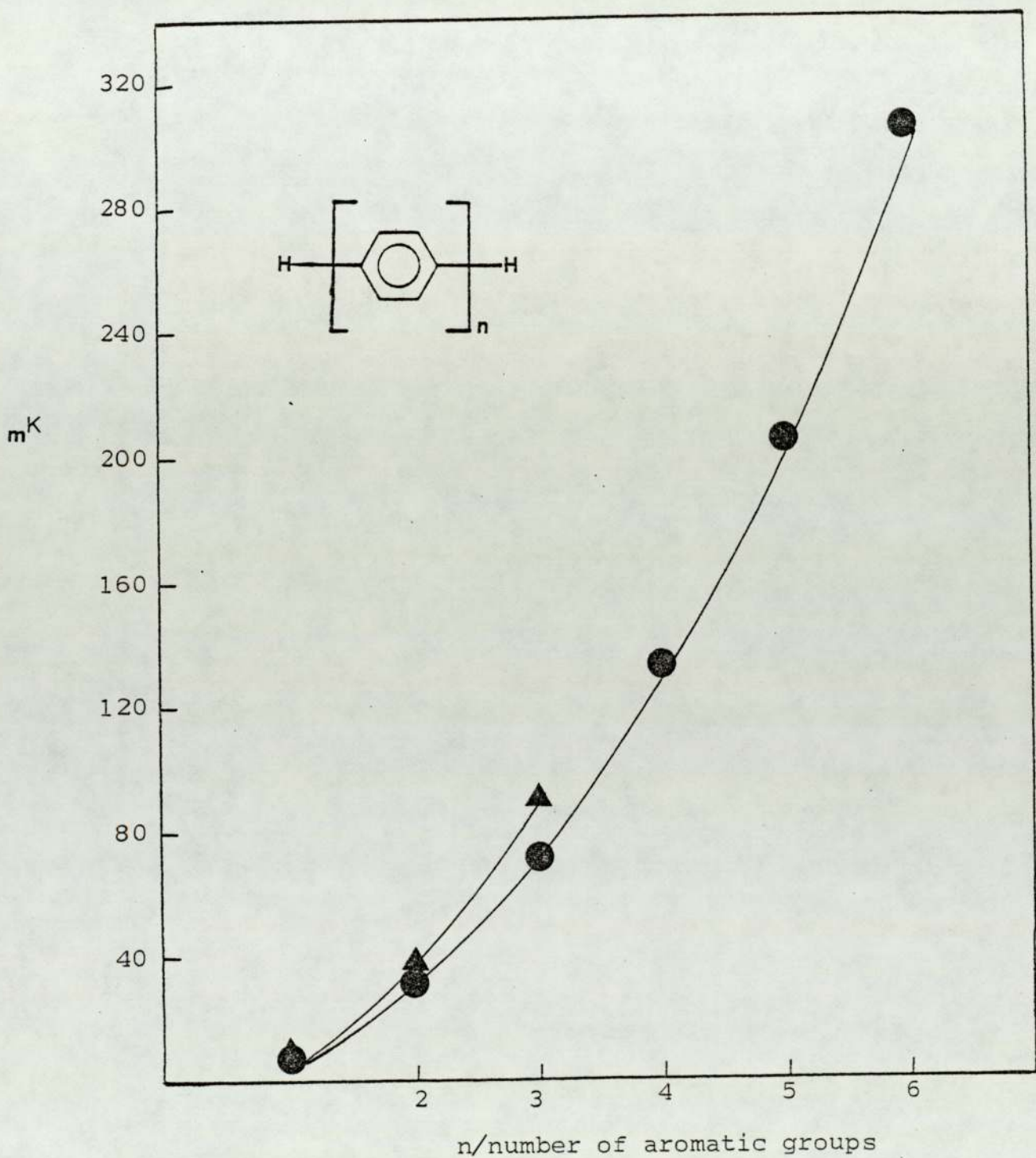


Figure 6.4 Molar Kerr constants, m_K as a function of the number of aromatic units for the oligophenylene compounds: (●) theoretical and (▲) experimental values

Solution Molar Kerr Constant of Iodine-Aryl Complexes

The solution molar Kerr constant of an iodine-aryl complex may be calculated using the following alligation relationship⁽⁹⁾

$${}_mK_{13} = f_1 {}_mK_1 + f_2 {}_mK_2 + f_3 {}_mK_3 \quad (6.11)$$

where f_1 , f_2 and f_3 are the mole fractions of aryl compound, iodine and the complex, respectively and ${}_mK_1$, ${}_mK_2$ and ${}_mK_3$ are the corresponding molar Kerr constants. Rearranging equation (6.11) yields

$${}_mK_3 = \frac{{}_mK_{13} - (f_1 {}_mK_1) - (f_2 {}_mK_2)}{f_3} \quad (6.12)$$

For a 0.2% w/v iodine in benzene, the calculated solution molar Kerr constant was $10.2 \times 10^{-26} \text{ V}^{-2} \text{ m}^5 \text{ mol}^{-1}$. The molar Kerr constant, ${}_mK_1$ of benzene and the molar Kerr constant, ${}_mK_2$ of iodine were determined to be $6.9 \times 10^{-26} \text{ V}^{-2} \text{ m}^5 \text{ mol}^{-1}$ and $6.54 \times 10^{-25} \text{ V}^{-2} \text{ m}^5 \text{ mol}^{-1}$ respectively. The mole fraction, f_1 of benzene and the mole fraction, f_2 of iodine and the mole fraction, f_3 of the benzene-iodine complex were 0.999, 2.15×10^{-4} and 4.8×10^{-4} respectively.

Substitution of the above values into equation (6.12) yields a value of $67.6 \times 10^{-24} \text{ V}^{-2} \text{ m}^5 \text{ mol}^{-1}$ for the molecular Kerr constant, ${}_mK_3$ of the benzene-iodine bimolecular complex.

The solution Kerr constants and the molar Kerr constants for the o, p- and m-xylene-iodine complexes were similarly obtained. A summary of the results is given in

Solvent	ϵ_1	ϵ_{12} (0.2% w/v I_2)	α	$\epsilon_1\alpha$	Equilibrium constant ^a	μ_{C-T} (Debye)
CCl_4	2.227	2.232	1.22			
Benzene	2.2725	2.276	0.52	1.2	0.2	5.6
Toluene	2.379	2.38	0.49	1.17	0.32	
o-xylene	2.568	2.569	0.22	0.57	0.42	3.7
p-xylene	2.27	2.272	0.47	1.07	0.41	5.3
m-xylene	2.374	2.376	0.48	1.14	0.54	5.4

Table 6.02 Dielectric data for solutions of I_2 (0.2% w/v) in various solvents at 298 K

^a Values taken from reference 88

table (6.01).

6.03 Solution Molar Kerr Constant of TCNQ-xylene
Complexes

The experimental Kerr constants B_{12} and dielectric permittivities, ϵ_{12} for solutions of 0.1% (w/v) TCNQ in the various aryl solvents were determined as described in section 6.03. A summary of the results is given in table (6.03) and (6.04).

For the 0.1% (w/v) solutions of TCNQ in the ortho, meta and para xylenes, all the TCNQ was assumed to be in the complex state.

The equilibrium constants are not known for these systems as far as the author is aware. The consequence of this assumption will be discussed subsequently.

The solution molar Kerr constants were calculated using equation (6.13).

$${}_m K_{13} = f_1 {}_m K_1 + f_2 {}_m K_2 + f_3 {}_m K_3 \quad (6.13)$$

where f_1 , f_2 and f_3 are the mole fractions of the xylenes, TCNQ and the TCNQ-xylenes complex respectively and ${}_m K_1$, ${}_m K_2$ and ${}_m K_3$ are the corresponding molar Kerr constants.

For a 1:1 complex formed using all of the available TCNQ, it follows that $f_2 = 0$ and that f_3 may be calculated from

Solvent	$10^{14} B_1$ ($v^{-2} m$)	$10^{14} B_{13}$ ($v^{-2} m$)	$10^{27} K_1$ ($v^{-2.5} m^5 mol^{-1}$)	$10^{27} K_{13}$ ($v^{-2.5} m^5 mol^{-1}$)	$10^{27} K_3$ ($v^{-2.5} m^3 mol^{-1}$)
o-xylene	1.77	2.72	32.2	49.5	29400 ± 460
p-xylene	1.53	1.67	32.7	38.0	8900 ± 400
m-xylene	1.34	1.35	27.0	27.6	1050 ± 300

Table 6.03 Kerr effect data for solutions of TCNQ (0.1% w/v)
in various solvents at 298 K

Solvent	ϵ_1	ϵ_{13} (0.1% w/v TCNQ)	α	$\epsilon_1 \alpha$	μ_{CT}
o-xylene	2.568	2.571	1.57	4.03	8.9
p-xylene	2.270	2.271	0.44	0.99	4.6
m-xylene	2.374	2.391	8.5	20.17	20.2

Table 6.04 Dielectric data for solutions of TCNQ (0.1% w/v)
in various solvents at 298 K

the total number of moles of TCNQ.

Therefore

$${}_m K_{12} = f_1 {}_m K_1 + f_2 {}_m K_3 \quad (6.14)$$

$$\text{and } {}_m K_3 = \frac{{}_m K_{12} - f_1 {}_m K_1}{f_2} \quad (6.15)$$

Equation 6.15, therefore, permits the calculation of the molar Kerr constants, ${}_m K_3$ for the TCNQ-xylene complexes.

For a 0.1% (w/v) solution of TCNQ in o-xylene, the solution molar Kerr constant, ${}_m K_{12}$ was determined to be $4.95 \times 10^{-26} \text{ v}^{-2} \text{ m}^5 \text{ mol}^{-1}$ and the Kerr constant, ${}_m K_1$ for o-xylene was $3.2 \times 10^{-26} \text{ v}^{-2} \text{ m}^5 \text{ mol}^{-1}$. The mole fractions, f_1 of o-xylenes and mole fraction, f_2 of the TCNQ were calculated to be 0.999 and 0.00059 respectively.

Substituting the above values into equation (6.15) gave a molar Kerr constant for TCNQ-o-xylene complex of $2.98 \times 10^{-23} \text{ v}^{-2} \text{ m}^5 \text{ mol}^{-1}$.

A similar approach was used to calculate the molar Kerr constant of TCNQ-complexes formed with p- and m-xylenes.

A summary of the results is given in table 6.03.

6.04 Discussion of Results

The experimentally determined Kerr constants B_1 for the solvents carbon tetrachloride, benzene, toluene, o-xylene, p-xylene and m-xylene at 298K are presented in table 6.01 along with the corresponding Kerr constants for 0.2% w/v solutions of iodine in these materials. The Kerr constant increment $\delta B (= B_{12} - B_1)$ was observed to be relatively small ($0.03 \times 10^{-14} \text{ V}^{-2}_m$) for the solution of iodine in carbon tetrachloride. It has been noted previously that iodine molecules in a carbon tetrachloride medium may be regarded as 'free' and equivalent to the gaseous form of iodine. Thus, the Kerr constant increment, in this instance may be attributed solely to uncomplexed iodine molecules. Much larger Kerr constant increments were found for the aryl solvents. The largest increment was $0.62 \times 10^{-14} \text{ V}^{-2}_m$ found for the o-xylene-iodine system. The increments found for the aryl-iodine systems have been interpreted as the sum of Kerr effect contributions from 'free' iodine and from aryl-iodine complexes. Strictly speaking the observed increments must also reflect the decrease of 'free' aryl molecules. Although the latter contribution is expected to be small for dilute solution of iodine in pure aryl compounds its effect was still taken into account when calculating the molar Kerr constants of the complexes.

Although a comparison of experimental Kerr constants, B_{12} is quite useful it is much more informative to examine the molar Kerr constants which relate more directly to

molecular structure via optical anisotropies and molecular dipole moments. It is interesting that the molecular Kerr constant ($654 \times 10^{-27} \text{ V}^{-2} \text{ m}^5 \text{ mol}^{-1}$) determined for the iodine molecule is nearly an order of magnitude greater than that ($67 \times 10^{-27} \text{ V}^{-2} \text{ m}^5 \text{ mol}^{-1}$) found for chlorine⁽⁹⁰⁾, indicating that iodine molecules are considerably more polarizable, along the bond axis, than chlorine molecules; an observation reflecting the well known differences in general chemical behaviour of these two halogen molecules. Referring to the contents of table 6.01 it can be seen that the experimental molar Kerr constants of the aryl-iodine complexes cover a wide range of values. Even a brief examination of the molar Kerr constants for the xylene-iodine complexes reveals that there must be considerable differences between their optical anisotropic and/or dipole moments.

Similarly, the experimentally determined Kerr constants for solutions of TCNQ (0.1% w/v) in o, p and m-xylene at 298K are presented in table 6.03. An attempt to perform similar determinations with benzene and toluene was not successful due to the extreme insolubility of TCNQ in these solvents. It is interesting that the solution Kerr constants for the solutions of TCNQ in these solvents (o, p and m-xylene) exhibited similar trends to the solution Kerr constants of iodine in these solvents. Thus, the o-xylene produced the largest Kerr constant increment followed by the p-xylene solution. The m-xylene gave by far the smallest solution Kerr constant.

Referring to the dielectric data shown in table 6.04, the dipole moment values quoted for the complexes have been calculated from the dielectric increments resulting from the formation of the complex. Thus, the dielectric increment was attributed solely to the complex. These dipole moments indicate the highest positive value (20.2D) for the m-xylene-TCNQ system. The calculated dipole moments for the o-xylene and p-xylene systems (8.9 and 4.6 respectively) are much smaller than obtained for the m-xylene system. It is anticipated that these dipole moments would be acting in a direction more or less at right angle to the plane of maximum polarizability of the complex and this would effectively produce a negative Kerr constant from the θ_2 term (see Chapter 7). If the dipole moment acting at right angle to plane of maximum polarizability is large enough, the overall Kerr constant of the complex may be negative. It would therefore appear that the dipole moment associated with the TCNQ-complex in the m-xylene system was sufficient to substantially offset the positive contribution to the Kerr constant but not large enough to produce an overall negative Kerr constant. The effect of the dipolar term, θ_2 would be smaller for the o-xylene and p-xylene system as indicated by the calculated dipole moments of their complexes. This would consequently be reflected in the effects they produce on the magnitude and sign of the Kerr constant of the complex.

Since the Kerr constants depend on anisotropy (θ_1) and dipole moment (θ_2) contributions, the magnitude and sign

of the Kerr constants would depend on which of these factors is dominant. It may be seen that the dipole moment calculated for the complex in the o-xylene system (8.9D) is greater than that calculated for the complex in the p-xylene system (4.6D). However, the Kerr constant of the o-xylene-TCNQ complex is larger than the Kerr constant of the p-xylene-TCNQ complex. This could probably be due to a greater anisotropy of the o-xylene-TCNQ complex compared to the anisotropy of the p-xylene-TCNQ complex.

In Chapter 7, theoretical Kerr constants are calculated for various aryl-TCNQ system. In this chapter a more detailed examination of the electro-optical properties and possible molecular structures of p-oligophenylene-TCNQ complex will be undertaken.

Colton and Henn⁽⁸⁹⁾ have previously indicated that even a completely substituted benzene (hexamethylbenzene) exhibits a considerable overlap with the TCNQ molecule. The predicted donor-acceptor arrangement for benzene-TCNQ and hexamethylbenzene-TCNQ (drawn by Colton and Henn) together with overlap diagrams for o-, p- and m-xylene-TCNQ using the same basis are shown in figure 6.2.

Although little information has been reported about the detailed structure of the TCNQ-aryl complexes, structures of aromatic complexes with a similar molecule, tetracyanoethylene (TCNE) have been reported in relatively more

detail. For example, in naphthalene⁽⁹¹⁾, pyrene⁽⁹²⁾ and perylene⁽⁹³⁾ complexes the donor and acceptor molecules were observed to alternate in stacks of 1:1 stoichiometry. Adman et al⁽⁹⁴⁾ showed using overlap diagrams, that the TCNE molecule lies almost directly above a p-p' vector of a given benzene ring of the particular polycyclic hydrocarbon. They suggested that the TCNE molecule is always associated with the centre of a particular benzene ring of an electron donor and not with the periphery of the ring, and that it is associated with a ring at the periphery and not the centre of the larger polycycles.

Although there remains much work to be done before the electro-optical behaviour of aryl-TCNQ complexes can be fully interpreted in terms of their molecular structures it has been demonstrated that a combination of dielectric and Kerr effect techniques can provide useful information about structure and electrical properties of charge-transfer complexes in solution.

6.05 TCNQ-Complexes of Phenylene Oligomers in 1,4-Dioxane

Poly(p-phenylene) and the oligomers are known to form charge-transfer complexes with both n- and p-type dopants. The most extensively studied complexes are those formed with AsF_5 , $NOBF_4$ and lithium naphthalide (see section 2.09). Tetracyanoquinodimethane (TCNQ) has been used similarly to dope polymers for the purpose of enhancing their electrical conductivity. A notable example is the

doping of poly(n-vinylcarbazole) with TCNQ which is discussed in Chapter 8.

Although TCNQ has for sometime been known to form a charge transfer complex with the polyphenylene compounds, detailed investigations of the structure of the complex have been relatively sparse. This is mainly due to the extreme insolubility of the poly(p-phenylenes) and the oligomer in the majority of solvents that would be considered suitable for a complex.

The present chapter describes a study (using mainly dielectric and electro-optical Kerr effect techniques) of the oligomers soluble in 1,4-dioxane.

6.06 Preparation of TCNQ-Oligophenylene Complexes

All the TCNQ-complexes of the oligomers (biphenyl, m-biphenyl benzene, terphenyl) were prepared in 1,4-dioxane.

Solutions of biphenyl and m-biphenyl benzene-TCNQ complexes were each prepared by dissolving 2% and 0.1% (w/v) of oligomer and TCNQ respectively in 1,4-dioxane. These were shaken in a stoppered flask for approximately 24 hours at room temperature. Solution of terphenyl-TCNQ complex were prepared by dissolving 1% of oligomer and 0.1% of TCNQ in 1,4-dioxane. The solubility of terphenyl in 1,4-dioxane is poor (< 2%).

The freshly prepared solutions of oligophenylenes and TCNQ possessed an intense red colour similar to that observed for solutions of TCNQ in the ortho-, meta- and para-xylenes.

6.07 Solution Molar Kerr Constants of Oligophenylenes and Oligophenylene-TCNQ Complexes

The estimation of the molar Kerr constant of solutes at infinite dilution was first adopted by Le Fèvre⁽⁹⁰⁾. The procedure involves the extrapolation of measurements of four experimental parameters to infinite dilution before calculating the Kerr constant of a solute. This is facilitated by the following relationships which are assumed to apply at high dilution for the permittivity (ϵ_{12}), density (d_{12}), refractive index (n_{12}) and experimental Kerr constant (B_{12}) of the solution.

$$\epsilon_{12} = \epsilon_1 (1 + \alpha w_2) \quad (6.16)$$

$$d_{12} = d_1 (1 + \beta w_2) \quad (6.17)$$

$$n_{12} = n_1 (1 + \gamma w_2) \quad (6.18)$$

$$B_{12} = B_1 (1 + \delta w_2) \quad (6.19)$$

Thus, by making measurements for a series of solutions with different weight fractions, w_2 of solute, the values of α , β , γ and δ may be evaluated. These values, together with equation (6.20) may then be used to calculate the specific Kerr constant of the solute at infinite dilution, $\omega_s(K_2)$.

$$\alpha({}_sK_2) = \left[(1 - \beta + \gamma + \delta - H\gamma - J\alpha\epsilon_1) \right] {}_sK_1 \quad (6.20)$$

where $H = 4n_1^2 / (n_1^2 + 2)$ (6.21)

and $J = 2 / (\epsilon_1 + 2)$ (6.22)

${}_sK_1$ is the specific Kerr constant of the solvent.

In practice for polar solutes, β and γ are usually very small relative to the other contributions denoted by α and δ . Thus, a simplified version of equation (6.20) may be used, namely:

$${}_sK_2 = (1 + \delta - J\alpha\epsilon_1) {}_sK_1 \quad (6.23)$$

The majority of measurements were made on dilute solutions ($\approx 2\%$ w/v) of the solutes in the solvent 1,4-dioxane at 298 K.

The permittivity and specific Kerr constant of 1,4-dioxane were taken to be 2.209 and $0.138 \times 10^{-25} \text{ V}^{-2} \text{ m}^5 \text{ Kg}^{-1}$ respectively⁽¹²¹⁾. The coefficients, α and δ were determined from the gradients of plots of ϵ_{12} vs w_2 and B_{12} vs w_2 , respectively. Solute specific Kerr constants ${}_sK_2$ were then calculated using equation (6.23).

6.08 Molar Kerr Constants of TCNQ-Oligophenylene Complexes in Solution in 1,4-dioxane at 298

The composition of a quantity W_g , of a solution of complex may be expressed as follows:

$w_1 \times W$ dioxane
 $w_2 \times W$ biphenyl
 $w_3 \times W$ TCNQ

where w_1 , w_2 and w_3 are the weight fractions of dioxane, biphenyl and TCNQ respectively.

Given that the molecular weight of TCNQ equals 204, then the total number of moles of TCNQ per W solution will be:

$$\frac{w_3 \times W}{204}$$

If it is assumed that all the TCNQ is incorporated in a 1:1 complex with the aryl molecule, then the weight of complex present in W of solution will then be given by:

$$\left(\frac{w_3 \times W}{204}\right) M_C$$

where M_C is the molecular weight of the complex. Hence the weight fraction of complex, w_4 , will be given by:

$$w_4 = \frac{w_3 \times W \times M_C}{204}$$

The number of moles of aryl molecule involved in the formation of the complex is equal to $w_3 \times W / 204$ and the total weight of aryl molecules incorporated in the complex will be given by

$$\frac{w_3 \times W \times M}{204}$$

where M is the molecular weight of the aryl moiety.

It therefore follows that the weight of uncomplexed aryl molecules may be expressed as

$$w_2 \times W - \frac{w_3 \times W \times M}{204}$$

and the weight fraction of the uncomplexed aryl molecules, w_2' , will then be given by:

$$w_2' = \left(w_2 - \frac{w_3 \times M}{204} \right)$$

The solution specific Kerr constant, sK_{13} for the aryl-TCNQ complex in 1,4-dioxane may then be calculated using the following relationship:

$$sK_{13} = w_1 sK_1 + w_2' sK_2 + w_3 sK_3 + w_4 sK_4 \quad (6.24)$$

where w_4 and sK_4 are the weight fraction and specific Kerr constant of the aryl-TCNQ complex, respectively.

For the formation of a 1:1 complex the term $w_3 sK_3$ equals zero and equation (6.24) reduces to

$$sK_{13} = w_1 sK_1 + w_2' sK_2 + w_4 sK_4 \quad (6.25)$$

Substituting for w_2' and w_4 yields

$$sK_{13} = w_1 sK_1 + \left(w_2 - \frac{w_3 \times M}{204} \right) sK_2 + \left(\frac{w_3 \times M_C}{204} \right) sK_4 \quad (6.26)$$

Rearranging to find sK_4

$$sK_4 = sK_{13} - w_1 sK_1 - \left(w_2 - \frac{w_3 \times M}{204} \right) sK_2 \frac{204}{w_3 \times M_C} \quad (6.27)$$

enable the specific Kerr constant of the complex to be readily obtained.

For the biphenyl-TCNQ system, the values for ${}_sK_{13}$, ${}_sK_1$ and ${}_sK_2$ were $0.209 \times 10^{-25} \text{ V}^{-2} \text{ m}^5 \text{ Kg}^{-1}$, $0.138 \times 10^{-25} \text{ V}^{-2} \text{ m}^5 \text{ Kg}^{-1}$ and $2.18 \times 10^{-25} \text{ V}^{-2} \text{ m}^5 \text{ Kg}^{-1}$ respectively.

Substituting these quantities into equation (6.27) gives a value of $25.4 \times 10^{-25} \text{ V}^{-2} \text{ m}^5 \text{ Kg}^{-1}$ for the specific Kerr constant of the TCNQ-biphenyl complex and a corresponding molar Kerr constant ${}_mK_4$ of $9.09 \times 10^{-22} \text{ V}^{-2} \text{ m}^5 \text{ mol}^{-1}$ (${}_mK_4 = {}_sK_4 \times \text{molecular weight of complex}$).

The same procedure was used to calculate the molar Kerr constant of terphenyl-TCNQ complex and m-biphenyl benzene-TCNQ complex in solution in 1,4-dioxane at 298 K. The results of these calculations are summarised in table 6.06.

6.09 Discussion of Results

The dielectric and Kerr effect data for the oligophenylenes, biphenyl, m-biphenyl benzene and terphenyl in solution in 1,4-dioxane at 298 K are presented in table 6.05. Also included in this table are the corresponding experimental specific and molar Kerr constants of these molecules calculated using procedures described earlier. The molar Kerr constants in the final column of table 6.05 were calculated using polarizabilities ${}^*b_1 = 11.32 \times 10^{-24}$, $b_2 = 11.32 \times 10^{-24}$, $b_3 = 7.19 \times 10^{-24}$ for the phenyl nucleus and $b_1 = 2.8 \times 10^{-24}$, $b_2 = 0.73 \times 10^{-24}$, $b_3 = 0.77 \times 10^{-24}$ for the carbon-carbon bond between the phenyl rings. These calculations were carried out using the computer program

* units in cm^3

Sample	$10^{14} B_{12}$ ($v^{-2} m$)	δ	α	$10^{27} s K_2$ ($v^{-2} m^5 Kg^{-1}$)	$10^{27} m K_2$ ($v^{-2} m^5 mol^{-1}$)
2% Biphenyl	0.098	15.2	0.35	218	33 ± 7 (31)
2% m-Biphenyl- benzene	0.123	32.5	0.35	456	105 ± 22 (69.8)
1% Terphenyl	0.098	29.3	1.82	390	90 ± 20 (69.8)

Table 6.05 Kerr effect and dielectric data for solutions of oligophenylenes in 1,4-dioxane at 298 K. $m K_2$ in parenthesis are theoretical values

Sample	$10^{14} B_{13}$ ($v^{-2} m$)	δ	α	$10^{27} s K_4$ ($v^{-2} m^5 Kg^{-1}$)	$10^{27} m K_4$ ($v^{-2} m^5 mol^{-1}$)
2% Biphenyl	0.114 (0.100)	24.5	16.8	254	910 ± 130
2% m-Biphenyl- benzene	0.116 (0.125)	26.3	0.81	-115	-370 ± 70
1% Terphenyl	0.117 (0.100)	54.3	4.3	734	820 ± 230

Table 6.06 Kerr effect and dielectric data for solutions of TCNQ (0.1%) and oligophenylene in 1,4-dioxane at 298 K.

Sample	ϵ_{12}	ϵ_{13}	μ_{CT}^D
2% Biphenyl	2.224	2.246	23.0
2% m-Biphenyl- benzene	2.234	2.245	6.2
1% Terphenyl	2.252	2.252	11.7

Table 6.07 Dielectric data for solutions of TCNQ-oligophenylene in 1,4-dioxane at 298 K. ϵ_{12} and ϵ_{13} denotes the dielectric permittivities of the pure oligophenylene solution and the solution of the TCNQ complexes respectively

described in Appendix 2.

For biphenyl there is good agreement between the experimental Kerr constant, $33 \times 10^{-27} \text{ V}^{-2} \text{ m}^5 \text{ mol}^{-1}$ and the theoretical Kerr constant, $31 \times 10^{-27} \text{ V}^{-2} \text{ m}^5 \text{ mol}^{-1}$.

The theoretical molar Kerr constants calculated for m-biphenylbenzene and terphenyl are identical ($69.8 \times 10^{-27} \text{ V}^{-2} \text{ m}^5 \text{ mol}^{-1}$) because the polarizability of the aromatic nuclei and consequently those of the molecules is isotropic along directions lying in the plane of these molecules. The experimental molar Kerr constants of m-biphenylbenzene and terphenyl were determined to be $105 \times 10^{-27} \text{ V}^{-2} \text{ m}^5 \text{ mol}^{-1}$ and $90 \times 10^{-27} \text{ V}^{-2} \text{ m}^5 \text{ mol}^{-1}$ respectively. The difference between these two values may not be significant in view of the fact that the error bars associated with these values are overlapping. However, despite these reservations it is likely that the Kerr constant of m-biphenylbenzene is slightly greater than that of its isomeric form, terphenyl, because its non-linear structure will give rise to a small dipole moment, lying in a direction coincident with the axis of symmetry of m-biphenylbenzene which would increase the magnitude of the positive Kerr constant. By way of illustration, a dipole moment of 0.75 D would raise the theoretical Kerr constant from $70 \times 10^{-27} \text{ V}^{-2} \text{ m}^5 \text{ mol}^{-1}$ ($\mu = 0$) to $110 \times 10^{-27} \text{ V}^{-2} \text{ m}^5 \text{ mol}^{-1}$.

The experimental molar Kerr constants found for m-biphenyl-

benzene and terphenyl are significantly greater than the theoretical values calculated using tabulated bond and group polarizabilities taken from the literature. These differences are not great and probably arise from changes in the polarizability of the phenyl moiety when it is incorporated in an extensive conjugated system.

Attempts were made to measure the Kerr effect of solutions of the higher molecular weight oligophenylenes (e.g. p-quarterphenyl, p-quinquiphenyl) but their extremely poor solubility in solvents suitable for making Kerr effect measurements prohibited such an analysis. Figure 6.05 shows experimental and theoretical molar Kerr constants for several oligophenylenes. The theoretical values were calculated assuming that the molecules are rod-like and planar.

The addition of small amounts of the powerful electron acceptor TCNQ to solutions of the oligophenylenes gave rise to substantial changes in the experimental solution Kerr constants. Referring to Column 1 in table 6.06 the entries in parenthesis are the solution Kerr constants estimated for the 1,4-dioxane-oligophenylenes-TCNQ systems based on ideal mixing of the solutes i.e. no specific solute-solute interactions. For biphenyl and terphenyl the experimental solution Kerr constants, B_{13} , are 14% and 17% greater than the corresponding values predicted for the ideal solutions. These are significant differences and indicate that there are specific inter-

actions between biphenyl and TCNQ and between terphenyl and TCNQ. For convenience it will be assumed that these specific interactions result in the formation of a 1:1 complex although it is recognised that the stoichiometry and exact concentration of the complex cannot be established from Kerr effect measurements alone. This problem will be discussed subsequently. It is interesting to note that the addition of TCNQ to solutions of m-biphenylbenzene produces a significant lowering of the solution Kerr constant indicating the formation of a complex possessing a negative Kerr constant.

The experimental molar Kerr constants listed in the final column of table 6.06 were calculated from the solution Kerr constants B_{13} assuming that all of the TCNQ is in a complexed form. Thus, these molar Kerr constants represent minimum values of the molar Kerr constant of the oligophenylene-TCNQ complexes. It is important to appreciate that the experimental molar Kerr constants calculated for the complexes are underestimated quantities. The experimental molar Kerr constants found for the complexes are substantially greater than those found for the constituent molecules. These results indicate that the polarizability and/or anisotropy of polarizability of the complexes greatly exceeds that of the separate molecules.

Calculation of Molecular Kerr Constant of Bimolecular
Complexes using Bond Polarizabilities

7.01 Introduction

Previous chapters have described the measurement of molecular Kerr constant of complexes formed between a variety of donor and acceptor molecules in solution.

From a consideration of the magnitude and sign of the experimentally determined molecular Kerr constant it is possible to deduce a limited amount of information regarding the overall shape and electrical properties of the complexes. In this chapter a more detailed analysis of the molecular structure and electro-optic properties of the complexes will be undertaken based on the calculation of molecular Kerr constants using bond polarizabilities and electric dipole moments.

Theoretical Considerations:-

Le Fèvre and his many co-workers have consistently demonstrated that for a large variety of organic molecules the electrical and optical molecular polarizabilities may be represented by appropriate tensor sums of the constituent bond polarizabilities. It is known that the anisotropy of molecular polarizability is very dependent on the

overall shape of molecules. Thus, by comparing experimental and theoretical molecular Kerr constant of a molecule (typically a solute molecule) it is possible to deduce useful information concerning its structure and conformation. This approach can be extended to cover solute-solvent and solute-solute interaction. Indeed, departures of solutes from ideality due to association between molecules are readily studied using the electro-optical Kerr effect, provided that scattering is minimal and specific absorption effects are recognised and taken into account.

The molecular Kerr constant of a molecule is normally regarded as the sum of two contributions, a term (θ_1) associated with induced electric dipole moments and a second term (θ_2) associated with permanent electric dipole moments.

$$\text{Thus } m^K = \frac{2\pi N}{9} (\theta_1 + \theta_2) \quad (7.01)$$

The first term, θ_1 is usually referred to as the induced anisotropy term and its magnitude, which is always positive is a measure of the anisotropy of optical and electrical polarizability. N is Avogadro's number.

The form of θ_1 is

$$\theta_1 = \frac{1}{45KT} \frac{(\epsilon - 1)}{(n^2 - 1)} \left[(b_1 - b_2)^2 + (b_2 - b_3)^2 + (b_3 - b_1)^2 \right] \quad (7.02)$$

In this expression b_1 , b_2 and b_3 are the principal electrostatic polarizabilities of the molecule, ϵ is the dielectric constant and n is the refractive index. T and K are the

temperature and Boltzmann's constant respectively.

The dipole term, θ_2 , sometimes referred to as the orientation term, is given by:

$$\theta_2 = \frac{1}{45K^2T^2} \left[(\mu_1^2 - \mu_2^2)(b_1 - b_2) + (\mu_2^2 - \mu_3^2)(b_2 - b_3) + (\mu_3^2 - \mu_1^2)(b_3 - b_1) \right] \quad (7.03)$$

Where μ_1 , μ_2 and μ_3 are the components of the permanent dipole moment vector along directions parallel to b_1 , b_2 and b_3 .

From the Langevin-Born-Gans Theory, the Kerr constant of the medium is

$$B = \frac{\pi\nu(n^2 + 2)^2(\epsilon + 2)^2(\theta_1 + \theta_2)}{27n\lambda} \quad (7.04)$$

Where ν is the number of molecules per unit volume and λ is the wavelength of the light used to make measurements.

On rearranging equation (7.04) we obtain

$$\theta_1 + \theta_2 = \frac{B 27 n \lambda}{\pi\nu(n^2 + 2)^2(\epsilon + 2)^2} \quad (7.05)$$

which may be substituted into equation (7.01) to give:

$$m^K = \frac{6 n B \lambda}{(n^2 + 2)(\epsilon + 2)^2} \frac{N}{\nu} \quad (7.06)$$

The quotient N/ν may be shown, by simple manipulation, to be equal to M/d , where M and d are the molecular weight and density respectively. So finally we obtain:

$$m^K = \frac{6 n B \lambda M}{(n^2 + 2)(\epsilon + 2)^2 d} \quad (7.07)$$

Thus, using equations(7.01 - 7.03), together with a knowledge of molecular polarizabilities b_1, b_2, b_3 and corresponding dipole moment components μ_1, μ_2 and μ_3 , the theoretical molecular Kerr constant may be calculated. Such a value may then be compared with the corresponding experimental value calculated by substituting experimentally determined values of B, n, ϵ and d into equation 7.07.

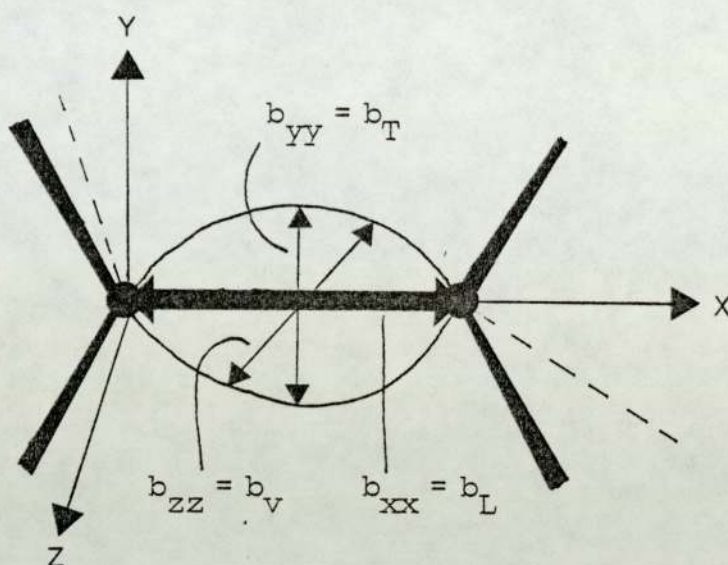
However, before a comparison may be made between theoretical and experimental molecular Kerr constants the molecular polarizabilities have first to be calculated.

It is assumed that the electro-static and optical polarizability of a molecule can be represented by a single polarizability tensor, T_m . This assumption implies that the electrostatic and optical polarizabilities are related by a scaling factor. The molecular polarisability tensor T_m is given by the tensor sum of the bond polarizability tensors T_i . The latter posses the general form⁽⁹⁵⁾.

$$T_i = \begin{vmatrix} b_L & 0 & 0 \\ 0 & b_T & 0 \\ 0 & 0 & b_V \end{vmatrix} i \quad (7.08)$$

The diagonal components, b_L, b_T, b_V of the tensor of the i^{th} bond T_i correspond to the principal axes of the electro-

optical polarizability ellipsoid of the i^{th} bond in the molecule.



The electrostatic polarizability tensor of a molecule may be written in the following form:

$$T_m = \sum_{i=1}^N S_i T_i S_i^{-1} \quad (7.09)$$

Where N is the number of bonds in the molecule and S_i is a 3×3 transformation matrix for representing the bond polarizability tensor **with** an arbitrarily chosen reference coordinate system. The matrix S_i^{-1} is the inverse of S_i . For transformation using Cartesian co-ordinate S_i^{-1} is simply the transpose of S_i . The transformation matrix S_i depends on the relative orientation of the i^{th} bond and the bond chosen as a reference co-ordinate system. S_i is expressed as a serial product of the intervening bond transformation matrices ${}_i R_j$. Thus:

$$S_i = \prod_{j=0}^{i-1} R_j \quad (7.10)$$

where j indexes the bonds linking the i^{th} bond to the reference bond, such that $j=0$ corresponds to the reference bond and $j=R+1$ to the i^{th} bond. The index i serves merely as a label for the bonds and is not involved with the ordinal numbering of the bonds that connect the reference bond to the i^{th} bond. Bond transformation matrices required by equation (7.10) are given by⁽⁹⁵⁾

$$R_j = \begin{vmatrix} \cos \theta_j & \sin \theta_j & 0 \\ \sin \theta_j \cos \phi_j & -\cos \theta_j \cos \phi_j & \sin \phi_j \\ \sin \theta_j \sin \phi_j & -\cos \theta_j \sin \phi_j & -\cos \phi_j \end{vmatrix} \quad (7.11)$$

where the elements of the transformation matrix, R_j , are functions of the bond rotation angle ϕ_j and the bond angle supplement θ_j of the j^{th} intervening bond. Application of equations (7.08 - 7.11) yields molecular polarizability tensors which have the general form:

$$T_m = \begin{vmatrix} b_{xx} & b_{xy} & b_{xz} \\ b_{yx} & b_{yy} & b_{yz} \\ b_{zx} & b_{zy} & b_{zz} \end{vmatrix} \quad (7.12)$$

If the components of the permanent dipole vector expressed in the reference co-ordinate system are μ_x , μ_y and μ_z , then the molecular Kerr constant may be calculated using the following equations:

$$m^K = N(\theta_1 + \theta_2)/2\epsilon_0 \quad (7.13)$$

$$\theta_1 = \left[(b_{xx} - b_{yy})^2 + (b_{yy} - b_{zz})^2 + (b_{zz} - b_{xx})^2 + 6b_{xy}b_{xy} + 6b_{zx}b_{zx} + 6b_{yz}b_{yz} \right] P_D/45P_EKT \quad (7.14)$$

$$\theta_2 = \left[(\mu_x^2 - \mu_y^2)(b_{xx} - b_{yy}) + (\mu_y^2 - \mu_z^2)(b_{yy} - b_{zz}) + (\mu_z^2 - \mu_x^2)(b_{zz} - b_{xx}) + 6\mu_x\mu_y b_{xy} + 6\mu_y\mu_z b_{yz} + 6\mu_z\mu_x b_{zx} \right] /45K^2T^2 \quad (7.15)$$

where P_D and P_E are the distortion and electronic polarisation, respectively. Diagonalisation of the molecular electro-optical polarizability tensor, T_m , enables equations (7.14 - 7.15) to be simplified, since the terms involving off-diagonal elements of T_m disappear.

A computer program, 'Kerr Constants' written in Basic for the Apple II computer was used to calculate the molecular polarizability tensor, the molecular dipole moment and the induced, dipolar and total molecular Kerr constants. A detailed description of the structure and use of this program is presented in Appendix 2.

7.02 Theoretical Molar Kerr Constant of Iodine Complexes

The principal polarizabilities of iodine were estimated from the knowledge of its refractive index, density, molecular weight and its experimentally determined molar Kerr constant.

Theoretically, the molar Kerr constant can be expressed

in terms of polarizabilities (b) and dipole moments (μ) (induced and permanent).

$$\text{Thus } m^K = \frac{2\pi N (\theta_1 + \theta_2)}{9} \quad (7.01)$$

where θ_1 is known as the induced term and θ_2 as the dipolar term.

Since the iodine molecule is symmetrical, it has no net dipole moment. Therefore θ_2 becomes zero

Equation (7.01) then reduces to:

$$m^K = \frac{2\pi (\theta_1)}{9} \quad (7.16)$$

$$\text{But } \theta_1 = \frac{1}{45KT} \left[(b_1 - b_2)^2 + (b_2 - b_3)^2 + (b_3 - b_1)^2 \right] \quad (7.17)$$

For the cylindrically symmetric iodine molecule, we may assume $b_2 = b_3$. Then equation (7.17) reduces to:

$$\theta_1 = \frac{1}{45KT} \left[(b_1 - b_2)^2 \right] \quad (7.18)$$

Therefore from (7.16) and (7.18)

$$(b_1 - b_2)^2 = \frac{9 m^K}{2\pi} \frac{45KT}{2} \quad (7.19)$$

Molar refraction is also related to the principal polarizabilities by the following equation:

$$R = \frac{4\pi N}{9} (b_1 + b_2 + b_3) \quad (7.20)$$

If $b_2 = b_3$

$$\text{Then } R = \frac{4\pi N}{9} (b_1 + 2b_2) \quad (7.21)$$

But molar refraction can also be represented by the following equation:

$$R = \frac{(n^2 - 1)}{(n^2 + 2)} \frac{M}{d} \quad (7.22)$$

where n is the refractive index, M the molecular weight and d the density.

From equation (7.21) and (7.22):

$$b_1 = \frac{9}{4\pi N} \frac{(n^2 - 1)}{(n^2 + 2)} \frac{M}{d} - 2b_2 \quad (7.23)$$

and from equation (7.19):

$$b_1 = \sqrt{\frac{9}{2\pi} \frac{K}{m} \frac{45KT}{2}} + b_2 \quad (7.24)$$

Combining equation (7.23) and (7.24), so as to eliminate b_1 , we obtain:

$$b_2 = \frac{9}{4\pi N} \frac{(n^2 - 1)}{(n^2 + 2)} \frac{M}{d} \pm \sqrt{\frac{9}{2\pi} \frac{K}{m} \frac{45KT}{2} \times \frac{1}{3}} \quad (7.25)$$

The polarizabilities b_1 and b_2 can therefore readily be calculated. The polarizability b_3 is readily evaluated since it is simply equal to b_2 .

The calculated principal polarizabilities are $18.6 \times 10^{-24} \text{ cm}^3$, $9.29 \times 10^{-24} \text{ cm}^3$ and $9.29 \times 10^{-24} \text{ cm}^3$ for b_1 , b_2 and b_3 respectively. These polarizability values were used in the program described in Appendix 2 to calculate the molar Kerr constant of the iodine complexes.

7.03 Theoretical Kerr Constant of Tetracyanoquinodimethane

In order to calculate the molar Kerr constant of a molecule it is necessary to have a complete knowledge of the electrostatic polarizability tensor and the permanent electric dipole moment of the molecule. The symmetrical structure of TCNQ will ensure that its time-averaged dipole moment is zero. The molecular polarizabilities b_1 , b_2 and b_3 may be calculated by the tensorial addition of the individual bond polarizabilities b_L , b_T and b_V .

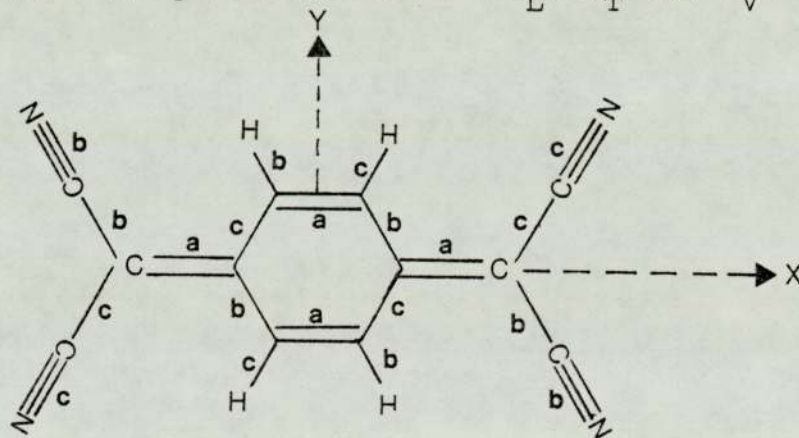


Figure 7.1 Structure of TCNQ molecule

Figure 7.1 shows the structure of the TCNQ molecule. All the bond angles were assumed to be close to 120° . For the purpose of calculation it is convenient to classify the bonds in terms of their orientation in the X-Y plane. (The plane in which lie all of the atoms). Bonds lying along the direction of the X-axis are labelled with the letter 'a'. Bonds which may be considered as rotated clockwise (-60°) about the Z-axis are designated with a

Compounds	Principal Polarizabilities (esu)/10 ²⁴			μ (Debyes)
	b_1	b_2	b_3	
Benzene	11.32	11.32	7.19	0
Toluene	13.75	13.03	8.7	0.37
P-xylene	15.75	15.18	10.24	0
O-xylene	15.6	15.3	12.05	0.62
M-xylene	15.3	15.6	12.05	0.37
Iodine	18.6	9.29	9.29	0
TCNQ	29.16	18.76	11.12	0
Biphenyl	21.34	21.34	13.5	0
M-Biphenyl- Benzene	31.36	31.36	19.6	0
Terphenyl	31.36	31.36	19.6	0

Table 7.01 Principal polarizabilities of the aryl compounds.

The polarizability values for benzene, toluene and the xylenes were obtained from reference 120.

Values for iodine, TCNQ and the oligophenylenes were calculated.

'b'. An equivalent set of bonds labelled 'c' may be regarded as having been rotated anticlockwise ($+60^\circ$) about the Z-axis from a direction initially parallel to the X-axis. The description of the molecule is consistent with the view that each bond is oriented along the X-axis of a local invariant cartesian co-ordinate system. It is the latter (for bond types 'c' and 'b') that has been rotated through 60° relative to the co-ordinate system (X, Y, Z) affixed to the molecule.

Bond polarizabilities (in cm^3) for the relevant bonds are as follows: (97)

	b_L	b_T	$b_V \times 10^{24}$
C - H	0.65	0.65	0.65
C = C	2.80	0.73	0.77
C - C	0.97	0.26	0.26
C - (C \equiv N)	4.03	1.54	1.54

It follows that the total polarizability contributions b_1 , b_2 and b_3 for bonds 'a', 'b' and 'c' are:

$$\begin{aligned}
 a b_1 = 11.2, \quad a b_2 = 2.92, \quad a b_3 = 3.08, \quad b b_1 = 10, \quad b b_2 = 3.6, \\
 b b_3 = 3.6, \quad c b_1 = 10, \quad c b_2 = 3.6, \quad c b_3 = 3.6 \quad \text{respectively.}
 \end{aligned}$$

These values together with the appropriate rotational angle (0 , -60° or $+60^\circ$) were used in the computer program "Kerr Constants" (See Appendix 2) to give the diagonalised molecular polarizability tensor and the molar Kerr constant of TCNQ at 298 K. The principal components of the

molecular polarizability tensor (b_1 , b_2 and b_3) were found to be 29.2, 18.8 and 11.2 (10^{-24} cm^3). The corresponding theoretical molar Kerr constant was calculated to be $1.24 \times 10^{-25} \text{ v}^{-2} \text{ m}^5 \text{ mol}^{-1}$. This value is nearly 17 times greater than that determined for TCNQ in solution in 1,4-dioxane at 298 K. Such a large difference between experimental and theoretical Kerr constants is normally indicative of either a significant departure from the tensorial additivity of bond polarizabilities and/or a substantial degree of association between the solvent and solute molecules. In the former case it is known that the presence of extensive conjugation in unsaturated systems may give rise to increased optical and electrical anisotropies (usually referred to as exaltation). Le Fèvre's^(95,98) studies of this effect for a series of α , ω -diphenyl polyenes $\text{Ph}(\text{CH}=\text{CH})_n \text{Ph}$, showed that for $n=1$ the experimental Kerr constant was approximately 120 times greater than that calculated using bond polarizabilities deduced from saturated chemical system. It is difficult to estimate the magnitude of this effect for TCNQ, but it is believed that the difference between experimental and theoretical molar Kerr constants cannot be attributed entirely to the effects of exaltation. The other possible contributing factor alluded to briefly is that resulting from the association between TCNQ and 1,4-dioxane. It is well known that both of these molecules are able to form complexes with a variety of donor and acceptor molecules. A detailed discussion of the complexing ability of TCNQ has already been given. For 1,4-dioxane a few comments are

Compound	Minimum K_m^3		Mean K_m^3		Maximum K_m^3	
	Experimental	Theoretical	Experimental	Theoretical	Experimental	Theoretical
Benzene	5300	5283(9.1)	6760	6569(10.15)	7700	7713(11)
Toluene	1960	1917(5.8)	2290	2260 (6.3)	2620	2632(6.8)
O-xylene	25600	25393(18.7)	30600	30516(20.5)	35600	35305(22.05)
P-xylene	14600	14511 (17)	15100	15028(17.3)	15600	15553(17.6)
M-xylene	-270	12.3 (0)	30	30.5 (0.5)	330	332 (2.1)

Table 7.02 Experimental molecular Kerr constant, $K_m^3 \times 10^{27}$ ($v^{-2} m^5 mol^{-1}$) and corresponding calculated dipole moment, μ_C enclosed in brackets for the iodine-aryl complexes

Compound	Molecular Kerr Constants ${}_m K_3$			
	Minimum	Mean		Maximum
		Experimental	Theoretical	
O-xylene	24800	29400	253 (911)	34000
P-xylene	8500	8900	210 (794)	9300
M-xylene	750	1050	182 (783)	1350
Biphenyl	780	910	238 (858)	1040
M-Biphenyl- Benzene	-440	-370	-369 (-30)	-300
Terphenyl	590	820	346 (990)	1050

Table 7.03 Experimental molecular Kerr Constant ${}_m K_3 \times 10^{27}$
 $(\text{v}^{-2} \text{m}^5 \text{mol}^{-1})$ for TCNQ-aryl complexes.

Theoretical ${}_m K_3$ values enclosed in brackets were from altered principal polarizabilities of TCNQ ($b_1 = 50$, $b_2 = 18.76$, $b_3 = 11.12$)

in order. It is known that 1,4-dioxane will dissolve a variety of metal salts, when the lattice energy of the salt is outweighed by the heat of solvation of the metal ion by the molecules of 1,4-dioxane. It is partly for this reason that care has to be exercised in the drying of 1,4-dioxane using anhydrous metal salts. Considering the strong electron withdrawing effects of the cyano groups of TCNQ, which make this molecule a powerful electron acceptor, it would seem reasonable to anticipate that TCNQ would interact quite strongly with the lone pair electron of the oxygens of 1,4-dioxane. Such an interaction would be expected to be favoured by a boat-like configuration of the 1,4-dioxane molecule.

Although the formation of a 1:1 bimolecular complex between TCNQ and 1,4-dioxane has not been proven it is useful to depict a possible juxtaposition of the two molecules in diagrammatic form as shown in figure 7.2.

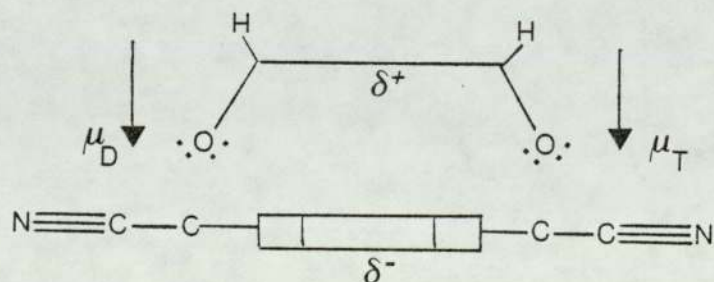


Figure 7.2 Structure of predicted 1,4-dioxane-TCNQ complex.

Polarization of the complex indicated by the partial charges δ^+ and δ^- together with the dipole moment contribution of 1,4-dioxane will result in a diminution of the molar Kerr constant since the resultant dipole moment μ_T is normal to the axis of maximum optical polarizability.

Dielectric and Electro-Optical Properties of Poly(N-vinyl-Carbazole) in Solution with Tetracyanoquinodimethane.8.01 Introduction

The photo-induced and bulk electrical conductivity of poly(N-vinylcarbazole), PVK, has been a subject of intensive investigation. The system is particularly interesting because the intrinsic semi-conductivity ($\approx 10^{-14} \text{ ohm}^{-1} \text{ cm}^{-1}$) of the polymer may be greatly enhanced by treatment with various dopant molecules such as TCNQ and I_2 . These dopants also influence the photo conductivity of the polymer by shifting the absorption spectrum into the visible region. In the pure PVK, conduction is dominated by holes which are long-lived and photo injected from metal electrodes. The unusual performance of this photo conductive polymer has been connected with its tendency to take up a helical conformation with successive aromatic side chains lying parallel to each other in a stack along which electron transfer is relatively easy⁽⁹⁹⁾. The addition of equimolar amounts of electron acceptor e.g. tetracyanoquinodimethane (TCNQ) and trinitrofluorenone (TNF) leads to increased photo conductance and is particularly useful in the generation of significant conductance under visible radiation. This is achieved by the formation of charge-transfer complexes (which strongly absorb in the visible region) between pendant carbazole residues acting as donor

groups and acceptor dopant molecules. The conductance is then dominated by electrons rather than holes. For a more detailed discussion of the application of PVK photoconductive systems, see Chapter 1.

In PVK:TCNQ complexes, the carbazole side group acts as the donor and TCNQ is the electron acceptor. As a direct result of the PVK:TCNQ complex formation, there is a charge transfer band in the absorption spectrum at 600 nm (100,101).

The PVK:TCNQ and PVK:TNF complexes are the systems mostly studied. In both cases complete complexing with the repeat units of PVK does not occur. The degree of complexing (ratio of complexed acceptor molecules to the stoichiometric amount) has been found to depend on component mole ratio. For example the degree of complexing was observed to decrease with the increase of acceptor concentration from 80% for a PVK:TCNQ mole proportion of 50:1 to 60% for 10:1 ratio.

Poly(N-vinylcarbazole), exists in various stereoregular forms because of the presence of an asymmetrical carbon in the repeat unit of the polymer. Proton and ^{13}C n.m.r. studies have indicated that synthetic routes used to prepare the polymer have a marked effect on its stereostructure (102-105). The various stereoregular forms of PVK therefore provide an interesting opportunity to study the effects of tacticity on the electrical and photo-

electrical properties of the pure polymer and when complexed with various dopants. Although some work has been done on the dielectric properties of PVK, Beevers and Mumby⁽¹⁰⁶⁾ were the first to present a detailed study in which the dielectric and electro-optical data were correlated with ^{13}C n.m.r. spectra for well characterised fractions of different stereostructural forms of PVK. Although the exact nature of these various structures has been the subject of much interesting discussion, broadly speaking there appear to be three main types of stereostructure as judged by NMR Spectroscopy⁽¹⁰⁷⁻¹¹⁴⁾, x-ray diffraction⁽¹¹⁵⁻¹¹⁸⁾ and measurements of glass transition temperature⁽¹¹⁹⁾.

8.02 Synthesis and Characterisation of Stereoregular Poly(N-vinylcarbazole)

The various stereoregular forms of PVK employed in this work were prepared and characterised in this laboratory⁽⁶¹⁾. For the sake of completeness a brief description of the preparative procedures will be given here.

N-vinylcarbazole was polymerised in solution using three different types of initiator. The polymerisation reactions were carried out in purpose-built glass reaction vessels (approximately 250 cm^3) fitted with glass-tight PTFE-glass joints and Suba Seals. The reaction vessels could be attached to a vacuum line for charging with solvent. All the solvents were distilled, dried over alumina and re-

distilled before use. The N-vinylcarbazole monomer (Fluka Ltd., Purum grade) was used as received. For all the polymerisation reactions the concentration of the monomer was approximately 0.5 m (97 g l^{-1}).

(1) Initiation using aluminium chloride:

The vinyl monomer was placed in the reaction vessel and toluene was added by distillation under nitrogen. The solution was thermally equilibrated at 298 K before adding a suspension of aluminium chloride (0.20 g) in toluene. The aluminium chloride was purified by subliming the material twice under vacuum. The concentration of the initiator was 0.5 mol % (0.0025 m) of the monomer concentration. The polymerisation was allowed to proceed for 18.5 hours at 298 K under dry nitrogen gas. The polymer sample prepared in this manner will be referred to as sample S1.

(2) Initiation with boron trifluoride etherate:

The vinyl monomer and freshly distilled toluene (150 cm^3) were placed in the reaction vessel. A small quantity (0.17 cm^3) of the initiator boron trifluoride etherate was injected into the reaction flask using a gas-tight syringe. The concentration of the initiator was 0.5% (0.0025 m) of the monomer concentration and the polymerisation time was 18.5 hours. All of these operations were conducted under an atmosphere of dry nitrogen. For convenience, polymers produced by this procedure will be referred to as S2.

(3) Initiation with azobisisobutyronitrile

A solution of the monomer in benzene (140 cm^3) was evacuated and degassed several times. The initiator, azobisisobutyronitrile (0.123 g) in solution in benzene ($\approx 6 \text{ cm}^3$) was injected into the reaction vessel through a Suba Seal. The concentration of the initiator was 1.00% (0.005 m) of the monomer concentration. The polymerisation reaction was allowed to proceed for 7 hours at 343 K under the vapour pressure of the solution. Polymer obtained by this procedure will be referred to as S3.

All of the polymerisations were terminated by pouring the reaction mixtures into methanol (500 cm^3). The polymers were purified by repeated precipitation (at least three times) by the dropwise addition of a 1% w/v solution of the polymer in toluene into methanol (500 cm^3), while vigorously stirring the mixture.

A commercial sample of PVK, prepared by the thermal polymerization of N-vinylcarbazole, was obtained from Polymer Consultants Ltd. London. This sample was purified by several precipitations in the manner previously described, and will subsequently be referred to as sample S4.

The polymer samples S1 - S4 prepared by the methods described above had a very broad distribution of molecular weight ($M_w/M_n > 9$) as judged by gel permeation chromatog-

raphy, with the exception of sample S3, which was estimated to have a polydispersity index of ca 2.9. The polymer samples S1 - S4 were fractionated to produce fractions possessing a range of molecular weights and a variety of polydispersity indices. This was achieved by dissolving the polymers in toluene to give an approximately 1% w/v solution and sufficient methanol was slowly added to produce a faint turbidity at 333 K. The temperature of the solution, which was controlled to within ± 0.05 K, was slowly decreased by a few degrees until a portion ($\sim 10\%$) of the polymer had precipitated. The temperature was kept constant for several hours during which time the flask was shaken regularly to permit the solution and the precipitated polymer to attain thermodynamic equilibrium. After allowing the system to form a well-defined boundary between the two phases the uppermost solution was carefully removed by decantation. The remaining layer represented the required fraction. This was dissolved in toluene, reprecipitated by adding methanol and dried. Further fractions were produced from the remaining solution by repeating the above procedure at successively lower temperatures down to a final temperature of 273 K.

The fractions of the PVK samples were characterised in terms of number-average and weight-average polystyrene equivalent molecular weights, M_n and M_w , respectively, using a Waters gel permeation chromatograph fitted with Styrogel columns with nominal porosities 10^3 , 10^4 , 10^5 and 10^6 nm. This combination of columns produced a satisfactory

separation for the majority of the PVK fractions. However, some of the higher molecular weight fractions were excluded from the columns and for these samples no reliable values of molecular weight and polydispersity index were obtained.

The absolute weight-average molecular weights of the various samples were also determined using a low-angle light-scattering (LALLS) unit attached to the eluent output of the GPC instrument.

One of the earliest carbon-13 NMR Spectra of poly(N-vinylcarbazole) was that published by Tsu chishashi et al⁽¹¹²⁾. They assigned most of the absorption peaks by comparing the spectrum of the polymer with those obtained for the model compound n-propyl carbazole. Kawamura and Matsuzaki⁽¹¹⁴⁾ completed the assignment of the peaks in the carbon-13 spectrum of PVK and observed that the shapes and relative intensities of the methine and methylene carbon absorptions depended on the method of polymerisation. The absorptions of the methine carbon of samples of PVK prepared by radical routes were observed to be split into a 'triplet', while those for samples of PVK obtained by cationic methods were split into a 'doublet'. It was tentatively assumed that the polymers of n-vinylcarbazole, obtained via radical polymerization, possessed a high proportion of syndiotactic sequences, and that PVK prepared using BF₃ etherate was predominantly isotactic and that PVK synthesised using Al(Et)Cl was composed of stereoblock

structures. Williams and Froix⁽¹¹³⁾ have reported carbon-13 spectra for samples of PVK prepared using synthetic methods similar to those described previously. However, the spectrum obtained by these authors for PVK initiated by BF_3 etherate, closely resembles the NMR spectrum published by Kawamura and Matsuzaki⁽¹¹⁴⁾ for PVK prepared using $\text{Al}(\text{Et})\text{Cl}_2$. Williams and Froix deduced that the methine peak was comprised of absorptions due to mr, rr and mm triads (where m and r respectively denote meso and racemic dyads of consecutive repeat units) and that the methylene carbon-13 peak was the sum of absorptions associated with rmr, mrm, rrr, mrr, mnr and mm tetrad stereostructures. By measuring the relative intensities of these various contributions these authors were able to draw certain conclusions regarding the spatial distribution of the pendant carbazole groups. Williams and Froix refuted the notion that PVK molecules consist of long blocks of either isotactic or syndiotactic sequences. However, the text of their paper notes that there is an increase in racemic content for cationically prepared PVK whereas the corresponding NMR data apparently indicate a decrease in racemic content, in agreement with the observations of Okamoto et al⁽¹¹⁰⁾.

The NMR spectral data for the PVK samples used in the present study⁽⁶¹⁾ and supported by the published work of Williams and Froix⁽¹¹³⁾ indicate that cationically prepared PVK possesses 54% meso dyads and 46% racemic dyads and that radically prepared PVK is comprised of 41% meso

dyads and 59% racemic dyads. For the PVK sample obtained by thermal initiation(S4), Beevers and Mumby obtained⁽¹⁰⁶⁾ a close match between calculated and experimental dipole moments using a value of 1:7 for the ratio of meso dyads to racemic dyads, respectively.

8.03 Preparation of PVK:TCNQ complexes in Solution in 1,4 Dioxane

Solutions of the PVK samples S1 - S4 (1% w/v) in 1,4-dioxane were prepared by dissolving accurately weighed quantities (~ 1 g) of polymer in 100 cm^3 of 1,4-dioxane. Granular forms of the polymers were first crushed into powders to aid the dissolution. In some cases, sonification was employed to aid the dissolution of the polymers. Generally the polymer-solvent mixture was allowed to stand for at least 24 hours to ensure that all the material has gone into solution. The solutions were transparent and viscous.

Similarly, the PVK:TCNQ complexes were prepared by dissolving 1 g of polymer and 0.1 g TCNQ in 100 cm^3 of 1,4-dioxane. This gave an intensely green, viscous solution of the TCNQ-polymer complexes. Solubility of the polymer-TCNQ complexes was rather poor ($\sim 1 - 2\%$ w/v) in 1,4-dioxane and the solution was therefore kept in stoppered flasks in a water bath maintained at about 333 K for 2 - 3 hours to aid dissolution.

8.04 Kerr Effect of the PVK Samples S1 - S4 and their TCNQ Complexes

All the measurements of the Kerr effect of solutions of PVK samples S1 - S4 and their corresponding TCNQ complexes were made at 298 K. Although some difficulties were experienced due to the attenuation of light by the intense green solution of the polymer complexes, reproducible results were obtained with these materials.

Figures 8.1, 8.2, 8.3 and 8.4 show plots of the rotation of plane polarized light α' , versus the square of applied voltages for the polymer samples S1, S2, S3 and S4, respectively, in 1,4-dioxane at 298 K. These figures also include data for the pure polymers in 1,4-dioxane at 298 K.

These data indicate that PVK samples S2 and S4 exhibited an increased Kerr effect when complexed with TCNQ whilst samples S1 and S3 produced a decreased Kerr effect as a consequence of complex formation with TCNQ. This is apparent by comparing the gradients of the plots of α' versus V^2 for the pure polymers and their corresponding TCNQ complexes.

The experimental Kerr constants, B, for the pure polymer samples S1 - S4 and the Kerr constants of their corresponding TCNQ complexes were determined as previously described in section 3.08. These are given in table 8.1. All the PVK samples S1 - S4 gave negative experimental Kerr constants,

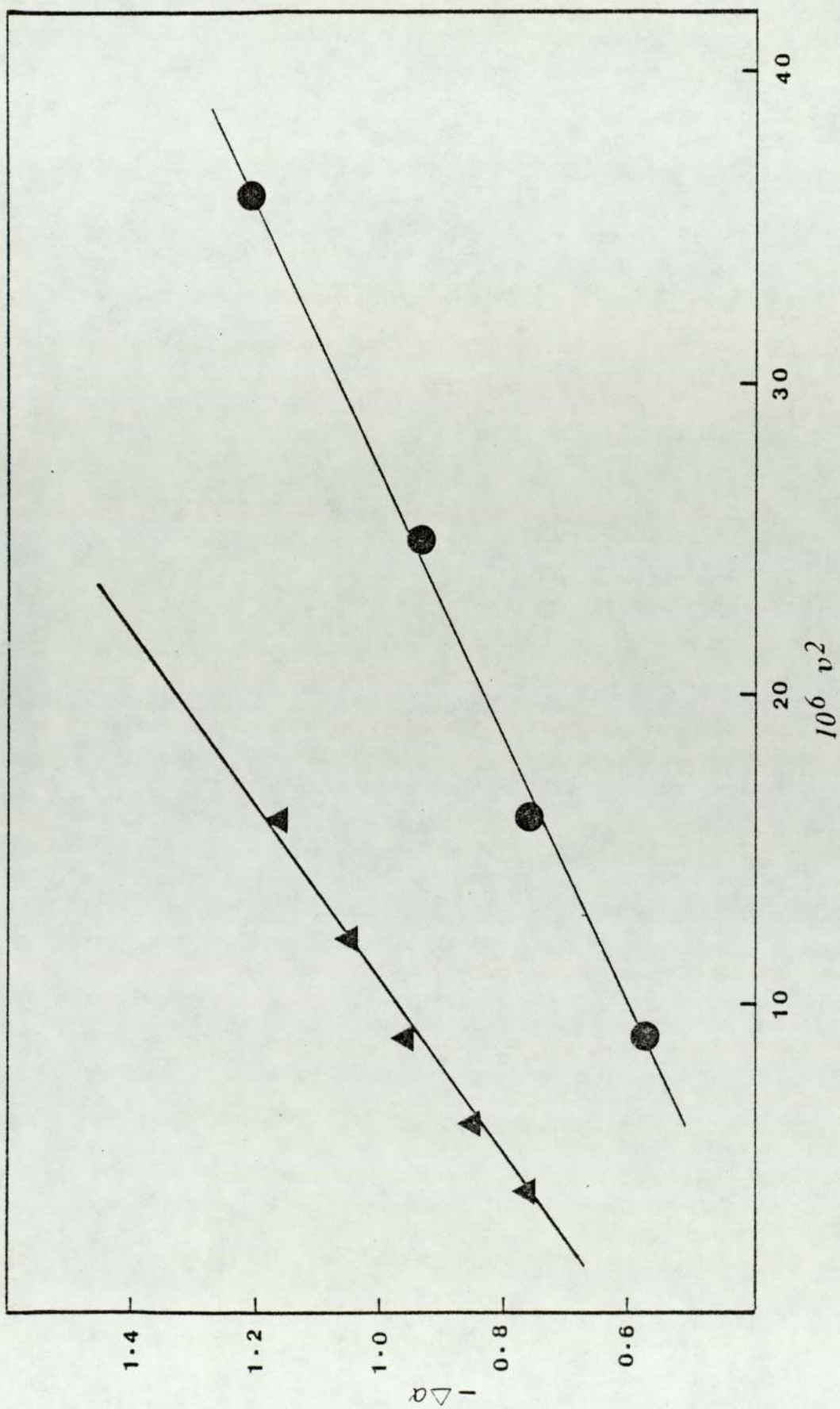


Figure 8.1 Rotation of plane-polarised light as a function of the square of applied voltage for PVK sample S1 (▲) and the TCNQ complex (●) in 1,4-dioxane at 298 K

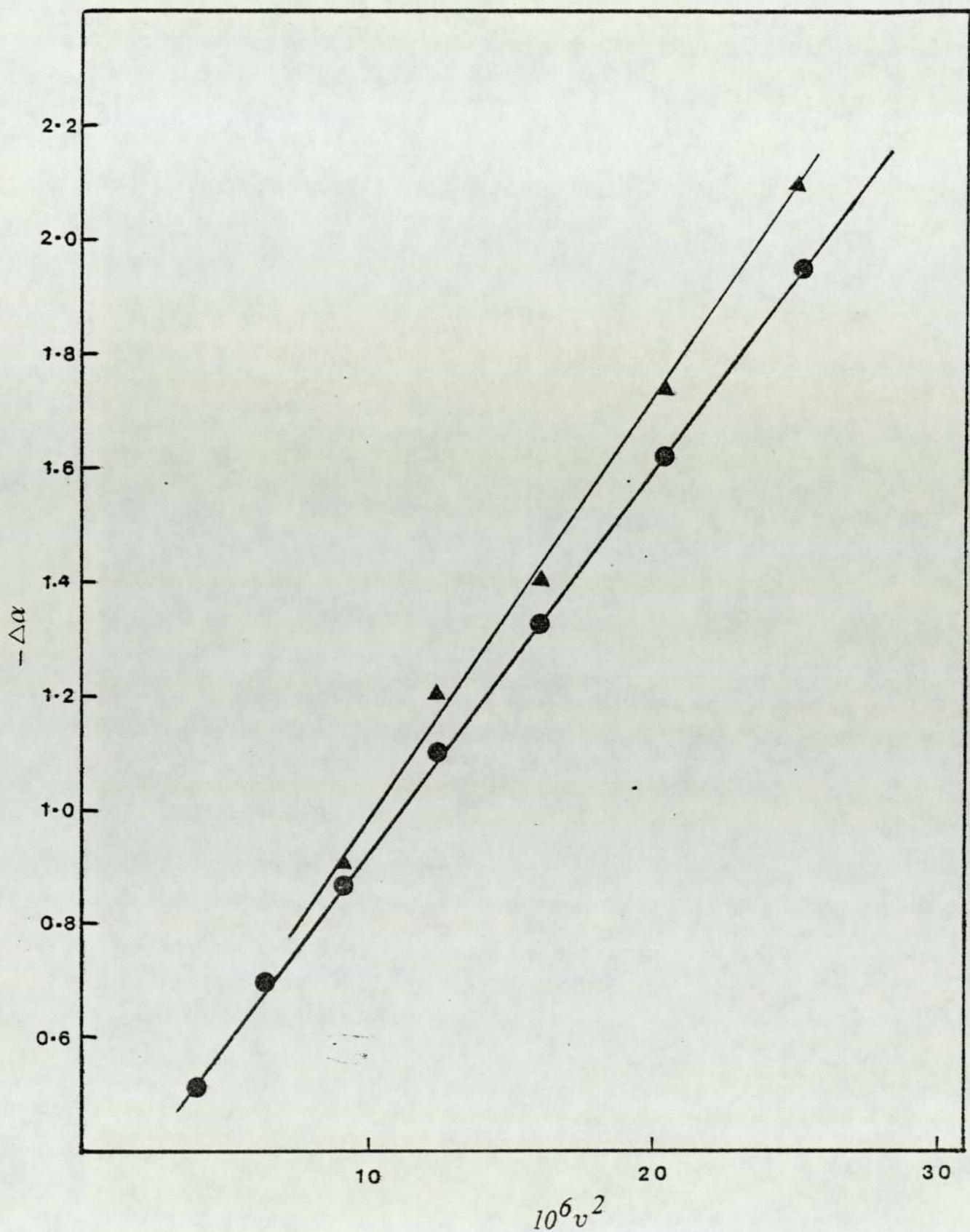


Figure 8.2 Rotation of plane-polarised light as a function of the square of applied voltage for PVK sample S2 (●) and the TCNQ complex (▲) in 1,4-dioxane at 298 K

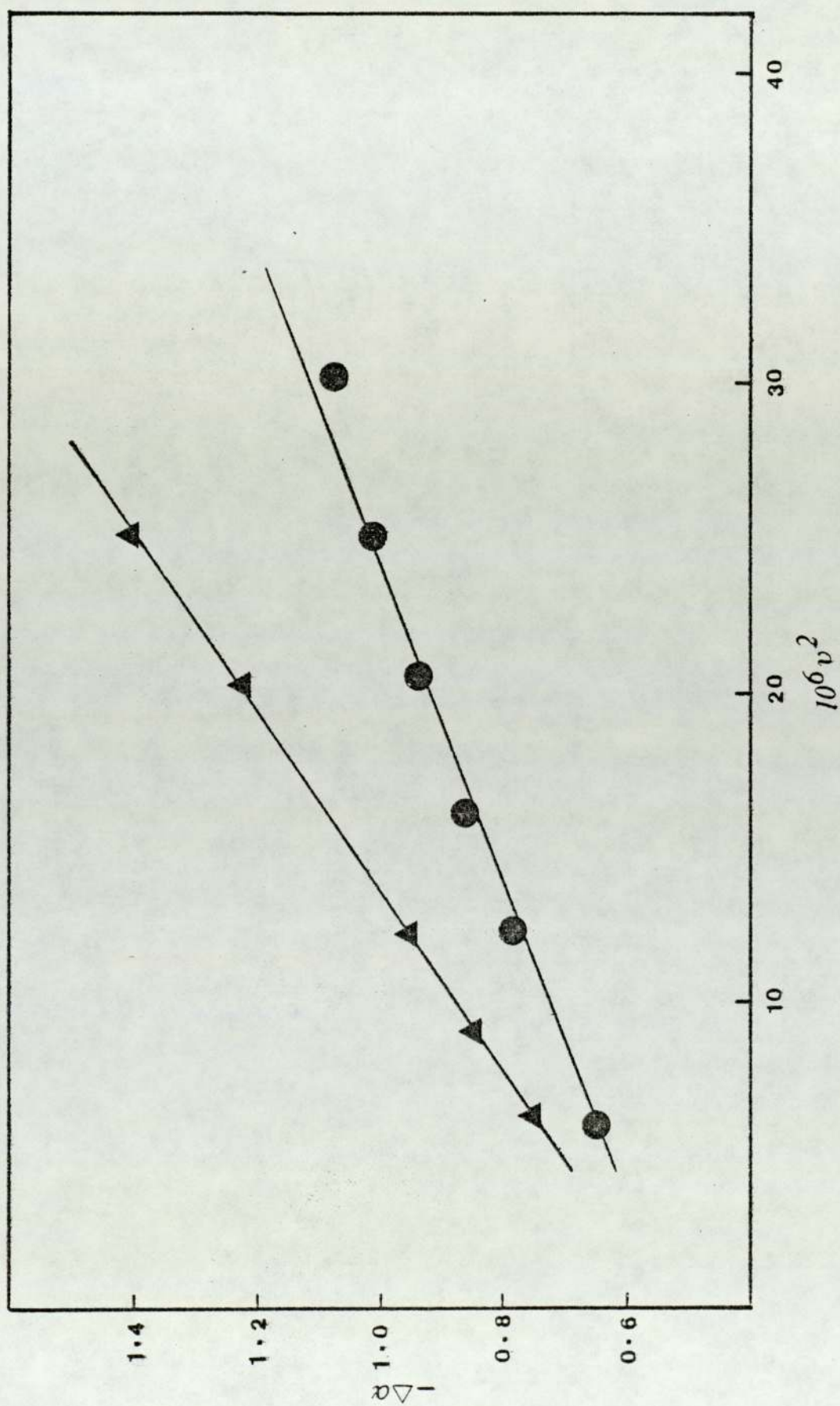


Figure 8.3 Rotation of plane-polarised light as a function of the square of applied voltage for PVK sample S3 (▲) and the TCNQ complex (●) in 1,4-dioxane at 298 K

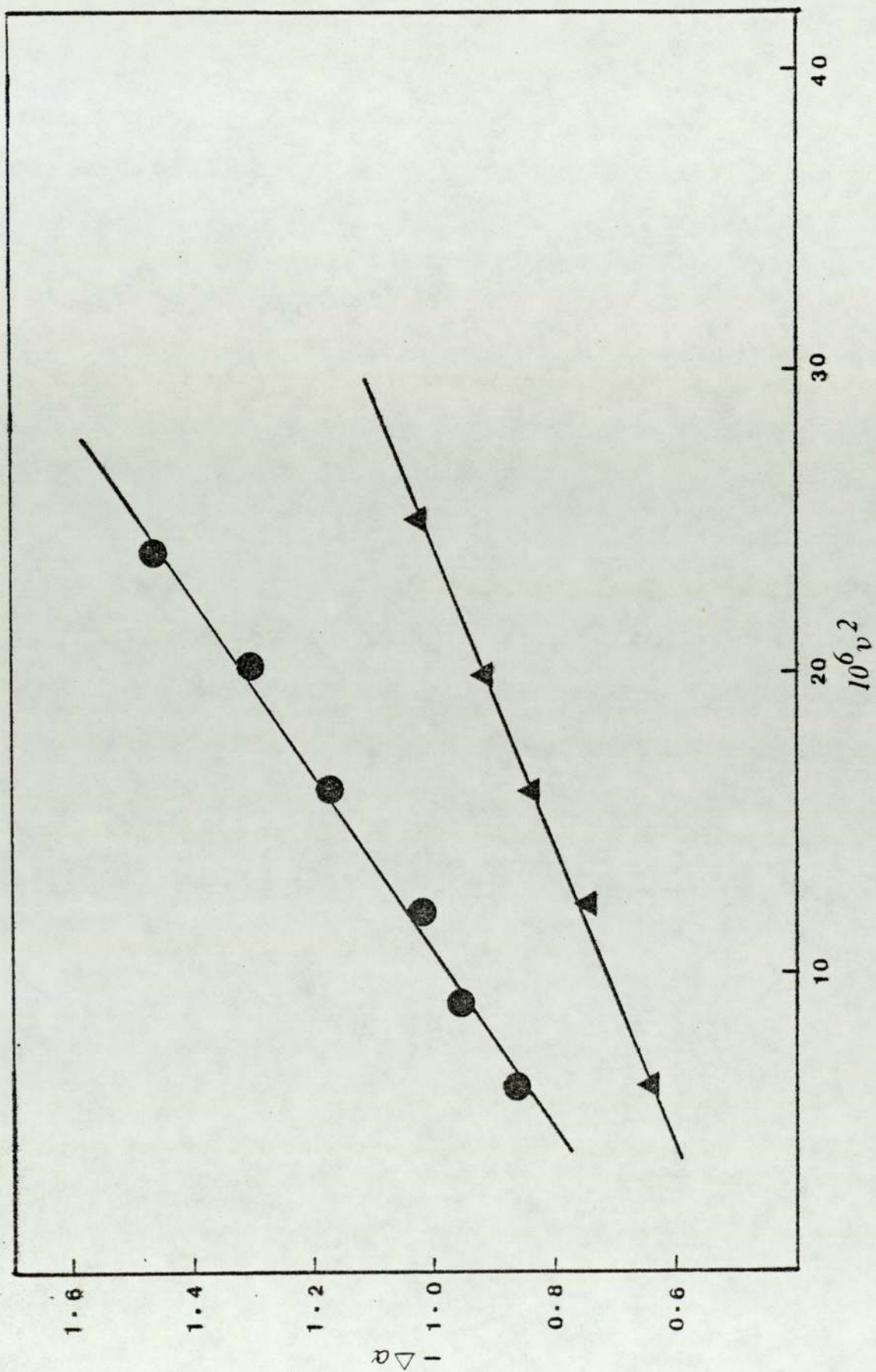


Figure 8.4 Rotation of plane-polarised light, as a function of the square of applied voltage for PVK sample S4 (\blacktriangle) and the TCNQ complex (\bullet) in 1,4-dioxane at 298 K

S1	v^2	9.0	16.0	25.0	36.0	
	α'	0.57	0.77	0.94	1.20	
S1-TCNQ complex	v^2	4.0	6.25	9.0	12.25	16.0
	α'	0.76	0.84	0.95	1.05	1.16
S2	v^2	9.0	12.25	16.0	20.25	25.0
	α'	0.87	1.11	1.34	1.63	1.96
S2-TCNQ complex	v^2	9.0	12.25	16.0	20.25	25.0
	α'	0.9	1.2	1.41	1.74	2.1
S3	v^2	9.0	12.25	16.0	20.25	25.0
	α'	0.84	0.94	1.05	1.21	1.4
S3-TCNQ complex	v^2	9.0	12.25	16.0	20.25	25.0
	α'	0.98	1.05	1.15	1.2	1.27
S4	v^2	6.25	9.0	12.25	16.0	20.25
	α'	0.64	0.74	0.83	0.91	1.03
S4-TCNQ complex	v^2	6.25	9.0	12.25	16.0	20.25
	α'	0.87	0.95	1.02	1.17	1.3

Table 8.1 Rotation of plane polarized light as a function of the square of the applied voltage v for pure PVK samples and their TCNQ complexes in 1,4-dioxane at 298 K

PVK Samples	$-10^{14} B_{12}$ ($v^{-2} m$)	$-10^{14} B_{13}$ ($v^{-2} m$)	ΔB_{23}	$-\delta_{12}$	$-\delta_{13}$	$\Delta\delta_{23}$
S1	0.58	0.46	0.12	678	516	162
S2	0.86	0.94	-0.08	1077	1184	-107
S3	0.397	0.22	0.177	443	204	239
S4	0.297	0.36	-0.063	305	396	-91

Table 8.2 Kerr effect data for PVK samples and their TCNQ complexes in 1,4-dioxane at 298 K

B_{13} and B_{23} denotes the solution Kerr constant of the complex and the additional increment in the solution Kerr constant due to the presence of TCNQ.

δ_{13} and δ_{23} are the corresponding delta values

PVK Solutions in 1,4-Dioxane	Frequency readings (Hz)	Permittivity ϵ	Dielectric increment $\Delta\epsilon$
S1 Polymer Complex	98,863	2.245 (8)	+0.001
	98,862	2.246 (8)	
S2 Polymer Complex	98,848	2.262 (5)	-0.0022
	98,850	2.260 (3)	-0
S3 Polymer Complex	98,863	2.245 (8)	-0.0023
	98,865	2.243 (5)	
S4 Polymer Complex	98,812	2.302 (7)	-0.0123
	98,823	2.290 (4)	

Table 8.3 Dielectric data for various samples of PVK and their TCNQ

complexes in solution in 1,4-dioxane.

(Air = 100,000 Hz; 1,4-dioxane = 98896 Hz; ϵ_1 dioxane = 2.209)

PVK Samples	\bar{M}_w	$-10^{14} B_{12}$ (v^{-2}_m)	$-\delta$	ϵ_{12}	$\epsilon_{12} - \epsilon_1$
S2/F1	231,000	0.74	915	2.2606	0.053
S2/F2	2,880,000	0.73	901	2.2817	0.073
S2/F3	7,050,000	0.744	920	2.2587	0.050
S2/F4	13,600,000	0.79	987	2.2684	0.059
S1/F1	5,360,000	0.422	476	2.2569	0.048
S1/F2	329,000	0.383	423	2.2541	0.045
S1/F3	966,000	0.453	520	2.2532	0.044

Table 8.4 Kerr effect data for a 1% w/v solution of various molecular weights of PVK samples (S2/F1, S2/F2, S2/F3, S2/F4, BF_3 initiated and S1/F1, S1/F2, S1/F3, $AlCl_3$ initiated) in 1,4-dioxane at 298 K

B. It is interesting to note that samples S1 and S3 produced TCNQ complexes with decreased solution Kerr constant with respect to the solution Kerr constant of the pure polymer, and the magnitudes of the decreases were similar (δB_{23} for S1 = 0.12 and δB_{23} for S3 = 0.177). Similarly, the PVK samples S2 and S4 produced complexes with larger solution Kerr constants than the corresponding pure polymers. The differences between the solution Kerr constant of the complex and the pure polymer for these samples are similar. (δB_{23} for S4 = -0.063 and δB_{23} for S2 = -0.08).

S1 type PVK sample ($AlCl_3$ initiated) forms TCNQ complex with smaller Kerr constants than those found for the pure polymer. This is only possible if the complex formation is accompanied by a decrease in the optical anisotropy compared to that of the pure polymer. It could also be due to a smaller dipole moment associated with the complex compared to the repeat unit of the pure polymer. However, the dielectric increment (see table 8.3) suggests that the resultant dipole moment of the complex is greater than that of the pure polymer. The dipole moment contribution to the Kerr constant therefore appears to be rather insignificant with respect to the anisotropy contribution.

For the polymer sample S2 (BF_3 initiated) the complex formation is accompanied by an increase in Kerr constant which would tend to suggest an increased anisotropy and/or an increased dipole moment as a result of complex formation.

The negative dielectric increment further favours the anisotropy change as the dominant factor in the determination of the Kerr constant.

Similarly, S3 type PVK samples (AZBN initiated) form a TCNQ complex with a substantial decrease of the Kerr constant with respect to the pure polymer. The most probable explanation for this change could be the decrease in anisotropy as a result of the formation of the complex and/or a smaller resultant dipole moment associated with the complex. However, the magnitude of the dielectric increment suggests an insignificant change in dipole moment. A decrease in optical anisotropy as a result of complex formation would make the dipole moment term a dominant factor in determining the magnitude of the Kerr constant of the complex.

For the PVK type S4 (thermally initiated) the formation of the TCNQ complex produced a substantial increase in the Kerr constant. This may arise from a change in conformation as a result of the complex formed with TCNQ or it could be due to larger resultant dipole moment. However, the dielectric data (see table 8.3) for the complex indicate a negative dielectric increment, thus appearing to rule out the significance of the dipole moment contribution to the Kerr constant. A significant change in conformation adopted by the complexed PVK molecule appears to be responsible for the increase in Kerr constant of the complex with respect to the pure polymer. It is

interesting to note that dipole moment calculations on the PVK type S4 by Beevers and Mumby⁽¹⁰⁶⁾ suggested that it has the highest degree of stereoregularity with an estimated ratio of 1:7 for meso dyads to racemic contents respectively. Thus it has a racemic content nearest to syndiotactic PVK.

8.05 Investigation of Molecular Weight Dependence on Kerr Constant for PVK Samples

The dependence of Kerr constants and dipole moments on molecular weight for the pure PVK samples was investigated. Dielectric and Kerr effect measurements were performed on various molecular weights of PVK types S1 and S2. A summary of the results is given in table 8.4.

Both the Kerr effect and the dielectric data indicate no significant changes with molecular weight of these samples. For example the PVK sample S2/F1 ($\bar{M}_w = 7,050,000$) has a solution Kerr constant, B_{12} of $0.744 \times 10^{-14} \text{ v}^{-2} \text{ m}$. Similarly the dielectric increment ($\epsilon_{12} - \epsilon_1$) for the sample S2/F1 is 0.053 and the dielectric increment for the sample S2/F3 is 0.050.

8.06 Dielectric Permittivities of PVK and PVK:TCNQ Complexes in Solution in 1,4-Dioxane

The static dielectric permittivities of PVK samples S1 - S4 and their TCNQ complexes has been determined in 1,4-

dioxane at 298 K and according to the procedure described previously in section 3.11. The data of the dielectric measurements are summarised in table 8.3. Only PVK sample S1 showed an enhanced dielectric increment attributable to the formation of a complex with TCNQ ($\delta\epsilon = 0.001$). Samples S2, S3 and S4 on the other hand showed a decreased dielectric constant when they form complexes with TCNQ. The PVK samples S2 ($\delta\epsilon = -0.0022$) and samples S3 ($\delta\epsilon = -0.0023$) show a comparable decrease in dielectric constant with the formation of the complex. The PVK sample S4 appeared to be modified to a greater extent than the other samples as evident in the magnitude of the dielectric increment ($\delta\epsilon = -0.0123$).

In principle, it should be possible to calculate, using measured dielectric permittivities, the molecular dipole moment of the complex formed between the carbazole units and a molecule of TCNQ. However, there are a number of difficulties associated with this exercise.

Firstly, it is necessary to have an accurate estimate of the concentration of complex formed in solution since it is absolutely essential that the dielectric increment is apportioned between free (uncomplexed) carbazole groups, free TCNQ molecules and the PVK:TCNQ complex.

Secondly, the experimentally determined dielectric increment must be very accurate, which in practice was found to be a difficult constraint to satisfy mainly due to the rather poor solubility of the PVK:TCNQ complex.

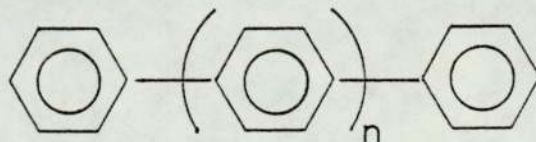
However, despite these reservations concerning the interpretation of the solution dielectric permittivities they are sufficiently accurate to be used in the $(\epsilon + 2)^2$ term appearing in equation (6.9) used to calculate molecular Kerr constant.

CHAPTER 9

General Conclusions and Suggestions for Future Work

In this chapter the main conclusions of the preceding chapters are discussed and enlarged upon. Suggestions are also made for extending certain aspects of the research.

It has been demonstrated, using mainly chromatographic techniques, in conjunction with infra-red spectroscopy and carbon-hydrogen analysis, that the preparation of oligophenylenes and polyphenylenes can be carried out using a variety of synthetic techniques starting with benzene, 1,4-dibromobenzene or biphenyl. It has been shown that the amount of extractable, low-molecular weight material is very dependent on the synthetic route and reaction conditions. Analytical gel permeation chromatography has permitted the separation and identification of para-substituted oligophenylenes.



with $n = 0 - 6$

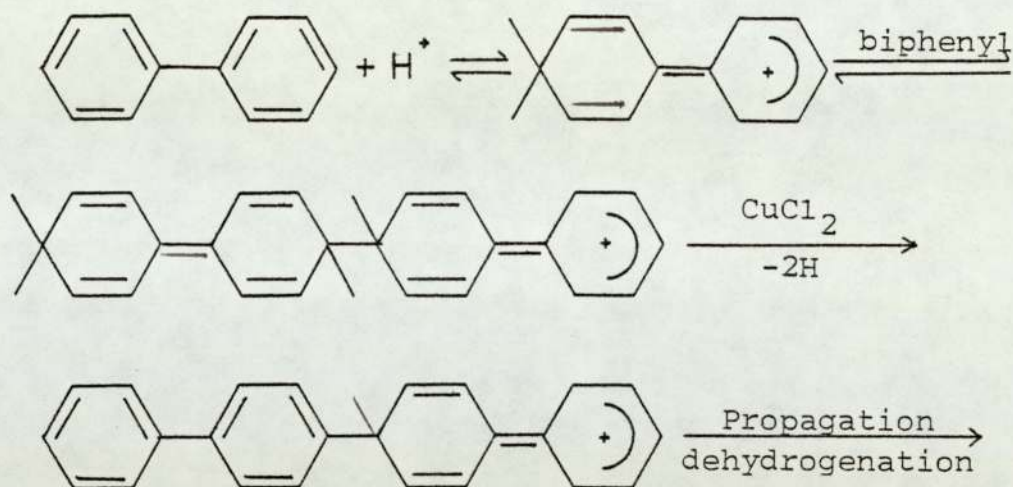
The quantity of chloroform extractable oligomeric species from polymers produced by reactive para-coupling of benzene

dramatically increases when the polymerization is carried out in the presence of substantial volume proportions of an 'inert' solvent (e.g. cyclohexane). However, even small quantities of ethereal types of solvents were found to severely inhibit the polymerization process, indicating a substantial degree of complexation between the solvent and the 'catalyst' (particularly with AlCl_3).

The Kovacic method of preparing polyphenylenes was repeated in this laboratory. Analysis of the chloroform extractable material using analytical GPC revealed that the extracts were composed of a very wide range of non-para substituted poly-aryls, in addition to the linear polyphenylenes.

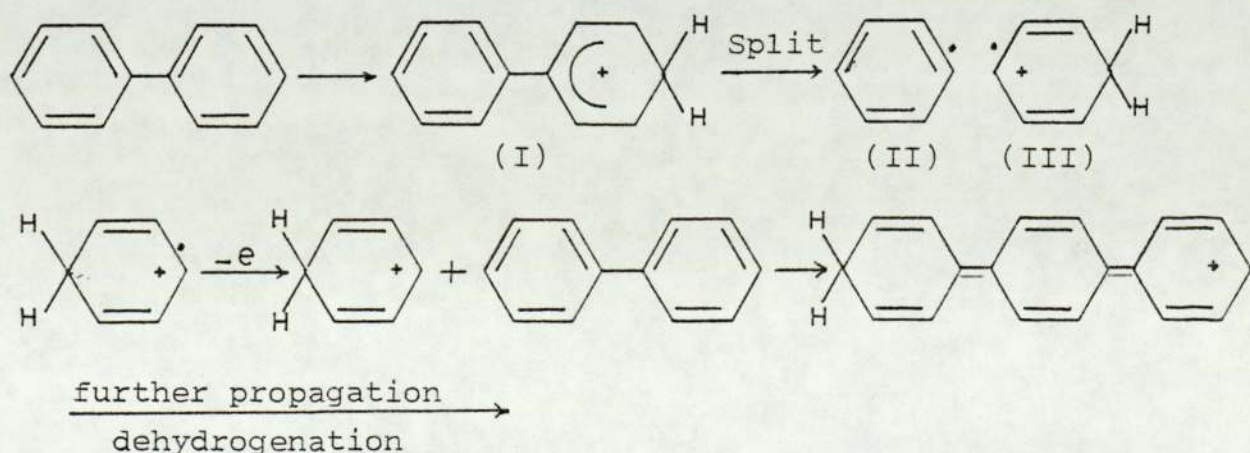
The polymerization of biphenyl in solution in cyclohexane employing Kovacic types of catalyst mixtures, resulted in high yields of predominantly para-substituted oligophenylenes. Analytical gel permeation chromatography indicated almost entirely para-substituted products over the range $n = 2-7$. An interesting feature of this synthetic procedure was that it produced substantial quantities of odd-numbered oligophenylenes.

The simplest polymerization scheme for biphenyl is one in which there is an irreversible propagation step and a termination stage. Kovacic and Lange⁽¹²²⁾ first proposed that the polymerization proceeded by an oxidative cationic mechanism similar to that advanced for the benzene polymerization as described earlier. Thus:



However, this scheme would produce only even-membered oligophenylenes. An element of reversibility (depolymerization), in which either one or two phenyl units are removed from the main oligomeric chain, is a possible explanation for the production of odd and even membered oligophenylenes from biphenyl monomer. More elaborate explanations can be devised to account for these observations.

One of these involves the formation of an initiator complex comprised of a single phenyl unit similar to that believed to exist for the reductive polymerization of benzene. We therefore propose the following scheme in an attempt to account for the formation of the odd-numbered phenylene oligomer.



The scheme involves the formation of biphenyl cation which splits to form two reactive species, a phenyl radical and a phenyl radical cation. The radical cation loses its lone electron to form the cation and propagates cationically by reacting with a neutral biphenyl molecule. Although the reaction conditions did not permit the detection of benzene, trace amounts were observed by Kovacic and Lange⁽¹²²⁾. We anticipated the formation of benzene to occur through hydrogen abstraction by the phenyl radical species (II) or by a proton loss from the radical-cation (III). This hypothesis would also account for the relatively large concentrations of terphenyl and quinquiphenyl during solution polymerization of biphenyl. The noticeable reduction in non-para-substituted oligomers may well be due to the mutual directing influence of the phenyl moieties of biphenyl.

Polyphenylene and oligophenylenes were also synthesized by a transition-metal catalysed carbon-carbon coupling method. This procedure gave good yields of polymer and quite high proportion of chloroform extractable oligophenylenes. However, elemental analysis showed that the oligomers contain bromine atoms, presumably in the terminal para positions. In view of this it is probably more appropriate to describe these oligomers as 1,4 -dibromo-para-oligophenylenes.

Analysis of the extracted mixtures of oligomers showed that the polymerization reaction was almost 100% para-

coupling between the growing oligomer and the monomer, 1,4-dibromobenzene. The presence of terminal bromine atoms in the oligomers formed from the coupling of 1,4-dibromobenzene enables these species to be regarded as possible precursors or blocks that may be incorporated into the backbone of flexible polymer molecules such as those of the polysiloxanes or polyvinyls. Flory⁽¹²³⁾ has shown that some of the oligophenylenes exhibit mesogenic (liquid crystal) behaviour in their melts. Other workers^(124,125) have demonstrated that interesting mesogenic behaviour can be induced in polymers of relatively simple structure by incorporating mesogenic groups either in the backbone of the polymer or by their attachment to flexible side-chains.

An important aspect of the investigations described in the preceding chapters was that involved with the doping of polymers in order to greatly enhance their electrical conductivity. Because of the intractable nature of the majority of polymer-dopant systems it is very difficult to study their detailed molecular structure. A partial solution to this problem is achieved by examining the properties of complexes formed between oligomers and dopant molecules when dissolved in a suitable solvent. In this way it should then be possible to derive information concerning the nature of the electronic interactions between the polymers and dopant molecules.

A comparative study was undertaken of the dielectric and Kerr effect behaviour of o-, m- and p-xylenes in the pure state and with small amounts of added iodine and TCNQ.

Although the measurements of dielectric permittivity indicated relatively small differences in the degree of complexation of the xylenes with iodine and TCNQ, the molecular Kerr constants of the complexes were found to differ quite considerably for the three xylene systems.

The magnitudes and signs of the molar Kerr constants found for the o-, m- and p-xylene/iodine system and o-, m- and p-xylene/TCNQ system indicated that the complexes are either substantially more polarizable or substantially more anisotropic than the sum effect of their constituent molecular components. Significantly smaller molar Kerr constants were found for the iodine and TCNQ complexes of toluene. The methyl substituents and their substituted pattern appear to play an important role in determining the electronic properties of the xylene-acceptor complexes, probably through their ability to donate negative charge via a +I inductive effect. The net polarization of the complexes is also dependent on the interactions between the permanent dipole moment of the xylene molecule (m- and o-xylene only) and the electrons of either the iodine or TCNQ molecules. Interactions of a similar nature are not ruled out for p-xylene which despite a zero dipole moment, possesses a non-zero quadrupole moment that can interact with the electrons of I_2 and TCNQ. In the calculation of the molar Kerr constants of the complexes certain approximations were made that would lead to an underestimation of these quantities. Thus, a more accurate determination (where applicable) would be expected to increase, not decrease the magnitudes of the molar Kerr constants.

Similar studies were also carried out for benzene, biphenyl, terphenyl and m-biphenylbenzene. These studies were performed in solutions in 1,4-dioxane at 298 K, except for benzene which was studied in the pure state.

The molar Kerr constants determined for the benzene-iodine complex ($6.8 \times 10^{-24} \text{ v}^{-2} \text{ m}^5 \text{ mol}^{-1}$) which is approximately ten times larger than the value ($6.5 \times 10^{-25} \text{ v}^{-2} \text{ m}^5 \text{ mol}^{-1}$) measured for iodine in carbon tetrachloride, indicates that there are substantial changes in either the polarizability or anisotropy of polarizability of the molecules as a result of complex formation and/or that the complex is endowed with a modest dipole moment. The latter proposal appears to be supported by dielectric data (see table 6.02) obtained for solutions of iodine in benzene. Although complexes formed from benzene and TCNQ were made it was not possible to study their dielectric and electro-optical properties because of insufficient solubility in acceptable solvents.

The Kerr effect data for solutions of biphenyl, terphenyl and m-biphenylbenzene indicates that there are marked departures from ideality in the presence of TCNQ. The molar Kerr constants of the aryl molecules and TCNQ are very small compared to those of the resultant complexes and it is anticipated that these differences will be increased if the concentration of complex is decreased relative to the concentration of free (not complexed) TCNQ.

Dielectric and Kerr effect techniques were also used to

investigate the nature and extent of complex formation between TCNQ and various stereoregular forms of poly(N-vinyl carbazole). The results of these experiments have shown quite clearly that stereoregularity has a marked effect on complex formation between TCNQ and poly(N-vinyl-carbazole), as judged by differences in the corresponding molar Kerr constants of the complexes. However, no evidence was found for any dependence of the Kerr constants on molecular weight or dispersity of molecular weight.

The performance of the poly(N-vinyl carbazole) as a photoconductive polymer described in earlier sections, has been attributed to its tendency to adopt helical conformation in which successive aromatic side-chains are parallel to each other and in so doing permit relatively easy transfer of electrons along the molecular framework. In complexes formed between TCNQ and PVK, the TCNQ molecules are believed to be interleaved with the carbazole side-groups in a 'herring-bone' fashion, so as to maximise orbital overlaps between donor (carbazole) and acceptor (TCNQ) groups. It would seem reasonable to expect that the photoconductive behaviour of PVK-TCNQ complexes would be affected by the stereoregularity of the polymer molecule since this would influence the formation of a regular helical structure. Further studies are necessary concerning this particular aspect of the work in order that measurements of photoconductivity may be correlated with electro-optical data derived for the TCNQ complexes for the various stereoregular forms of PVK.

APPENDIX 1.

OPTICAL THEORY OF THE KERR EFFECT

A1-I The Use of a Quarter Wave Retarder

The diagram in Figure A1-1 of the electric vectors of the light before entering, and after leaving, the various optical components, serves to illustrate the use of a quarter wave plate. The parallel beam of incident light, whose electric vectors are randomly oriented, is plane polarized at an angle of 45° to the direction of the applied electric field, E , by the polarizer. The electric vector,

$$\bar{V}_{45} = a \sin \omega t, \quad (A1-1)$$

may be resolved into the parallel and perpendicular components

$$\bar{V}_\perp = a \sin \omega t \sin 45^\circ \quad (A1-2)$$

and
$$\bar{V}_\parallel = a \sin \omega t \cos 45^\circ \quad (A1-3)$$

respectively. On passing through a birefringent sample the parallel component is retarded relative to the perpendicular component by a phase difference, δ , and the resultant waveform becomes

$$\bar{V}'_\parallel = a \sin (\omega t - \delta) \sin 45^\circ. \quad (A1-4)$$

The parallel and perpendicular components of the electric vector may each be further resolved into two components at 45° to the direction of the applied electric field. These components are

$$\bar{V}'_{45} = a \sin \omega t \cos^2 45^\circ + a \sin (\omega t - \delta) \sin^2 45^\circ \quad (A1-5)$$

and

$$\bar{V}'_{135} = a \sin \omega t \cos^2 45^\circ \sin 45^\circ - a \sin (\omega t - \alpha) \sin 45^\circ \cos 45^\circ, \quad (A1-6)$$

respectively. Component, \bar{V}'_{45} , suffers a relative phase retardation of $\pi/2$ (90°) on passing through the quarter wave plate. The waveform emerging from the quarter wave plate may now be represented by the

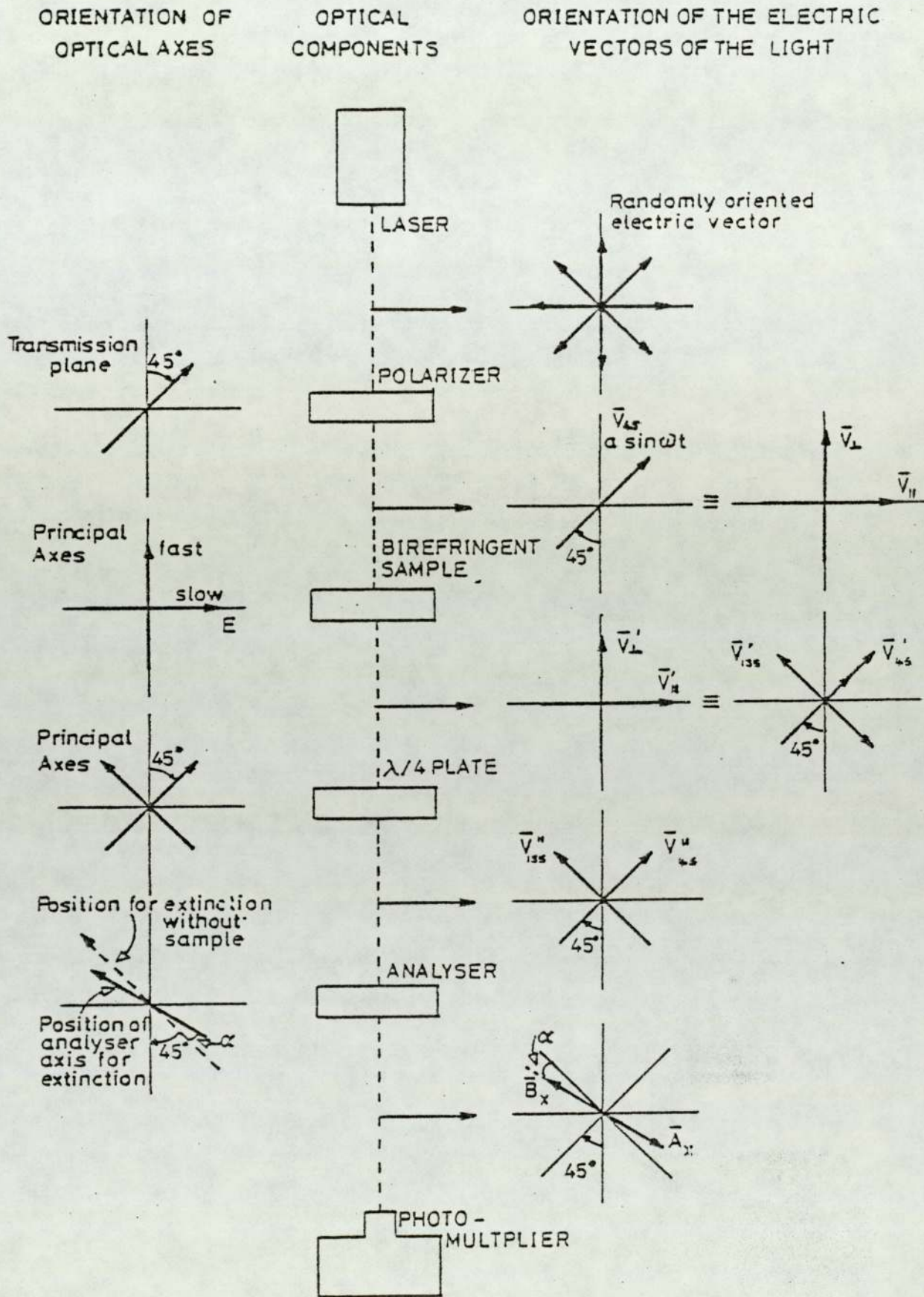


Figure A1-1 Electric vectors of light before entering, and after leaving, the various optical components of the electro-optical Kerr effect apparatus.

following orthogonal electric vectors

$$\bar{V}_{45}'' = a \sin(\omega t - \pi/2) \cos^2 45^\circ + a \sin(\omega t - \delta - \pi/2) \sin^2 45^\circ \quad (A1-7)$$

and

$$\bar{V}_{135}'' = a \sin \omega t \cos 45^\circ \sin 45^\circ - a \sin(\omega t - \delta) \sin 45^\circ \cos 45^\circ \quad (A1-8)$$

Since,

$$\sin 45^\circ = \cos 45^\circ$$

the two components may be simplified to give

$$\bar{V}_{45}'' = a \cos^2 45^\circ \left[\sin(\omega t - \pi/2) + \sin(\omega t - \delta - \pi/2) \right] \quad (A1-9)$$

and

$$\bar{V}_{135}'' = a \cos^2 45^\circ \left[\sin \omega t - \sin(\omega t - \delta) \right]. \quad (A1-10)$$

Applying the identity,

$$\sin x \pm \sin y = 2 \sin \frac{1}{2}(x \pm y) \cos \frac{1}{2}(x \mp y),$$

enables equations (A1-9) and (A1-10) to be rewritten in the form

$$\bar{V}_{45}'' = 2a \cos^2 45^\circ \left[\sin \frac{1}{2}(\omega t - \pi/2 + \omega t - \delta - \pi/2) \cos \frac{1}{2}(\omega t - \pi/2 - \omega t + \delta + \pi/2) \right] \quad (A1-11)$$

$$\text{and } \bar{V}_{135}'' = 2a \cos^2 45^\circ \left[\sin \frac{1}{2}(\omega t - \omega t + \delta) \cos \frac{1}{2}(\omega t + \omega t - \delta) \right]. \quad (A1-12)$$

These further simplify to give

$$\bar{V}_{45}'' = 2a \cos^2 45^\circ \cos \delta/2 \sin(\omega t - \pi/2 - \delta/2) \quad (A1-13)$$

$$\text{and } \bar{V}_{135}'' = 2a \cos^2 45^\circ \sin \delta/2 \cos(\omega t - \delta/2). \quad (A1-14)$$

Since,

$$\sin(x - \pi/2) = -\cos x$$

equation (A1-13) may be written in the form

$$\bar{V}_{45}'' = -2a \cos^2 45^\circ \cos \delta/2 \cos(\omega t - \delta/2). \quad (A1-15)$$

Thus, it can be seen that the two orthogonal components,

$$\bar{V}_{45}'' = -2a \cos^2 45^\circ \cos \delta/2 \cos(\omega t - \delta/2) \quad (A1-15)$$

$$\text{and } \bar{V}_{135}'' = 2a \cos^2 45^\circ \sin \delta/2 \cos(\omega t - \delta/2), \quad (A1-14)$$

have the same phase relationship, and differ only in their relative amplitudes. Therefore, the light emerging from the quarter wave plate is polarized and may thus be completely extinguished by the analyser when the latter is rotated by an amount $s\alpha_n$ from its normally crossed

position. The above procedure corresponds to the measurement of the static electro-optical Kerr effect.

AL-II Measurement of Phase Difference, δ , Using Static Electric Fields

Consider the waveform of the light after having passed through the sample and the quarter wave plate. The two orthogonal components of the electric vector of the light are expressed by equations (A1-15) and (A1-14). These components, \bar{V}_{4s}'' ($\equiv \bar{A}$) and \bar{V}_{13s}'' ($\equiv \bar{B}$), may be resolved (see Figure A1-2(a)) into two pairs of components, \bar{A}_x and \bar{B}_x , and \bar{A}_y and \bar{B}_y , such that \bar{A}_x and \bar{B}_x cancel one another, and \bar{A}_y and \bar{B}_y augment each other. In other words \bar{A}_y and \bar{B}_y , together, represent plane polarized light with the direction of the electric vector denoted by $s\alpha_n$. Referring to Figure A1-2(a), it can be seen that

$$\frac{\sin s\alpha_n}{\cos s\alpha_n} = \frac{\bar{A}_x/\bar{A}}{\bar{B}_x/\bar{B}} = \frac{\bar{B}}{\bar{A}} \quad (\text{A1-16})$$

Substituting expressions for components $\bar{A}(\equiv \bar{V}_{4s}'')$ and $\bar{B}(\equiv \bar{V}_{13s}'')$, as defined by equations (A1-15) and (A1-14), into equation (A1-16) one obtains

$$\frac{\sin s\alpha_n}{\cos s\alpha_n} = \frac{2a\cos^2 45^\circ \sin \delta/2 \cos(\omega t - \delta/2)}{-2a\cos^2 45^\circ \cos \delta/2 \cos(\omega t - \delta/2)}, \quad (\text{A1-17})$$

which may be readily simplified to give

$$\frac{\sin s\alpha_n}{\cos s\alpha_n} = \frac{\sin \delta/2}{-\cos \delta/2} \quad (\text{A1-18})$$

Hence,

$$\tan s\alpha_n = -\tan \delta/2 \quad (\text{A1-19})$$

and therefore,

$$s\alpha_n = -(\delta/2) \pm 2n\pi \quad (\text{A1-20})$$

Thus, for rotations of the analyser of less and 180° the relation

$$s\alpha_n = -\delta/2 \quad (\text{A1-21})$$

may be employed to determine the electrically-induced phase retardation, δ .

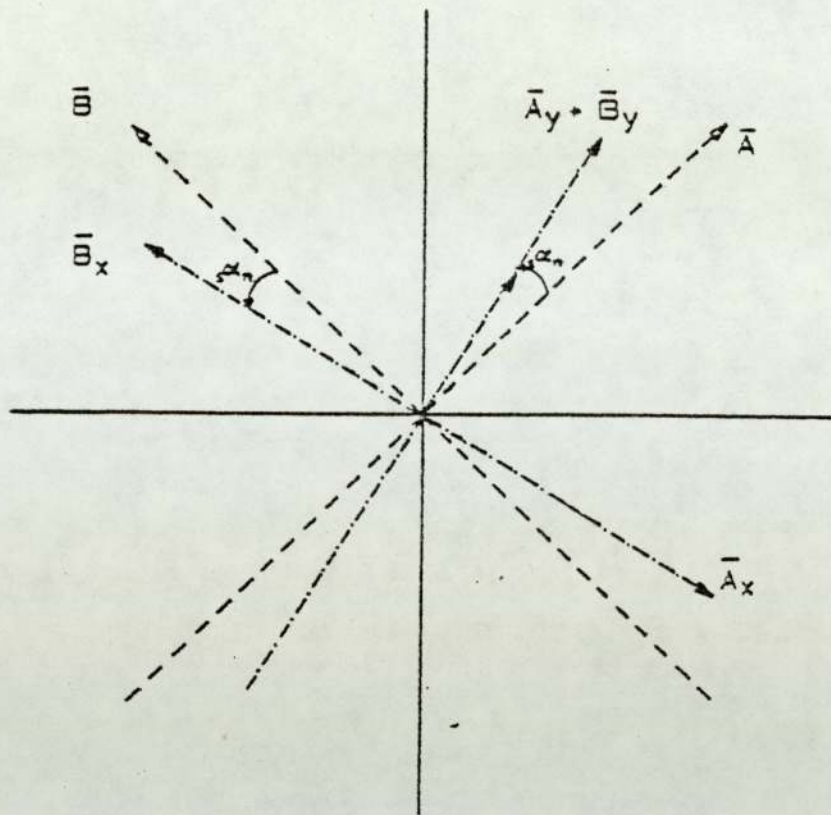


Figure A1-2(a) Resolved electric vector of light having passed through sample and quarter wave plate

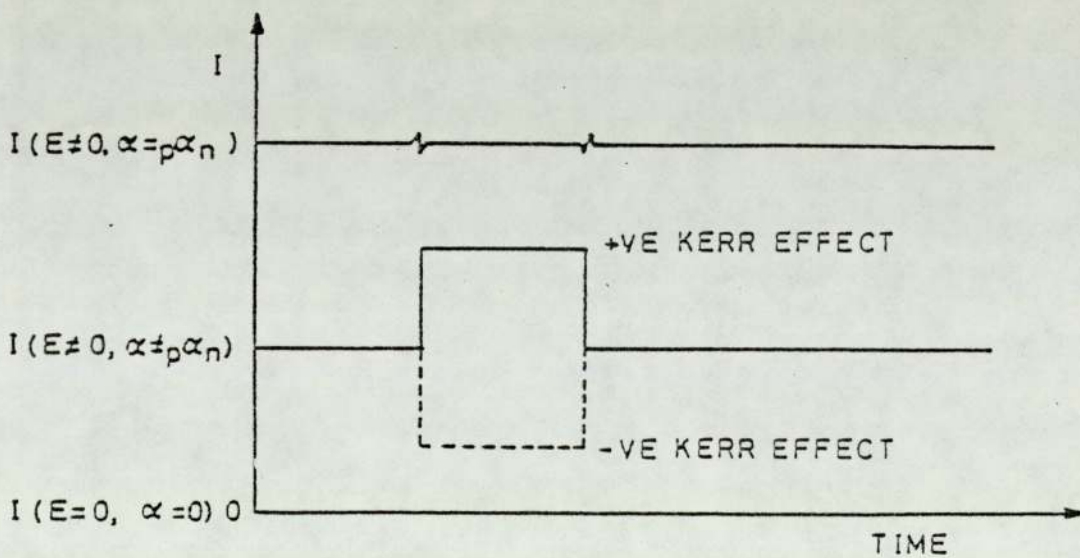


Figure A1 - 2(b) Optical pulse observed for different analyser rotations and electrical field conditions.

A1-III Measurement of the Phase Difference, δ , Using Pulsed Electric Fields

The symbol, $p\alpha_n$, denotes the rotation of the analyser, from its normally crossed position, required to null the pulse of light transmitted through the sample during the application of a short duration pulse of high voltage to the Kerr cell. In practical terms the amplitude of the pulse viewed on the oscilloscope is reduced, by rotation of the analyser, to the level corresponding to the absence of the applied electric field. See Figure A1-2(b).

The relationship between the transmitted intensity, I , of a plane polarized beam of light, the initial intensity, I_0 , and the rotation, α , of the analyser with respect to the nulled position is known as Malus' Law and may be expressed as

$$I = I_0 \sin^2 \alpha$$

Applying Malus' Law, the intensity of light transmitted by the analyser, when the applied electric field, E , is zero, is given by

$$I_{E=0} = I_0 \sin^2 \alpha. \quad (A1-22)$$

However, upon application of an electric field to the sample, the light transmitted by the sample becomes

$$I_{E \neq 0} = I_0 \sin^2(\alpha + \delta/2) \quad (A1-23)$$

If the electronically-induced pulse of light is nulled, by rotating the analyser, to the quiescent level then intensities $I_{E=0}$ and $I_{E \neq 0}$ become equal. Thus, from equations (A1-22) and (A1-23) we may write

$$I_0 \sin^2 p\alpha_n = I_0 \sin^2(p\alpha_n + \delta/2).$$

Thus,

$$\sin^2 p\alpha_n = \sin^2(p\alpha_n + \delta/2), \quad (A1-24)$$

and for arguments corresponding to less than 20° a satisfactory approximation is given by

$$p\alpha_n^2 = (p\alpha_n + \delta/2)^2 \quad (A1-25)$$

Expanding and rearranging equation (A1-25) gives

$$\rho_n^{\alpha} = -\delta/4 \quad (\text{A1-26})$$

Thus, for the pulsed mode of operation, expression (A1-26) describes the relationship between the angular rotation of the analyser, required to null the optical signal, and the electronically-induced phase retardation, δ .

On comparing equation (A1-26), with the corresponding relationship given by equation (A1-21) for the static d.c. method of operation, one would predict a higher signal-to-noise ratio in favour of the static method. This is indeed the case for birefringent samples which are not unduly perturbed by the application of a high voltage electric field. However, for samples which are somewhat electrically conductive, the signal-to-noise ratio is found to favour the pulsed electric field method, since the samples are less disturbed by the application of an electric pulse of short duration.

Program 1 (Kerr Constants) Calculation of Theoretical
Molar Kerr Constants

From a knowledge of bond polarizabilities, bond dipole moments and molecular geometry the optical anisotropy of a molecule can be calculated. The magnitude and sign of this molecular anisotropy is denoted by the symbol K_m and is called the molar Kerr constant when reference is being made to an Avogadro number of molecules. This appendix is chiefly concerned with a description of the structure and use of the computer program used in the calculation of the Kerr constants of bimolecular complexes. The theoretical aspects involved in the calculation of molar Kerr constants are discussed in detail in the first part of Chapter 7.

The computer program 'Kerr Constants' was designed to run on a bench top micro-computer (Apple II) since it was required that the program should be highly interactive. Maximum flexibility, concerning the input and changing of data was achieved by presenting the user with a series of menus. This type of structured programming allows the user to input and change parameters very quickly.

The program is capable of calculating Kerr constants of single molecules in isolation and Kerr constants of two molecules simultaneously. In the latter case it is

possible to orientate the molecules relative to each other and then calculate the total molar Kerr constant for the pair of molecules. This approach was employed in the calculation of the molar Kerr constants of bimolecular complexes between iodine (or tetracyanoquinodimethane) and a number of aryl compounds.

The computer program is organised into ten identifiable sections, each of which possesses a menu. The relationships between the menus is best appreciated via reference to figure A2-1 which shows a block outline of the structure of the program. The first section contains a master menu through which the smaller menus can be assessed.

The composition of the molecular polarizability tensors has already been discussed in Chapter 7. However, a few comments, regarding the juxtaposition of molecules 1 and 2 are in order. The angular relationship between molecules 1 and 2 is defined by two angles θ (tilt angle) and ϕ (rotate angle) as shown in figure A2-2. Thus molecule 2 may be rotated about the common z-axis and about its own y-axis. The angles may be regarded as angular displacements between the principle axes of the polarizability ellipsoid of molecule 2 with respect to the x, y and z axes of a rectangular Cartesian co-ordinate system centred on molecule 1. The electrostatic polarizabilities along directions parallel to the x, y and z axes are denoted by 1^b_x , 1^b_y , 1^b_z and by z^b_x , z^b_y , z^b_z for molecules 1 and 2 respectively.

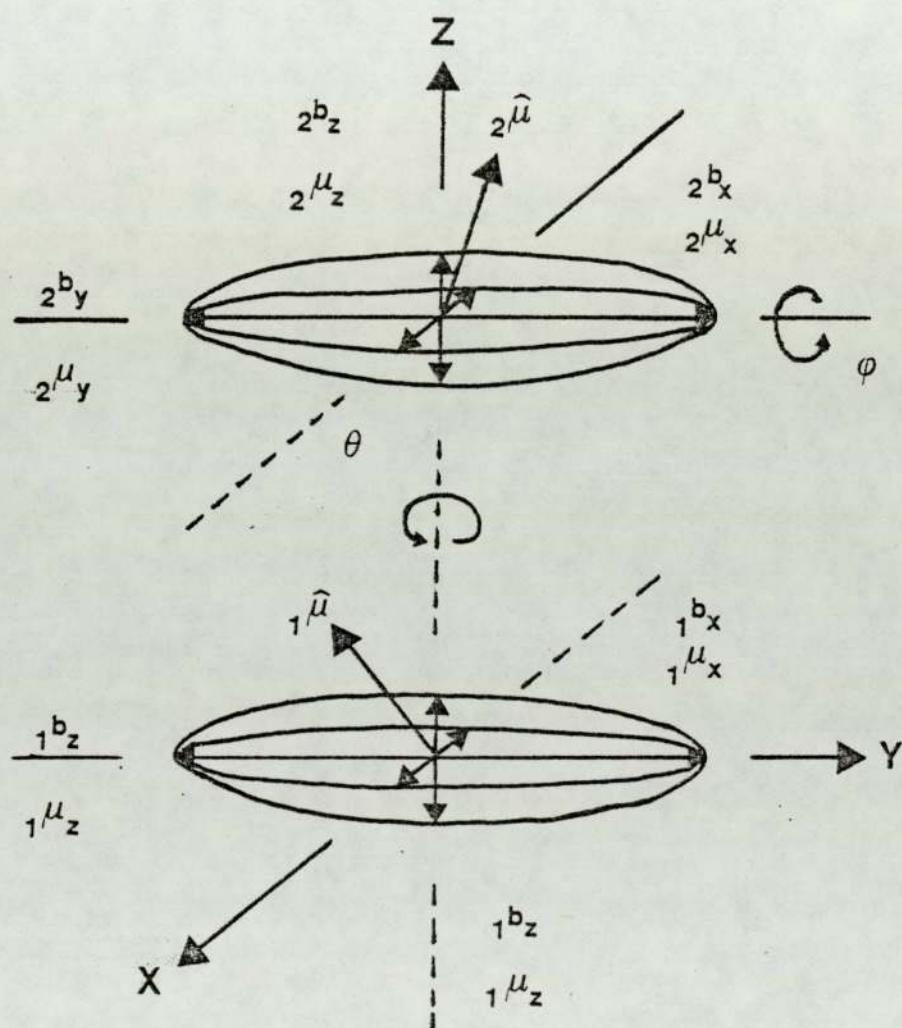


Figure A2.2 Juxtaposition of two molecules in a complex

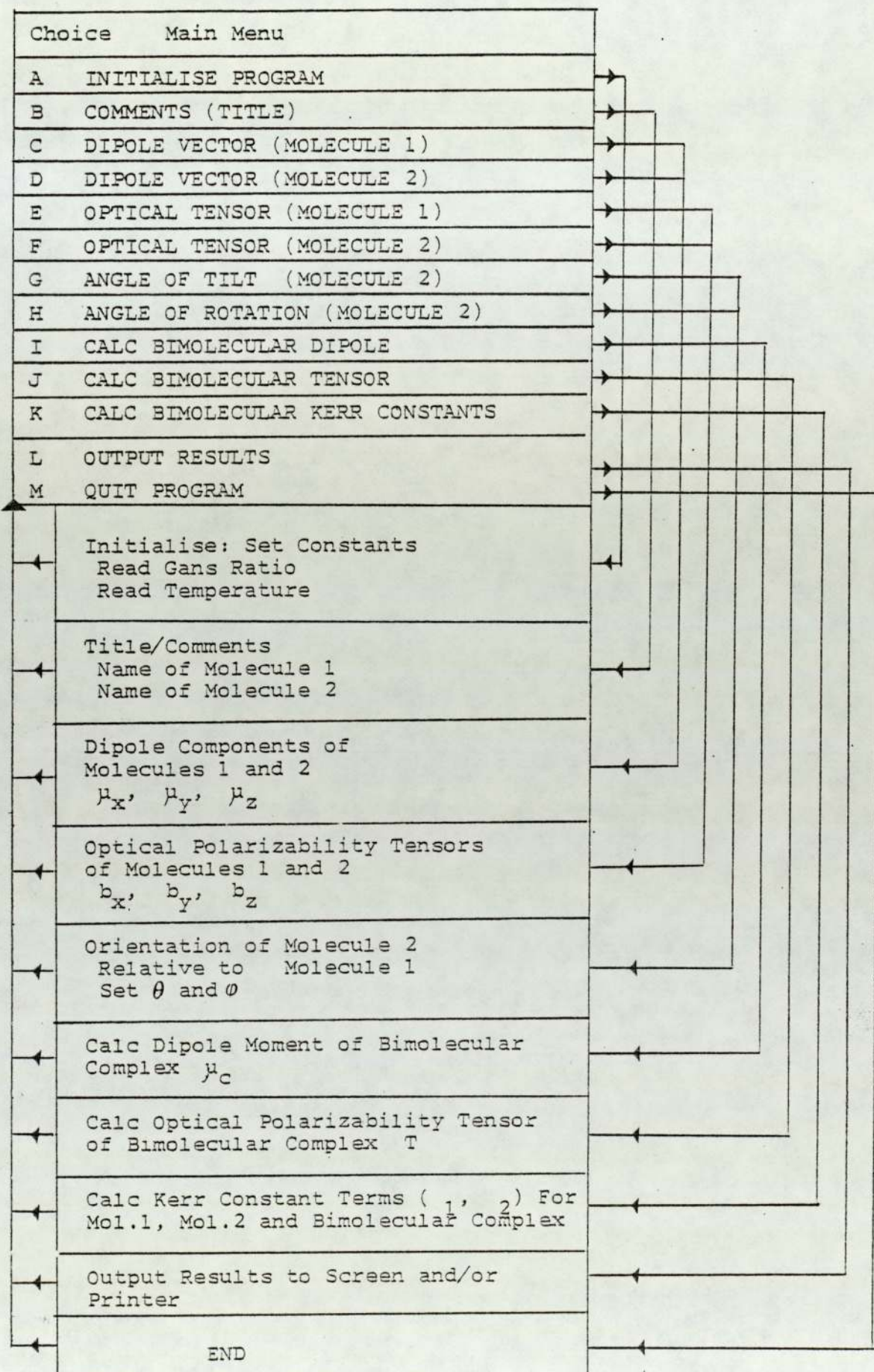


Figure A2-1 Block outline of structure of programme

The components of the dipole moments vectors of molecules 1 and 2, $1\mu_x$, $1\mu_y$, $1\mu_z$ and $2\mu_x$, $2\mu_y$, $2\mu_z$ are similarly assigned.

Auxillary Computer Programs

In addition to the main computer program 'Kerr Constants' described in Appendix 2 four other Basic (Apple II) programs were used to evaluate and manipulate experimental data.

These programs were primarily concerned with the calculation of the refractive indices of solutions, the calculation of molar Kerr constants at infinite dilution, evaluation of the permanent electric dipole moment and the calculation of molar Kerr constants using simple alligation formulae.

```

10 REM MOLAR KERR CONSTANT FOR A
20 REM BIMOLECULAR COMPLEX FORMED IN
30 REM SOLUTION.REQUIRES OPTICAL TENSOR
40 REM AND DIPOLE VECTOR OF EACH MOLECULE
50 REM *****
60 IN = 0
65 DIM DA(3),DB(3),PA(3,3),PB(3,3),U(3),T(3,3),T1(3,1),T2(3,1),P1(3,3)
66 DIM P2(3,3)
70 HOME
80 PRINT "CHOOSE OPTION (A-M)"
90 PRINT
100 PRINT "A INITIALISE (DO THIS FIRST)"
110 PRINT "B COMMENTS (TITLE ETC)"
115 PRINT
120 PRINT "C DIPOLE VECTOR (1)"
130 PRINT "D DIPOLE VECTOR (2)"
135 PRINT
140 PRINT "E OPTICAL TENSOR (1)"
150 PRINT "F OPTICAL TENSOR (2)"
155 PRINT
160 PRINT "G ANGLE OF TILT"
170 PRINT "H ANGLE OF ROTATION"
175 PRINT
180 PRINT "I CALC COMPLEX DIPOLE"
190 PRINT "J CALC COMPLEX TENSOR"
200 PRINT "K CALC KERR CONSTANTS"
204 PRINT
205 PRINT "(L) OUTPUT RESULTS"
206 PRINT
207 PRINT "(M) QUIT PROGRAM"
210 GET K$: IF K$ = "" THEN 210
215 FG = ASC (K$)
220 IF FG < 65 OR FG > 77 THEN 210
230 IF IN = 0 AND K$ < > "A" THEN 210
240 FG = FG - 64: HOME
250 ON FG GOSUB 1000,2000,3000,3000,4000,4000,5000,5000,7000,8000,9000,6000,10000
260 GOTO 70
437 PRINT "TOTAL=";MK(3) * 1.11265 * 10 ^ ( - 15);"INDUCED=";MK(4) * 1.11265 * 10 ^ ( - 15)

537 PRINT "TOTAL=";MK(3) * 1.11265 * 10 ^ ( - 15);"INDUCED=";MK(4) * 1.11265 * 10 ^ ( - 15)

637 PRINT "TOTAL=";MK(5) * 1.11265 * 10 ^ ( - 15);"INDUCED=";MK(6) * 1.11265 * 10 ^ ( - 15)

737 PRINT "TOTAL=";MK(5) * 1.11265 * 10 ^ ( - 15);"INDUCED=";MK(6) * 1.11265 * 10 ^ ( - 15)

```

```

1000 REM *****
1005 REM INITIALISE
1010 REM *****
1012 F1 = 10 ^ ( - 9): REM FACTOR FOR TERM A
1013 F2 = 10 ^ ( - 5): REM FACTOR FOR TERM B
1015 IN = 1
1020 K = 1.38052: REM BOLTZMANN
1030 N = 6.02252: REM AVOGADRO
1040 PI = 3.141593: REM OBVIOUS
1050 HOME
1060 PRINT "CHOOSE OPTION(1-3)": PRINT
1070 PRINT "(1) GANS RATIO"
1080 PRINT "(2) TEMPERATURE/K"
1090 PRINT "(3) RETURN TO MAIN MENU"
1100 GET K$: IF K$ = "" THEN 1100
1110 FG = VAL (K$)
1120 IF FG < 1 OR FG > 3 THEN 1100
1130 HOME
1140 ON FG GOTO 1300,1400,1999
1300 PRINT
1310 PRINT "GANS RATIO ";GA
1320 PRINT "CHANGE VALUE ?(Y/N)"
1330 GET K$: IF K$ = "" THEN 1330
1340 IF K$ = "N" THEN 1050
1350 IF K$ < > "Y" THEN 1330
1360 INPUT "GANS RATIO :";GA
1370 GOTO 1050
1400 PRINT
1410 PRINT "TEMPERATURE/K ";T
1420 PRINT "CHANGE TEMPERATURE ?(Y/N)"
1430 GET K$: IF K$ = "" THEN 1430
1440 IF K$ = "N" THEN 1050
1450 IF K$ < > "Y" THEN 1430
1460 INPUT "TEMPERATURE/K: ";T
1470 GOTO 1050
1999 RETURN
2000 REM *****
2005 REM COMMENTS/TITLE
2010 REM *****
2015 HOME
2020 PRINT "CHOOSE OPTION 1-4"
2025 PRINT
2030 PRINT "(1) TITLE/COMMENTS"
2035 PRINT
2040 PRINT "(2) NAME OF MOLECULE 1"
2050 PRINT "(3) NAME OF MOLECULE 2"
2055 PRINT
2060 PRINT "(4) RETURN TO MENU"
2070 GET K$: IF K$ = "" THEN 2070
2080 FG = VAL (K$)
2090 IF FG < 1 OR FG > 4 THEN 2070
2095 HOME
2100 ON FG GOTO 2300,2400,2500,2999
2110 GOTO 2015
2300 PRINT
2310 PRINT "TITLE/COMMENTS": PRINT
2315 PRINT T$: PRINT

```

```

2320 PRINT "CHANGE THESE ?(Y/N)"
2330 GET K$: IF K$ = "" THEN 2330
2340 IF K$ = "N" THEN 2015
2350 IF K$ < > "Y" THEN 2330
2360 PRINT "NEW TITLE AND/OR COMMENTS:"
2365 INPUT T$
2370 GOTO 2015
2400 PRINT
2410 PRINT : PRINT "NAME OF MOLECULE 1": PRINT : PRINT NA$: PRINT
2420 PRINT "CHANGE NAME ?(Y/N)"
2430 GET K$: IF K$ = "" THEN 2430
2440 IF K$ = "N" THEN 2015
2450 IF K$ < > "Y" THEN 2430
2460 INPUT "NEW NAME: ";NA$
2470 GOTO 2015
2500 PRINT
2510 PRINT "NAME OF MOLECULE 2": PRINT : PRINT NB$: PRINT
2520 PRINT "CHANGE NAME ?(Y/N)"
2530 GET K$: IF K$ = "" THEN 2530
2540 IF K$ = "N" THEN 2015
2550 IF K$ < > "Y" THEN 2530
2560 INPUT "NEW NAME: ";NB$
2570 GOTO 2015
2999 RETURN
3000 REM *****
3005 REM   DIPOLE VECTORS
3010 REM *****
3015 HOME
3020 PRINT "CHOOSE OPTION 1-3": PRINT
3030 PRINT "(1) DIPOLE VECTOR 1"
3040 PRINT "(2) DIPOLE VECTOR 2": PRINT
3045 PRINT "(3) RETURN TO MAIN MENU"
3050 GET K$: IF K$ = "" THEN 3050
3060 FG = VAL (K$)
3070 IF FG < 1 OR FG > 3 THEN 3050
3080 HOME
3090 ON FG GOTO 3300,3500,3999
3095 GOTO 3015
3300 PRINT "DIPOLE VECTOR 1 (X,Y,Z)": PRINT
3310 PRINT "X,Y,Z: ";DA(1),DA(2),DA(3): PRINT
3320 PRINT "CHANGE THESE ?(Y/N)"
3330 GET K$: IF K$ = "" THEN 3330
3340 IF K$ = "N" THEN 3015
3350 IF K$ < > "Y" THEN 3330
3360 INPUT "X,Y,Z";DA(1),DA(2),DA(3)
3370 GOTO 3015
3500 PRINT "DIPOLE VECTOR 2 (X,Y,Z)": PRINT
3510 PRINT "X,Y,Z: ";DB(3),DB(2),DB(1)
3520 PRINT "CHANGE THESE ?(Y/N)"
3530 GET K$: IF K$ = "" THEN 3530
3540 IF K$ = "N" THEN 3015
3550 IF K$ < > "Y" THEN 3530
3560 INPUT "X,Y,Z";DB(3),DB(2),DB(1)
3570 GOTO 3015
3999 RETURN

```

```

4000 REM *****
4005 REM   OPTICAL TENSORS
4010 REM *****
4015 HOME
4020 PRINT "CHOOSE OPTION(1-3)": PRINT
4030 PRINT "(1) TENSOR 1"
4040 PRINT "(2) TENSOR 2": PRINT
4050 PRINT "(3) RETURN TO MAIN MENU"
4060 GET K$: IF K$ = "" THEN 4060
4070 FG = VAL (K$)
4080 IF FG < 1 OR FG > 3 THEN 4060
4090 HOME
4100 ON FG GOTO 4300,4600,4999
4110 GOTO 4015
4300 PRINT "TENSOR 1:": PRINT
4310 FOR I = 1 TO 3
4320 PRINT PA(I,1);PA(I,2);PA(I,3): NEXT I
4330 PRINT : PRINT "CHANGE THESE ?(Y/N)"
4340 GET K$: IF K$ = "" THEN 4340
4350 IF K$ = "N" THEN 4015
4360 IF K$ < > "Y" THEN 4340
4370 FOR I = 1 TO 3: PRINT "TYPE IN RAW" I
4380 INPUT PA(I,1),PA(I,2),PA(I,3): NEXT I
4390 GOTO 4015
4600 PRINT "TENSOR 2:": PRINT
4610 FOR I = 1 TO 3
4620 PRINT PB(I,3),PB(I,2),PB(I,1): NEXT I
4630 PRINT : PRINT "CHANGE THESE ?(Y/N)"
4640 GET K$: IF K$ = "" THEN 4640
4650 IF K$ = "N" THEN 4015
4660 IF K$ < > "Y" THEN 4640
4670 FOR I = 1 TO 3: PRINT "TYPE IN RAW"; I
4680 INPUT PB(I,1),PB(I,2),PB(I,3): NEXT I
4690 GOTO 4015
4999 RETURN
5000 REM *****
5005 REM   TILT AND ROTATE ANGLES
5010 REM *****
5015 HOME
5020 PRINT "CHOOSE OPTION (1-4)": PRINT
5030 PRINT "(1) ANGLE OF TILT"
5040 PRINT "(2) ANGLE OF ROTATION"
5045 PRINT
5050 PRINT "(3) CALC NEW TRANSFORM MATRIX"
5055 PRINT
5060 PRINT "(4) RETURN TO MAIN MENU"
5070 GET K$: IF K$ = "" THEN 5070
5080 FG = VAL (K$)
5090 IF FG < 1 OR FG > 4 THEN 5070
5100 HOME
5110 ON FG GOTO 5200,5400,5600,5999
5115 GOTO 5015
5200 PRINT : PRINT "ANGLE OF TILT": THETA: PRINT
5220 PRINT "CHANGE THIS VALUE ?(Y/N)"
5230 GET K$: IF K$ = "" THEN 5230
5240 IF K$ = "N" THEN 5015
5250 IF K$ < > "Y" THEN 5230
5260 INPUT "NEW ANGLE/DEGREES:": THETA
5270 GOTO 5015

```

```

5400 PRINT : PRINT "ANGLE OF ROTATION";PHI: PRINT
5420 PRINT "CHANGE THIS VALUE ?(Y/N)"
5430 GET K$: IF K$ = "" THEN 5430
5440 IF K$ = "N" THEN 5015
5450 IF K$ < > "Y" THEN 5430
5460 INPUT "NEW ANGLE/DEGREES:";PHI
5470 GOTO 5015
5600 RD = 2 * PI / 360
5610 TA = THETA * RD:RA = PHI * RD:SB = SIN (TA):CT = COS (TA):SP = SIN (RA):CP = COS (R
    A)
5620 TR(1,1) = CT:TR(1,2) = SB:TR(1,3) = 0
5630 TR(2,1) = SB * CP:TR(2,2) = - CT * CP:TR(2,3) = SP
5640 TR(3,1) = SB * SP:TR(3,2) = - CT * SP:TR(3,3) = - CP
5650 GOTO 5015
5999 RETURN
6000 REM *****
6005 REM  OUTPUT RESULTS
6010 REM *****
6015 HOME :T$ = "KERR EFFECT-BIMOLECULAR COMPLEXES"
6020 PRINT "CHOOSE OPTIONS(1-7)": PRINT
6030 PRINT "(1) COMPLEX (SCREEN)"
6040 PRINT "(2) COMPLEX (PRINTER)"
6050 PRINT
6060 PRINT "(3) MOLECULE 1 (SCREEN)"
6070 PRINT "(4) MOLECULE 1 (PRINTER)"
6080 PRINT
6090 PRINT "(5) MOLECULE 2 (SCREEN)"
6100 PRINT "(6) MOLECULE 2 (PRINTER)"
6110 PRINT
6120 PRINT "(7) EXIT TO MAIN MENU"
6130 GET K$: IF K$ = "" THEN 6130
6140 FG = VAL (K$)
6150 IF FG < 1 OR FG > 7 THEN 6130
6160 HOME
6170 ON FG GOTO 6200,6300,6400,6500,6600,6700,6999
6175 GOTO 6015
6200 REM COMPLEX (TO SCREEN)
6205 PRINT T$: PRINT : PRINT "MOLECULE 1 ";NA$: PRINT : PRINT "MOLECULE 2 ";NB$: PRINT
6210 PRINT "DIPOLE VECTOR (X,Y,Z)(DEBYES):PRINT
6215 PRINT U(1),U(2),U(3): PRINT
6220 PRINT "OPTICAL POLARISABILITY TENSOR (ESU*10^24)"
6225 FOR I = 1 TO 3: PRINT T(I,1),T(I,2),T(I,3): PRINT ;: NEXT I: PRINT
6230 PRINT "MOLECULAR KERR CONSTANT (ESU)"
6235 PRINT "TOTAL = ";MK(1);" INDUCED = ";MK(2)
6236 PRINT "(SI)"
6237 PRINT "TOTAL = ";MK(1) * 1.11265 * 10 ^ ( - 15);" INDUCED = ";MK(2) * 1.11265 * 10 ^
    ( - 15)
6240 PRINT : PRINT "PRESS A KEY FOR MENU"
6242 GET K$: IF K$ = "" THEN 6242
6244 GOTO 6015
6300 REM COMPLEX (TO PRINTER)
6301 PR# 2
6305 PRINT T$: PRINT : PRINT "MOLECULE 1 ";NA$: PRINT : PRINT "MOLECULE 2 ";NB$: PRINT
6310 PRINT "DIPOLE VECTOR (X,Y,Z)(DEBYES)": PRINT
6315 PRINT U(1),U(2),U(3): PRINT
6320 PRINT "OPTICAL POLARISABILITY TENSOR (ESU*10^24)"
6325 FOR I = 1 TO 3: PRINT T(I,1),T(I,2),T(I,3): NEXT : PRINT
6330 PRINT "MOLECULAR KERR CONSTANT (ESU)": PRINT

```

```

6335 PRINT " TOTAL = ";MK(1);" INDUCED = ";MK(2)
6336 PRINT "(SI)"
6337 PRINT " TOTAL = ";MK(1) * 1.11265 * 10 ^ ( - 15);" INDUCED = ";MK(2) * 1.11265 * 10 ^
( - 15)
6340 PRE 0: GOTO 6015
6400 REM MOLECULE 1 (TO SCREEN)
6405 PRINT "MOLECULE 1": PRINT
6410 PRINT "DIPOLE VECTOR (X,Y,Z)(DEBYE)": PRINT
6415 PRINT DA(1),DA(2),DA(3): PRINT
6420 PRINT "OPTICAL POLARISABILITY TENSOR (ESU*10^24)": PRINT
6425 FOR I = 1 TO 3: PRINT PA(I,1),PA(I,2),PA(I,3): NEXT I: PRINT
6430 PRINT "MOLECULAR KERR CONSTANT (ESU)": PRINT
6435 PRINT " TOTAL = ";MK(3);" INDUCED = ";MK(4): PRINT
6436 PRINT "(SI)"
6437 PRINT " TOTAL = ";MK(3) * 1.11265 * 10 ^ ( - 15);" INDUCED = ";MK(4) * 1.11265 * 10 ^
( - 15): PRINT
6440 PRINT : PRINT "PRESS A KEY FOR MENU"
6442 GET K$: IF K$ = "" THEN 6442
6444 GOTO 6015
6500 REM MOLECULE 1 (TO PRINT)
6501 PRE 2
6505 PRINT "MOLECULE 1";NA$: PRINT
6510 PRINT DA(1),DA(2),DA(3): PRINT
6515 PRINT ,DA(1);DA(2);DA(3): PRINT
6520 PRINT "OPTICAL POLARISABILITY TENSOR (ESU*10^24)": PRINT
6525 FOR I = 1 TO 3: PRINT PA(I,1),PA(I,2),PA(I,3): NEXT I: PRINT
6530 PRINT "MOLECULAR KERR CONSTANT (ESU)": PRINT
6535 PRINT " TOTAL = ";MK(3);" INDUCED = ";MK(4): PRINT
6536 PRINT "(SI)"
6537 PRINT " TOTAL = ";MK(3) * 1.11265 * 10 ^ ( - 15);" INDUCED = ";MK(4) * 1.11265 * 10 ^
( - 15): PRINT
6540 PRE 0: GOTO 6015
6600 REM MOLECULE 2 (TO SCREEN)
6605 PRINT "MOLECULE 2";NB$: PRINT
6610 PRINT "DIPOLE VECTOR (X,Y,Z)(DEBYES)": PRINT
6615 PRINT DB(1);DB(2);DB(3): PRINT
6620 PRINT "OPTICAL POLARISABILITY TENSOR (ESU*10^24)": PRINT
6625 FOR I = 1 TO 3: PRINT PB(I,1),PB(I,2),PB(I,3): PRINT : NEXT I: PRINT
6630 PRINT "MOLECULAR KERR CONSTANT (ESU)": PRINT
6635 PRINT " TOTAL = ";MK(5);" INDUCED = ";MK(6): PRINT
6636 PRINT "(SI)"
6637 PRINT " TOTAL = ";MK(5) * 1.11265 * 10 ^ ( - 15);" INDUCED = ";MK(6) * 1.11265 * 10 ^
( - 15): PRINT
6640 PRINT : PRINT "PRESS A KEY FOR MENU"
6642 GET K$: IF K$ = "" THEN 6642
6644 GOTO 6015
6700 REM MOLECULE 2 (TO PRINTER)
6701 PRE 2
6705 PRINT "MOLECULE 2 ";NB$: PRINT
6710 PRINT "DIPOLE VECTOR (X,Y,Z)(DEBYES)": PRINT
6715 PRINT DB(1),DB(2),DB(3): PRINT
6720 PRINT "OPTICAL POLARISABILITY TENSOR (ESU*10^24)": PRINT
6725 FOR I = 1 TO 3: PRINT PB(I,1),PB(I,2),PB(I,3): PRINT : NEXT I: PRINT
6730 PRINT "MOLECULAR KERR CONSTANT (ESU)": PRINT
6735 PRINT " TOTAL = ";MK(5);" INDUCED = ";MK(6): PRINT
6736 PRINT "(SI)"
6737 PRINT " TOTAL = ";MK(5) * 1.11265 * 10 ^ ( - 15);" INDUCED = ";MK(6) * 1.11265 * 10 ^
( - 15): PRINT
6740 PRE 0: GOTO 6015
6999 RETURN

```

```

7000 REM *****
7005 REM DIPOLE MOMENT OF COMPLEX
7010 REM *****
7015 HOME
7020 PRINT "CALCULATING-PLEASE WAIT"
7030 U(1) = TR(1,1) * DB(1) + TR(1,2) * DB(2) + TR(1,3) * DB(3) + DA(1)
7040 U(2) = TR(2,1) * DB(1) + TR(2,2) * DB(2) + TR(2,3) * DB(3) + DA(2)
7050 U(3) = TR(3,1) * DB(1) + TR(3,2) * DB(2) + TR(3,3) * DB(3) + DA(3)
7500 REM COULD PRINT OUT VECTOR U ?
8000 REM *****
8005 REM CALCULATE COMPLEX'S TENSOR
8010 REM *****
8015 HOME : PRINT "CALCULATING-PLEASE WAIT"
8020 FOR I = 1 TO 3
8030 FOR J = 1 TO 3
8040 SUM = 0
8050 FOR KK = 1 TO 3
8060 SUM = SUM + PB(I, KK) * TR(J, KK): NEXT KK
8070 P1(I, J) = SUM
8080 NEXT J: NEXT I
8090 FOR I = 1 TO 3
8100 FOR J = 1 TO 3
8110 SUM = 0
8120 FOR KK = 1 TO 3
8130 SUM = SUM + TR(I, KK) * P1(KK, J): NEXT KK
8140 P2(I, J) = SUM
8150 NEXT J: NEXT I
8160 FOR I = 1 TO 3
8170 FOR J = 1 TO 3
8180 T(I, J) = PA(I, J) + P2(I, J)
8190 NEXT J: NEXT I
8500 REM COULD PRINT OUT TENSOR ?
8999 RETURN
9000 REM *****
9005 REM CALCULATE KERR CONSTANTS
9010 REM *****
9015 HOME
9020 PRINT "CALCULATE KERR CONSTANTS": PRINT
9030 PRINT "CHOOSE OPTION (1-7)": PRINT
9040 PRINT "(1) COMPLEX (INDUCED+DIPOLE)"
9050 PRINT "(2) COMPLEX (INDUCED)"
9060 PRINT
9070 PRINT "(3) MOLECULE 1 (INDUCED+DIPOLE)"
9080 PRINT "(4) MOLECULE 1 (INDUCED)"
9090 PRINT
9100 PRINT "(5) MOLECULE 2 (INDUCED+DIPOLE)"
9110 PRINT "(6) MOLECULE 2 (INDUCED)"
9120 PRINT
9130 PRINT "(7) EXIT TO MAIN MENU"
9140 GET K$: IF K$ = "" THEN 9140
9150 FG = VAL (K$)
9160 IF FG < 1 OR FG > 7 THEN 9140
9170 HOME
9180 ON FG GOTO 9200, 9300, 9400, 9500, 9600, 9700, 9999
9190 RETURN
9200 REM COMPLEX'S KERR CONSTANT
9210 BC = (T(1,1) - T(2,2)) * (U(1) ^ 2 - U(2) ^ 2) + (T(2,2) - T(3,3)) * (U(2) ^ 2 - U(3) ^ 2)
9220 BC = BC + (T(3,3) - T(1,1)) * (U(3) ^ 2 - U(1) ^ 2) + 3 * U(1) * U(2) * T(1,2)
9225 BC = BC + 3 * U(2) * U(3) * T(2,3)
9230 BC = BC + 3 * (U(1) * U(3) * T(1,3) + U(2) * U(1) * T(2,1) + U(3) * U(2) * T(3,2))
9235 BC = BC + 3 * (U(3) * U(1) * T(3,1))

```

```

9300 AC = (T(1,1) - T(2,2)) ^ 2 + (T(2,2) - T(3,3)) ^ 2
9310 AC = AC + (T(3,3) - T(1,1)) ^ 2 + 3 * (T(1,2) ^ 2 + T(2,1) ^ 2)
9320 AC = AC + 3 * (T(1,3) ^ 2 + T(3,1) ^ 2 + T(2,3) ^ 2 + T(3,2) ^ 2)
9330 GOTO 9800: REM GO CALC MK
9400 REM MOLECULE 1 KERR CONSTANT
9410 B1 = (PA(1,1) - PA(2,2)) * (DA(1) ^ 2 - DA(2) ^ 2)
9415 B1 = B1 + (PA(2,2) - PA(3,3)) * ((DA(2) ^ 2 - DA(3)) ^ 2)
9420 B1 = B1 + (PA(3,3) - PA(1,1)) * (DA(3) ^ 2 - DA(1) ^ 2) + 3 * (DA(1) * DA(2) * PA(1,2))

9425 B1 = B1 + 3 * (DA(2) * DA(3) * PA(2,3))
9430 B1 = B1 + 3 * (DA(1) * DA(3) * PA(1,3) + DA(2) * DA(1) * PA(2,1) + DA(3) * DA(2) * PA(3,2))
9435 B1 = B1 + 3 * (DA(3) * DA(1) * PA(3,1))
9500 A1 = (PA(1,1) - PA(2,2)) ^ 2 + (PA(2,2) - PA(3,3)) ^ 2
9510 A1 = A1 + (PA(3,3) - PA(1,1)) ^ 2 + 3 * (PA(1,2) ^ 2 + PA(2,1) ^ 2)
9520 A1 = A1 + 3 * (PA(1,3) ^ 2 + PA(3,1) ^ 2 + PA(2,3) ^ 2 + PA(3,2) ^ 2)
9530 GOTO 9850: REM GO CALC MK
9600 REM MOLECULE 2 KERR CONSTANT
9610 B2 = (PB(1,1) - PB(2,2)) * ((DB(1) ^ 2 - DB(2)) ^ 2)
9615 B2 = B2 + (PB(2,2) - PB(3,3)) * (DB(2) ^ 2 - DB(3) ^ 2)
9620 B2 = B2 + (PB(3,3) - PB(1,1)) * (DB(3) ^ 2 - DB(1) ^ 2) + 3 * (DB(1) * DB(2) * PB(1,2))

9625 B2 = B2 + 3 * (DB(2) * DB(3) * PB(2,3))
9630 B2 = B2 + 3 * (DB(3) * DB(1) * PB(3,1))
9700 A2 = (PB(1,1) - PB(2,2)) ^ 2 + (PB(2,2) - PB(3,3)) ^ 2
9710 A2 = A2 + (PB(3,3) - PB(1,1)) ^ 2 + 3 * (PB(1,2) ^ 2 + PB(2,1) ^ 2)
9720 A2 = A2 + 3 * (PB(1,3) ^ 2 + PB(3,1) ^ 2 + PB(2,3) ^ 2 + PB(3,2) ^ 2)
9730 GOTO 9900
9800 REM CALC COMPLEX'S KERR CONSTANT
9805 MA = F1 * AC * GANS / (45 * K * T)
9810 MB = (F2 * BC) / (45 * K * K * T * T)
9815 MK(1) = (MA + MB) * 2 * PI * N / 9
9820 MK(2) = MA * 2 * PI * N / 9
9830 GOTO 9015
9850 REM CALC MOLECULE 1 KERR CONSTANT
9855 MA = F1 * A1 * GANS / (45 * K * T)
9860 MB = (F2 * B1) / (45 * K * K * T * T)
9865 MK(3) = (MA + MB) * 2 * PI * N / 9
9870 MK(4) = MA * 2 * PI * N / 9
9880 GOTO 9015
9900 REM CALC MOLECULE 2 KERR CONSTANT
9905 MA = F1 * A2 * GANS / (45 * K * T)
9910 MB = (F2 * B2) / (45 * K * K * T * T)
9915 MK(5) = (MA + MB) * 2 * PI * N / 9
9920 MK(6) = MA * 2 * PI * N / 9
9950 GOTO 9015
9999 RETURN
10000 REM *****
10005 REM QUIT PROGRAM ROUTINE
10010 REM *****
10020 HOME : PRINT "WANT TO QUIT PROGRAM ?(Y/N)"
10030 GET K$: IF K$ = "" THEN 10030
10040 IF K$ = "N" THEN RETURN
10050 IF K$ < > "Y" THEN 10040
10060 HOME : END
10070 RETURN

```

Program 2 Calculation of Solution Molar Refractions
and Refractive Indices

The molar refraction R_{12} of a two component ideal solution can be calculated using the alligation formula:

$$R_{12} = f_1 R_1 + f_2 R_2 \quad \text{A2.1}$$

where R_1 and R_2 are the molar refractivities of the solvent and solute, respectively and f_1 and f_2 are the corresponding mole fractions. The molar refraction of these components is given by the Lorenz-Lorentz relationship .

$$R_{1,2} = \frac{(n_{1,2}^2 - 1)}{(n_{1,2}^2 + 2)} \frac{M_{1,2}}{d_{1,2}} \quad \text{A2.2}$$

where n , M and d , with suitable subscripts, denote the refractive index, molecular weight and density of the pure components.

For solutions the molar refraction may be written as:

$$R_{12} = \frac{(n_{12}^2 - 1)}{(n_{12}^2 + 2)} \frac{M_{12}}{d_{12}} \quad \text{A2.3}$$

From a knowledge of the composition of the solution the molecular weight M_{12} and density d_{12} may be calculated using:

$$M_{12} = f_1 M_1 + f_2 M_2 \quad \text{A2.4}$$

$$\text{and } d_{12} = \frac{(w_1' + w_2') d_1 d_2}{w_1' d_2 + w_2' d_1} \quad \text{A2.5}$$

where w_1' and w_2' are the weight of solvent and solute, respectively.

Equations A2.1 - A2.5 enable the solution refractive index n_{12} , to be derived. The accompanying computer program requires the refractive index, molecular weight, density and weight fraction of the pure components of the solution. This program and the others to be described subsequently are well documented using REM statements.

```

10 REM LORENZ-LORENZ
20 HOME : PRINT
30 PRINT "DATA FOR COMPONENT 1": PRINT
40 INPUT "MOLECULAR WEIGHT =";M1
50 INPUT "DENSITY =";D1
60 INPUT "REFRACTIVE INDEX =";N1
70 PRINT
80 PRINT "DATA FOR COMPONENT 2"
90 INPUT "MOLECULAR WEIGHT =";M2
100 INPUT "DENSITY =";D2
110 INPUT "REFRACTIVE INDEX =";R2
120 PRINT
130 PRINT "DATA FOR SOLUTION OF 1 AND 2": PRINT
140 INPUT "WEIGHT OF COMPONENT 1=";W1
150 INPUT "WEIGHT OF COMPONENT 2=";W2
160 PRINT
170 PRINT "HIT-SPACE-BAR TO CONTINUE"
180 GET K$: IF K$ = "" THEN 180
190 REM CALCULATE MOLE FRACTIONS
200 F1 = (W1 / M1) / ((W1 / M1) + (W2 / M2))
210 F2 = 1 - F1
220 REM MOLAR REFRACTION OF 1
230 R1 = ((N1 * N1 - 1) * N1) / ((N1 * N1 + 2) * D1)
240 REM MOLAR REFRACTION OF 2
250 R2 = ((N2 * N2 - 1) * M2) / ((N2 * N2 + 2) * D2)
260 REM CALC. SOLN MOLAR REFRACTION

```

```

270 RS = F1 * R1 + F2 * R2
280 REM CALC.MOL.WT. OF SOLN
290 MS = F1 * M1 + F2 * M2
300 REM CALC. MOLAR VOL. OF 1
310 V1 = M1 / D1
320 REM CALC. MOLAR VOL. OF 2
330 V2 = M2 / D2
340 REM CALC. MOLAR VOL. OF SOLN
350 VS = F1 * V1 + F2 * V2
360 REM CALC. DENSITY OF SOLN
370 DS = MS / VS
380 REM CALC REFRACTIVE INDEX OF SOLN
390 NS = SQR ((MS + 2 * RS * RS) / (MS - DS * RS))
400 REM PRINT TO SCREEN
410 HOME
420 PRINT "COMPONENT 1": PRINT
430 PRINT "MOLAR VOLUME=";V1
440 PRINT "MOLAR REFRACTION=";R1
450 PRINT
460 PRINT "COMPONENT 2": PRINT
470 PRINT "MOLAR VOLUME=";V2
480 PRINT "MOLAR REFRACTION=";R2
490 PRINT
500 PRINT "SOLUTION"
510 PRINT "MOLAR VOLUME=";VS
520 PRINT "MOLAR REFRACTION=";RS
530 PRINT "REFRACTIVE INDEX=";NS
540 PRINT
550 PRINT "HIT-SPACE-BAR TO CONTINUE"
560 GET K$: IF K$ = "" THEN 560

```

```
570 HOME
580 PRINT "HIT KEY H FOR MORE DATA"
590 PRINT "HIT KEY S TO STOP"
600 GET K$: IF K$ = "" THEN 600
610 IF K$ = "H" THEN 20
620 PRINT : PRINT : PRINT
630 PRINT "END*****"
640 END
```

Program 3 Calculation of Infinite Dilution Molar
Kerr Constants

By measuring the experimental Kerr constant, B_{12} , refractive index n_{12} , static dielectric permittivity ϵ_{12} and density d_{12} of a series of solutions containing different weight fractions w_2 of solute it is possible to calculate the molar Kerr constant of the solute at infinite dilution. The approximate equation will be reproduced here with no description or definition of the variables since this aspect has been adequately dealt with in Chapter 6. The computer program requires the molecular weights of the solvent and solute, the refractive index of the solvent, the static permittivity of the solvent and the density of the solvent. The constants α , β , γ and δ which are deduced from the initial gradients of ϵ , d , n and B against the weight fraction of solute are also required. (See equations 6.16 - 6.22).

The computer program calculates the specific and molar Kerr constants of the solute in solution at infinite dilution.

```

2  REM INFINITE DILUTION KERR CONSTANTS
4  REM 1,2,3 DENOTE SOLVENT,SOLUTE,SOLUTION, RESPECTIVELY
6  REM K1,K2,K3 MOLECULAR KERR CONSTANTS
8  REM S1,S2,S3 SPECIFIC KERR CONSTANTS
10 REM D1,D2,D3 DENSITIES
12 REM E1,E2,E3 DIELECTRIC PERMITTIVITIES
14 REM N1,N2,N3 REFRACTIVE INDICES
16 REM B1,B2,B3 EXPERIMENTAL KERR CONSTANTS
17 REM M1,M2,M3 MOLECULAR WEIGHTS
18 REM W1,W2 WEIGHT FRACTIONS
20 REM ALPHA (AL) SLOPE OF E3 VS. W2
22 REM BETA (BE) SLOPE OF D3 VS. W2
24 REM GAMMA (GA) SLOPE OF N3 VS. W2
26 REM DELTA (DE) SLOPE OF B3 VS. W2
28 REM LB WAVELENGTH OF KERR EXPERIMENT
30 LB = 632.8E - 09
32 HOME
35 PRINT : PRINT "SOLVENT DATA": PRINT
40 INPUT "DIELECTRIC PERMITTIVITY = ";E1
50 INPUT "DENSITY = ";D1
60 INPUT "REFRACTIVE INDEX = ";N1
70 INPUT "KERR CONSTANT, B = ";B1
75 INPUT "MOLECULAR WEIGHT = ";M1
80 PRINT : PRINT "SOLUTION DATA": PRINT

```

```

90 INPUT "ALPHA (SLOPE E3 VS.W2) = ";AL
100 INPUT "BETA (SLOPE D3 VS.W2) = ";BE
110 INPUT "GAMMA(SLOPE N3 VS.W2) = ";GA
120 INPUT "DELTA (SLOPE B3 VS.W2) = ";DE
124 INPUT "SOLUTE MOLECULAR WEIGHT =" ;M2
130 REM CALCULATE SOLUTE AND SOLVENT KERR CONSTANTS
140 S1 = 6 * LB * N1 * B1 / D1
150 S1 = S1 / ((E1 + 2) * (E1 + 2) * (N1 * N1 + 2) * (N1 * N1 + 2))
160 K1 = S1 * M1
170 H = (4 * N1 * N1) / (N1 * N1 + 2)
180 J = 2 / (E1 + 2)
190 S2 = (1 - BE + GA + DE - H * GA - J * AL * E1) * S1
194 K2 = S2 * M2
200 PRINT : PRINT "CALCULATED PARAMETERS": PRINT
210 PRINT "SOLVENT SPECIFIC KERR CONSTANT = ";S1
220 PRINT "SOLVENT MOLECULAR KERR CONSTANT = ";K1
230 PRINT : PRINT "SOLUTE SPECIFIC KERR CONSTANT = ";S2
240 PRINT "SOLUTE MOLECULAR KERR CONSTANT = ";K2
250 PRINT : INPUT "CHANGE SOLVENT ?" ;A$
260 IF A$ = "Y" GOTO 32
270 PRINT : INPUT "CHANGE SOLUTE ?" ;B$
280 IF B$ = "Y" GOTO 80
290 HOME : VTAB 15: HTAB 10: PRINT "**** END ****": END

```

Program 4 Calculation of Dipole Moments

This computer program calculates the permanent electric dipole moment of solute molecules in dilute solution using the Debye-Guggenheim relationship. This approach does not necessitate a knowledge of the density of the solutions. Variables required by the program are the refractive index, static permittivity and density of the pure solvent together with the temperature used in the measurement of the solution static permittivities. The initial gradient of the graph of solution permittivity versus weight fraction of solute is also required. The **computer** program is well described in the REM statements.

```

5 HOME
10 PRINT "GUGGENHEIM - DEBYE PROGRAM"
20 INPUT "TEMPERATURE =" ; T
30 INPUT "MOL. WT. SOLUTE =" ; M2
35 M2 = M2 / 1000
40 INPUT "SOLVENT PERMITTIVITY =" ; E1
50 INPUT "SOLVENT REFRACTIVE INDEX =" ; N1
60 INPUT "SOLVENT DENSITY =" ; D1
70 INPUT "GRADIENT OF E12 VS. W2 PLOT =" ; G
80 E = 8.854E - 12
90 K = 1.38012
100 N = 6.02217
110 TE = 27 * E * K * T
120 TE = TE * G * M2 / D1
130 TE = TE / (N * (E1 + 2) * (N1 * N1 + 2))
140 DM = SQR (TE)
150 PRINT
160 PRINT "DIPOLE MOMENT X E30 = " ; SQR (TE) * 1.0E07
170 PRINT
180 PRINT "REPEAT CALC.?(YORN)"
190 GET K$; IF K$ = "" THEN 190
200 IF K$ = "Y" THEN GOTO 5
210 IF K$ = "N" THEN GOTO 230
220 GOTO 180
230 HOME
240 PRINT "***** END OF PROGRAM"
250 END

```

Program 5 Calculation of Solute Molar Kerr Constants
Using Alligation Formulae

This is a general program used for the analysis of electro-optic data obtained for solutions that approximate to ideal behaviour. Although the relevant equations have been described in detail in an earlier chapter, the principal expressions will be given here for the sake of convenience. (Further details are given in Chapter 7).

Solution molar Kerr Constant

$${}^m K_{12} = f_1 {}^m K_1 + f_2 {}^m K_2 \quad \text{A2.6}$$

where ${}^m K_1$ and ${}^m K_2$ are the molar Kerr constants of the solvent and solute respectively.

For a pure medium the molar Kerr constant may be expressed in terms of the experimental Kerr constant B, refractive index n, static dielectric permittivity ϵ , density d, molecular weight and the wavelength of light used to measure n and B. Thus:

$${}^m K_{\sigma} = \left[\frac{6 \lambda n M B}{(\epsilon + 2)^2 (n + 2)^2 d} \right]_{\sigma} \quad \text{A2.7}$$

where σ denotes the appropriate subscript for solution (12), solvent (1), or solute (2).

The subscript on the RHS of equation A2.7 implies that the quantities within the square brackets are each appropriately

subscripted (except λ).

The computer program requests information concerning the solvent (but not ${}_mK_2$) and the solution. It then proceeds to calculate the molar Kerr constant of the solute using data for a given concentrations of solutes. The calculation is normally repeated for additional concentration and a mean value of ${}_mK_2$ is eventually derived.

For systems where the solubility of the solute was very low several solutions corresponding to the maximum possible solubility were analysed and the corresponding solute Kerr averaged. Although this approach may 'hide' non-linearities (in plots of B_{12} versus w_2) it leads to improved experimental errors. The majority of the electro-optical work was performed on solution possessing solute concentration of less than 1% and it is unlikely that departures from linearity would be significant. This was confirmed by carrying out dilution tests on soluble solutes and the graphs of B_{12} against w_2 were found to be linear for concentrations up to approximately 2% by weight.

```

2  REM ELECTRO-OPTIC CALCULATIONS
4  REM LN-REFRACTIVE INDEX WAVELENGTH
6  REM LB-KERR EFFECT WAVELENGTH
8  REM REM 1,2,3 DENOTE SOLVENT, SOLUTE AND SOLUTION PROPERTIES RESPECTIVELY
10 REM M1,M2,M3 MOLECULAR WEIGHTS
12 REM B1,B2,B3 EXPERIMENTAL KERR CONSTANTS
14 REM E1,E2,E3 DIELECTRIC PERMITTIVITIES
16 REM N1,N2,N3 REFRACTIVE INDICES
18 REM D1,D2,D3 DENSITIES
20 REM R1,R2,R3 MOLAR REFRACTIONS
22 REM P1,P2,P3 MOLAR POLARISATIONS
24 REM V1,V2,V3 MOLAR VOLUMES
26 REM K1,K2,K3 MOLECULAR KERR CONSTANTS
28 REM W1,W2 WEIGHTS OF SOLVENT AND SOLUTE
30 REM F1,F2 MOLE FRACTIONS
40 INPUT "REFRACTIVE INDEX WAVELENGTH/NM ? =" ;LN
50 INPUT "KERR-EFFECT WAVELENGTH/NM ? =" ;LB
55 PRINT : PRINT "SOLVENT DATA": PRINT
60 INPUT "MOLECULAR WEIGHT =" ;M1
70 INPUT "REFRACTIVE INDEX =" ;N1
80 INPUT "PERMITTIVITY =" ;E1
90 INPUT "KERR CONSTANT,B =" ;B1
100 INPUT "DENSITY =" ;D1
110 REM CALCULATE SOLVENT PARAMETERS
120 V1 = M1 / D1
125 PRINT "SOLVENT MOLAR VOLUME =" ;V1
130 N1 = N1 * LN / LB
135 PRINT "CORRECTED SOLVENT REFRACTIVE INDEX =" ;N1

```

```

140 R1 = (N1 * N1 - 1) * M1 / ((N1 * N1 * + 2) * D1)
145 PRINT "SOLVENT MOLAR REFRACTION =" ;R1
150 P1 = (E1 - 1) * M1 / ((E1 + 2) * D1)
155 PRINT "SOLVENT MOLAR POLARISATION =" ;P1
160 K1 = 6 * LB * N1 * M1 * B1 / D1
170 K1 = K1 / ((E1 + 2) * (E1 + 2) * (N1 * N1 + 2) * (N1 * N1 + 2))
175 PRINT "SOLVENT MOLECULAR KERR CONSTANT =" ;K1
180 PRINT : PRINT "SOLUTE DATA": PRINT
190 INPUT "MOLECULAR WEIGHT =" ;M2
200 INPUT "REFRACTIVE INDEX =" ;N2
210 INPUT "PERMITTIVITY =" ;E2
220 INPUT "KERR CONSTANT,B =" ;B2
230 INPUT "DENSITY =" ;D2
240 REM CALCULATE SOME SOLUTE PARAMETERS
250 V2 = M2 / D2
255 PRINT "SOLUTE MOLAR VOLUME =" ;V2
260 N2 = N2 * LN / LB
265 PRINT "CORRECTED SOLUTE REFRACTIVE INDEX =" ;N2
270 R2 = (N2 * N2 - 1) * M2 / ((N2 * N2 + 2) * D2)
275 PRINT "SOLUTE MOLAR REFRACTION =" ;R2
280 P2 = (E2 - 1) * M2 / ((E2 + 2) * D2)
285 PRINT "SOLUTE MOLAR POLARISATION =" ;P2
290 PRINT : PRINT "SOLUTION DATA": PRINT
300 INPUT "WEIGHT OF SOLVENT =" ;W1
310 INPUT "WEIGHT OF SOLUTE =" ;W2
320 INPUT "PERMITTIVITY =" ;E3
330 INPUT "REFRACTIVE INDEX =" ;N3
340 INPUT "DENSITY =" ;D3
350 REM CALCULATE SOLUTION PARAMETERS
360 F1 = (M1 / W1) / (M1 / W1 + M2 / W2)

```

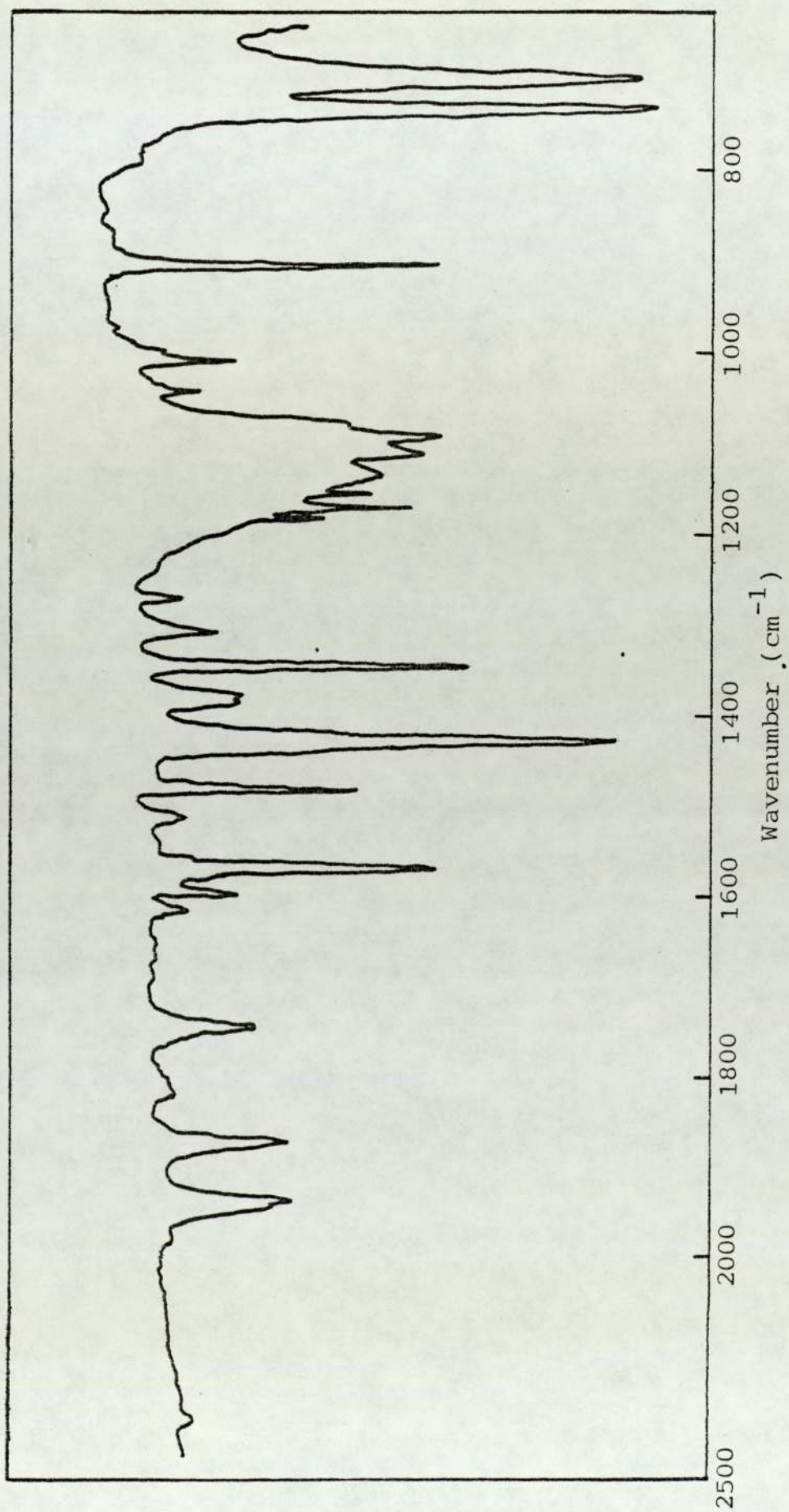
```

365 PRINT "MOLE FRACTION OF SOLVENT =" ; F1
370 F2 = 1 - F1
375 PRINT "MOLE FRACTION OF SOLUTE =" ; F2
380 M3 = F1 * M1 + F2 * M2
385 PRINT "SOLUTION MOLECULAR WEIGHT =" ; M3
390 V3 = F1 * V1 + F2 * V2
395 PRINT "SOLUTION MOLAR VOLUME =" ; V3
400 N3 = M3 * LN / LB
410 IF D3 > 0 GOTO 430
420 D3 = M3 / V3
430 IF N3 > 0 GOTO 460
440 R3 = F1 * R1 + F2 * R2
450 N3 = SQR ((2 * R3 * D3 + 2 * M3) / (M3 - D3 * R3)) : GOTO 470
460 R3 = (N3 * N3 - 1) * M3 / ((N3 * N3 + 2) * D3)
464 PRINT "SOLUTION REFRACTIVE INDEX =" ; N3
465 PRINT "SOLUTION MOLAR REFRACTIVITY =" ; R3
470 P3 = (E3 - 1) * M3 / ((E3 + 2) * D3)
475 PRINT "SOLUTION MOLAR POLARISATION =" ; P3
480 K3 = 6 * LB * N3 * M3 * B3 / D3
490 K3 = K3 / ((E3 + 2) * (E3 + 2) * (N3 * N3 + 2) * (N3 * N3 + 2))
495 PRINT "SOLUTION MOLECULAR KERR CONSTANT =" ; K3
500 REM CALCULATE SOLUTE MOLECULAR KERR CONSTANT
510 K2 = (K3 - F1 * K1) / F2
520 PRINT : INPUT "ALTER SOLVENT DATA ?" ; A$
530 IF A$ = "Y" GOTO 55
540 INPUT "CHANGE SOLUTE ?" ; B$
550 IF B$ = "Y" GOTO 180
560 INPUT "ALTER SOLUTE CONCENTRATION ?" ; C$
570 IF C$ = "Y" GOTO 290
580 INPUT "CHANGE KERR EFFECT WAVELENGTH ?" ; D$

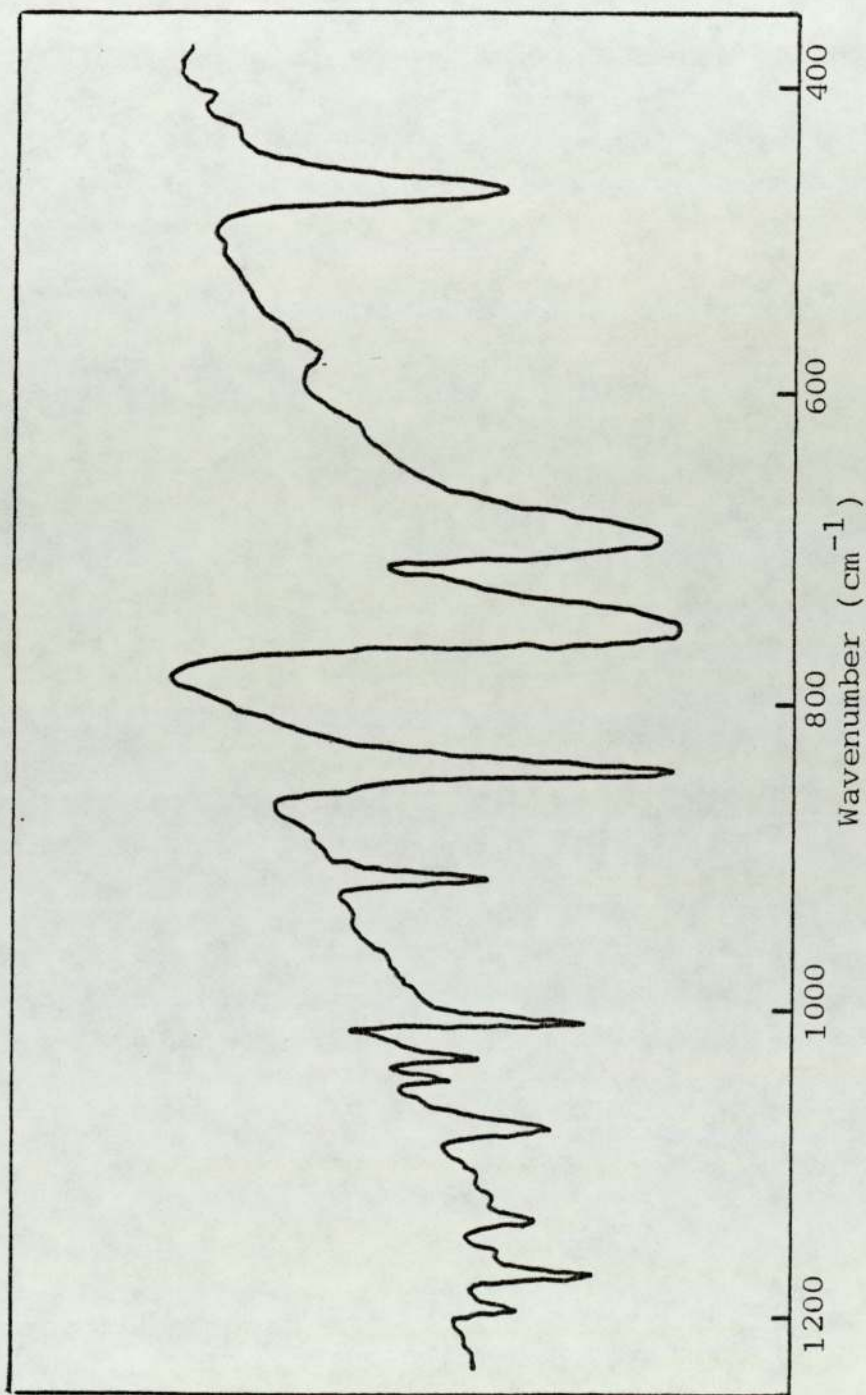
```

590 IF D\$ = "Y" GOTO 40

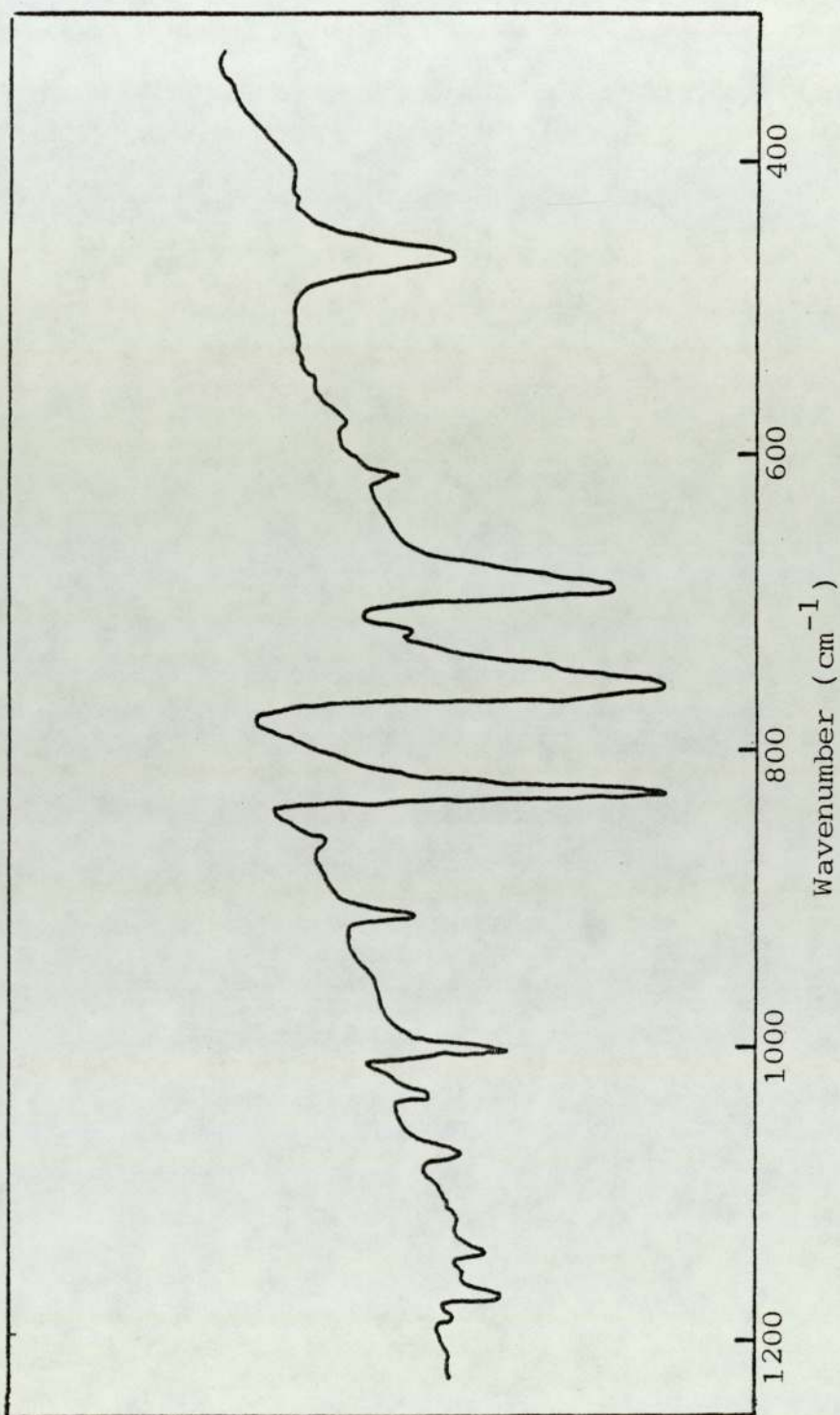
600 HOME : VTAB 15: PRINT "**** END ****": END



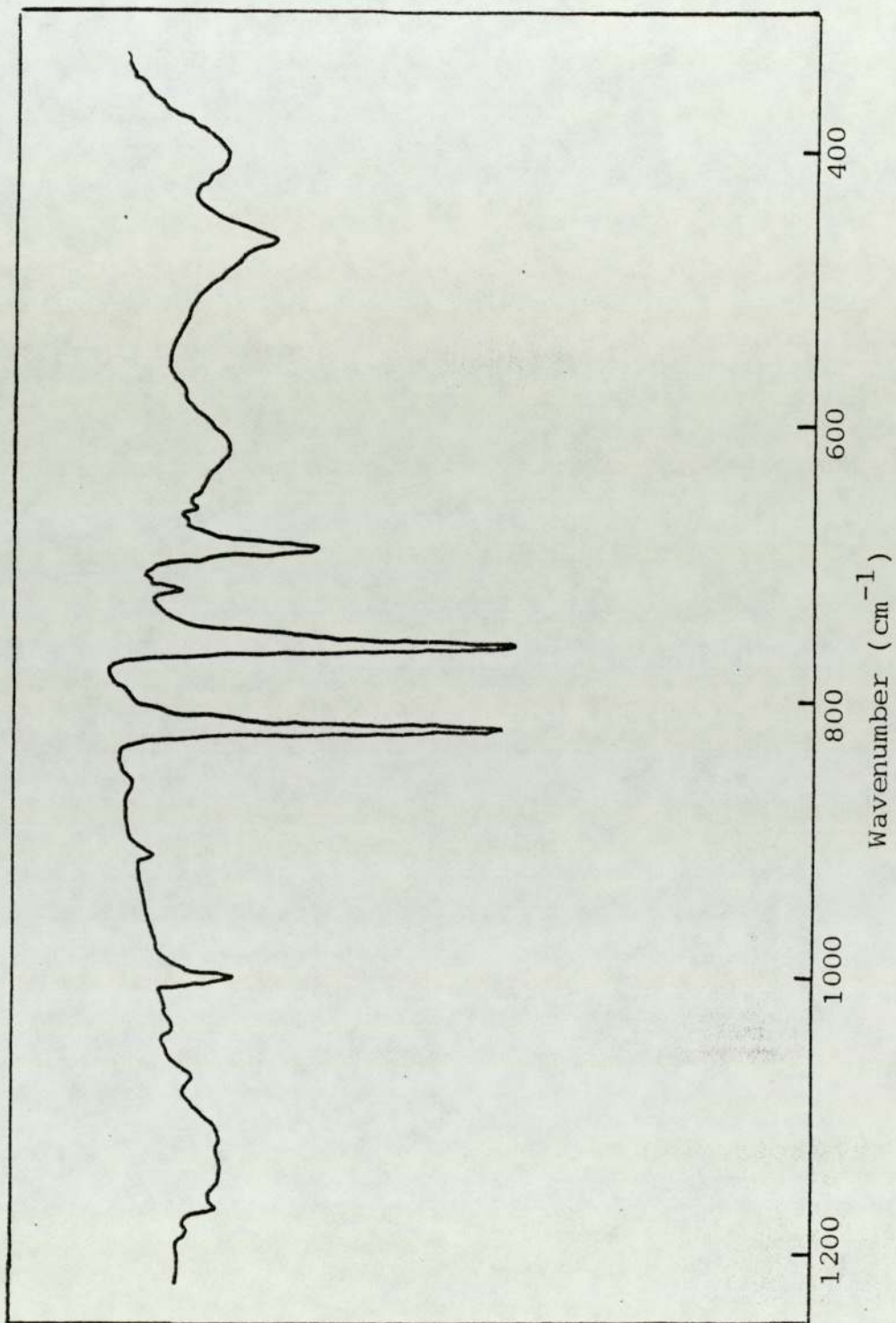
I.R. Spectra of Biphenyl



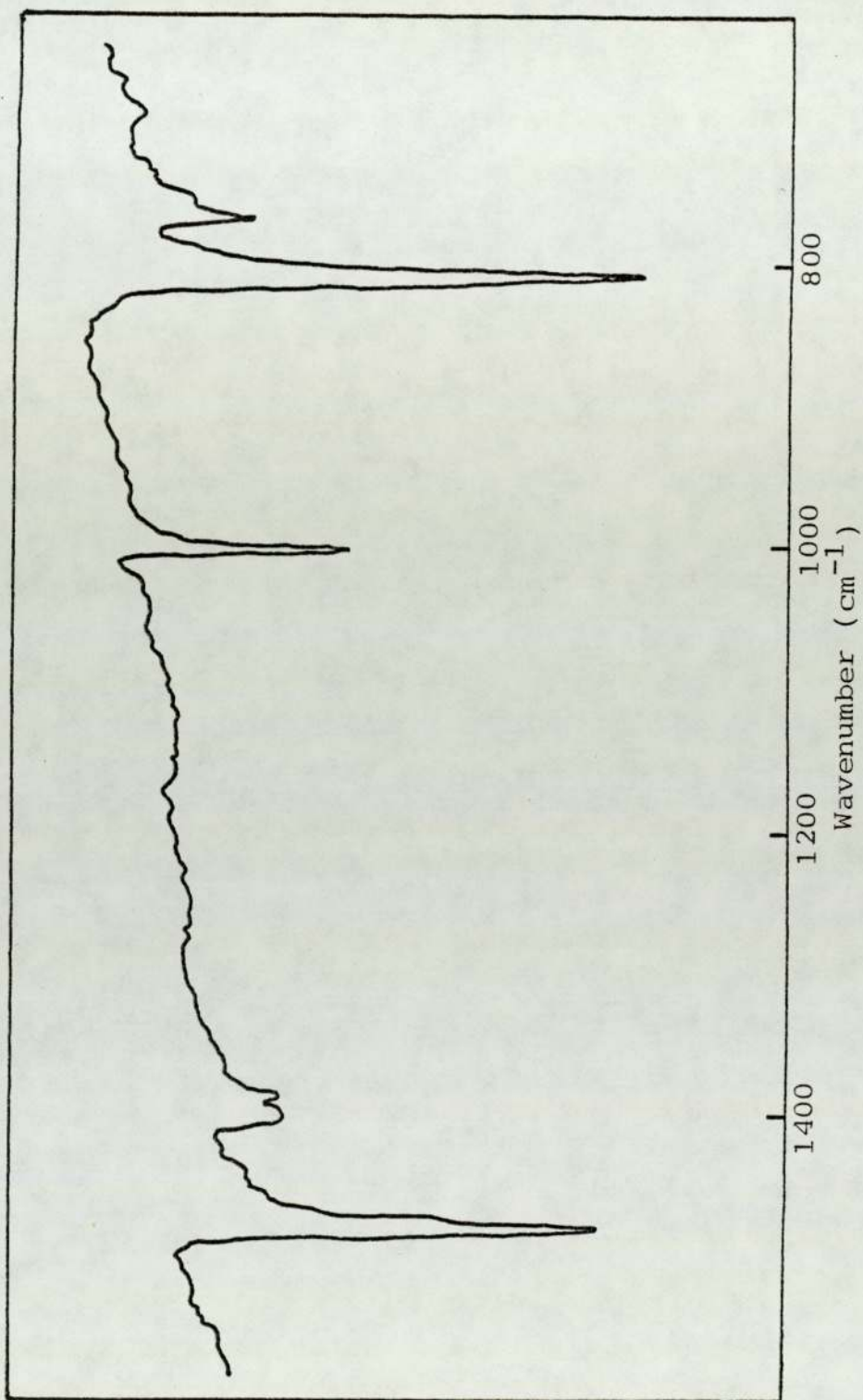
I.R. Spectra of Terphenyl



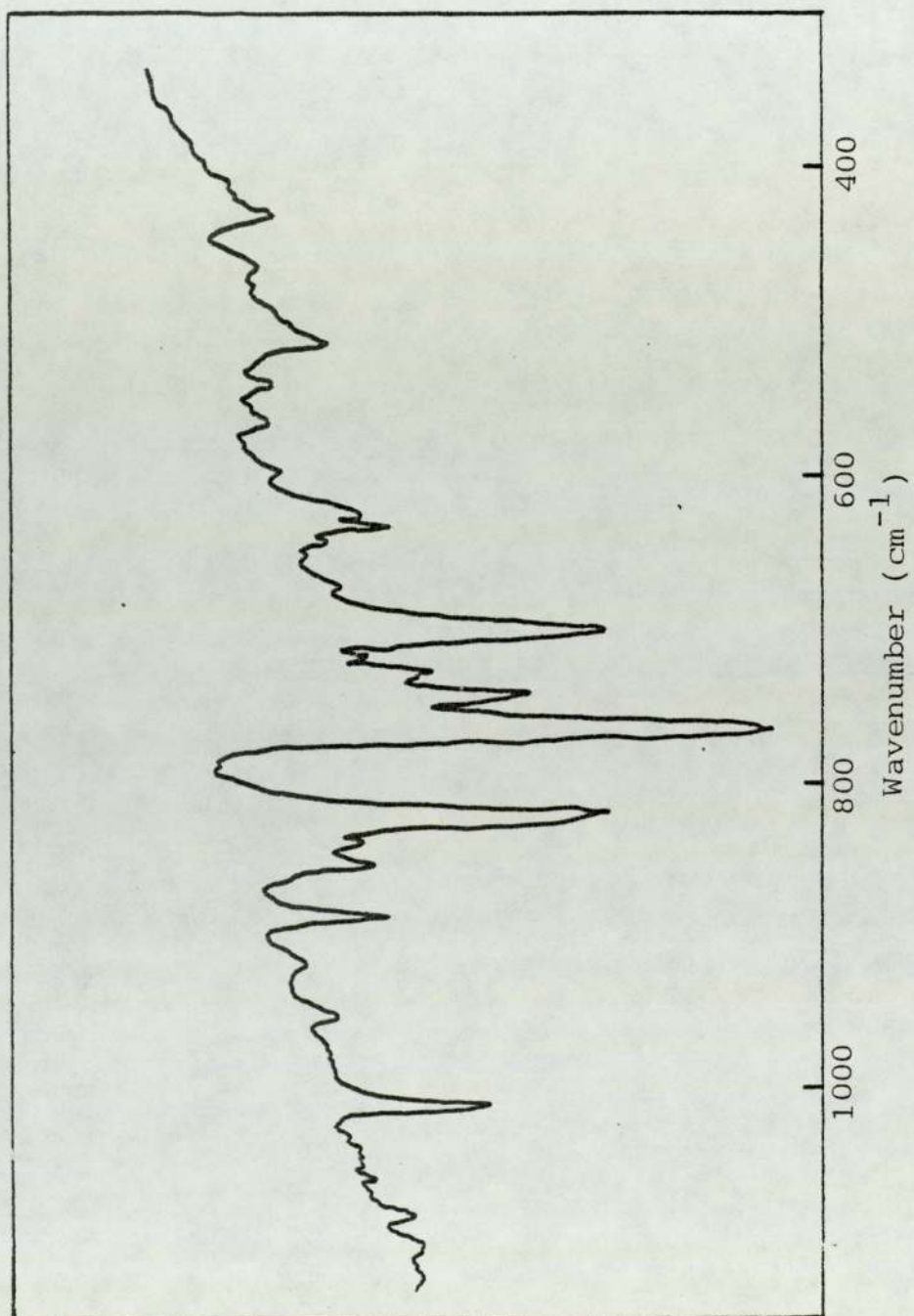
I.R. Spectra of P-Quarterphenyl



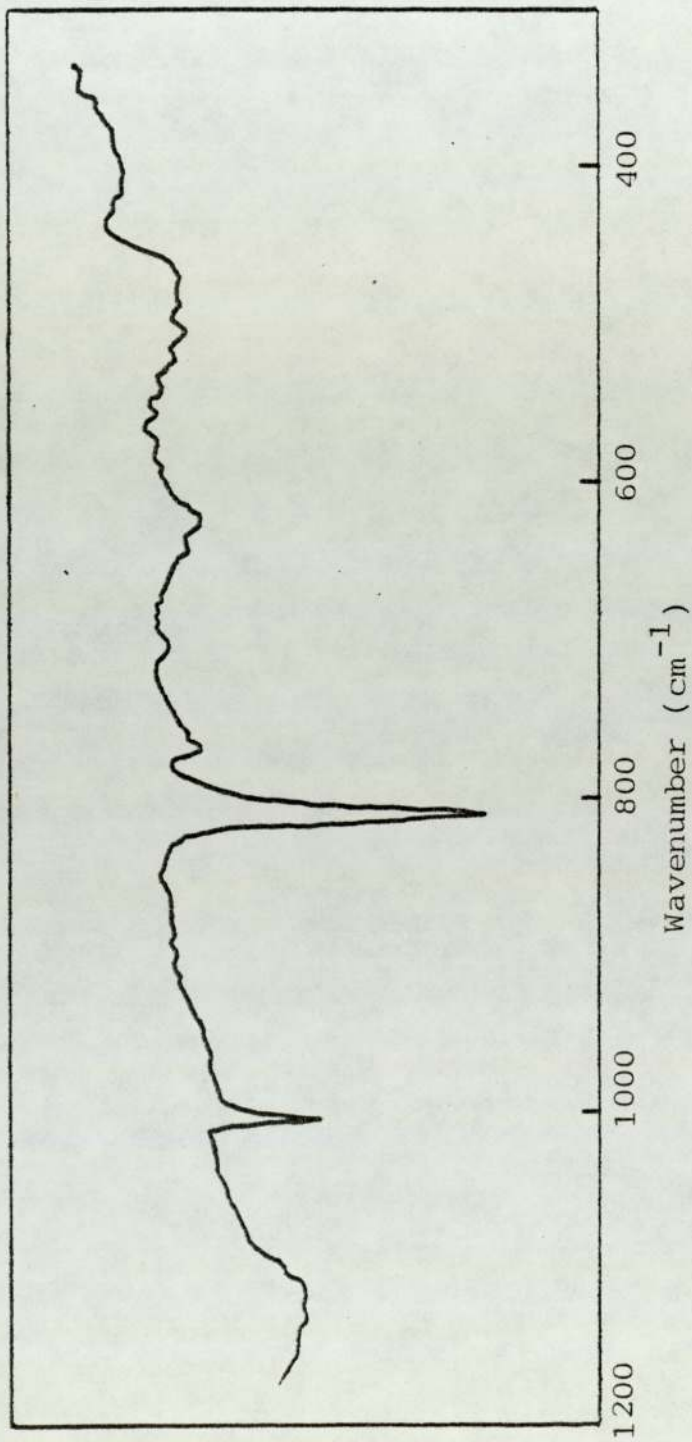
I.R. Spectra of P-Quinquephenyl



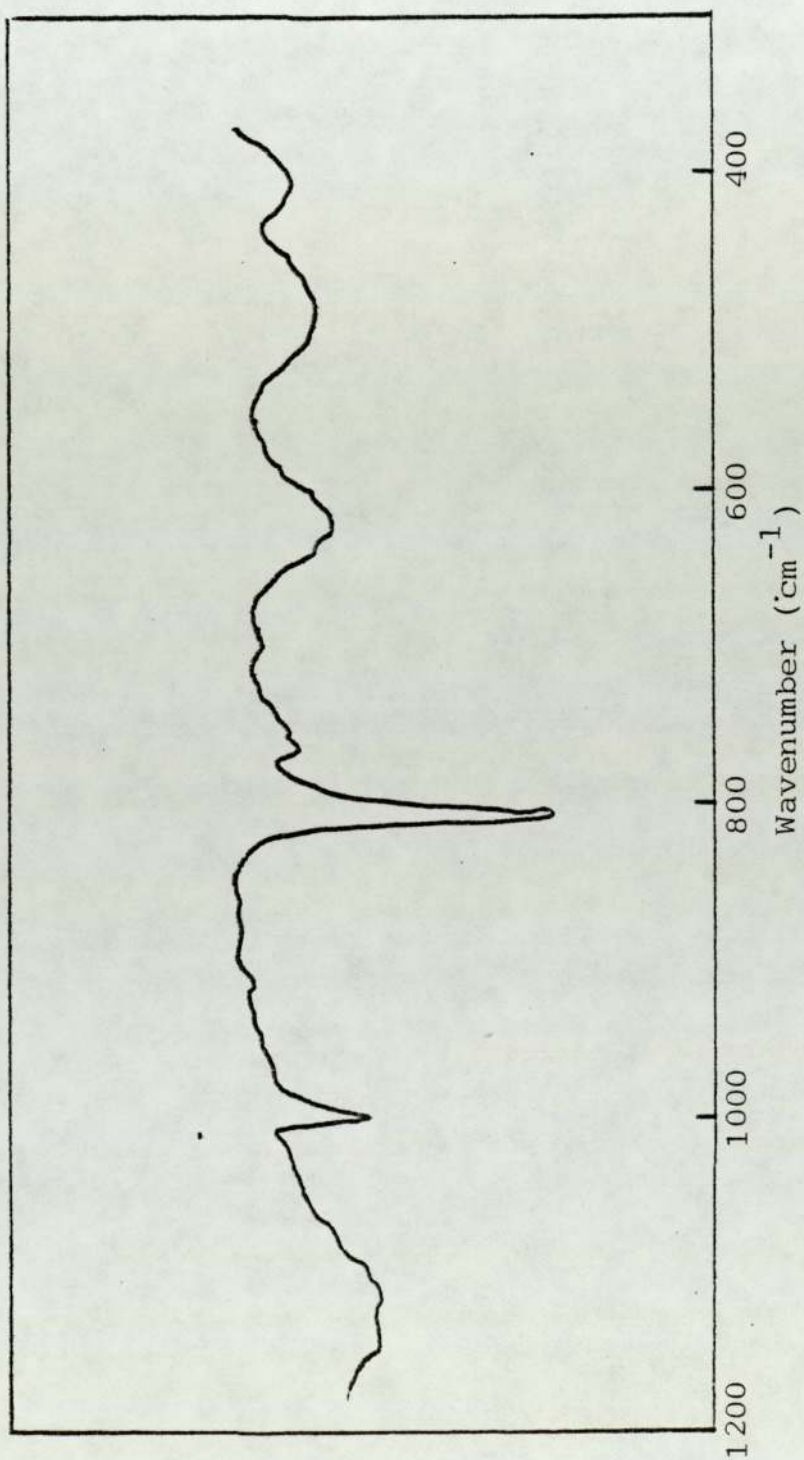
I.R. Spectra of polymer sample P1



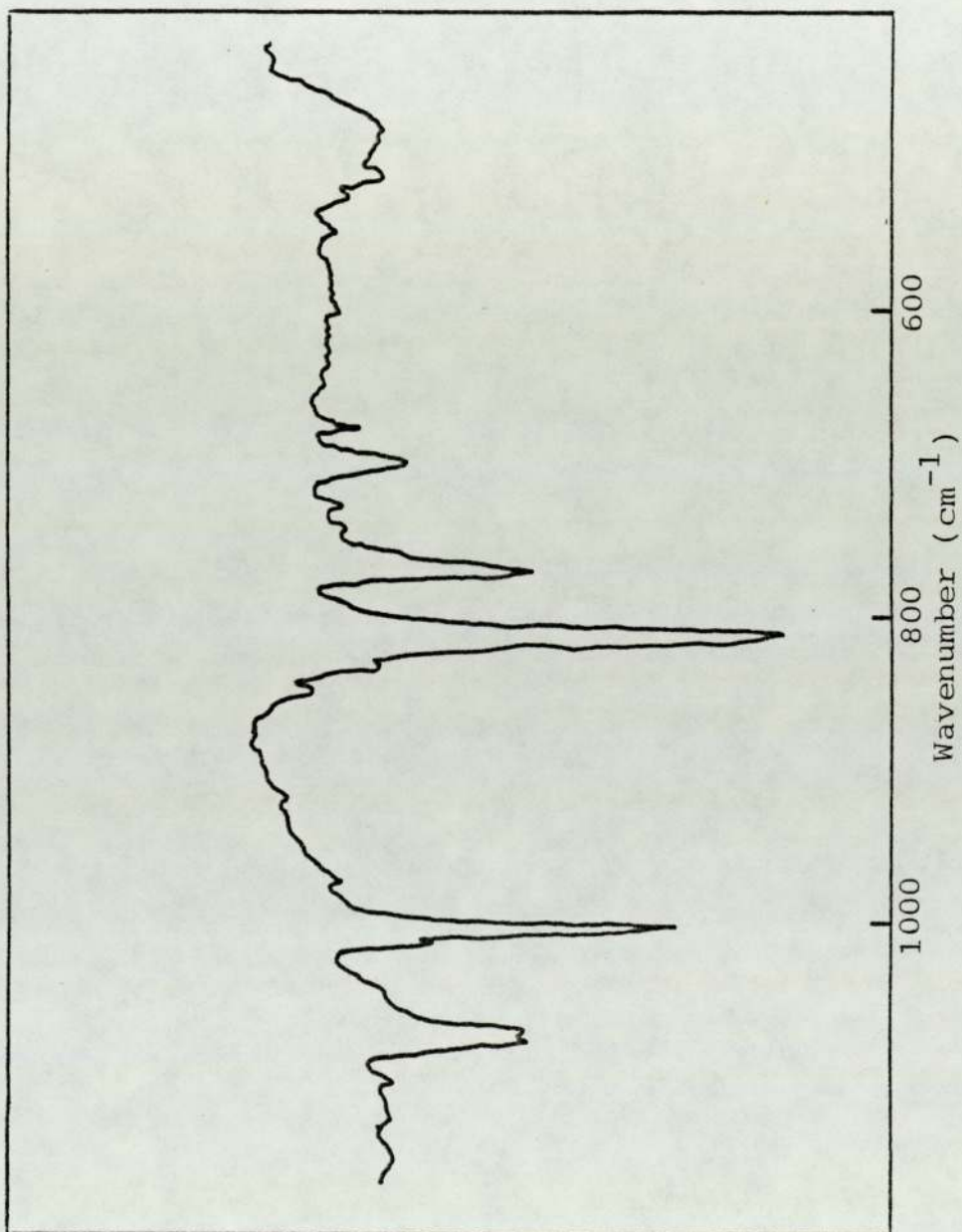
I.R. Spectra of Polymer Sample P4



I.R. Spectra of Polymer Sample P5



I.R. Spectra of Polymer Sample P6



I.R. Spectra of polymer sample P7

REFERENCES

1. MacDiarmid, A.G., Heeger, A.J. *Synthetic Metals* 1980, 1, 101-118
2. Yamamoto, T., sanechika, K., Yamamoto, A. *J. Pol. Sci., Polymer letter. Ed.* 1980, 18, 9-13
3. Ivory, D.M., Miller, G.G., Sowa, J.M., Shacklette, L.W., Chance, R.R., Baughman, R.H. *J. Chemical Physics.* 1979, 71, 1506-1511
4. Shacklette, L.W., Chance, R.R., Ivory, M.D., Miller, G.G., Baughman, R.H. *Synthetic Metals* 1980, 1, 307-320
5. Baughman, R.H., Bredas, J.L., Chance, R.R., Elsenbaumer, R.L., Shacklette, L.W. *Chem. Rev.* 1982, 82, 209-222
6. Baughman, R.H., Hsu, S.L., Anderson, L.R., Pez, G.P., Signorelli, A.J. *NATO Conf. Ser., (Ser.)* 6, 1979, 187
7. Bredas, J.L., Andre, J.M., Delhalle, J. *J. Mol. Structure* 2, 34-38 (1979)
8. Chance, R.R., Shacklette, L.W., Miller, G.G., Ivory, D.M., Elsenbaumer, R.L., Baughman, R.R. *J. Chem. Soc. Chem. Comm.* 1980, 347
9. Tabor, B.J., Magre, E.P., Boon, J. *Eur. Polym. J.* 1971, 7, 1127
10. Duke, C.S., Paton, A. *Org. Coat. Plast. Chem.* 1980, 43, 863
11. Bredas, J.L., Chance, R.R., Baughman, R.H., Silbey, R. *Int. J. Quantum Chem. Symp.* 1981, 15, 30
12. Charbonneau, G.P., Delugeard, Y. *Acta Crystallogr. Sect. B* 1977, 33, 1586
13. Noordik, J.H., Schreurs, J., Gould, R.O., Mooij, J.J., de Boer, E. *J. Phys. Chem.* 1978, 82, 1105
14. de Boer, E., Klaasen, A.A.K., Mooji, J.J., Noordik, J.H. *Pure Appl. Chem.* 1979, 51, 73
15. Rabolt, J.F., Clarke, T.C., Kanazawa, K.K., Reynolds, J.R., Street, G.B. *J. Chem. Soc. Chem. Commun.* 1980, 348
16. Pummerer, R., Bittner, K., *Ber.* 57, 84 (1924)
17. Pummerer, R., Seligsberger, L., *ibid.* 64, 2477 (1931)
18. Kuhn, R. *Ann.* 475, 131 (1929)
19. Nozaki, T., Tamura, M., Harada, Y., Saito, K. *Bull. Chem. Soc. Japan*, 33, 1329, (1960)

20. Kern,W., Wirth,H.O., Kunststoffe-Plastics, 6, 12
(1958)
21. Busch,M., Weber,W. J. Prakt. Chem. 146, 1, (1936)
22. Krizewsky, Turner. J. Chem. Soc. 1919, 115, 560
23. Kovacic,P., Koch,F.W. J. Org. Chem. 28, 1864,
(1963)
24. Marvel,C.S., Hartzell,G.E., J. Am. Chem. Soc., 81,
448 (1959)
25. Speight,J.G., Kovacic,P., Koch,F.W., J. Macromol.
Sci. Rev. C5, 295 (1971)
26. Pepper,D.C., Friedel-Crafts and Related Reactions.
Vol.11, G.A.Olah, Ed. Wiley-Interscience, New York,
1964, 1293
27. Kovacic,P., Kyriakis,A. J. Amer. Chem. Soc., 85,
454 (1963)
28. Mano,E.B., Alves,L.A., J. Polym. Sci. A-1, 10,
655-671 (1972)
29. Parker,V.D., Svanholm,U. J. Amer. Chem. Soc. 98,
2942 (1976)
30. Engstrom,G.G., Kovacic,P. J. Polymer Sci., 15,
1253-1468 (1972)
31. Williams,G.H., Homolytic Aromatic Substitution,
Pergamon Press, 1960, p.57
32. Shelton,J.R., Uzelmeier,C.W. J. Am. Chem. Soc. 88,
5222 (1966)
33. Olah,G.H., Flood,S.H., Moffat,M.E. J. Amer. Soc.,
86, 1065 (1964)
34. Olah,G.A., Kuhn,S.J., Hardie,B.A. J. Amer. Chem. Soc.
86, 1055 (1964)
35. Kovacic,P., Oziomek,J., Macromolecular Synthesis,
2, 23, (1966)
36. Ingold,K.U. Free Radicals, Vol.1, J.K.Kochi Ed.,
Wiley, New York 1973, p.66
37. Kochi,J.K. Free Radicals, Vol.1, J.K.Kochi Ed.,
Wiley, New York 1973, Chap.11
38. Thomas,J.K. J. Phys. Chem. 71, 1919 (1967)
39. Walling,C., Free Radicals in Solution, Wiley,
New York, 1957, p.169, 418

40. Kovacic,P., Wu,C. J. Poly. Sci. 47, 45 (1960)
41. De Tar,D.F., Long,R.A.J., Rendleman,J., Bradley,J.,
Duncan,D. J. Amer. Chem. Soc. 89, 4051 (1967)
42. Kochi,J.K. J. Amer. Chem. Soc. 85, 1958 (1963)
43. Struble,D.L., Beckwith,A.L.J., Gream,G.E.,
Tetrahedron Letters, 1970, 4795
44. Kochi,J.K. J. Amer. Chem. Soc., 78, 4815 (1956)
45. Kochi,J.K., Subramanian,R.V. J. Amer. Chem. Soc.
87, 1508 (1965)
46. Hey,D.H., Liang,K.S.Y., Perkins,M.J.,
Tetrahedron Letters 1967, 1477
47. Willard,H.H., Merritt,L.L.Jr., Dean,J.A. Instrumental
Methods of Analysis, 4th Ed., D.Van Nostrand, New York,
1965, p.151
48. Kovacic,P., Hsu,L.C. J. Polymer Sci. A-1, 4, 5-28
(1966)
49. Kovacic,P., Jones,M.B., Lanska,D. J. Polym. Sci.
19, 89-101 (1981)
50. Kirkland,E.V., Funderburk,O.P., Wadsworth,F.T.,
J. Org. Chem., 23, 1631 (1958)
51. Kovacic,P., Durham,J.E. J. Poly. Sci., Poly. Chem
Ed., 15, 2701-2706 (1977)
52. Amma,E.L., Turner,R.N., Abstracts of Papers,
144th. National Meeting of the American Chemical Soc.,
Los Angeles, April 1963
53. Olah,G.A., Meyer,M.W. In Friedel Crafts and
Related Reactions. Olah,G.A. Ed. Interscience,
New Yprk, 1963, Vol.1 Chapt.8.
54. Baughman,R.H., Shacklette, L.W., Elsenbaumer,R.L.,
Chance,R.R., Sowa,J.M., Ivory,D.M., Granville,G.M.
J. Chemical Soc., Chemical Communication,
361-362 (1982)
55. Tamao,K., Sumitani,K., Kumada,M. J. Am. Chem. Soc.,
94, 4374 (1972)
56. Yamamoto,T., Hayashi,Y., Yamamoto,A. Bull. Chem. Soc.
Japan, 51 (7), 2091-2097 (1978)
57. Shacklette,L.W., Eckhardt,H., Chance,R.R., Miller,G.G.,
Ivory,D.M., Baughman,R.H. J. Chemical Physics 1980
73 (8), 4098-4102

58. Gans, R. 'Asymmetrie Von Gasmolekeln. Ein Beitrag zur Bestimmung der Molekularen Forms', *Annalen der Physik*, Vol. 65 (10), p.97-123, (1921)
59. Debye, P., Sack, H. 'Handbuch der Radiologie' Vol. 6, Ch. 2, p.69 and p.179 (1934)
60. Stuart, H.A. 'Die Struktur des freien Molekuls', Ch. 7, p.415, Springer, Berlin (1952)
61. Mumby, S.J. Ph.D. Thesis, University of Aston in Birmingham, 1983
62. des Coudres, T. *Verhandl. Ges. deutsch Naturforsch, Arzte*, 65, 67 (1893)
63. Tamao, K., Sumitani, K., Kumada, M. *J. Am. Chem. Soc.*, 94, 4374 (1972)
64. Yamamoto, T., Hayashi, Y., Yamamoto, A. *Bull. of Chem. Soc. of Japan*, 51 (7), 2091-2097 (1978)
65. Jozefowicz, M. Ph.D. Thesis, University of Paris 1963
66. Kovacic, P., Feldman, M.B., Kovacic, J.P., Lando, J.B. *J. Appl. Polym. Sci.* 12, p.1735-1743 (1968)
67. Toussaint, C.J., Vos, G. *J. Chem. Soc., B*, 813 (1966)
68. Porath, J., Flodin, P. *Nature*, 1959, 183, 1657
69. Moore, J.C. *J. Polymer Sci., A-2* (1964) 835
70. Joustra, M., Soderquist, B., Fischer, L. *J. Chromatography* 28 (1967) 21
71. Kusch, P., Zahn, H. *Angew. Chem. Intern. Ed. Engl.*, 4 (1965) 696
72. Determann, H., Lueben, G., Wieland, T. *Makromol. Chem.* 73 (1964) 168
73. Heitz, W., Ullner, H., Hoecker, H. *Makromol. Chem.*, 48 (1961) 160
74. Martin, A.J.P., Synge, R.L.M. *Biochem. J.*, 1941, 35, 1358
75. Beckmann, E.Z. *Physik. Chem.* 5, 76 (1889)
76. Lachman, A. *Physik Chem.* 25, 50 (1903)
77. Hilderbrand, J.H., Glascock, B.L., *IBID*, 31 26 (1909)
78. Walker, O.J., *Transfaraday Society*, 31, 1432 (1935)

79. Hilderbrand, J.H., Benesi, H.A., *ibid*, 70, 3978 (1948)
80. Friedel, C., Crafts, J., *Compt. rend.*, 85, 74 (1877)
81. Mazzetti, De Carli, *Gazz Chim. ital*, 58, 36 (1928)
82. Hepp, *Ann.*, 215, 376 (1882)
83. Fairbrother, F. *Nature*, 160 87 (1947); *J. Chem. Soc.* 1051 (1948)
84. Schlenk, W., *Ann.*, 368, 277 (1909)
85. Nijl, D., Kainer, H., Rose-Innes, A.C. *J. Chem. Phys.*, 30, 765 (1959)
86. Kepler, R.G., Bierstedt, P.E., Merrifield, R.E., *Physics Review Letters*, 5, 503 (1960)
87. Melby, L.R., Hardner, R.J., Hertler, W.R., Mahler, W., Benson, R.E., Mochel, W.E. *J. Am. Chem. Soc.* 82, 6408 (1960)
88. Robert, D.B., Johannes, G., Larry, K. *J. Am. Chem. Soc.* 94, (19), 6861-6862 (1972)
89. Colton, R.H., Henn, D.E. *J. Chem. Soc. (B)*, 1532 (1970)
90. Le Fevre, C.G. and Le Fevre, R.J.W. *The Kerr Effect: Its Measurement and Applications in Chemistry; Rev. Pure Appl. Chem.*, Vol.5 (4), p.261-318 (1955)
91. Williams, R.M., Wallwork, S.C., *Acta Cryst.*, 22, 899 (1967)
92. Kuroda, A., Ikemoto, I., Akamatu, H. *Bull. Chem. Soc. Japan* 39, 547 (1966)
93. Ikemoto, I., Kuroda, H. *Bull. Chem. Soc. Japan*, 40, 2009 (1967)
94. Adman, E., Rosenblum, M., Sullivan, S., Margulis, T.N., *J. Am. Chem. Soc.*, 89, 4540 (1967)
95. Aroney, M.J., Corfield, M.G., Le Fevre, R.J.W. *J. Chem. Soc.* 648-652 (1964)
96. Flory, P.J. *Statistical Mechanics of Chain Molecules*, Inter-Science, New York, 1969
97. Le Fevre, R.J.W., Orr, B.J., Ritchie, G.L.D. *J. Chem. Soc. B.* 1966, 273
98. Le Fevre, R.J.W., *J. & Proce. Royal Society of New South Wales*, Vol.95, p.1-11 (1961)

99. Blythe,A.R. 'Electrical Properties of Polymers',
Cambridge University Press (1979)
100. Taniguchi,A., Kanda,S., Kusabayashi,T., Mikawa,H.,
Ito,K. Bull. Chem. Soc. Japan 37, 1386 (1964)
101. Kuczkowski,A., Dreger,Z., Slupkowieki,T., Jachym,B.
Polymer 20, 1161 (1979)
102. Okamoto,K.I., Yamada,M., Itaya,A., Kimura,T.,
Kusabayashi,S. Macromolecules 1976, 9, 645
103. Williams,D.J., Froix,M.F. Polymer Preparation 1977,
18, 445
104. Karvamura,T., Matsuzaki,K. Makromol. Chem. 1978,
179, 1003
105. Terrell,D.R., Evers,F., Smoorenburg,H.,
van den Bogaerts,H.M. J. Polym. Sci., Polym. Phys.
Ed. 1982, 20, 1933
106. Beevers,M.S., Mumby,S.J. Polymer Communications,
25, 173-175 (1984)
107. Robin,P., Pouget,J.P., Comes,R., Gibson,H.W.,
Epstein,A.J. Polymer 1983, 24, 1559
108. Heller,J., Tieszen,D.O., Parkinson,D.B. J. Polymer
Sci. Part A 1963, 1, 125
109. Yoshimoto,S., Akana,Y., Kimura,A., Hirata, H.,
Kusabayashi,S., Mikawa,H. Chem. Comm. 1969, 17,
987
110. Okamoto,K.I., Yamada,M., Itaya,A., Kimura,T.,
Kusabayashi,S. Macromolecules 1976, 9, 645
111. Froix,M.F., Williams,D.J., Goedde,A.O.
Macromolecules 1976, 9, 81
112. Tsuchihashi,N., Hataro,M., Sohma,J. Makromol. Chem.
1976, 177, 2739-2747
113. Williams,D.J., Froix,M.F. Polymer Preprints 1977,
18, 445
114. Kawamura,T., Matsuzaki,K. Makromol. Chem. 1978,
179, 1003
115. Kimura,A., Yoshimoto,S., Akana,Y., Hirata,H.,
Kusabayashi,S., Mikawa,H., Kasai,N. J. Polym. Sci.
Polym. Phys. 1970, 8, 643
116. Crystal,R.G. Macromolecules 1971, 4, 379
117. Griffiths,C.H. J. Polym. Sci. Polym. Phys. 1975,
13, 1167

118. (a) Griffiths, C.H. J. Polym. Sci. Poly. Lett. 1978, 16, 271
 (b) Griffiths, C.H. 'Characterisation of Metals and Polymer Surfaces (Symp.)' 1976, 2, 233
 (c) Sundararajan, P.R., Zamiu, J. Polymer 1979, 20, 1567
119. (a) Bergfjord, J.A., Powell, R.C., Stolka, M. J. Polym. Sci. Polym. Phys. 1979, 711
 (b) Terrel, D.R., Evers, F., Smoorenburg, H., van der Bogaert, H.M. J. Polym. Sci. Polym. Phys. 1982, 20, 1933
120. Aroney, M.J., Pratten, S.J. J. Chem. Soc. Faraday Trans. 1, 1984, 80, 1201-1204
121. Aroney, M.J., Battaglia, M.R., Ferfoggia, R., Millar, D. and Pierens, R.K., 'The Kerr Constant of Water and other Pure Liquids at 633 nm', J.C.S., Faraday II, Vol.72, p.724-726 (1976)
122. Kovacic, P., Lange, R.M. J. Org. Chem. 29, 2416-2420 (1964)
123. (a) Flory, P.J., Irvine, P.A., Da Cheng Wu, J. Chem. Soc. Faraday Trans. 1, 1984, 80, 1795-1806
 (b) Flory, P.J., Irvine, P.A. J. Chem. Soc. Faraday Trans., 1, 1984, 80, 1807-1819
 (c) Flory, P.J., Irvine, P.A. J. Chem. Soc. Faraday Trans., 1, 1984, 80, 1821-1830
124. Finkelmann, H., Rehage, G. Makromol. Chem. Rapid Commun. 1, 733-740 (1980)
125. Aguilera, C., Ringsdorf, H. Polymer Bull. 12, 93-98 (1984)